Mycobacterium tuberculosis glycolipids and their effects on HIV-1 infection and replication

Thesis submitted in accordance with the requirements of

the University of Liverpool for the degree of Doctor in Philosophy

By

Marion Pouget

October 2018

Abstract

Human Immunodeficiency Virus type 1 (HIV-1) and *Mycobacterium tuberculosis* (*Mtb*) co-infection results in a rapid loss of numerous immunological functions and ultimately leads to death when not treated. The WHO estimated in 2015 that 13 million people were infected by both pathogens, with 390,000 deaths related to tuberculosis among HIV-infected individuals. *Mtb* and HIV-1 can induce profound changes in the host immune response resulting in *Mtb* infections causing active disease or the exacerbation of HIV-1 infection. For aiding in the development of new treatments a better understanding of the interactions between both pathogens and the host is crucial. This thesis follows this perspective by aiming to characterise the impact *Mtb* glycolipids have on modulating HIV-1 infection and to identify *Mtb* strains that differentially modulate HIV-1 infection and immune cell innate signalling.

A technique was developed allowing for incorporation of *Mtb* glycolipids into liposomes, thereby mimicking the lipid distribution and antigen presentation found within the mycobacterial cell wall. Liposomes were produced with total lipid extracts from various pathogenic and non-pathogenic mycobacteria strains: BCG, *M. smegmatis*, and *Mtb* H37Rv, HN878, CDC1551 and EU127. We demonstrated the successful incorporation of specific mycobacterial cell wall glycolipids into liposomes. In order to study the impact of these *Mtb* glycolipids on the immune response, potentially influencing HIV-1 infection (indirectly), we measured the effect of *Mtb* liposomes on macrophage, DC and $CD4^+$ T cell activation *in vitro* by measuring cytokine production and expression of cellular activation markers. From these analyses we demonstrated a strong heterogeneity of *Mtb* liposome effects on modulating immune cell responses depending on cell type and the *Mtb* strains studied. The *Mtb* generated liposomes were subsequently tested in the context of various HIV-1 *in vitro* co-culture systems using both HIV-1 X4 and R5 strains. We investigated the effects on HIV-1 *cis*-infection and *trans*-infection mediated by DCs, believed to be involved with HIV-1 transmission and disease progression. We observed that *Mtb* glycolipids differentially modified cytokines and chemokines production from infected cells. These modulations are associated with heterogenous impacts on HIV-1 infection depending on virus tropism, the culture system being tested and *Mtb* strains. *Mtb* glycolipids did not show the capacity to interfere with HIV-1 cell attachment and cell entry *via* co-receptors recognition. However, HIV-1 *trans*-infection mediated by DC-SIGN receptor was impaired in the presence of *Mtb* glycolipids from BCG, H37Rv and EU127 strains. SL1 and TDM glycolipids were identified to

be involved in DC-SIGN recognition and impairment of HIV-1 *trans*-infection. These findings indicate that variant strains of *Mtb* have differential effects on modulating immune activation, primarily through DC interactions, and which affect HIV-1 infection and/or replication, which in all likelihood will influence HIV-1 disease course in co-infected individuals.

Finally, in the perspective of better understanding the role of extra-vesicles (EVs) in influencing HIV-1 infectivity in the context of *Mtb* co-infection, we developed and compared different techniques for generating EVs from plasma, namely utilising ultra-centrifugation and gel filtration.

Acknowledgments

Firstly, I would like to thank Bill and Georgios for giving me the chance to join their research team and the opportunity to complete a thesis under their supervision. Through their guidance and mentorship, I achieved to become an improved researcher and scientist. I would like to thank them for their support and kindness in both professional and personal matters that lasted from the first night I arrived in Liverpool until now.

I would like to express my gratitude to the PathCo family for their support in this project and particularly Anastasia Koch and Robert J. Wilkinson from the University of Cape Town for providing all the clinical samples; Apoorva Bhatt from the University of Birmingham for the lipid extracts and TLC analysis; and Carolina Herrera from the Imperial College London for the Luminex analysis.

From the Paxton Lab, I would like to thank especially Jordan for the help in HIV-DNA quantification assays. I will not forget the laughs we shared together on a daily basis as well as the pub quizzes, nights-outs in Liverpool (and Manchester) and his tremendous gift for singing with the correct lyrics. I am thankful for Alessandra whom shared her experimental knowledge with me during her time in the lab. She has been of a great support during my PhD by providing me comfort and lending me an ear when confronted by different hardships.

Thank you to Jeoffrey, Lindsay, Raquel, Charlene and Fernanda for having been my family in Liverpool. Without them my life there wouldn't have been the same. They made my time in Liverpool what it is, for living with me all the good and the bad that we came across either at the lab or outside of work. Jeoffrey, his singing and his peculiar French music tastes made me able to manage my homesickness; Fernanda and Raquel provided me their Spanish sunlight in a foggy and rainy Liverpool. I give a special thought to Lindsay and Charlene whom helped me to stabilise my mental state and *vice versa*.

It would be impossible to forget John and Dan, for having always been there when I needed to blow off some steam with a pint at the pub (or several), I express my gratitude. I would like to thank, from the IGH, Stavros, Marie, Rong, Noon, Amer, Murad, Emma, Murielle, Laura, Janet, Libby, Yasmin and Wes for their availability and kindness when I needed them.

I would like to thank Pauline and Gwenaelle for their eternal friendship, love and kind heartedness despite the many miles between us.

Finally, last but not least, I would like to express my sincere gratitude to my family who made me who I am today. I wouldn't have been able to be here without their unconditional support. They pushed me to go through my fears, to accomplish my goals and uphold my aspirations. I would like to dedicate my thesis to my Mother, Annie, whom always sacrificed herself for the well-being of her children.

Declaration of Authorship

I declare that except where indicated by specific reference in the text, this work is my own work. Work done in collaboration with, or with the assistance of other, is indicated as such and acknowledged.

Table of Contents

List of Figures

List of Tables

List of Appendixes

List of Abbreviations

ADAM17	ADAM metallopeptidase domain 17
AG	Arabinoglactan
AIDS	Acquired Immune Deficiency Syndrome
AP-1	Activator protein 1
APC	Antigen-presenting cell
APOBEC	Apolipoprotein B mRNA editing enzyme catalytic polypeptide-like
ARD	Antiviral drug
ART	Antiretroviral therapy
ARV	AIDS-associated retrovirus
BCG	Bacillus Calmette-Guérin
bp	Base pair
BSA	Bovine serum albumin
CA	Capsid
CCR5	CC chemokine receptor 5
CD	Cluster of differentiation
CDC	Centre of Disease Control
C/EBP	CCAAT enhancer binding proteins
cGAS	GMP-AMP synthase
Ch	Cholesterol
CR	Complement receptor
CTL	Cytotoxic T cell
CXCR4	CXC chemokine receptor 4
DC	Dendritic cell
DC-SIGN	Dendritic cell-specific ICAM-3-grabbing non-integrin
DMEM	Dulbecco's modified eagle medium
dsDNA	Double stranded DNA
EDTA	Ethylenediaminetetraacetic acid
ELISA	Enzyme-linked immune-enzymatic assay
EMB	Ethambutol
Env	Envelope
ESCRT-I	Endosomal sorting complexes required for transport
Esx-1	ESAT-6 secretion system 1
EV	Extracellular vesicles
FBS	Foetal bovine serum
FI	Fusion inhibitor
Gag	Group specific antigen protein
G-CSF	Granulocyte colony-stimulating factor
GFP	Green fluorescent protein
GM-CSF	Granulocyte-macrophage colony-stimulating factor
gp	Glycoprotein
HBV	Hepatitis B virus
HCV	Hepatitis C virus
HEPES	4-(2-hydroxyethyl)-1-piperazineethanesulfonic acid
HIV	Human Immunodeficiency Virus
HLA	Human leukocyte antigen
HTLV-III	Human T-Lymphotropic Virus type III
iDC	Immature dendritic cell
IL	Interleukin

IFI16	Gamma-interferon-inducible protein 16
IFN	Interferon
IN	Integrase
INH	Isoniazid
INSTI	Integrase stand transfer inhibitor
IP	Interferon gamma-induced protein
IRIS	ART immune reconstitution inflammatory syndrome
I-TAC	Interferon-inducible T-cell alpha chemoattractant
LAM	Lipoarabinomannan
LAV	Lymphadonepathy-Associated Virus
LC	Langerhans cell
LEDGF	Lens epithelium-derived growth factor
LM	Lipomannan
LPS	Lipopolysaccharide
LTR	Long terminal repeat region
MA	Matrix protein p17/mycolic acid
ManLAM	Mannose-capped LAM
M-CSF	Macrophage colony-stimulating factor
mDC	Mature dendritic cell
MDM	Monocyte drive macrophage
MDR	Multi-drug resistance
MFI	Median fluorescence intensity
MHC	Major histocompatibility complex
MIG	Monokine induced by gamma interferon
Mincle	Macrophage inducible C-type lectin
MIP	Macrophage inflammatory proteins
MR	Mannose receptor
MUV	Multilamellar vesicles
Mtb	*Mycobacterium tuberculosis*
MVB	Multivesicular compatment
NC	Nucleocapsid p7
Nef	Negative Regulatory Factor
NFAT	Nuclear factor of activated T cells
NF-κB	Nuclear factor κB
NK	Natural killer cell
NPC	Nuclear pore complex
NNRTI	Non-nucleoside reverse transcription inhibitor
NRTI	Nucleoside reverse transcription inhibitor
ORF	Open reading frames
PAMP	Pathogen-associated molecular pattern
PBMC	Peripheral Blood Mononuclear cell
PBS	Phosphate-buffered saline
PC	Phosphatidylcholine
PCR	Polymerase chain reaction
PDIM	Phthiocerol dimycocerosate
PFA	Paraformaldehyde
PG	Peptidoglycan
PHA-p	Phytohemagglutinin p
PI3P	Phosphatidylinositol 3-phosphate
PI	Protease inhibitor
PIC	Pre-integration complex
PIM	Phosphatidylinositol mannoside

PM	Plasma membrane
Pol	Polymerase
Poly(I:C)	Polyinosinic:polycytidylic acid
PR	Protease p11
PRR	Pathogen-recognition receptor
pTEFb	Positive transcription elongation factor
PVDF	Polyvinylidene difluoride
PZA	pyrazinamide
qPCR	Quantitative PCR
RANTES	Regulated on activation, normal T cell expressed and secreted
RER	Rough endoplasmic reticulum
RIF	Rifampicin
RIPA	Radioimmunoprecipitation assay
RLU	Relative light units
RNApol-II	RNA polymerase II
RNase H	Ribonuclease H
RPMI	Roswell Park Memorial Institute medium
RT	Room Temperature/Reverse-transcriptase
RTF	Reverse transcription complex
SAMHD1	SAM domain and HD domain-containing protein 1
SDF-1	Stromal cell-derived factor 1
SDS-PAGE	Sodium dodecyl sulfate–polyacrylamide gel electrophoresis
SEC	Size exclusion chromotography
SIV	Simian Immunodeficiency Virus
SL	Sulfolipid
Sp	Specificity protein
ssRNA	Single stranded RNA
SU	Env surface sub-unit gp120
SUV	Small unilamellar vesicles
TAR	Trans-activation response element
Tat	Trans-activator of transcription
TB	Tuberculosis
TBS	Tris-buffered saline
TDM	Trehalose dimycolate
TEMED	Tetramethylethylenediamine
TGF	Transforming growth factor
TLC	Thin-layer chromatography
Th	T helper
TM	Env transmembrane sub-unit gp41
TNF	Tumour necrosis factor
TLR	Toll-like receptor
UC	Ultra-centrifugation
V3	Variable loop 3
Vif	Viral infectivity factor
Vpr	Viral protein r
Vpu	Viral protein u
YFP	Yellow fluorescent protein
XDR	Extensively drug-resistance

Introduction

Human Immunodeficiency Virus HIV is a lentivirus causing Acquired Immune Deficiency Syndrome (AIDS). We count in 2017, 36.9 million people living with HIV and 1.8 million newly infected. Despite the increasing availability of Antiretroviral Therapy (ART), approximately 1 million deaths are attributed to HIV-1 each year. Tuberculosis (TB) is the most common disease to be diagnosed in people living with HIV and provides for the highest mortality rates amongst HIV-infected patients (390,000 tuberculosis-related death in 2015), especially in sub-Saharan Africa (WHO).

I. HIV-1 Infection

The Centre of Disease Control (CDC) observed in 1981, an increase of rare opportunistic infections such as *Pneumocystis carinii* pneumonia and Kaposi sarcomas (Gottlieb *et al.*, 1981; Masur *et al.*, 1981). These infections were linked with a severe immune deficiency syndrome named AIDS in 1982. In 1983, researchers from the Pasteur Institute identify the lymphadenopathy-associated virus (LAV) in AIDS patients without demonstrating the causality between infection and AIDS (Barré-Sinoussi *et al.*, 1983). However in 1984, the CDC announced the isolation of the etiological agent of AIDS: the Human T-Lymphotropic Virus type III (HTLV-III) (Popovic *et al.*, 1984). HTLV-III and LAV, as well as a third virus named AIDS-associated retrovirus (ARV) described in 1984 (Levy *et al.*, 1984), were later characterised to be the same virus (Ratner, Gallo and Wong-Staal, 1985) and renamed HIV in 1986. A second retrovirus was isolated in West African patients (Clavel *et al.*, 1986) and named HIV type 2 (HIV-2) against the first described named HIV type 1 (HIV-1). The two viruses shared similar genetic and biological properties, but compared to HIV-1, HIV-2 is less virulent and transmissible (Marlink *et al.*, 1994; Vidya Vijayan *et al.*, 2017). Phylogenetic analysis established links between HIV-1 groups and the simian immunodeficiency virus SIV_{cpz} (virus infecting chimpanzees) and SIV_{gor} (virus infecting gorillas). HIV-1 is divided into four genetic subgroups M, O, N (Gao *et al.*, 1999; Takehisa *et al.*, 2009) and more recently P (Plantier *et al.*, 2009) where subgroup M is responsible of the majority of HIV-1 cases.

i. Viral Particle

HIV is a lentivirus belonging to the *Retroviridae* family. As a retrovirus, it is characterised by a genome composed of positive single stranded RNA. Two copies of RNAs are encased by nucleocapsid p7 (NC) forming the core of the viral particle. The association of ARN/p7 and viral proteins essential for viral replication are contained in a conical capsid composed of protein p24 (CA). The capsid is surrounded by a cavity defined by the matrix protein p17 (MA) fixed in lipids and incorporating the viral envelope protein (Env). The Env consists of a lipid bilayer membrane, derived from the host cell budding and a viral trimeric envelope protein complex. The trimeric structure is composed of a transmembrane sub-unit gp41 (TM) and a surface sub-unit gp120 (SU). All the above elements form a viral particle which range in size between 80-120nm and represented Figure 1 (Barré-Sinoussi, 1996; Ganser-Pornillos, Yeager and Sundquist, 2008; Ganser-Pornillos, Yeager and Pornillos, 2012).

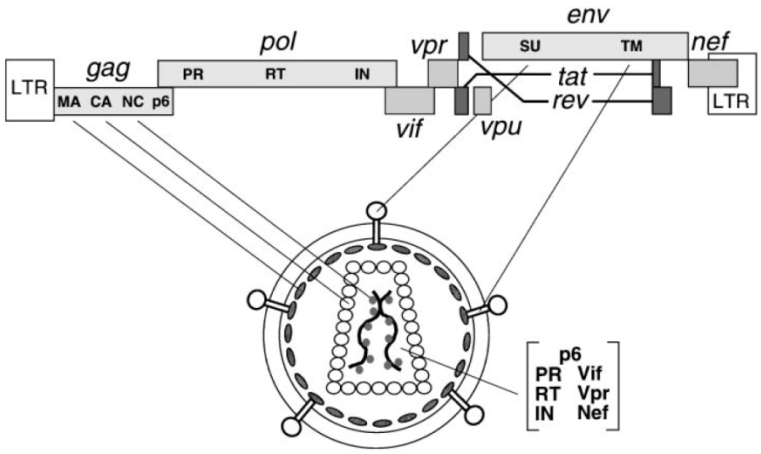

Figure 1 : Organisation of HIV-1 genome and virion

Adapted from (Frankel and Young, 1998)
HIV-1 genome encodes nine open reading frames. Three of these encode the Gag, Pol, and Env polyproteins. The four Gag proteins, MA (matrix), CA (capsid), NC (nucleocapsid), and p6, and the two Env proteins, SU (gp120) and TM (gp41), are structural components that make up the core of the virion and outer membrane envelope. The three Pol proteins, PR (protease), RT (reverse transcriptase), and IN (integrase), provide essential enzymatic functions and are also encapsulated within the particle. HIV-1 encodes six additional proteins: Vif, Vpr, and Nef found in the viral particle; Tat and Rev, essential in virus replication; and Vpu. The retroviral genome is encoded by an~9-kb RNA and two genomic-length RNA molecules are also packaged in the particle.

ii. Viral Genome

The two copies of single stranded RNA (ssRNA) are approximately 9.7 kb in length each. Retroviruses are distinguished by the capacity to retro-transcribe the viral RNA molecules into double strained DNA (dsDNA) using the viral reverse-transcriptase (RT) protein

incorporated into the virion. At the 5' and 3' ends of the genome, two identical non-coding regions are found and called the long terminal repeat (LTR) regions. The LTRs are involved with the control of viral gene expression and integration of the viral genome into the host chromosome and encompasses nine viral open rending frames (ORF). The 5' LTR contains transcription regulatory factors promoting viral genome expression.

The ORFs *gag*, *pol* and *env* encode for polyproteins common to all retroviruses. Gag and Pol precursors are cleaved by the viral protease p11 (PR) and Env by the cellular furin protein. Gag is proteolytically cleaved to produce MA, CA, NC and p6 viral proteins fundamental for virus assembly while the Pol precursor produces protease PR, RT and integrase (IN). The RT is involved in reverse-transcription of viral RNA into DNA and the IN regulates the integration of the linear viral DNA obtained after the retro-transcription. Finally, Env precursor gp160 is cleaved in gp120 and gp41 to form the Envelope protein. The ORFs *Tat* and *Rev* encode for proteins important in viral replication and pathogenicity including *vif*, *vpr*, *vpu* and *nef*. Tat and Rev play an essential role in the viral life-cycle, whilst Vif, Vpr, Vpu and Nef are involved in viral pathogenesis (Frankel and Young, 1998; Tang, Kuhen and Wong-Staal, 1999).

iii. Replicative cycle

The life-cycle of HIV-1 is divided into several stages (Appendix 1). The first step is the attachment of the virus at the surface of the target cell followed by the fusion of the viral and cell membrane allowing the entry of the capsid into the cells. The viral RNA genome is then reverse-transcribed into DNA in the cytoplasm and translocated to the nucleus for integration. The proviral DNA is then transcribed and subsequently translated to express the viral proteins required for production of immature virions containing two copies of viral genome. After budding of new virions, maturation occurs, allowing for the production of mature viral particles capable of infecting new cells.

a) Entry to target cells

The functional envelope protein of HIV is composed of a trimer of non-covalently linked gp120 to gp41 molecules. The gp120 sub-unit initiates entry of the virus by initially binding to the CD4 receptor present on the surface of various cells, such as lymphocytes, macrophages and dendritic cells (DCs). Viral gp120 has a high affinity with CD4 and once bound a conformational change occurs exposing the variable loop 3 (V3) of gp120 and

allowing the molecule to bind to its secondary co-receptors, which are typically CCR5 and CXCR4. The simultaneous binding of receptor and co-receptor with gp120 induces disruption of the interaction between the gp120 and gp41 trans-membrane fusion protein. The N-terminal of gp41 inserts into the host membrane and allows for fusion to occur *via* a typical spring-loaded mechanism allowing for the membranes to fuse and the capsid structure to enter the cell (Figure 2) (Wilen, Tilton and Doms, 2012).

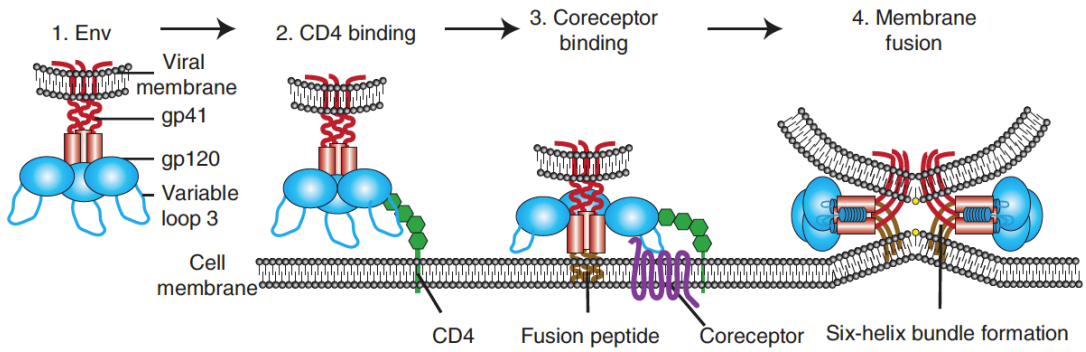

Figure 2 : HIV-1 entry

Adapted from (Wilen, Tilton and Doms, 2012)
1. HIV Env, composed of gp120 and gp41 subunits, attaches to the host cell by **2.** binding CD4 *via* gp120. This causes conformational changes in Env, allowing **3.** co-receptor binding mediated in part by the V3 loop of Env. This initiates **4.** the membrane fusion process as the fusion peptide of gp41 inserts into the target membrane, followed by six-helix bundle formation and complete membrane fusion.

The co-receptors utilised during virus entry define the tropism of HIV-1, where CCR5 (R5) viruses utilise the CCR5 chemokine receptor and CXCR4 (X4) viruses use the CXCR4 receptor for entry, whilst some viruses (R5X4) utilise both and are termed dual-tropic viruses.

b) Reverse Transcription

Once the core has entered the cell it is uncoated through removal of CA p24 protein to release the viral RNA genome with its associated enzymes into the cytoplasm. The capsid is brought to the nucleus by interactions with the micro-tubular system and disassembled in the process (Arhel *et al.*, 2006; Ambrose and Aiken, 2014; Campbell and Hope, 2015). During transportation, the reverse transcription complex (RTF) is formed and RNA reverse transcription is initiated with binding of the host transfer RNA ($tARN^{Lys3}$) on the primer binding site (PB) at the 5' end of the genome. RT allows for the generation of a minus stranded DNA molecule and degrades the complementary RNA by its RNase H activity. The DNA-tRNA hybrid subsequently produced is then transferred to the 3' end of the genome and used as a primer for the synthesis of the first DNA strand. The ssRNA molecule is

degraded by RT, except the PP site that serves for priming synthesis the second DNA strand. After degradation of the tRNA, hybridisation at the PB site occurs and for elongation of the second DNA strand by RT and allowing for the generation of dsDNA and its LTRs (U3-R-U5) (Appendix 2) (Hu and Hughes, 2012; Modrow *et al.*, 2013). The viral DNA associated with cellular and viral proteins (such as MA, CA, Vpr, or IN), form the pre-integration complex (PIC) which is then translocated to the nucleus through the nuclear pore complex (NPC) (Jayappa, Ao and Yao, 2012).

c) Integration and gene expression

Once in the nucleus, the integration of the viral dsDNA into the host genome is mediated by the integrase protein (IN). Integration process occurs preferentially in actively transcribed units to favour efficient viral gene expression. IN catalyses two distinct reactions: the 3'-processing where nucleotides are added at its 3' ends, and stand transfer where the viral DNA ends are inserted into host chromosomal DNA. The integration process is facilitated with the help of host factors such as LEDGF that promotes viral integration in transcriptionally active regions by binding IN (Craigie and Bushman, 2012; Kvaratskhelia *et al.*, 2014; Grawenhoff and Engelman, 2017). A fraction of non-integrated viral DNAs can remain in the nucleus in circular forms (1-LTR or 2-LTR) or linear forms (Ruggiero *et al.*, 2017).

Integrated HIV-1 DNA, termed provirus, is then transcribed using the cellular transcriptional machinery, following early and late phases. The 5'-LTR region possesses a number of regulatory sequences similar to human cellular genes that allow for fixation of host transcription factors promoting gene expression such as Sp, NF-κB, C/EBP, NFAT or AP-1.

Initially, the proviral DNA is transcribed by the cellular RNA polymerase II (RNApol-II) enzyme, allowing for the synthesis of mRNAs. The majority of the transcripts produced are short due to the low stability of the RNApol-II protein. However, full transcripts are produced that are subsequently multiply spliced and which migrate to the cytoplasm allowing for the expression of the regulatory proteins Tat, Rev and Nef. Once the proteins Tat and Rev are produced in sufficient quantity they promote the late transcription of the provirus genome. Tat is a trans-activator that interacts with the TAR region of new HIV-1 transcripts allowing for the recruitment of the positive transcription elongation factor (pTEFb) and thereby promoting elongation of the transcript. The protein Rev binds to the RRE structure of unspliced or partially spliced HIV-1 transcripts and enables for them to be exported from the

nucleus. The HIV-mRNA produced then is translated into the last viral proteins (Lawn *et al.*, 2001; Karn and Stoltzfus, 2012; Modrow *et al.*, 2013).

d) Viral particle assembly, budding and maturation

The HIV-mRNA unspliced or partially spliced forms encode polyproteins Env, Gag and Gag-Pol. The newly synthesised viral proteins are assembled to form new viral particles. The Env polyproteins are transported from the rough endoplasmic reticulum (RER) to lipid rafts within the cellular membrane *via* the typical secretory pathways. Gag and Gag-Pol precursors generate viral proteins involved in particle assembly. Gag precursors contain MA, CA, NC and p6 domains. Gag recruits the viral genomic RNA (by the NC domain) to migrate and multimerise (by the CA domain) at the plasma membrane under the same rafts. After incorporation of Env (by the MA domain), the endosomal sorting complex, required for transport (ESCRT-I), is recruited *via* the p6 domain catalysing membrane fission and completing the budding process. Additionally, the p6 protein of Gag additionally allows for recruitment of Vpr, Vif and Nef to associate with viral particles before budding. The particles released are immature until the protease p11 cleaves Gag and Gag-Pol into the appropriate structural proteins. Once maturation is complete the new viral particles are fully infectious and ready to start a new replicative cycle (Appendix 3) (Freed, 2015).

iv. <u>Pathogenesis and transmission</u>

a) Course of HIV Infection

Infection with HIV-1 is characterised by three clinical stages: primary/acute, asymptomatic and AIDS (Figure 3). The HIV-1 acute phase of infection lasts for between 3 to 6 weeks and is associated with an expansion of viral replication and reduction in the number of $CD4^+$ T lymphocytes. At the end of the primo-infection, the immune system recovers partially with an increase in $CD4^+$ T cells counts and a decrease in viral load. The following asymptomatic phase can typically last for 6 to 11 years in the absence of antiretroviral treatment (ART) and is characterised by the control of viral load by the immune system. However, residual replication leads to chronic inflammation and a progressive decline in $CD4^+$ T cell number. When $CD4^+$ T cells go below 200 cells/L, the immune system is unable to sufficiently control opportunistic infections and the patient is declared immunocompromised, termed AIDS and which subsequently leads to death (Modrow *et al.*, 2013; Maartens, Celum and Lewin, 2014).

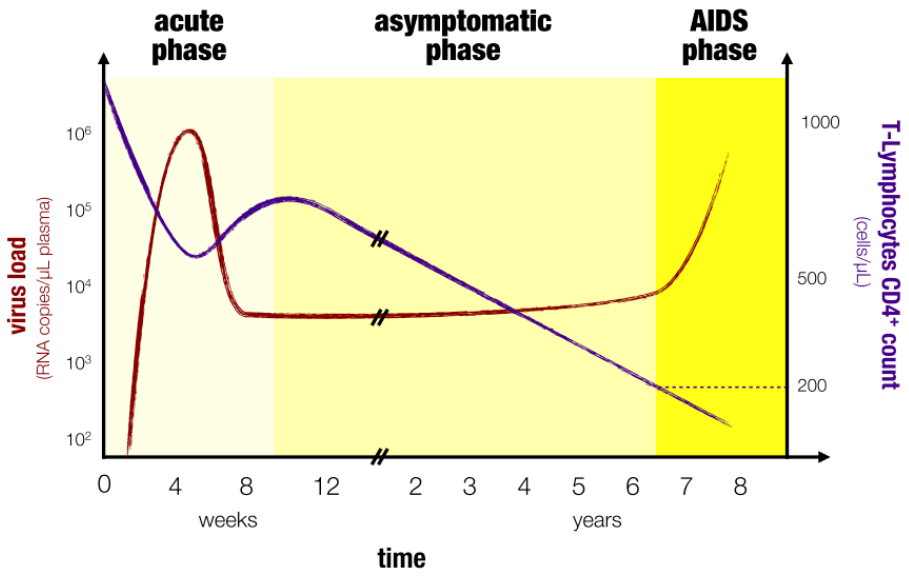

Figure 3 : Course of HIV-1 infection

Adapted from (Alizon and Magnus, 2012)
Relationship between plasma HIV-1 load increase and $CD4^+$ T-cell loss over the course of infection in untreated patients.

b) Primary Infection

Infection with HIV-1 occurs when virus particles reach the bloodstream *via* injury, blood transfusion, mother-to-child transmission during pregnancy, delivery or lactation, or *via* mucous membranes as encountered during sexual intercourse (conjunctiva, rectum and genital mucosa). The first target cells for HIV-1 are likely DCs and macrophages present at the site of infection and which also includes Langerhans cells (LCs) (Appendix 4). DCs and macrophages are permissive for HIV-1 R5 infection by expression of CD4 and the CCR5 receptors, where for LC entry of the virus is mediated by endocytosis. Consequently, DCs and macrophages play a crucial role in the initial phase of infection and represent viral reservoirs (Lawn, Butera and Folks, 2001; Wu, 2008; Modrow *et al.*, 2013; Maartens, Celum and Lewin, 2014). Individuals homozygous for a 32bp deletion in the CCR5 gene (CCR5-Δ32) have been described to have $CD4^+$ lymphocytes refractory for infection with CCR5 using viruses, rendering them naturally resistant to infection (Huang *et al.*, 1996; Paxton *et al.*, 1996; Wu *et al.*, 1997; Hütter *et al.*, 2009). HIV-1 CXCR4 tropic viruses are found later in infection and evolve from viruses using CCR5 and can be found in 50% of infected individuals later in their disease course (Schuitemaker *et al.*, 1992). However, positive selection of HIV-1 (R5) and restriction of HIV-1 (X4) viruses during transmission represents a key mechanism for virus propagation as CXCR4 using viruses are associated with rapid loss of $CD4^+$ T cells due to their strong cytopathogenic effect (Turville *et al.*, 2004).

Infected cells activate the immune response recruiting new target cells (DCs and macrophages) to important anatomical sites *via* production of chemokines and subsequent migration to lymph nodes. There, the virus proliferates by infection of monocytes, macrophages and T lymphocytes, inducing the generation of adaptive immune responses, both cellular and humoral. Because of the physical contact between antigen-presenting cells (APCs) or infected cells and T cells through virological synapses, the virus can be transmitted from cell to cell. This mechanism can occur between infected macrophages or $CD4^+$ T cells and uninfected lymphocytes, or between DCs and $CD4^+$ T cells (Lawn, Butera and Folks, 2001; Wu, 2008; Modrow *et al.*, 2013; Maartens, Celum and Lewin, 2014). In the case of DCs, the capture of infectious virions transmitted to uninfected T cells, occurs by attachment of the glycoprotein Env *via* mannose receptor or C-type lectin receptor. This mechanism is called *trans*-infection (Sallusto *et al.*, 1995; Gummuluru, KewalRamani and Emerman, 2002; McDonald *et al.*, 2003; Turville *et al.*, 2003; Garcia *et al.*, 2005; Wu, 2008).

During primary infection, HIV-1 replication occurs initially within lymph nodes (first week of infection) and is then disseminated in plasma (resulting in peak replication during the second week of infection). HIV-1 replication subsequently declines to a stable level (typically after 4 weeks of infection) and relates to the establishment of effective innate and adaptive immune response that can control viral replication (Lawn, Butera and Folks, 2001; Wu, 2008; Modrow *et al.*, 2013; Maartens, Celum and Lewin, 2014).

c) Anti-viral response and chronic infection

As mentioned above, the immune response against HIV-1 is initiated by infected cells *via* the recognition of pathogen-associated molecular patterns (PAMPs) from viral elements by pathogen-recognition receptors (PRRs) expressed by immune cells. PRRs are receptors that mediate immunity including Toll-like receptors (TLRs) (present on the cell surface or in endosomes) or cGAS and IFI16 (present in the cytosol). Endosomal TLR7 and TLR8 recognise HIV-1 ssRNA, while cGAS and IFI16 will recognise the viral dsDNA generated from the RT step in the replication cycle. The activation of those signalling pathways activate the expression of various transcription factors leading to production of type I IFNs, cytokines (IL-1β, IL-6 and TNF-α) and chemokines for recruitment of immune cells such as macrophages, DCs, NK, T and B cells to the site of infection (Mogensen *et al.*, 2010; Altfeld and Gale, 2015; Lahaye and Manel, 2015). IFN responses are crucial for anti-viral activity through promoting expression of anti-viral proteins such as tetherin, that blocks budding and release of viral particle (Neil,

Zang and Bieniasz, 2008; Perez-Caballero *et al.*, 2009) or APOBEC-3G and SAMHD1, that inhibit reverse transcription (Okeoma *et al.*, 2010; Goldstone *et al.*, 2011; Laguette *et al.*, 2011; Wang *et al.*, 2011; Harris and Dudley, 2015). Additionally, some chemokines produced are the natural ligands for the appropriate HIV-1 chemokine co-receptors, and consequently can block HIV-1 entry. It is the case for SDF-1, natural ligand of CXCR4 (Bleul *et al.*, 1996), as well as MIP-1α, MIP-1β and RANTES the natural ligands of CCR5 (Cocchi *et al.*, 1995).

The host antiviral immune responses mounted include the induction of cytotoxic T cells (CTL) responses characterised by the proliferation of $CD8^+$ T cells, whereas induced $CD4^+$ T-helper responses are weaker. The environment of pro-inflammatory cytokines produced by the immune response during infection can positively modulate HIV-1 replication (Kedzierska and Crowe, 2001). TNF-α is described to enhance HIV-1 replication in macrophages and T lymphocytes *via* NF-κB pathway (Folks *et al.*, 1989; Okamoto *et al.*, 1989; Foli *et al.*, 1997; Muñoz-Fernández *et al.*, 1997) as well as IL-1 (Granowitz *et al.*, 1995) and IL-6 (Foli *et al.*, 1997).

HIV-1 has developed several strategies to escape the effects of the immune response. The viral accessory proteins Nef, Vpu, Vpr and Vif are determinants in modulating viral pathogenesis and disease progression. The Nef protein has been described to decrease expression of CD4 and MHC-I on the cell surface, thereby modulating infection. Depletion in CD4 at the surface of the cell can prevent superinfection and enhance release of new viral particle, whereas MHC-I down-regulation can inhibit recognition of the infected cells by cytotoxic T cells (Pereira and DaSilva, 2016). Vpu is a viroporin protein that can induce a reduction in CD4 expression at the cell surface and enhance the released of virions by promoting reorganisation of raft structures and budding (González, 2015). Vpr contributes to HIV-1 pathogenesis through an array of mechanisms, notably promoting early T cell activation facilitating productive HIV-1 infection of non-activated T cells and secretion of TNF-α, IL-6 or IL-8 (González, 2017). Vif is required for HIV-1 replication and can induce degradation of APOBEC proteins, a cellular RNA editing enzyme restricting HIV-1 reverse transcription as mentioned above (Goila-Gaur and Strebel, 2008).

Mutations frequently occur in MHC class-I CTL epitopes found in many of the viral proteins described above and this therefore limits the efficacy of CTL responses in controlling HIV-1 infection (J. Kim *et al.*, 2018). The progression of HIV-1 disease is related to the balance between viral replication and the cellular immune response mediated through $CD8^+$ CTL and

the exhaustion of infected $CD4^+$ T cells, thereby reducing virus production and replication. During chronic asymptomatic HIV-1 infection, persistent viral replication and production, leads to the loss of $CD4^+$ T lymphocytes associated with constant systemic immune activation.

d) Extracellular vesicles and HIV-1 infection

Extracellular vesicles (EVs or exosomes), are small vesicles ranging in size between 150 to 1,000nm and are secreted from the plasma membrane (PM) by direct budding or by fusion of internal multivesicular compartments (MVB) with the PM (Figure 4).

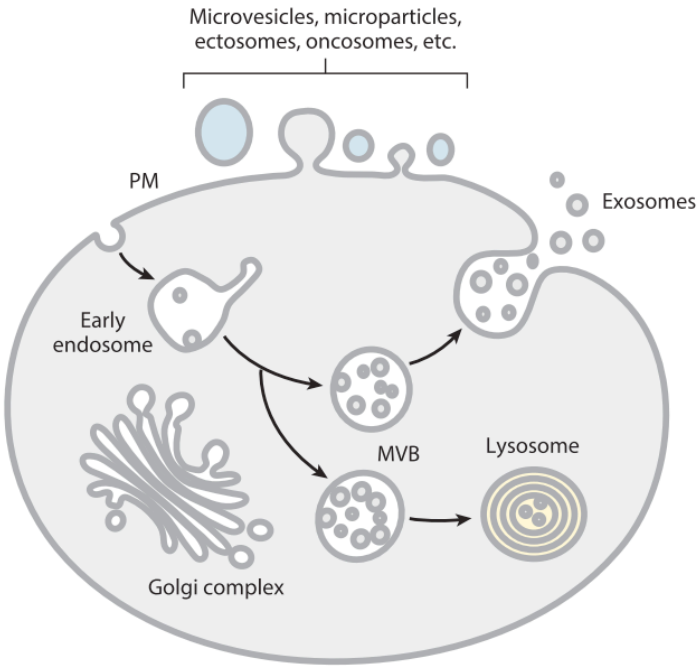

Figure 4 : EVs production from different intracellular origins

Adapted from (Colombo, Raposo and Théry, 2014)
Schematic representation of the different types of membrane vesicles released by eukaryotic cells, either by direct budding from the plasma membrane (PM) or by fusion of internal multivesicular compartments (MVB) with the PM.

EVs can be produced by different cell types into the extracellular environment and can be detected in various biological fluids such as blood, urine, saliva, amniotic fluid, ascites, bronchoalveolar lavage, synovial fluid, semen and breast milk (Gould and Raposo, 2013; Raposo and Stoorvogel, 2013; Colombo, Raposo and Théry, 2014; Iraci *et al.*, 2016).

HIV-1 and EVs are generated by similar pathways (Fang *et al.*, 2007; Usami *et al.*, 2009) leading to incorporation of HIV-1 products into EVs such as Nef, Env, Gag, HIV-1 nucleic acids and microRNA, facilitating virus replication and pathogenicity (Kadiu *et al.*, 2012; Arenaccio,

Chiozzini, Columba-Cabezas, Manfredi, Affabris, *et al.*, 2014; Madison and Okeoma, 2015; Hildreth, 2017).

As mentioned previously, the viral protein Nef can promote HIV-1 infection. When the protein is incorporated into EVs, it has been described to be able to activate HIV-1 replication and modulate inflammation (Arenaccio, Chiozzini, Columba-Cabezas, Manfredi and Federico, 2014b; Lee *et al.*, 2016). Additionally, EVs produced from infected cells can induce activation of latent HIV-1 genomes in $CD4^+$ T cells and macrophages *via* TNF-α through ADAM17 incorporated in EVs (Arenaccio *et al.*, 2015). Recently, Tang *et al.* demonstrated the ability of exosomal Tat to activate latent HIV-1 in CD4+ T lymphocytes (Tang *et al.*, 2018). Furthermore, EVs can modulate the inflammatory environment during infection through generating favourable conditions for viral replication. Sampey *et al.* revealed in 2015, a role of exosomal TAR RNA in modulating inflammation where EVs from HIV-1 infected cells induced secretion of IL-6 and TNF-β in macrophages, suggesting activation of the TLR pathway by EVs (Sampey *et al.*, 2015). EVs can also modulate HIV-1 entry *via* cell to cell contact by influencing the expression or availability of membrane receptors. This is the case for the CCR5 and CXCR4 co-receptors that can be transferred *via* EVs making cells more susceptible to HIV-1 infection (Mack *et al.*, 2000; Rozmyslowicz *et al.*, 2003). Additionally, the surface molecules CD45, CD86 and MHC-II can be released *via* EVs from HIV-1 infected cells influencing the evasion of the immune system (Esser *et al.*, 2001).

Some EVs can have a protective and negative impact on HIV-1 infection. As viral proteins, cellular components with anti-viral activity can be incorporated in EVs. APOBEC-3G has been described to be transferred from cell to cell *via* EVs thereby protecting cells against HIV-1 infection (Khatua *et al.*, 2009; Okeoma *et al.*, 2010). Additionally, cytokines can be transferred in EVs including IL-4, IL-13 and TNF-α which can block HIV-1 infection by reducing expression of co-receptors needed for viral entry (Lane *et al.*, 1999; Bailer, Lee and Montaner, 2000; Creery *et al.*, 2006; Li *et al.*, 2013). It has been described that EVs secreted by T lymphocytes can incorporate the CD molecule into the vesicles and thereby block HIV-1 infection (de Carvalho *et al.*, 2014), as well as EVs form $CD8^+$ T cells that can inhibit HIV-1 transcription in infected cells (Tumne *et al.*, 2009). Also, Näslund *et al.* showed in 2014 that EVs isolated from breast milk can inhibit DC mediated HIV-1 *trans*-infection by binding to DC-SIGN (Näslund *et al.*, 2014). However, because of the cytolytic replication of HIV-1, the implication of the anti-viral activity from EVs might be hidden.

v. *Treatment*

ART consists of a combination of antiretroviral drugs to inhibit viral replication and prevent disease progression. Antiviral drugs (ARD) are classified according to the specific phase of the viral life-cycle they target (Appendix 1).

a) *Entry inhibitors*

Maraviroc is a CCR5 antagonist that binds to the CCR5 receptor inhibiting interaction with HIV-1 gp120 (Dorr *et al.*, 2005). Resistance to this molecule can occur due to the hyper-variability within the V3 loop (Yuan *et al.*, 2011). Enfuvirtide (T20) is fusion peptide (fusion inhibitors FI) blocking gp41 folding and HIV-1 entry. However, rapid accumulation of mutations in gp41 can thwart its action (Carmona *et al.*, 2005).

b) *Reverse transcriptase inhibitors*

The reverse transcription step in the viral life-cycle (ssRNA to dsDNA synthesis) has been heavily targeted in the development of ARDs. There are two main categories of drugs targeting reverse transcription: nucleoside and non-nucleoside reverse transcription inhibitors (NRTIs and NNRTIs respectively). NRTIs are analogues of the cellular nucleotides lacking a 3'OH group on the deoxyribose. The incorporation of NRTI instead the natural substrate, leads to premature stops in the formation of DNA chain during reverse transcription. NNRTIs are non-competitive inhibitors to reverse transcription. They bind to RT inducing conformational changes leading to the loss of the enzymes affinity for nucleotides (De Clercq, 2013).

c) *Integration inhibitors*

To inhibit integration of viral dsDNA, ARTs target the integrase IN protein. The integrase strand transfer inhibitors (INSTIs) bind to the active site of the integrase, blocking binding to the enzyme on its catalytic site essential for promoting integration (Métifiot, Marchand and Pommier, 2013).

d) *Assembly inhibitors*

These drugs interfere with the generation of functional proteins and the virus assembly process by inhibiting p11 protease activity. PIs are competitive inhibitors that prevent

cleavage of Gag and Gag-Pol precursor by interacting with the active site of p11. These inhibitors are commonly used in multi-therapy approaches even if its bioavailability is not optimum (De Clercq, 2013).

e) Limitations of ART

The introduction of ART has increased the duration of the asymptomatic period and the life expectancy of infected people. Commonly, ART consists of a combination of two NRTIs with either INSTI, PI or NNRTI. However, ART only controls disease and does not cure it. Indeed, upon treatment interruption a virus rebound is observed which associates with a drop in $CD4^+$ T lymphocyte numbers due to reactivation of virus from latently infected reservoirs. Subsequent activation of latent viruses from $CD4^+$ T lymphocytes and monocytes/macrophages lineages in the absence of treatment represents a major obstacle for virus eradication and total recovery for patients (Le Douce *et al.*, 2012).

vi. HIV-1 and co-infections

The immunodeficiency caused by HIV-1 infection increases the risk of co-infection leading to higher risk of morbidity and mortality for infected individuals. Additionally, despite administration of ART in co-infection situations, the restoration of the immune response to normal level is not always achieved. Historically, HIV-1 was identified because of the increase in *Pneumocystis carinii* pneumonia and Kaposi's sarcomas opportunistic diseases. Today, many other pathogens have been associated with significant detrimental effects for co-infected individuals, through loss of immunity, and these include infection with *Cryptococcus*, Hepatitis B virus (HBV), Hepatitis C virus (HCV), *Plasmodium* and *Mycobacterium tuberculosis* (*Mtb*) (Chang *et al.*, 2013). In this Thesis, we focused on studying the *in vitro* effects of *Mtb* on HIV-1 infection.

II. *Mycobacterium tuberculosis* Infection

The *Mtb* bacillus responsible for tuberculosis (TB) disease appeared 70,000 years ago. During the industrial revolution, TB became epidemic but its incidence decreased though the 20th century in developed countries. The introduction of the Bacillus Calmette-Guérin (BCG)

vaccine in 1921 along with associated antimicrobial drugs reduced considerably the incidence of disease. However, the incidence of TB has increased since the 1980's due to a number of factors, including deterioration of health conditions, the generation of antibiotic resistant strains and the emergence of the HIV-1 pandemic (Bates and Stead, 1993; Daniel, 2006; Bañuls *et al.*, 2015).

i. Mtb *composition*

Mtb is a bacillus measuring 2-4 µm characterised by a slow generation time of 12-24h under optimal conditions. The *Mtb* H37Rv genome, a standard pathogenic strain of TB, consists of $4.4x10^6$ bp containing approximately 4,000 genes classified according to function (Smith, 2003). The bacteria cell wall confers to *Mtb* a strong impermeable barrier to toxic compounds and drugs and plays a major role in *Mtb* pathogenesis. The mycobacterial cell envelope is divided into three sections: the plasma membrane, the cell wall core and the capsule (Figure 5).

The mycobacterial cell envelope is complex and composed of a plasma membrane surrounded by a cell wall skeleton constituting 60% of its dry mass composed of diverse lipids presented within an outer capsule. The cell wall core consists of peptidoglycans (PG) in covalent attachment with arabinogalactan (AG) linked to mycolic acids (MA) by esterification. Free lipids associated with MA together form the mycobacterial outer membrane. It is composed of various and complex lipids such as glycolipids, trehalose dimycolate (TDM), phthiocerol dimycocerosate (PDIM/DIM), sulfolipids (SLs), phosphatidylinositol mannosides (PIM), lipomannan (LM) and lipoarabinomannan (LAM) (Hoffmann *et al.*, 2008; Zuber *et al.*, 2008; Angala *et al.*, 2014; Bansal-Mutalik and Nikaido, 2014; Grzegorzewicz *et al.*, 2016; Singh *et al.*, 2018).

Importantly, the nature and the quantity of mycobacterial cell wall components can vary between *Mtb* isolates and can significantly impact on bacterial host interactions (Cywes *et al.*, 1997; Ehlers and Daffé, 1998; Torrelles and Schlesinger, 2010).

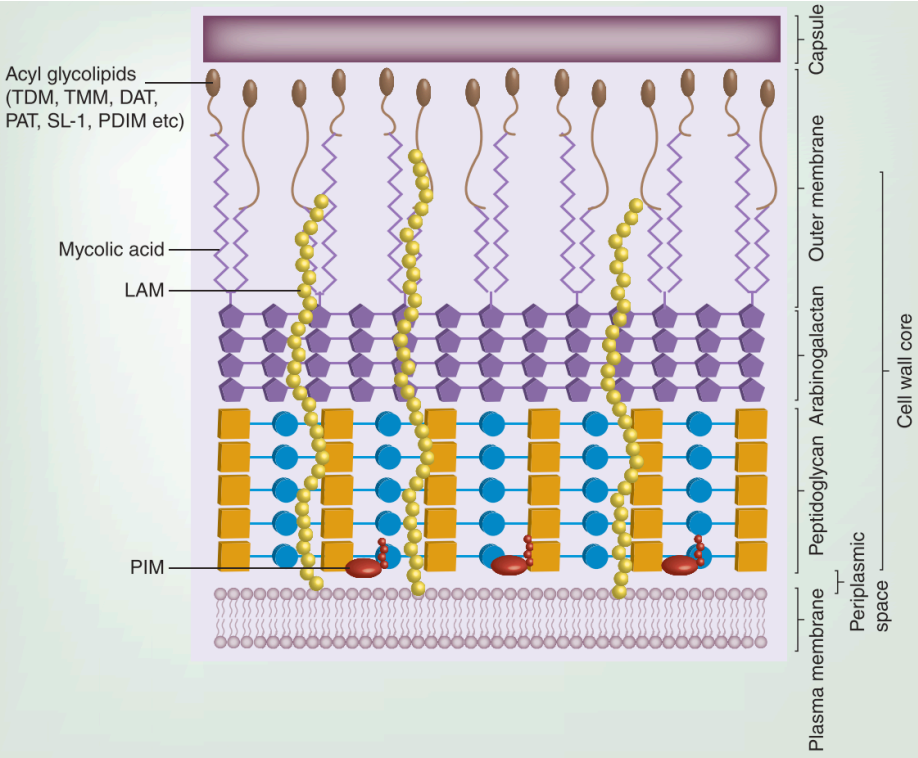

Figure 5 : Structure of the* Mtb *cell envelope

Adapted from (Singh *et al.*, 2018)
The *mycobacterial* cell envelope is mainly composed of three different covalently linked layers composed of plasma membrane, periplasmic space, cell wall core, outer membrane and capsule. PG (Peptidoglycan), AG (Arabinogalactan) and mycolic acids form the cell wall core. The outer membrane of the cell envelope contains various free acyl lipids DAT (Diacyltrehalose), TAT (Triacyltrehalose), PAT (Polyacyltrehalose), TDM (Trehalose 6,6'-dimycolate), SL-1 (Sulfolipid-1), PDIM (Phthiocerol dimycocerosate), PGL (Phenolic glycolipid), etc. that are intercalated with the mycolic acids. The outer layer called the capsule, mainly contains polysaccharides and surface proteins. LAM (Lipoarabinomannan) is shown both in the outer membrane and plasma membrane. PIM (Phosphatidylinositol mannoside) is shown to be associated with plasma membrane and PG.

ii. Pathogenesis

Mtb infection starts when bacteria dispersed in the air, from an individual with active pulmonary TB, reaches the alveoli of the host. The bacteria are rapidly phagocytised by macrophages, typically resulting in the bacillus being destroyed. However, *Mtb* can survive and start to replicate in infected cells and to spread to other organs through the lymph system and the peripheral blood. After initiation of the adaptive immune response, migration of immune cells (including neutrophil and lymphocytes) to site of primary infection occurs and can form a cellular infiltrate, termed granuloma, in order to contain the spread of the bacteria. Granulomas are considered lesions which benefit both the host and *Mtb* (Smith, 2003; Philips and Ernst, 2012; Delogu, Sali and Fadda, 2013).

The initial stage of TB infections starts 3 to 8 weeks after *Mtb* ingestion when the pathogen is disseminated within the lymphatic circulation to lymph nodes in the lung forming Ghon complexes (granuloma). The second stage of disease is characterised by bacterial spread to other organs, including other regions of the lungs through blood circulation and can typically last for three months. Once the bacteria reach the pleural space, severe chest pain appears and can last for up to two years. The resolution of Ghon complexes can take up to three years if the disease doesn't progress (Smith, 2003).

a) Mtb *entry*

Mtb is rapidly phagocytised by alveolar macrophages (resident cells) as well as neutrophils, monocytes derived macrophages (MDM) and DCs. The bacteria is recognised by immune cells *via* interactions with different cellular receptors: Mannose receptor (Kang *et al.*, 2005), C-type lectin (DC-SIGN, Dectin-1), scavenger receptors (Class A and B), complement receptors (CR1, CR3), inducing opsonisation or phagocytose of *Mtb* (Smith, 2003; Philips and Ernst, 2012). Mannose-capped LAM (ManLAM), from the mycobacteria envelope, is recognised by mannose receptors (expressed my macrophages) (Schlesinger, Hull and Kaufman, 1994; Ehlers and Daffé, 1998) and DC-SIGN (major receptor involved in *Mtb* recognition by DCs) (Geijtenbeek *et al.*, 2003; Tailleux *et al.*, 2003). PIM_6 can also interact with DC-SIGN (Driessen *et al.*, 2009) while TDM interacts with macrophage inducible C-type lectin (Mincle) (Ishikawa *et al.*, 2009). The origin of the receptors involved in bacteria uptake determines the intracellular outcome of the bacteria (Smith, 2003; Philips and Ernst, 2012; Stanley and Cox, 2013).

b) Intracellular trafficking

Most of the time the maturation of the phagosome with phagosome-lysosome fusion occurs leading to the bacteria being destroyed as the bacillus is subject to a hostile environment, characterised by acid pH, reactive oxygen intermediates and lysosomal enzymes (Figure 6, **route e**). However, in some case, the bacteria interfere with the phagosome maturation process and replicates. Various studies support the theory that *Mtb* inhibits phagosome maturation by interacting with host molecules which reside in a compartment similar to an early endosome (Figure 6, routes **a** and **f**) (Philips, 2008). The mycobacterial phagosome can interfere with Rab5 activity blocking Rab7 bound on phagosome membranes and the production of phosphatidylinositol 3-phosphate (PI3P) (Philips and Ernst, 2012; Stanley and Cox, 2013). Mycobacterial lipids TDM and ManLAM have been described to play a role in the

perturbation of phagosome maturation (Fratti *et al.*, 2003; Indrigo, Hunter and Actor, 2003). However, studies support that *Mtb* can replicate in the cytoplasm by phagosomal escape (Leake, Myrvik and Wright, 1984; McDonough, Kress and Bloom, 1993) *via* membrane damage caused by the Esx-1 secretion system (Figure 6 routes **b** and **c**) (van der Wel *et al.*, 2007; Houben *et al.*, 2012). Depending on the bacteria route, *Mtb* grows either inside the un-maturated phagosome or in the cytosol.

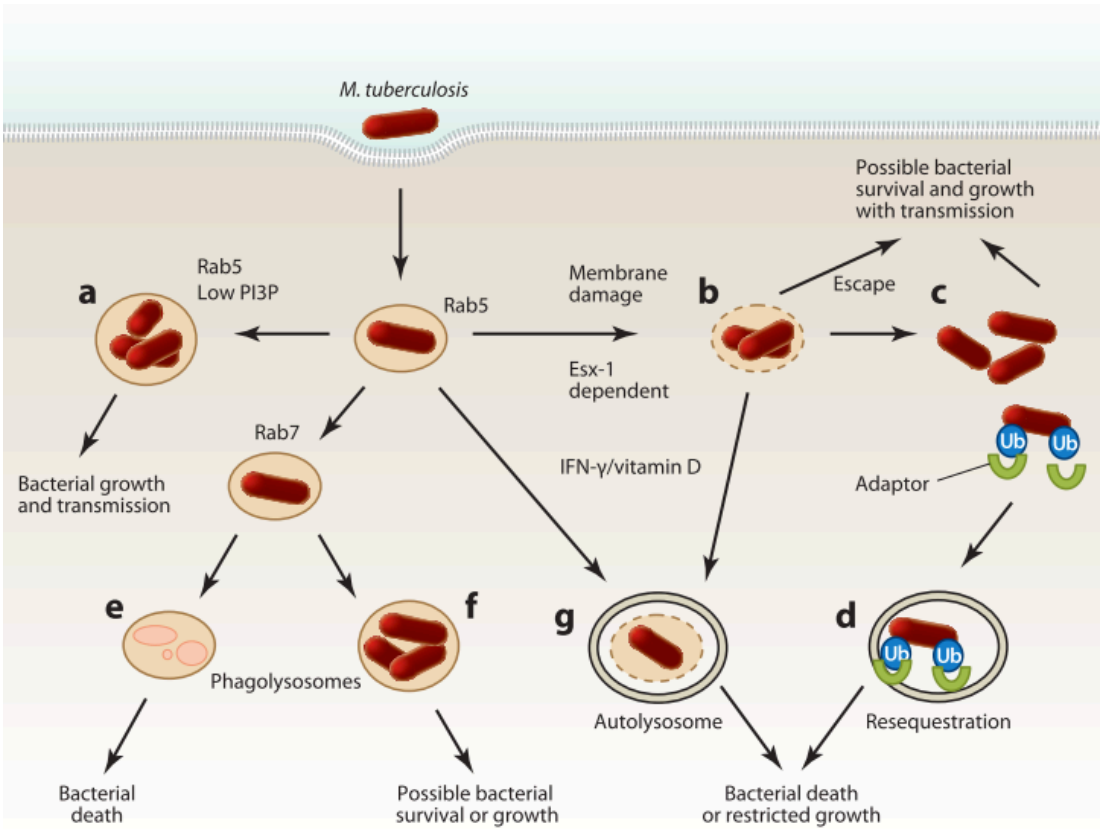

Figure 6 :* Mycobacterium *routes after phagocytose

Adapted from (Philips and Ernst, 2012)
a. *Mtb* can prevent phagosome maturation and grow in an early endosome–like compartment by inhibiting phosphatidylinositol 3-phosphate (PI3P) generation on the phagosome and impairing the recruitment of active, GTP-bound Rab7 while retaining Rab5. **b.** The Esx-1 system permeabilises the phagosomal membrane, allowing direct cytosolic access. **c.** In some cases, this process may result in the escape of the bacteria into the cytosol. The extent of cytosolic growth may depend upon cell type. **d.** the cytosolic bacteria are recognised by the host ubiquitin system and are sequestered in a membrane-bound compartment. **e.** Some ingested bacteria fail to prevent phagosome maturation, and they are delivered to the lysosome, where their replication is curtailed. **f.** In certain contexts, they may be able to grow in lysosomes. **g.** IFN-γ and vitamin D can overcome the early endosome–like arrest of *Mtb*, thereby promoting delivery of bacteria to autolysosomes, where growth is curtailed.

Infected macrophages can engage autophagy characterised by formation of autolysosomes containing the bacteria leading to the destruction of the bacteria (Figure 6 route **g**) or antigen presentation. Cytosolic bacteria can join this pathway by ubiquitination and sequestration *via* adaptor proteins (Figure 6 route **d**). *Mtb* is then released from infected macrophages by inducing cell apoptosis or necrosis (Philips and Ernst, 2012).

c) Granuloma

Activation of the immune response by *Mtb* results in macrophage recruitment to the site of infection, inducing aggregation and forming a granuloma. The *Mtb* released from early infected macrophages are rapidly ingested by surrounding macrophages contributing to early bacterial growth (Davis and Ramakrishnan, 2009). Various *Mtb* components have been described to be implicated in the initiation of granuloma formation such as LM, PIMs, TDM and LAMs (Puissegur *et al.*, 2007).

d) Immune Responses induced by Mtb *components*

Mtb components (PAMPs) are recognised by different elements of the innate immune response that is essential for defence against progressive *Mtb* infection. The bacteria expresses multiple TLRs agonists with predominant TLR2 ligands such as LM (Quesniaux *et al.*, 2004) and PIMs (Banaiee *et al.*, 2006) and *Mtb* DNA that can be recognised by TLR9 (Bafica *et al.*, 2005). Depending of the *Mtb* lineage, the bacteria will preferentially activate TLR2 or TLR4 pathways, resulting in the differential modulation of cytokine production. Compared to the H37Rv and HN878 strains, *Mtb* from the Beijing lineage activated macrophage *via* TLR4 (Carmona *et al.*, 2013). Activation of macrophages mediated by TLR2 enhanced vitamin D receptor and hyrdolaxylase, promoting antimicrobial responses (Liu *et al.*, 2006) and activation of TNF-α production (Underhill *et al.*, 1999). Additionally, TLRs mediate the interaction of *Mtb* induced activation/maturation of DCs and production of numerous cytokines including TNF-α, IL-6, IL-10, and IL- 12 *in vitro* (Hickman, Chan and Salgame, 2002; Jang *et al.*, 2004).

In parallel, mycobacterial PG can interact with the receptor NOD2 in the macrophage cytosol, inducing production of pro-inflammatory cytokines (Ferwerda *et al.*, 2005; Divangahi *et al.*, 2008). The C-type lectin receptor Dectin-1 is a PRR expressed by macrophages, DCs, neutrophils and T cells recognising α-glucan from *Mtb* (Dinadayala *et al.*, 2004). Dectin-1 mediated recognition induces Th1 and Th17 responses characterised by production of IL-17

(van de Veerdonk *et al.*, 2010), DC responses *via* IL-12p40 production (Rothfuchs *et al.*, 2007) and macrophage responses with TNF-α, RANTES, IL-6 and G-CSF production (Yadav and Schorey, 2006). Additionally, DC-SIGN can promote maturation of phagosomes and production of IL-10 leading to the induction of an anti-inflammatory response (Gringhuis *et al.*, 2007; Tanne *et al.*, 2009).

The interactions of *Mtb* PAMPs with host PRRs induce cell activation and secretion of cytokines crucial for immune cell recruitment and clearance of the bacteria. TNF-α plays a crucial role in TB protection (Flynn *et al.*, 1995) by containing latent TB (Mohan *et al.*, 2001) and inhibiting bacterial growth and macrophage death (Clay, Volkman and Ramakrishnan, 2008). IFN-γ induced by IL-12 and IL-18 production, promotes $CD4^+$ T cell recruitment and CTL mediated bacteria killing. Additionally, the cytokines IL-1, IL-6 and IL-23 are important for promoting the pro-inflammatory response (Hossain and Norazmi, 2013). However, *Mtb* infection can induce upregulation of IL-4 and IL-10 cytokines, increasing disease progression and down-regulating macrophage and DC activity. The role of type I IFNs remains unclear as it could induce anti-inflammatory responses. The balance between pro- and anti-inflammatory responses will in all likelihood determine TB progression (Philips and Ernst, 2012; Hossain and Norazmi, 2013).

e) Extracellular-vesicles and Mtb *infection*

EVs from *Mtb* infection originate from the cytoplasmic membrane origin, proteomic analyses revealed that EVs are principally composed of proteins involved in host-pathogen interaction (Lee *et al.*, 2015). *Mtb* EVs can participate in immune stimulations, indeed, EVs produced from infected macrophages can promote immune responses by activation of uninfected macrophages *via* induction of pro-inflammatory cytokines (Bhatnagar *et al.*, 2007) or T cell activation (Giri and Schorey, 2008). Also, EVs derived from infected APCs can present processed antigen to T cells (Ramachandra *et al.*, 2010) or DCs (Jurkoshek *et al.*, 2016). However, several studies support that *Mtb* have utilised EV trafficking to export lipoglycan and lipoproteins that impair host immune response (Athman *et al.*, 2015, 2017). Additionally, EVs can impair bacterial survival, Alvarez-Jimenez *et al.* described recently that EVs released from infected neutrophils promote macrophage autophagy (Alvarez-Jiménez *et al.*, 2018).

iii. Treatment

The current treatment for *Mtb* infections include a cocktail of rifampicin (RIF), isoniazid (INH), pyrazinamide (PZA), and ethambutol (EMB), resulting in clearance of the bacteria after 6-9 months. The high prevalence of *Mtb* disease is explained by the lack of availability of medications and the growing problem of MDR-TB. Treatment for MDR-TB towards two years is associated with toxic effects of the drugs. Furthermore, the development of treatment against MDR-TB induced development of extensively drug-resistant tuberculosis (XDR-TB). The development of novel chemotherapeutic options is crucial to treat MDR-TB (Hoagland *et al.*, 2016).

III. *Mycobacterium tuberculosis* and HIV-1 co-infection

HIV-TB co-infection results in a rapid loss of numerous immunological functions and ultimately leads to death when not treated. WHO estimated in 2015 that 13 million people were infected by both pathogens. *Mtb* and HIV-1 can induce profound changes in the host immune system resulting in an increase of *Mtb* infections to active disease or the exacerbation of HIV infection.

i. TB reactivation by HIV

TB/HIV-1 co-infected patients are 21-34 times more likely to develop active TB disease than those only infected with *Mtb*. Furthermore, people living with HIV-1 are facing emerging threats with increase in prevalence of drug-resistant TB and where multi-drug resistant (MDR-TB) and extensively drug resistant TB (XDR-TB) strains over the last years (WHO). HIV-1 infection increases the risk of acquiring primary *Mtb* infection by 2.2 to 5.5 fold (Chang *et al.*, 2013) and facilitate *via* different mechanisms *Mtb* growth/dissemination (Pathak, Wentzel-Larsen and Åsjö, 2010) and activation of latent TB (Diedrich and Flynn, 2011). HIV-1 infection induces a global dysfunction of the immune responses. A strong depletion of $CD4^+$ T cells is observed in the context of co-infection (Law *et al.*, 1996; Kalsdorf *et al.*, 2009; Geldmacher *et al.*, 2010) decreasing the ability to contain *Mtb* infection. This phenomenon is illustrated by disruption in IFN-γ, TNF and IL-2 production (Kalsdorf *et al.*, 2009). HIV-1 infection enhances the expression of receptors involved in *Mtb* entry such as CD14 (Rosas-Taraco *et al.*, 2006) or impairment with DCs antigen presentation (Singh *et al.*, 2016).

Additionally, bacterial survival is improved with inhibition of macrophage phagocytosis and apoptotic responses with notable interactions of the viral protein Nef with adaptor proteins required for phagocytose (Mazzolini *et al.*, 2010), and with the autophagy regulator beclin 1 (Patel *et al.*, 2007, 2009; Kyei *et al.*, 2009). Because of the depletion of $CD4^+$ cells, the granuloma formation can be disturbed leading to a systemic disease in co-infected patients, where extrapulmonary TB has been described only in patients with HIV-1 infection (Naing *et al.*, 2013).

ii. Exacerbation of HIV infection by Mtb *infection*

a) HIV replication at sites of Mtb *infection*

Various studies described the influence of *Mtb* infection on HIV-1 replication. In co-infected patients, enhancement of HIV replication were found on sites of *Mtb* infection in the lung (Nakata *et al.*, 1997) and pleural space (Lawn *et al.*, 2001). Additionally, in HIV-1-infected patients with pulmonary TB, HIV-1 viral load is higher compared to non-TB symptomatic HIV-1-infected patients (Toossi *et al.*, 2001). *In vitro*, *Mtb* have been described to activate virus replication in monocyte lineages or primary macrophages (Shattock, Friedland and Griffin, 1993; Goletti *et al.*, 1996; Toossi *et al.*, 2001) by activation of LTR transcription (Zhang, Nakata, *et al.*, 1995).

b) Immune responses induced by Mtb *components*

A large range of molecular components from *Mtb* (or PAMPs) are engaged in PRRs recognition by macrophages. Several studies described the involvement of *Mtb* PAMPs in activation of PRRs signalling pathways leading to modification/translocation of transcription factors resulting in enhancement of HIV-1 LTR activity (summarised Appendix 5). Indeed, the engagement by *Mtb* components of the TLR4, TLR2 and TLR9, induce a signal transduction MyD88-dependent and MyD88-independent cascade activating the MAPK and NF-κB (Falvo *et al.*, 2011; Philips and Ernst, 2012; Hussein *et al.*, 2014; Kawasaki and Kawai, 2014), resulting in activation of HIV-1 replication (Bafica *et al.*, 2003; Equils *et al.*, 2003; Hernández *et al.*, 2012; Rodriguez *et al.*, 2013). Additionally, the engagement of the C-type lectins family with *Mtb* ligands receptors, such as DC-SIGN, can induce NF-κB pathways (Tailleux *et al.*, 2003; Geijtenbeek *et al.*, 2003; Koppel *et al.*, 2004; Neyrolles, Gicquel and Quintana-Murci, 2006; Driessen *et al.*, 2009; Gringhuis *et al.*, 2009; Ehlers, 2010; Falvo *et al.*, 2011; Lugo-Villarino *et al.*, 2011; Philips and Ernst, 2012; Hussein *et al.*, 2014). The observations of up-regulation of

HIV-LTR activity is correlated by reactivation of latent HIV-1 in T cells *via* TLR2 engagement in *Mtb* infection (Larson *et al.*, 2017).

c) Establishment of a favourable environment for HIV-1 infection

As we described previously, the pro-inflammatory cytokine production induced by the immune response, can heighten HIV-1 replication by activation of the NF-κB pathway. In the context of *Mtb* co-infection, the immune response engaged against the bacillus, can increase HIV-1 replication, such as TNF and IL-6 (Ranjbar *et al.*, 2009). In parallel, down-regulation of anti-inflammatory responses, such as IL-10 and TGF-β induced by co-infection lead to an exaggerated pro-inflammatory response, providing a benefit to the virus (Goletti *et al.*, 1998; Chetty *et al.*, 2014; Tomlinson *et al.*, 2014). Additionally, HIV-1 entry is facilitated by an augmentation of co-receptor expression from cytokine production induced by *Mtb* infection (Hoshino *et al.*, 2004; Rosas-Taraco *et al.*, 2006; Kalsdorf *et al.*, 2013; Wahid Ansari, Kamarulzaman and Schmidt, 2013) and associated with down-regulation of RANTES (natural ligand of CCR5 receptor, inhibiting HIV-1 entry) (Rosas-Taraco *et al.*, 2006). *Mtb* can enhance HIV cell-to-cell transmission. For instance, the bacillus can increase the efficacy of virus transmission from infected MDM to T cells (Mancino *et al.*, 1997). Additionally, because of the recruitment and association in granuloma of with immune cells (caused by *Mtb*), the propagation of virus can be facilitated (Bell and Noursadeghi, 2018). HIV-1 *trans*-infection mediated by DCs is enhanced in the presence of *Mtb*, the bacillus infection inducing perturbation in virus antigen presentation by the cell (Reuter *et al.*, 2010).

Overall, *Mtb* creates a favourable environment for HIV-1 replication, as *Mtb* infection leads to the activation and induction of immune responses, including activation of macrophages/DCs, recruitment of lymphocytes, co-receptor expression and production of pro-inflammatory cytokines (Figure 7).

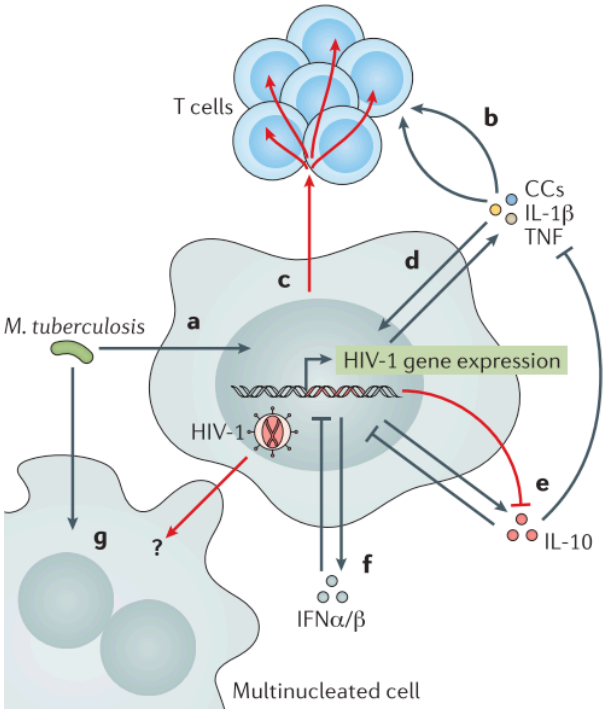

Figure 7 :* Mtb *increasing HIV-1 replication and propagation

Adapted from (Bell and Noursadeghi, 2018)
Innate immune signalling pathways in macrophages can increase HIV-1 transcription through activation of the transcription factors. **a.** The host cell response to innate immune activation by *Mtb* leads to the production of a range of pro-inflammatory cytokines and chemokines inducing **b.** local recruitment of T cells. **c.** The accumulation of activated T cells provides a population of cells permissive to HIV-1 and allows for rapid virus propagation by direct cell–cell spread. **d.** The pro-inflammatory cytokines also promote transactivation of virus replication through the action of the transcription factors. **e.** HIV-1 attenuation of IL-10 responses to *Mtb* favours the virus by reducing IL-10-mediated inhibition of HIV-1 transcription by promoting pro-inflammatory responses. **f.** *Mtb* induces type 1 interferon responses in macrophages, which would be expected to promote an antiviral state, any autocrine or paracrine inhibition of HIV-1 replication is transient. **g.** *Mtb* can cause macrophage polyploidy through activation of the cell cycle coupled to cytokinesis failure.

iii. Impact on treatments

ART treatment improves the immune response, reducing primary TB and latent TB reactivation (Suthar *et al.*, 2012). However, under anti-TB treatment and ART, immune reconstitution inflammatory syndrome (IRIS) can develop in some co-infected patients (Lawn, Bekker and Miller, 2005; Müller *et al.*, 2010) which is associated with extrapulmonary TB in most cases (Meintjes *et al.*, 2008). The risk of TB in patients is associated with early HIV-1 infection before the initiation of ART. BCG vaccination administrated in infants with a high prevalence of tuberculosis is not recommended by the WHO in HIV-infected patients due to its opportunistic potential. The development of new TB vaccines would be of benefit in cases of HIV-1 co-infected infants. Finally, a better understanding of the immunological disorders

observed in HIV-1/TB co-infected individuals would lead to the development of appropriate immunomodulatory therapy.

IV. Aims of the project

In 2015, the WHO has estimated 390,000 deaths related to TB in HIV-infected individuals. Because of the complexity of the immune response there are multiple ways that *Mtb* can modulate HIV-1 infection and *vice versa*. The better of understanding of interactions between the host with HIV-1 and *Mtb* simultaneously is crucial when considering developing improved treatments. This thesis project follows this perspective by aiming to characterise the impact *Mtb* glycolipids have on modulating HIV-1 infection and to identify *Mtb* strains that differentially modulate HIV-1 infection and immune cell innate signalling.

For this purpose, a technique allowing us to best mimic lipid distribution and antigen presentation on the mycobacterial cell wall was developed. Total lipid extracts from various mycobacterial strains BCG, *M. smegmatis* and *Mtb* from diverse origins (H37Rv, HN878, CDC1551 and EU127) were associated in liposomes. The composition and physical properties of generated liposomes were characterised by Thin-layer chromatography (TLC) and NanoSight technology to be used in *in vitro* assays. To understand the impact of *Mtb* glycolipids on the immune responses that can potentially influence HIV-1 infection (indirectly), the effect of *Mtb* liposomes on macrophages, DCs and $CD4^+$ T cells activations were analysed *in vitro* by measuring cytokine production and cellular expression markers (Chapter 2).

The direct impact of *Mtb* glycolipids associated in liposomes on HIV-1 infection was analysed. We investigated liposome effects on HIV-1 *cis*-infection (Chapter 3) and *trans*-infection mediated by DCs involved in HIV-1 transmission (Chapter 4). In both cases, two different approaches were used. In order to analyse interferences from *Mtb* glycolipids with HIV-1 cell attachment and cell entry *via* co-receptors CCR5 or CXCR4, a pseudo-typed viral particle system was developed. HIV-1 pseudo-typed viruses (either CCR5 or CXCR4 using tropic) produced by co-transfection of 293T cells were used to infect TZM-bl cells expressing reporter proteins to enable monitoring HIV-1 infectivity. To characterised DC-SIGN mediated HIV-1 capture/transfer, the Raji-DC-SIGN cell line was used, in parallel to immature and mature DCs from healthy donors, on TZM-bl *trans*-infection assays. The second approach

developed, used fully replicative competent HIV-1 where infections were performed on $CD4^+$ T lymphocytes from healthy donors *in vitro* and monitored for virus replication by measuring p24 production, HIV-1 DNA quantification and cytokine production. For *trans*-infection analysis using the replicative system viral capture/transfer was mediated by immature DCs to $CD4^+$ T cells. Additionally, an *in vitro* system was tested where immature DCs and $CD4^+$ T lymphocytes were co-cultured simultaneously, more resembling *in vivo* physiological conditions (Chapter 4).

Finally, in the perspective of better understanding the role of EVs on influencing HIV-1 infectivity in the context of TB co-infection, we developed and compared different techniques for generating EVs from plasma, namely utilising Ultra-centrifugation (UC) and gel filtration (Chapter 5).

Chapter 1: Material and Methods

I. Liposomes generation and characterisation

i. Mycobacterium *total lipids extract*

a) Isolation of total lipid composition

The isolation of total lipids from the all the *Mycobacteria* tested, have been performed in collaboration with Dr A. Bhatt, University of Birmingham. To isolate total lipids from *Mycobacteria*, standard procedures were performed as described Dobson *et al.*, 1985. Bacterial cultures were pelleted in 8ml glass tubes with PTFE caps. 2ml of solvent $CHCl_3$:MeOH:H_20 was added to the pellet and kept at 50°C for 3h. The tube was then centrifuged at 3,000rpm and the supernatant transferred into a new tube. 1.75ml of chloroform and 750µl of water were then added to the supernatant, mixed and centrifuged again. The organic phase located at the bottom was then transferred to a new tube and washed 2x by addition of 2ml of $CHCl_3$:MeOH:H_20 3:47:48. After vortexing and centrifugation, the upper aqueous phase was discarded. After the final wash, the lower phase was transferred into a new tube to a heat block under air flow at 55°C. The amount of dried pellet was then calculated.

b) H37Rv lipids fractionation

This technique was performed in collaboration with Dr A. Bhatt (University of Birmingham). Total lipid extract from H37Rv bacteria (2mg) was fractioned using a silica column. The column was pre-washed with chloroform (3x void volume) before the sample was added. Once the input sample was added onto the column, 100ml of chloroform was added to start flow through collection. A mix of $CHCl_3$:MeOH solvent was passed through the column with a progressive increase in the proportion of methanol as follows:

- $CHCl_3$:MeOH 99:1: collection tubes numbered 1-8
- $CHCl_3$:MeOH 98:2, collection tubes numbered 9-15
- $CHCl_3$:MeOH 97:3 collection tubes numbered 16-23
- $CHCl_3$:MeOH 95:5 collection tubes numbered 24-31
- 93:7 collection tubes numbered 32-49

- 90:10 collection tubes numbered 50-57
- 80:20 collection tubes numbered 57-63.

c) Lipids used for liposome generation

All dried lipid pellets were solubilised in $CHCl_3$:MeOH 2:1 (Table 1.1), chloroform ($CHCl_3$, Sigma Aldrich, UK) methanol (MeOH, Sigma Aldrich, UK). Phosphatidylcholine and cholesterol were solubilised in chloroform.

Table 1.1 : List of total lipids extracts and lipids solutions

Total lipids extracts	Strains	Origin
	Mycobacterium tuberculosis	HN878, Bejing strain donated by A. Bhatt (University of Birmingham)
		CDC155 donated by A. Bhatt (University of Birmingham)
		EU127 from clinical isolate donated by A. Koch and R. J. Wilkinson (University of Cape Town)
		EU111 from clinical isolate donated by A. Koch and R. J. Wilkinson (University of Cape Town)
		Ex30 from clinical isolate donated by A. Koch and R. J. and Wilkinson (University of Cape Town)
		H37Rv from W. Jacobs (Albert Einstein College of Medicine)
		H37Rv MA from C. Sassetti (University of Massachusetts)
		papA1Δ (H37Rv mutant ΔSL-1) donated by A. Bhatt (University of Birmingham)
	Mycobacterium chelonae	donated by A. Bhatt (University of Birmingham)
	Mycobacterium marinum	donated by A. Bhatt (University of Birmingham)
	Mycobacterium bovis	BCG donated by A. Bhatt (University of Birmingham)
	Mycobacterium smegmatis	MC2155 donated by A. Bhatt (University of Birmingham)
	Staphylococcus aureus	Donated by A. Kadioglu (University of Liverpool)
	Corynebacterium glutamicum	donated by A. Bhatt (University of Birmingham)
Lipids solutions	Phosphatidylcholine	L-α-Phosphatidylcholine from egg yolk (Sigma Aldrich, UK)
	Cholesterol	(Sigma Aldrich, UK)
	Sulpholipids-1	From H37Rv (BEI Resources)
	PDIM	From H37Rv (BEI Resources)
	TDM	From H37Rv (BEI Resources)
	PIMs	From H37Rv (BEI Resources)

ii. Liposomes generation

"Liposome" is a generic term describing hydrated lipid dispersion which may be large or small, unilamellar or multilamellar vesicles (Mayer, Hope and Cullis, 1986). Here, small unilamellar vesicles (SUV) were produced by initially forming a thin dry lipid film that was hydrated in an aqueous medium. The lipid films were obtained by mixing different lipids in solution with organic solvent ($CHCl_3$ or $CHCl_3$:MeOH), and the solvents were then evaporated with the use of nitrogen gas. After the hydration step, multilamellar vesicles (MUV) were obtained by mechanical agitation. To reduce the size of produced SUV the preparations were finally sonicated (Figure 1.1).

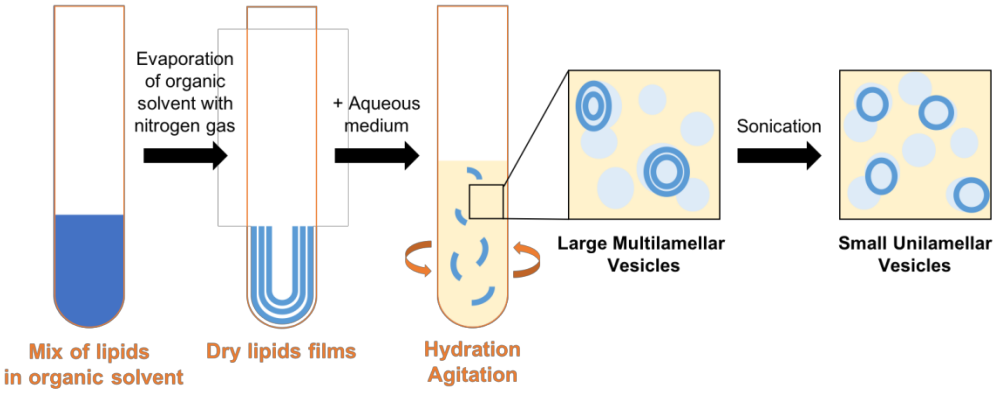

Figure 1.1 : Liposome preparation

Liposomes were generated with phosphatidylcholine (PC) and cholesterol (Ch) in different proportions (Table 1.2). Lipids were mixed together (2mg in total) and then evaporated with nitrogen gas for 30min. Liposomes were hydrated by addition of Roswell Park Memorial Institute (RPMI-1640, ThermoFisher scientific, UK), Dulbecco Modified Eagle Medium (DMEM, ThermoFisher scientific, UK), Phosphate-Buffered Saline (PBS, ThermoFisher scientific, UK), or sterile water (for TLC analyses). Liposomes were then incubated at 55°C for 30min with vortexing to achieve a final concentration of liposomes of 10mg/ml. The preparations were subsequently sonicated for 30min at 4°C. All liposomes were stored at 4°C for one month maximum.

For NanoSight analyses of liposomes, 0.8PC:0.2Ch liposomes were filtered using the Avanti® Mini-Extruder system after sonication. Liposome solutions were filtered through a 100nm or 200nm polycarbonate filter under 50°C temperature to produce 100nm and 200nm 0.8PC:0.2Ch liposome diameters.

Table 1.2 : List of liposomes generated and composition

Liposomes		Composition and Proportion				
		Phosphatidyl-choline	Cholesterol	Total lipids extract	SL-1	PDIM
Liposomes without lipids from *Mycobacterium* or other micro-organism	PC	100%	-	-	-	-
	0.9PC:0.1Ch	90%	10%	-	-	-
	0.8PC:0.2Ch	80%	20%	-	-	-
	0.6PC:0.4Ch	60%	40%	-	-	-
Liposomes with lipids from *Mycobacterium* or others	*Mtb* HN878	60%	20%	20%	-	-
	Mtb CDC1551					
	Mtb EU127					
	Mtb EU111					
	Mtb Ex30					
	Mtb H37Rv					
	Fraction 1 (from H37Rv 1-9 collection tube)					
	Fraction 2 (from H37Rv 10-13)					
	Fraction 3 (from H37Rv 14-18)					
	Fraction 4 (from H37Rv 19-27)					
	Fraction 5 (from H37Rv 28-32)					
	Fraction 6 (from H37Rv 33-36)					
	Fraction 7 (from H37Rv 37-44)					
	Fraction 8 (from H37Rv 45-63)					
	Mtb H37Rv MA					
	papA1Δ					
	papA1Δ + SL1	60%	20%	19%	1%	-
	PDIM	78%	20%	-	-	2%
	M. chelonae	60%	20%	20%	-	-
	M. marinum					

Table 1.2 continued

Liposomes		Composition and Proportion				
		Phosphatidyl-choline	Cholesterol	Total lipids extract	SL-1	PDIM
Liposomes with lipids from *Mycobacterium* or others	BCG	60%	20%	20%	-	-
	M. smegmatis					
	S. aureus					
	C. glutamicum					

iii. Thin-Layer Chromatography (TLC)

Thin-Layer Chromatography (TLC) is a solid-liquid form of chromatography allowing for the separation of lipids depending of their polarity. The technique was used here to characterise the lipid composition of the H37Rv bacterial strain and its lipid fractionation; and the composition of the *Mtb* liposomes generated. As for the total lipids isolations and fractionations, this was performed in collaboration with Dr A. Bhatt, University of Birmingham. In both cases, 10µl of sample was spotted and dried on a silica gel 60 F254 plate (Sigma Aldrich, UK). Sample separation occurred in 60:16:2 $CHCl_3$:MeOH:H_2O solvent and was visualised by staining with molybdophosphoric acid (MPA) and charring. For H37Rv fractions analyses, fractions (1-9) were pooled as fraction 1, (10-13) pooled as Fraction 2, (14-18) pooled as Fraction 3, (19-27) pooled as Fraction 4, (28-32) pooled as Fraction 5, (33-36) pooled as Fraction 6, (37-44) pooled as Fraction 7, and (45-63) pooled as fraction 8 from TLC separations and used for further analyses.

iv. Nanosight

Visualisation, particle concentration and the size distribution of the generated liposomes were evaluated using the NanoSight NS300 instrument (Malvern, UK) and using Nanoparticle Tracking Analysis (NTA) software. The liposomes in suspension were placed into a chamber where a laser beam passed through. In this way, the particles could be visualised by the camera and the Brownian motion of the particles indicating the particle size diameter using the Stokes Einstein equation, calculated by the NTA software. Videos were recording at camera level 13. The post-acquisition settings were with a minimum detection threshold 7, automatic blur and automatic minimum expected particle size. Liposome preparations were diluted 1:1000-1:2000 in PBS for each sample and three 60sec videos were recorded and analysed.

II. Immunology

i. PBMCs isolation

Venous blood samples from healthy donors collected in either EDTA or heparin collection tubes were processed by density gradient centrifugation using Histopaque®-1077 (Sigma Aldrich, UK) to allow for PBMC isolation. Blood was diluted 1:1 in PBS and layered over Ficoll

in 50ml tubes (20ml of diluted blood onto 15ml of Histopaque®-1077). Tubes were placed into centrifuge buckets, avoiding any disruption of the layer, to be spun at 1000g for 20min at 18-20°C (acceleration 1, brake 0). After centrifugation, the following layers were visible from the top to bottom of the tube: plasma and PBS, PBMC, Ficoll and red blood cells. The PBMC layer was carefully collected using a sterile plastic Pasteur pipette and transferred to 50ml tubes. PBS (Thermofisher, UK) was added up to 50ml and cells were washed by 8min centrifugation at 500g, 18-20°C (acceleration and brake 4). After the first wash, supernatant was discarded and the cell pellet was re-suspended in PBS; 10µl of cell suspension was taken for the cell count and the remaining cells were washed as described above. For cell count, 90µl of trypan blue 0.4% (Thermofisher, UK) was added to the cell suspension to allow for visualisation of dead cells. 10µl of the cell-trypan blue suspension was applied to a haemocytometer slide chamber. By using a microscope with a 10X objective alive (clear) and dead (blue) cells could be discriminated and live cells on one set of 4 corner squares counted. The total number of cells was then calculated with percentage viability determined.

ii. Monocytes derived macrophage (MDMs) isolation and culture

a) MDMs isolation and culture

Monocyte derived macrophages (MDMs) were isolated from fresh PBMCs by MACS® Separation (Miltenyi Biotech, UK) with positive selection of the $CD14^+$ cell population. PBMCs were washed in PBS and finally re-suspended in MACS buffer (80µl of buffer per 10^7 PBMCs) containing PBS with 0.5% bovine serum albumin (BSA, Sigma Aldrich, UK) and 2mM EDTA (ThermoFisher scientific, UK). Human magnetic CD14 MicroBeads (Miltenyi Biotech, UK) were added to the cells in suspension (10µl of beads per 10^7 total cells) and incubated for 15min at 4°C. During the incubation, LS MACS Columns (Miltenyi Biotech, UK) were placed on the magnetic separator and activated by passing through MACS buffer. Following incubation with the CD14 MicroBeads, the cells were pelleted and re-suspended in MACS buffer (500µl of buffer per 10^8 total PBMCs) and applied onto the column. Unbound cells ($CD14^-$ population) passed through the column and were collected in a 50ml tube for $CD4^+$ T cell isolation (Chapter 1 **Part II**. *Section iv.*). The LS column was washed with 1ml of MACS buffer (3x) before removing the column from the magnetic rack to elute the $CD14^+$ population with 5ml of MACS buffer and collected in a 15ml tube containing 1ml of buffer. 10µl of cell suspension was taken for determining cell counts and viability (as described in Chapter 1 **Part II.** *Section i*) and the remaining cells were pelleted by 8min centrifugation at

500g, 18-20°C (acceleration and brake 4). One aliquot of each population ($CD14^+$ and $CD14^-$) containing 1-0.5x10^6 cells (upon cell availability) was used for flow cytometry analysis (Chapter 1 **Part II.** *Section vi.a)*). The $CD14^+$ cell population was re-suspended at 1x10^6 cells/ml in RPMI-1640 containing L-glutamine, 10% AB^+ serum, 100U/ml penicillin and 100mg/ml streptomycin (Fisher Scientific, UK). The cells were then seeded in 6 well plates at 3ml per well, and incubated for 6-7 days at 37°C, 5% CO_2 to allow them to undergo differentiation.

b) MDMs incubated with liposomes

MDMs generated from 7 days of culture as described above were harvested and re-suspended in fresh media consisting of RPMI-1640 with L-glutamine, 10% AB^+ serum, 100U/ml penicillin and 100mg/ml streptomycin at 10^6 cells/ml. In a 96-well plate, 200µl of the cell suspension were seeded per well, then, 40µg of liposome suspension in RPMI-1640 was added per well with a total of 4 wells per condition. Liposomes tested: BCG, *M. smegmatis*, H37Rv, HN878, CDC1551 and EU127. 0.8PC:0.2Ch was used as a negative control and LPS (100ng/ml, Sigma Aldrich, UK) used as a positive control. After 18h of incubation at 37°C 5% CO_2, MDM were harvested and centrifuged for 5min at 1,400rpm, 18-20°C (acceleration and brake 4). The supernatant from 4 wells from the same condition were pooled and stored at -80°C before performing Lumniex® assays (Chapter 1 **Part II.** *Section vii.*).

iii. Monocytes derived dendritic cells (DCs) isolation, culture and maturation

a) iDCs isolation and culture

Immature monocytes derived dendritic cells (iDCs) were isolated from fresh PBMCs by MACS® Separation (Miltenyi Biotech, UK) with the positive selection of the $CD14^+$ cell population as described above for MDM (Chapter 1 **Part II.** *Section ii.a)*). The $CD14^+$ cells obtained after isolation were re-suspended at a density of 1x10^6 cells/ml in RPMI-1640 containing L-glutamine supplemented with 10% foetal bovine serum (FBS, Sigma Aldrich, UK), 100U/ml penicillin, 100mg/ml streptomycin, 70ng/ml human IL-4 (Fisher Scientific, UK) and 50ng/ml human GM-CSF (Fisher Scientific, UK). The cells were seeded in 6 well plates in 3ml media per well, and incubated at 37°C, 5% CO_2 through differentiation. After 3 days the media was replaced with fresh media containing IL-4 and GM-CSF. The iDCs were harvested

after 3-4 days of incubation. One aliquot of cells at 1-0.5x10^6 cells/vial was used for flow cytometry analysis.

b) iDCs maturation

Mature monocyte derived dendritic cells (mDCs) were isolated from fresh iDCs. At day 5-6 Poly(I:C) (20µg/ml, Sigma Aldrich, UK) or LPS (100ng/ml) were added to iDCs media. The mDCs cells were harvested after 18-24h of incubation at 37°C, 5% CO_2. The cell phenotypes where confirmed by flow cytometry analysis (Chapter 1 **Part II.** *Section vi.b)*).

c) iDCs maturation with liposomes

For iDCs maturation in the presence of liposomes, iDCs generated from 5-6 days of culture were harvested and re-suspended in fresh media containing RPMI-1640 supplemented with L-glutamine, 10% FBS, 100U/ml penicillin, 100mg/ml streptomycin. The cells were seeded in 6 well plates with 3ml per well at a density of 0.5x10^6 cells/ml. To each well 100µg of liposome suspension in RPMI-1640 was added per well with 2 wells per condition. Liposomes tested included: BCG, *M. smegmatis*, H37Rv, HN878, CDC1551 and EU127. Poly(I:C) and LPS were used as positive controls and in parallel iDCs without stimulation and 0.8PC:0.2Ch liposomes were included as negatives controls. After 18h of incubation at 37°C 5% CO_2, iDCs were harvested and analysed by flow cytometry, additionally, the supernatants from each condition were kept and stored at -80°C for Luminex® assays.

iv. <u>$CD4^+$ T lymphocyte isolation and culture</u>

$CD4^+$ T lymphocytes were isolated from fresh PBMCs using MACS® Separation (Miltenyi Biotech, UK). Frist, the $CD14^-$ cell population was isolated by negative selection as described above for MDM (Chapter 1 **Part II.** *Section ii.a)*). Secondly, after 4 days of activation and expansion of the $CD14^-$ population to lymphocytes, $CD4^+$ T lymphocytes were separated from $CD8^+$ T lymphocytes by negative selection using Dynabeads® CD8 (ThermoFisher scientific, UK). The $CD14^-$ isolated fraction from MACS® Separation were re-suspended at a density of 2x10^6 cells/ml in RPMI-1640 containing L-glutamine complemented with 10% FBS, 100U/ml penicillin, 100mg/ml streptomycin, 5µg/ml PHA-p (Sigma Aldrich, UK), 100U/ml human IL-2 (Fisher Scientific, UK) and incubated at 37°C, 5% CO_2. At day 2, the cells were re-suspended gently, counted and fresh IL-2 (100U/ml) was added to the media. At day 4 following cell activation and expansion the lymphocytes were harvested and pelleted by 8min

centrifugation at 500g, 18-20°C (acceleration and brake 4) to be re-suspended in isolation buffer (density of 10^7 lymphocytes/ml) containing PBS, with 0.1% BSA and 2mM EDTA. Dynabeads® CD8 were added to the cells in suspension (25µl of beads per 10^7 cells) and incubated for 30min at 4°C. The tube containing the cells incubated with the magnetic beads was then placed onto a magnetic rack to allow for the separation of $CD4^+$ T lymphocytes from the magnetically retained $CD8^+$ T lymphocytes. The $CD4^+$ cells were harvested, pelleted and re-suspended in RPMI-1640 containing L-glutamine supplemented with 10% FBS, 100U/ml penicillin, 100mg/ml streptomycin and 100U/ml human IL-2. One aliquot of each population ($CD4^+$ and $CD4^-$) containing 5-10 $x10^5$ cells were used for flow cytometry analysis. The $CD4^+$ T-lymphocytes were incubated at 37°C, 5% CO_2 for 24-48h before being used in assays.

v. *CD4⁺T lymphocytes and iDCs co-culture*

a) *CD4⁺T lymphocytes and iDCs co-culture*

The iDCs and $CD4^+$ T lymphocytes were both isolated from the same blood donor with the methods described above. In a 96-well plate $2x10^4$ iDCs were placed in culture with $2x10^5$ $CD4^+$ T lymphocytes per well in 200µl of RPMI-1640 containing L-glutamine supplemented with 10% FBS, 100U/ml penicillin, 100mg/ml streptomycin and 100U/ml human IL-2.

b) *CD4+T lymphocytes and iDCs with liposomes*

40µg of liposome suspensions in RPMI-1640 were added per well to iDCs and $CD4^+$ T lymphocyte co-culture, with a total of 4 wells per condition. Liposomes tested: BCG, *M. smegmatis*, H37Rv, HN878, CDC1551 and EU127. 0.8PC:0.2Ch is used as a negative control and LPS (100ng/ml, Sigma Aldrich, UK) as a positive control. After 7 days of incubation at 37°C 5% CO_2, the supernatant from 4 wells from the same condition were pooled and stored at -80°C before being processed for Lumniex® analysis.

vi. *Flow cytometry*

Flow cytometric analysis was performed to confirm each cellular fraction's phenotype by measuring expression of specific cellular markers relevant to the cell-type being assayed. Events were acquired using the BD Accuri™ C6 or BD FACSCelesta™ flow cytometers and the analysis was performed by using BD Accuri™ C6 Plus or FlowJo software, respectively.

a) CD14$^+$/CD14$^-$ PBMC population isolation

To confirm MACS® Separation of CD14$^+$ from the CD14$^-$ PBMC population, flow cytometry was performed for the detection of CD14 markers. Following isolation of the two population's, aliquots of 0.5x10^6 cells were pelleted by 1min centrifugation at 7,000rpm at room temperature (RT) and re-suspended in 40µl of MACS buffer. Cell suspensions were stained with the relevant antibody (Table 1.3) diluted following the manufacturer's recommendations (Biolegend, UK). After 30min incubation at 4°C, cells were washed 2x in PBS and centrifuged at 7,000rpm at RT for 1min. After the final wash cells were re-suspended in 100µl of 2% PFA solution (Sigma Aldrich, UK) and incubated for 30-45min at 4°C. Finally, the cells were re-suspended in PBS before undergoing analysis. Flow cytometry analysis was performed using the BD Accuri™ C6 and 10,000 events were recorded for each sample. Data analysis was performed using the BD Accuri™ C6 Plus software. For each population, three conditions were tested: cells alone, cells with antibody and cells with isotype matched control antibody.

b) iDCs maturation

The mDCs phenotypes were confirmed *via* flow cytometry by measuring specific markers of differentiation of DCs which include: DC-SIGN, CD40, CD86, CD80, and HLA-II. DCs were stained following the same protocol described above for PBMCs. BD FACS Celesta™ was used to record 10,000 events for each sample and data analyses was performed using FlowJo software.

c) CD4$^+$ T lymphocytes isolation

Flow cytometry was used to detect CD4$^+$ cell markers to confirm the enrichment of CD4$^+$ from CD14- cell populations using Dynabeads® CD8 depletion. Cells were stained following the same protocol described above for PBMCs and DCs. BD FACS Celesta™ was used to record 10,000 events for each sample and data analysis was performed using FlowJo standard software.

Table 1.3 : List of antibodies used in flow cytometry assays

Assays	Target (fluorochrome)	Company (Cat#)
$CD14^+/CD14^-$ PBMCs populations isolation	CD14 (PE)	BioLegend (325605)
iDCs maturation	DC-SIGN (PE)	BioLegend (330106)
	CD40 (APC)	BioLegend (334309)
	CD86 (PE)	BioLegend (305405)
	CD80 (APC)	BioLegend (305219)
	HLA-II (APC)	BioLegend (307609)
$CD4^+$T lymphocytes isolation	CD4 (PE)	BioLegend (300508)

d) HIV-1 infection

For the development of *in vitro* assays to study HIV-1 infection, flow cytometry was used to measure expression of different florescent markers (depending on the conditions) to measure infections as described in Chapter 1 **Part IV.** *Section iii.a)* and **Part V.** *Section iii.a)*.

vii. Luminex®

Supernatants from MDM, iDCs (Chapter 1 **Part II.** *Sections ii.b)* and *iii.c),* respectively) and HIV-1 *cis*-/*trans*-infection assays (Chapter 1 **Part V.** Sections *iii.b)* and *iv.b),* respectively) were assayed for a total of 27 soluble immune proteins quantified in four panels (listed Table 1.4) utilising the R&D Systems multiplex magnetic bead immunoassays and following manufacturer's instructions. The Luminex® assays were performed in collaboration with Dr C. Herrera, Imperial College London. Briefly, samples were spun and diluted appropriately for each panel. For detection of TGF-β 1, 2 and 3, samples required acid activation with 1N HCl followed by 1.2 N NaOH/0.5M HEPES neutralisation. Serially diluted standards and samples were incubated with a magnetic microparticle cocktail for 2h at RT on a horizontal orbital microplate shaker. Plates were then washed with wash buffer three times with a handheld magnetic plate washer prior to incubation with a biotin antibody cocktail for 1h at RT on the orbital shaker. Streptavidin-PE was added to each well after three washes. Plates were incubated for 30min, washed and microparticles resuspended in wash buffer. Finally, plates were read using a Luminex 200 System (Bio-Rad, Hercules, CA).

Table 1.4 : List of cytokines studied and kits used in Luminex® assays

Description	Company (Cat#)
Human Magnetic Luminex Assay (Ref GzWwKHKp) CCL3/MIP-1α (BR35) CXCL10/IP-10 (BR21) CXCL11/I-TAC (BR63) CXCL2/Gro beta/MIP-2α (BR27) CXCL8/IL-8 (BR18) CXCL9/MIG (BR52) G-CSF (BR54) GM-CSF (BR46) IFN-γ (BR29) IL-1α (BR38) IL-1β (BR28) IL-10 (BR22) IL-12 p70 (BR56) IL-18 (BR78) IL-23 (BR76) IL-27 (BR25) IL-6 (BR13) M-CSF (BR48) TNF-α (BR12)	Bio-Techne (LXSAHM-19)
Human Magnetic Luminex Assay (Ref GzWwKHKp) CCL5/RANTES (BR36) IFN-β (BR21) IL-15 (BR63) IL-12/23 p40 (BR67)	Bio-Techne (LXSAHM-04)
TGF-β Premixed Magnetic Luminex Performance Assay (Ref GHv98896) TGF-β1 TGF-β2 TGF-β3	Bio-Techne (FCSTM17-03)
Human Mag Luminex Perf Assay Base Ki t, XL Cyt Disc Panel - LUXLM000 IFN-α, XL Base Kit, XL Cytokine Discovery Panel (Ref bngrmtnr)	Bio-Techne (LUHM00) Bio-Techne (LUXLM9345)

III. Extra-vesicles (EVs) isolation and characterisation

i. Plasma isolation

In this thesis, extra-vesicles (EVs) were isolated from the plasma of healthy donors. In order to collect plasma, venous blood collected in EDTA or heparin tubes was centrifuged at 1,000g

for 20min at RT allowing separation of plasma from blood cells. The plasma (supernatant) was collected in 50ml tubes, aliquoted and stored at -80°C for.

ii. Isolation of EVs by differential centrifugations

a) Assay 1

For this approach, 1ml of plasma from healthy donors was diluted in PBS 1:1 in 2ml microcentrifuge tubes. To eliminate cell debris the sample was first centrifuged 5min at full speed (7,000g) at 4°C. 2ml cleared plasma in microcentrifuge tubes was then centrifuged 90min at full speed (7,000g) at 4°C. The supernatant was transferred to a new tube and stored at -80°C for subsequent analysis. The pellet containing the EV particles was re-suspended in 500µl PBS and stored at -80°C prior to testing in the appropriate assays.

b) Assay 2: Ultra-centrifugation

For this approach, EV isolation was performed on a larger scale and utilised the ultra-centrifugation protocol previously described (Théry *et al.*, 2006). 10ml of plasma from healthy donors was diluted 1:1 in PBS and centrifuged 30min at 10,000g at 4°C to remove cell debris. Supernatant was transferred to 5.9ml polycarbonate Quick-Seal® tubes (Beckman Coulter, UK) and heat-sealed using the specified Beckman device. Cleared plasma was centrifuged 2h at 100,000g at 4°C in a Beckman SW41 swing-bucket rotor. After centrifugation the supernatant was collected using a syringe and kept at -80°C until subsequent analysis. The pellets containing the EVs were re-suspended in 1ml of PBS, transferred to a clean tube and incubated 30min at RT to dislodge and separate EV particles. 25ml of PBS was added and the re-suspended pellet centrifuged for 2h 100,000g at 4°C as previously described. Following the wash step the second supernatant was collected and stored at -80°C for subsequent analysis. The pellet was re-suspended in 1ml PBS as described above and kept at -80°C for later analysis in the HIV-1 *trans*-infection assay (Chapter 1 **Part IV.** *Section iv.d)*).

iii. Isolation of EVs from Plasma by Gel Filtration (Size Exclusion Chromatography)

a) Assay 1: Gel Filtration Sephadex paired with concentration

For this approach, 1ml of plasma from healthy donor was diluted in PBS 1:1 in 2ml Eppendorf tubes. To eliminate cell debris the sample was centrifuged for 5min at full speed (7,000g) at 4°C and aliquoted. 2ml of cleared plasma was applied to a Sephadex G-25 column in PD-10 buffer (GE Healthcare, UK) to isolate the EVs from the plasma. The Sephadex G-25 column was first washed with 8ml of PBS. The cleared plasma was then eluted with PBS and collected. The eluate obtained was applied to an Amicon Ultra-15 30kDa filter (Merck Millipore, UK) and centrifuged 30min at 4,000g at 4°C to concentrate the EVs from plasma. The filtrate was removed and stored at -20°C to be subsequently utilised in HIV-1 *trans*-infection assays (Chapter 1 **Part IV.** *Section iv.d)*). The concentrate was washed once with 1ml PBS and centrifuged again for 30min at 4,000g at 4°C. After the wash step, the concentrate containing the EV particles was transferred to a clean Eppendorf tube and stored at -80°C before being analysed in HIV-1 *trans*-infection assays (Chapter 1 **Part IV.** *Section iv.d)*).

b) Assay 2: Gel Filtration Sepharose

For this approach EV isolation was performed following SEC as previously described (Böing *et al.*, 2014). An SEC column was constructed using a 10ml syringe (Becton Dickinson BD) stacked with 10ml of Sepharose CL-2B (Sigma Aldrich, UK). Prior to adding Sepharose, the tip of the syringe was compacted with nylon stocking to avoid leaking. The column was washed with 50ml of PBS then 2ml of cleared plasma diluted 1:1 in PBS was applied to the column and eluted with PBS. Twenty-six fractions of 500µl were collected and stored at -80°C before subsequent characterisation (Chapter 1 **Part III.** *Section iv*.) and analysis in the HIV-1 infection assays (Chapter 1 **Part IV.** *Sections iii.d)* and *iv.d)*) .

iv. Nanosight

As explained above for liposome characterisation, the NanoSight NS300 was used to visualise the EV particles isolated from plasma in order to estimate the concentration and size distribution. Videos were recorded at camera level 13. The post-acquisition settings were with a minimum detection threshold 7, automatic blur and automatic minimum expected particle size. Fractions collected from SEC were diluted (between 1:5-1:100) in PBS and for each sample 3x 60sec videos were recorded and analysed.

v. Bradford

The standard Bradford estimation method was used to quantify the amount of total protein present in the exosome preparations. The technique is based on an absorbance shift of the dye Coomassie Brilliant Blue G-250 in the presence of protein. Under acidic conditions the dye is predominantly red (A_{max}=470nm), but when the dye binds to protein it is converted to a blue colour (A_{max}=595nm). It is this blue protein-dye form that is detected at 595nm in the assay using a spectrophotometer. Quick Start™ Bradford Protein Assay Kit 1 (Bio-Rad, UK) was used with BSA (Bio-Rad) as a standard following the manufacturer's instructions. The Quick Start™ Bradford 1x dye reagents were warmed to RT. Standards and samples from the SEC isolation were diluted in PBS. Because the protein concentrations of samples were unknown, two standards were produced in parallel comprising of different ranges in concentration: Standard A 2,000-125µg/ml BSA and Standard B 25-1.25µg/ml. For the Standard A assay, 5µl of standard or sample were mixed with 250µl of 1x dye reagent per well in a 96-well plate. For Standard B assay, 150µl of standard or sample were mixed with 150µl of 1x dye reagent per well. Samples were quantified in duplicate. After 5-10min of incubation at RT the absorbance was read (595nm) using a spectrophotometer.

vi. Western Blot

To confirm isolation and characterise the EVs being isolated from plasma Western Blot analysis was used to detect the presence of specific EV proteins. This included testing for the TSG101 and CD63 markers with two different protocols using the Mini-PROTEAN®3 System (Bio-Rad, UK).

a) Protocol 1

Sample preparation

Fractions 1-7 and fractions 8-13 (following SEC isolation Chapter 1 **Part III.** *Section iii.*) were separately pooled and concentrated using the Amicon Ultra-0.5 membrane Ultracel-10 (Merk Millipore, UK) system. Samples were diluted in 1x RIPA Buffer (Sigma Aldrich, UK) and mixed 1:1 with 2x Laemilli buffer (Bio-Rad, UK) containing 5% β-mercaptoethanol (Bio-Rad, UK) and heated 10min at 100°C, after which 13µg of proteins (20µl) per well were loaded onto an SDS-PAGE gel.

SDS-PAGE

The following conditions were used for SDS-PAGE. 10% resolving gel composed of ProtoGel (GeneFlow, UK), ProtoGel Buffer (GeneFlow, UK), 10% ammonium persulfate (Sigma Aldrich, UK) and TEMED (Sigma Aldrich) and 4% stacking gel composed of stacking Buffer (0.5M Tris-HCl, 0.4% SDS (Fisher Scientific, UK)), ProtoGel, 10% ammonium persulfate and TEMED were used. The gel was run with SDS-PAGE running Buffer composed of SDS-PAGE Tank Buffer (10x) and Tris-Glycine SDS (GeneFlow, UK) and at 100V for 1h30.

Transfer

Following SDS-PAGE electrophoresis proteins were transferred to a PVDF membrane cut to size (Merk Millipore, UK) and using the appropriate gel transfer apparatus. The transfer was performed with standard Buffer composed 1x Tris-glycine Buffer (GeneFlow, UK) and 20% methanol (Sigma Aldrich, UK) at 250mA for 90min. To determine that protein transfer occurred PVDF membranes were stained with Ponceau S solution (Sigma Aldrich, UK) with agitation for 5-10min. Once the transferred proteins were visible and identified the membranes were washed with 0.1% PBS-Tween solution and then blotted for 2h at RT under agitation with blotting Buffer composed of 0.1% PBS-Tween and 5% milk.

Immuno-blotting

Primary antibody recognising TSG111 (ab83, Abcam, UK) was diluted 1:1000 in blotting buffer. The antibody was incubated with the membrane O/N at 4°C and with shaking. The membrane was washed 3x with PBS-Tween for 15min. The secondary antibody, goat anti-mouse (32430, ThermoFisher, UK) was diluted 1:100 and incubated with the membrane for 90min at RT. As previously described, the membrane was washed 3x with PBS-Tween, then probed with Pierce™ ECL Western Blotting Substrate (ThermoFisher, UK) and exposed.

b) Protocol 2

Sample preparation

The samples were prepared in reducing conditions as previously described and in non-reducing conditions where the 2x Laemilli buffer lacked β-mercaptoethanol.

SDS-PAGE

The same reagents were used as in Protocol 1 but electrophoresis was performed at 170V for 50min.

Transfer

The transfer was performed under the same conditions as in Protocol 1.

Immuno-blotting

Primary antibody recognising CD63 (ab193349, Abcam, UK) was used at 0.5µg/ml concentration and incubated overnight at 4°C. The same secondary antibody was used as in Protocol 1 using the same conditions.

IV. Virological assays – Generation of pseudo-typed viral particles

i. Viral production by transfection

Single-round infectious virus particle stocks were routinely generated through transfection of 292T cells with a combination of plasmids (Figure 1.2).

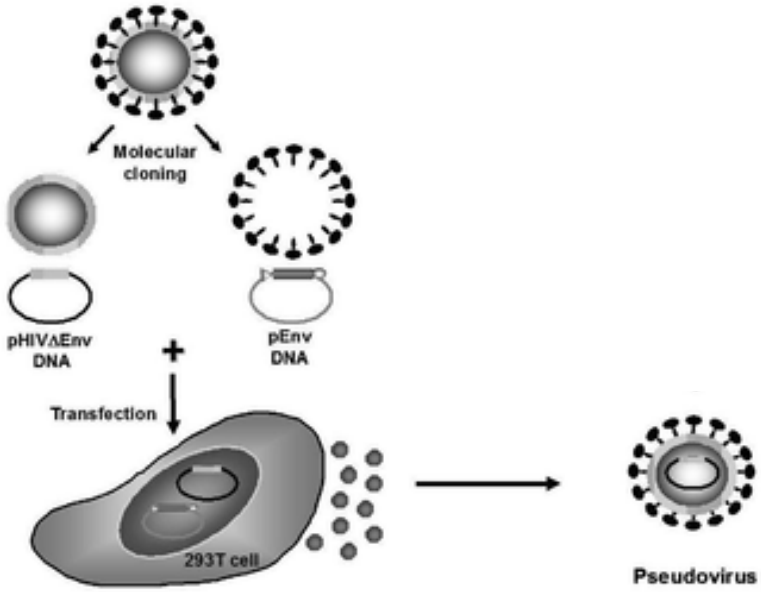

Figure 1.2 : Representation of pseudo-typed viral particle production

Adapted from (Ozaki *et al.*, 2012)

An expression plasmid containing the coding sequence for the HIV-1 envelope protein of either the following; JR-FL (utilising the CCR5 co-receptor, plasmid obtained from NIH AIDS Research and Reference Reagent Program), BAL (utilising the CCR5 co-receptor, plasmid obtained from NIH AIDS Research and Reference Reagent Program), LAI (utilising the CXCR4

co-receptor, plasmid obtained from NIH AIDS Research and Reference Reagent Program), or VSVg (a non-tropic envelope, plasmid obtained from NIH AIDS Research and Reference Reagent Program) was co-transfected along with pSG3Δenv, a plasmid coding for the proteins required for virus production (minus the intact envelope gene, Δenv from NIH AIDS). The transfected 293T cells thereby express the viral and envelope proteins required to generate a single-round infectious pseudo-typed virus particle, but since the incorporated viral genome of the produced viruses is Δenv the virus cannot generate new infectious virus particles following infection. 293T cells are human embryonic kidney cells, routinely maintained at 37°C 5% CO_2 in DMEM supplemented with 10% FBS, L-glutamine, 100U/ml penicillin and 100mg/ml streptomycin. One day prior to transfection $1.2x10^6$ cells were seeded in a 10cm dish. After 24h, the cells were transfected using the Lipofectamine standard method where 2µg of HIV-1 envelope plasmid and 2µg of the backbone pSG3Δenv plasmid were mixed in 300µl of OptiMEM (Thermo Fisher scientific, UK). Separately, 24µl of Lipofectamine was mixed with 276µl of OptiMEM and 300µl of this was added to the DNA mix. After 30min incubation at RT, the Lipofectamine/DNA mixture was added dropwise to 293T cells with 1ml of OptiMEM. After 6h, the media was replaced with fresh DMEM and the pseudo-typed virus stock (supernatant) was harvested after further 48h of incubation at 37°C 5% CO_2. Viruses were stored at -80°C and virus concentrations were quantified by measuring CA-p24 antigen levels as described below *Section ii.*

ii. Virus quantification by p24 ELISA

To measure HIV-1 viral stock concentrations, CA-p24 was quantified utilising a twin site sandwich HIV-1 p24 antigen ELISA (Aalto Bio Reagents, Ireland). The viral stock is lysed to release viral antigens and the p24 antigen is captured with a polyclonal antibody coated onto an ELISA plate. Bound p24 antigen is subsequently detected with an alkaline phosphatase conjugated anti-p24 monoclonal antibody and a luminescent detection system.

To coat the ELISA plate, 100µl of 5µg/ml antibody (D7320, Aalto Bio Reagents, Ireland) was added per well and incubated overnight at RT. The following day the plates were washed once with 1x TBS buffer pH7.5 containing 4.21g NaCl (Sigma Aldrich, UK), 15.1g Tris-Trizma base (Sigma Aldrich, UK) and H_2O. For blocking, 100µl of 2% milk-TBS is added per well and incubated for 1hr at RT. Coated plates could then be used or stored at -20°C for a maximum of 2 months.

To perform the ELISA, antigen coated plates were equilibrated at RT and washed once with 1x TBS buffer. The standards and samples to be tested were diluted using 0.1% Empigen-TBS (Sigma Aldrich, UK). Additionally, samples were pre-treated with 1% Empigen-TBS, dilution 1:1, prior to performing the dilutions to inactivate virus particles. 100µl per well of sample, standards, or controls were added in duplicate to the plate, and incubated for 3h at RT. Following incubation, plates were washed twice with 1x TBS buffer and tapped dry. Then, 100µl of conjugate (BC 1071-AP, Aalto Bio Reagents, Ireland) diluted 1:5000 in 20% sheep serum (Sigma Aldrich, UK), 0.05% Tween and 1x TBS, was added per well. After 1hr incubation at RT, plates were washed 4x with 0.1% Tween-PBS, and 2x with ELISA Light assay buffer (Thermo Fisher scientific, UK). Finally, plates were tapped dry before adding 50µl of ELISA Light Substrate (CSPD with Sapphire Substrate, Thermo Fisher scientific, UK). After 30-45min incubation at RT, luminescence was measured with FLUOStar® Omega luminometer (BMG LabTech).

iii. HIV-1 cis-*infection*

a) Optimisation of HIV-1 pseudo-typed virus stocks on GHOST cell-lines

GHOST cells (NIH AIDS) are derived from human osteosarcoma (HOS) cells and express GFP under control of Tat protein following HIV-1 infection. GHOST $CXCR4^+$, $CCR5^+$ and $CXCR4^+/CCR5^+$ cells were maintained at 37°C 5% CO_2 in DMEM supplemented with 10% FBS, 100U/ml penicillin, 100mg/ml streptomycin, 500µg/ml gentamycin G418 (Thermo Fisher scientific, UK), 100µg/ml hydromycin (Sigma Aldrich, UK) and 1µg/ml pyromycin (Sigma Aldrich, UK). One day prior to infection, $3x10^4$ cells per well were seeded in 96-well plates. After 24h the cells were infected with 2ng, 4ng or 8ng CA-p24 virus input within 50µl of total volume in supplemented DMEM as described above. Cells were infected with either pSG3-JF-FL, pSG3-LAI, pSG3-VSVg or pSG3Δenv pseudo-typed virus. pSG3Δenv pseudo-typed virus was used as a negative control and pSG3-VSVg pseudo-typed virus was used as a positive control. After 2h of incubation at 37°C 5% CO_2, 200µl of media was added. 48h post-infection at 37°C 5% CO_2 the supernatants were removed and the cells washed with PBS before being detached with 1% trypsin (Thermo Fisher scientific, UK) and collected in microcentrifuge tubes. GHOST cells were washed a second time in PBS, pelleted by 1min centrifugation at 7000rpm at RT and re-suspended in 100µl of 2% PFA solution. After 30-45min incubation at 4°C, the cells were re-suspended in PBS. The infection of GHOST cells was quantified by measuring GFP production by flow cytometry. BD Accuri™ C6 was used to record 10,000

events for each sample and data analysis was performed using the BD Accuri™ C6 Plus software.

b) TZM-bl cis-*infection*

TZM-bl cells (NIH AIDS) are HeLa cells that have been transformed to express luciferase under control of the HIV-1 Tat protein, expressed following HIV-1 infection. The cells are lysed to liberate the luciferase and thereby provide luminescence in the presence of enzyme substrate, where luminescence intensity correlates with the level of infection. TZM-bl cells were maintained at 37°C 5% CO_2 in DMEM complemented with 10% FBS, L-glutamine, 100U/ml penicillin and 100mg/ml streptomycin. *Cis*-infections were performed as described for GHOST cells, with 8ng CA-p24 virus input. After 48h of infection the cells were washed with PBS, and 20µl of lysis Buffer (Promega) was added per well. Luciferase activity was determined using the Luciferase Assay kit (Promega) and FLUOStar Omega luminometer (BMG LabTech) following the manufacturer's instructions.

c) TZM-bl cis-*infection in presence of liposomes*

To analyse the influence of liposome composition, varying in proportion of cholesterol, on HIV-1 *cis*-infection, two different assays were performed. In scenario one PC, 0.9PC:0.1Ch, 0.8PC:0.2Ch or 0.6PC:0.4Ch liposome suspension in DMEM was added to the cells at the same time virus was added. 8ng CA-p24 of pSG3-JR-FL pseudo-typed virus stock was mixed with 100ng or 1ng of liposomes in 50µl total volume and added to the TZM-bl cells. After 2h incubation at 37°C 5% CO_2, 200µl of media was added and the infection measured after 48h as described above. In the second scenario, liposome suspensions in DMEM were added to the cells prior to virus input. 50µl of 100ng or 1ng of liposome was added to the TZM-bl cells. After 30min incubation at 37°C and 5% CO_2, 8ng CA-p24 of pSG3-JR-FL was added and incubated for 2h as described above. Following this incubation, 200µl of media was added to each well and incubated for 48h at which point cells were lysed and luciferase activity was measured.

In parallel to the assays measuring the impact of liposome compositions on TZM-bl HIV-1 infection, the impact of liposomes on cell viability was measured. In this case, PC and 0.8PC:0.2Ch liposomes in suspension in DMEM were incubated on TZM-bl without virus. TZM-bl cells ($3x10^4$ per well) were seeded in 96-well plates and after 24h the cells were incubated with 1000ng, 100ng, 10ng and 1ng of liposome in 250µl total volume. After 48h

incubation at 37°C 5% CO_2 the media was removed and the cells harvested *via* trypsin treatment and fixed in 2% PFA. After fixation, the cells were re-suspended in PBS and the viability was analysed by flow cytometry. BD Accuri™ C6 was used to record 10,000 events for each sample and data analysis was performed using the BD Accuri™ C6 Plus software.

To analyse the influence of *Mycobacterium* liposomes on HIV-1 *cis*-infection the same assays were performed. 40µg of BCG, *M. smegmatis*, H37Rv, HN878, CDC1551, EU127 and 0.8PC:0.2Ch liposome suspensions were tested with 8ng of pSG3-BAL and pSG3-LAI where in one case liposome was added at the same time as virus and in a second where liposomes were pre-incubated with the target cells prior to virus input.

d) TZM-bl cis*-infection in presence of EVs*

To study the influence of EVs isolated from plasma by SEC (Chapter 1 **Part III.** *Section iii.*) a similar approach was used as with the liposome assay. Fractions 9-13 from SEC were pooled together and tested using the TZM-bl HIV-1 *cis*-infection assay. As with liposomes, 50µl EVs were either pre-incubated for 30min with TZM-bl cells or added at the same time as virus.

iv. HIV-1 trans*-infection*

a) Optimisation of HIV-1 trans*-infection*

For the optimisation of the HIV-1 *trans*-infection assay, the Raji and Raji-DC-SIGN cell-lines were utilised. Raji is an Epstein Barr Virus (EBV)-positive Burkitt's lymphoma cell-line (ATCC), and Raji-DC-SIGN cells are Raji cells transduced to express the DC-SIGN receptor protein. HIV-1 *trans*-infection is a mechanism whereby HIV-1 is captured by the DC-SIGN receptor and presented to target cells that it then infects *via* the classic CD4 and co-receptor *cis*-infection process. The routinely utilised *trans*-infection assay involves incubating HIV-1 with Raji (control) or Raji-DC-SIGN cells, washing and incubating with TZM-bl cells and measuring infection. Raji and Raji-DC-SIGN were cultured at 37°C 5% CO_2 in RPMI-1640 containing L-glutamine, supplemented with 10% FBS, 100U/ml penicillin and 100mg/ml streptomycin. One day prior to capture/transfer, $3x10^4$ TZM-bl cells per well were seeded on 96-well plates and cultured overnight. For the capture assay, $0.5x10^6$ Raji or Raji DC-SIGN cells were pelleted by 1min centrifugation at 7000rpm at RT, and mixed with 12.5ng CA-p24 pSG3Δenv, 25ng CA-p24 of pSG3-JR-FL and pSG3-BAL. After 2h incubation at 37°C 5% CO_2, the cells were washed 4x with ice cold PBS. The first supernatant is collected and 15µl of the supernatant is

added as an input control on TZM-bl cells. Raji and Raji-DC-SIGN cells were re-suspended in 45µl of DMEM containing 30ng/ml of Dextran and where 15µl of the suspension was used to infect TZM-bl cells. After 48h at 37°C 5% CO2, the TZM-bl cells were lysed and luciferase activity measured.

b) HIV-1 trans-*infection on TZM-bl in presence of liposomes*

To measure the influence of *Mycobacterium* liposomes on HIV-1 *trans*-infection, liposomes in RPMI-1640 suspension were added to Raji-DC-SIGN, iDCs or mDCs cells prior to capture of virus. Before capture, Raji-DC-SIGN, iDCs or mDCs cells were pre-incubated for 30min at 37°C 5% CO_2 with 100µg of liposome. Subsequently, 12.5ng CA-p24 pSG3Δenv, 12.5ng CA-p24 pSG3-LAI and 25ng CA-p24 of pSG3-BAL were added to cells for 2hr and as described above the cells were washed in PBS and re-suspended RPMI-1640 media and added to TZM-bl cells. After 48h, the infectivity of the TZM-bl cells was measured *via* luciferase activity.

c) HIV-1 trans-*infection in the presence of Mannan*

Mannan, an antagonist of the DC-SIGN receptor and an array of other C-type lectins, was used to determine receptor involvement in HIV-1 *trans*-infection. 20µg/ml or 2mg/ml of mannan (Sigma Aldrich, UK) was pre-incubated with Raji-DC-SIGN, iDCS or mDCs cells for 30min at 37°C 5% CO_2 prior to HIV-1 capture and transfer. The same methods were then performed as described previously with pSG3-LAI virus.

d) HIV-1 trans-*infection in presence of EVs*

HIV-1 *trans*-infection mediated by Raji-DC-SIGN cells was tested in the presence of EVs isolated from plasma using a range of different techniques as described **Part III.**. 50µl of preparation (supernatant, pellet or EVs) undiluted or diluted in PBS were incubated with $0.5x10^6$ Raji-DC-SIGN cells for 30min prior the virus capture. Subsequently, the procedure was similar to that described in the liposome assay Chapter 1 **Part IV.** *Section iv.c)*.

V. Virological assays - Replicative System

i. Viral production by transfection and viral growth

As described for HIV-1 pseudo-typed viral production Chapter 1 **Part IV.** *Section i.*, 293T cells were transfected with plasmids coding for full-length HIV-1. Two HIV-1 replication competent

viruses were produced: BAL-GFP virus recognising CCR5 and expressing GFP (Dorosko and Connor, 2010) and the LAI-YFP virus recognising CXCR4 and expressing YFP, donated by A. de Ronde (University of Amsterdam). The same transfection protocol was used as previously described for pseudo-typed virus production Chapter 1 **Part IV.** *Section i.*. Virus produced following 293T transfection were passaged and expanded on PM-1 cells, a T-lymphoid cell-line permissive for growth of macrophage and T cell tropic virus strains (NIH AIDS). PM-1 cells were maintained at 37°C 5% CO_2 in RPMI-1640 containing L-glutamine and supplemented with 10% FBS, 100U/ml penicillin and 100mg/ml streptomycin. At day 0, PM-1 cells ($2.5x10^6$) were inoculated with 1ml of virus supernatant from transfection of 293T cells in a 15ml tube and incubated at 37°C 5% CO_2. After 18-24h (day 1), the supernatant was removed and fresh PM-1 cells ($5x10^6$) were added in a total of 5ml media and incubated in a T25 flask with fresh media added (day 4). Fresh PM-1 cells and media were added (day 5 and day 8) to allow for virus propagation and maintaining a cell density approximating $1x10^6$ cells per ml. Viruses were harvested (day 11 and day 14), aliquoted and stored at -80°C. Each viral stock concentration was quantified by measuring CA-p24 antigen levels and by determining $TCID_{50}$/ml values described **Part V.** *Section ii.*. Furthermore, aliquots of supernatant (days 4, 8, 11 and 14) were stored at -80°C to monitor virus growth by quantifying HIV-1 CA-p24 production.

ii. Virus quantification by ELISA p24 and $TCID_{50}$/ml

To measure HIV-1 stock concentrations, CA-p24 was quantified using the antigen ELISA protocol 2 from Aalto Bio Reagents. In parallel, an estimation of $TCID_{50}$/ml of virus stock corresponding to 50% tissue culture infectious dose (TCID) was performed. $TCID_{50}$/ml values were determined utilising isolated $CD4^+$ T-lymphocytes enriched as described previously **Part II.** *Section iv.*. The assay was performed in 96-well culture plates with a starting dilution of virus stock at 1:5 in RPMI-1640 media. A succession of 1:5 dilutions (7 fold) was performed with 4 replicates per dilution tested. The volume of virus dilution per well was 100µl with a cell density of $2x10^5$ $CD4^+$ T-lymphocytes per well. The media composition used for the assay was RPMI-1640 containing L-glutamine complemented with 10% FBS, 100U/ml penicillin, 100mg/ml streptomycin and 100U/ml IL-2. The 96-well plate was prepared as follow:

- Columns 1 and 12: 200µl PBS added per well
- Columns 2 through 8: 100µl of cell suspension per well
- Columns 9 through 11: 100µl of media.

The plate was incubated at 37°C 5% CO_2 for 7 days. On day 7, samples were collected for p24 estimation by ELISA: 120µl of each well were harvested and transferred to a new 96-well plate. Virus supernatant was then inactivated by adding 10µl of 2% Empigen-TBS (final concentration 0.1%) and incubated at 56°C for 30min. A CA-p24 ELISA was then performed as described **Part IV.** *Section ii.*, to determinate the number of positive wells positive for CA-p24 (value above 3x standard deviation of control wells). The number of positive wells was multiplied by 2 and using the Muench formula the $TCID_{50}$/ml value was determined.

iii. HIV-1 cis-*infection*

a) Optimisation of HIV-1 cis-infection on CD4⁺T-lymphocytes

At day 0 in a 96-well tissue culture plate $CD4^+$ enriched T-lymphocytes ($2x10^5$/well) were mixed with 40, 200, 1000 or 3000 $TCID_{50}$/ml LAI-YFP or 500, 1000, 3000 $TCID_{50}$/ml BAL-GFP in 200µl total volume per well. Three plates with the same conditions were prepared (1 plate for 1 time point) with 3 replicates per condition per plate and incubated at 37°C 5% CO_2. At day 4, 7 and 10 post-infection, 100µl of supernatant was collected for CA-p24 production determination and 100µl of fresh media RPMI-1640 containing L-glutamine complemented with 10% FBS, 100U/ml penicillin, 100mg/ml streptomycin and 100U/ml IL-2 was added. From condition triplicates, supernatants were pooled and HIV-1 CA-p24 production was determined for each time point by ELISA (Chapter 1 **Part IV** *Section ii.*). In parallel (day 7, 10 and 14) $CD4^+$ T lymphocytes were harvested to measure the percentage of infected cells by FACS analysis. The cells from each condition in triplicate were pooled together, washed in PBS and fixed in 2% PFA before being analysed. After being re-suspended in PBS the cells were acquired by flow cytometry using BD FACS Celesta™ with 10,000 events recorded for each sample and data analysis performed using standard FlowJo software. For LAI-YFP virus, YFP expression was measured to evaluate the percentage of cells infected and GFP expression for BAL-GFP virus.

b) HIV-1 cis-*infection in presence of* Mycobacterium *liposomes*

To measure the influence of *Mycobacterium* liposomes on HIV-1 *cis*-infection, liposomes in suspension in RPMI-1640 were added at day 0 of infection. At day 0, in 96-well culture plates $CD4^+$ enriched T-lymphocytes ($2x10^5$/well) were mixed with 40µg of liposomes and 200 $TCID_{50}$/ml LAI-YFP or 500 $TCID_{50}$/ml BAL-GFP in 200µl total volume per well. BCG, *M. smegmatis*, H37Rv, HN878, CDC1551, EU127 and 0.8PC:0.2Ch liposomes were tested with

LPS used as positive control with 100ng/ml concentration per well. All these conditions were performed in quadruplicate. At day 4, 100µl per well of supernatant was collected for CA-p24 determination and replaced with 100µl of fresh media. At day 7, 50µl per well of supernatant was collected for CA-p24 quantification, then the supernatants left from quadruplicate wells were pooled. $CD4^+$ T-lymphocytes were pelleted by 7min centrifugation at 1,400rpm at RT. Supernatant was collected and stored at -80°C before performing Lumniex® assays **Part II.** *Section vii.*. Cell pellets were frozen at -80°C for subsequent DNA/RNA extraction as described **Part V.** *Section v.*.

iv. HIV-1 trans-*infection*

a) Optimisation of HIV-1 trans-infection in $CD4^+$ T lymphocytes via iDCs

$CD4^+$ T-lymphocytes and iDCs were both isolated from the same blood donor with the methods described **Part II.**. At day 0 of infection iDCs ($6x10^4$/well) were incubated 30min at 37°C 5% CO_2 with 40, 200, 1000, 3000 $TCID_{50}$/ml LAI-YFP or 500, 1000, 3000 $TCID_{50}$/ml BAL-GFP virus. The cells were then washed 4x with PBS and re-suspended in 300µl of media. 100µl of suspension was inoculated with $CD4^+$ T-lymphocytes ($2x10^5$/well) seeded in 100µl per well in a 96-well plate. The media used is the same as used for lymphocyte growth. Two plates with the same conditions were prepared in triplicate for each condition and incubated at 37°C 5% CO_2. At days 4, 7 and 10 post-infection, supernatants were collected in the same way as described for *cis*-infection optimisation for p24 quantification. At day 7 and 14 cells were harvested for FACS analysis (**Part V.** *Section iii.a)*).

b) HIV-1 trans-*infection in presence of* Mycobacterium *liposomes*

To measure the influence of *Mycobacterium* liposomes on HIV-1 *trans*-infection, liposomes in suspension in RPMI-1640 were added during capture and transfer of HIV-1. During virus capture iDCs ($8x10^4$) were incubated with 100µg of liposomes for 30min at 37°C 5% CO_2. The cells were washed and then re-suspended in 400µl of media. 100µl of the suspension was then inoculated on $CD4^+$ T-lymphocytes ($2x10^5$/well) seeded in 100µl per well in a 96-well plate. Finally, 40µg of liposomes were added per well. As for the study of the influence of liposomes on *cis*-infection, supernatants were collected at day 4 and 7 post-infection in a same way and the cells collected at day 7 for the same analysis.

v. HIV-1 DNA quantification

a) DNA/RNA extraction

For DNA and RNA extraction from HIV-1 infection assays, AllPrep DNA/RNA Mini Kit (Qiagen, UK) was used following the manufacturer's instructions. Frozen cell pellets were quickly thawed, mixed with 350µl of lysis Buffer RLT Plus and then incubated at 56°C for 30min to inactivate virus. The cell lysate homogenates were transferred to an AllPrep DNA spin column. After 30sec of centrifugation at 8000g the column (containing DNA) was kept at 4°C during RNA purification. RNA from the eluate was precipitated with 70% ethanol and transferred to an RNeasy spin column. The ethanol was removed by 30sec centrifugation, and the RNA washed successively with Buffers RW1 and RPE. Finally, RNA was eluted from the column with 50µl of RNase-free water. For DNA isolation the column was washed with Buffer AW1 and AW2 before DNA elution with 70µl of Buffer EB. RNA and DNA samples were stored at -80°C.

b) HIV-1 DNA quantification

To proceed to HIV-1 DNA quantification, we used similar techniques previously described by van der Sluis *et al.* and Vandergeeten *et al.* (van der Sluis *et al.*, 2013; Vandergeeten *et al.*, 2014). Total HIV-1 DNA was quantified using primers targeting the LTR region of the virus genome and designed to amplify only fully reverse transcribed DNA. Similar primers were used to quantify 2-LTR circular DNA. Integrated HIV-1 DNA was quantified using primers for the LTR and two primers targeting human Alu sequences that are randomly dispersed across the human genome. All the primers and probes used for those assays are shown Table 1.7. Cell input was quantified using primers targeting the CD3 gene and with a help of a standard based on 293T cells of known concentrations. To distinguish HIV-1 DNA markers, pre-amplifications were performed in 25µl reactions using reaction mixes and primers outlined Table 1.5 and 1.7. Pre-amplification products were then diluted in molecular grade water 1:10 (5µl product with 45µl water) and used as input for qPCR. Quantifications were performed in 20µl reactions using Supermix-UDG (Invitrogen, UK) with the Qiagen Rotor Gene RotorQ using primers and probes detailed in Table 1.6 and Table 1.7.

Table 1.5: Reaction mix for pre-amplification

Reagents 1x Reaction	HIV		CD3	
	Volume (µl)	Final Concentration	Volume (µl)	Final Concentration
Forward Primer 10000nM	0.3	120nM	0.75	300nM
Reverse Primer 10000nM	0.3	120nM	0.75	300nM
H_2O	16.9	-	16	-
10x PCR Buffer	2.5	1x	2.5	1x
$MgCl_2$ 50mM	1.5	3mM	1.5	3mM
Taq 5U/µl	0.25	0.05U/reaction	0.25	0.05U/reaction
dNTP 10nM	0.75	0.3nM	0.75	0.3nM
Total Master Mix:	**22.5**		**22.5**	
Total Sample:	**2.5**		**2.5**	

Table 1.6: Reaction mix for PCR

Reagents 1x Reaction	HIV		CD3	
	Volume (µl)	Final Concentration	Volume (µl)	Final Concentration
Forward Primer 10000nM	0.2	100nM	0.25	1250nM
Reverse Primer 10000nM	0.3	100nM	0.25	1250nM
Probe 10000nM	0.4	200nM	0.4	200nM
2x Supermix UDG	10	1x	10	1x
H_2O	2.8	-	2.7	-
Total Master Mix:	**13.6**		**13.6**	
Total Sample:	**6.4**		**6.4**	

Table 1.7 : Primers and probes used for quantification assays

Assay	Stage	Name	Function	Sequence
Total HIV-1	Pre-amplification	5'PFP	Forward: Total HIV-1	TAACCCTCAGATGCTGCATAWAAGCAGCYGCT
		3'PRP	Reverse: Total	AGCAAGCCGAGTCCTGCGTC
	qPCR	5'PF	Forward: Total HIV-1	GCCTCAATAAAGCTTGCCTTGA
		3'PR	Reverse: Total HIV-1	GGGCGCCACTGCTAGAGAT
		PPr	TaqMan Probe: Total HIV-1	5'-/56-FAM/CTGGTADCT/zen/AGAGATCCCTCAGA/3IABκFQ-3'
2-LTR	Pre-amplification	ULTRF1	Forward: 2-LTR	ATGCCACGTAAGCGAAACTCCTCAATAAAGCTTGCCTTGA
		ULTRR1	Reverse: 2-LTR	CTAACMAGAGAGACCCAGTAC
	qPCR	ULTRR2	Reverse: 2-LTR	GGTACTAGCTTGAAGCACCA
		Lambda T	Forward: 2-LTR & Total	ATGCCACGTAAGCGAAACT
		ULTR2 TaqMan	TaqMan Probe: 2-LTR	ACTCTGGTA/zen/ACTAGAGATCCCTCAGACC
Integrate	Pre-amplification	Alu1		TCCCAGCTACTGGGGAGGCTGAGG
		Alu2		GCCTCCCAAAGTGCTGGGATTACAG
		ULF1: 5'	Forward: Total	ATGCCACGTAAGCGAAACTCTGGGTCTCTCTDGTTAGAC
	qPCR	Lambda T	Forward: 2-LTR & Total	ATGCCACGTAAGCGAAACT
		UR2	Reverse: Total	CTGAGGGATCTCTAGTTACC
		UHIV TaqMan	TaqMan Probe: Total	CACTCAAGG/zen/CAAGCTTTATTGAGGC
CD3	Pre-amplification	HCD3 out 5'	Forward: CD3	ACTGACATGGAACAGGGGAAG
		HCD3 out 3'	Reverse: CD3	CCAGCTCTGAAGTAGGGAACATAT
	qPCR	HCD3 in 5'	Forward: CD3	GGCTATCATTCTTCTTCAAGGT
		HCD3 in 3'	Reverse: CD3	CCTCTCTTCAGCCATTTAAGTA
		CD3 TaqMan	TaqMan Probe: CD3	5'-/56-JOEN/ AGCAGAGAA/zen/CAGTTAAGAGCCTCCAT/3IABκFQ-3'

VI. Statistical Analysis

For all results, the statistical analyses were performed using GraphPad Prism 6.0 software. Unpaired sample comparisons were performed using the non-parametric rank test Mann Whitney and depict in Figures using the following: * for P value< 0.05, ** for P value< 0.01, *** for P value< 0.001, **** for P value< 0.0001.

Chapter 2: Impact of *Mycobacterium* liposomes on modulating immune responses

I. Introduction

In this Chapter, the research focus was on determining the influence of bacterial total lipid extracts from *M. bovis* BCG, *M. smegmatis*, *Mtb* H37Rv, HN878, CDC1551 and EU127 on modulating immune responses. An assay was developed where total lipid extracts from specific bacterial strains could be incorporated into liposomes, thereby mimicking lipid antigen as presented on the bacterial cell wall.

The mycobacterial cell envelope is complex and composed of different lipids such as AG and MA linked to PG and free lipids TDM, PDIM, SL, PIM, LM and LAM described in the Introduction. Lipids from the mycobacterial cell wall play important roles in structural and biological functions. Importantly, because of their localisation and properties, those lipids can modulate the host immune response and specifically interact with various cell receptors influencing *Mycobacterium* pathogenicity.

MA constitutes a natural barrier of the bacteria maintaining the shape and the integrity of the cell. The nature of its composition and oxygenation can modulate the cell wall viscosity and properties influencing *Mtb* pathogenicity (Barry *et al.*, 1998; Dubnau *et al.*, 2000). Oxygenated *Mtb* MA can modulate macrophage activation and differentiation (Vander Beken *et al.*, 2011; Dkhar *et al.*, 2014). Additionally, MA associated with PG and AG can be responsible for inflammatory activation of macrophage and DCs *via* TLR pathway signalling (Means *et al.*, 1999). Interestingly, *trans*-cyclopropanation of MA on TDM can suppress inflammation and *Mtb* virulence (Rao *et al.*, 2006). Additionally, MA can be recognised by specific T cells playing a protective role against *Mtb* infection (Zhao *et al.*, 2015).

The mycobacterial outer membrane contains various acyltrehaloses including TDM (also known as cord factor) and SL. TDM is a major contributor to inflammation (Ryll *et al.*, 2001; Geisel *et al.*, 2005; Linares *et al.*, 2012; Welsh, Hunter and Actor, 2013) and it has been

described to modulate macrophage activation (Ryll *et al.*, 2001; Indrigo, Hunter and Actor, 2002; Ishikawa *et al.*, 2009) and granuloma formation (Hamasaki *et al.*, 2000; Sakamoto *et al.*, 2013). Kan-Sutton *et al.*, showed that TDM presence reduces expression of MCH-II, CD1d, CD40, CD80 and CD86 at the surface of macrophages. Additionally, they described that TDM can supress antigen presentation and T cell stimulation (Kan-Sutton, Jagannath and Hunter, 2009). However, TDM properties are dependent on its composition/structure (Rao *et al.*, 2005, 2006) as well as the intracellular environment (Fischer *et al.*, 2001). SLs are sulphated trehalose esters with SL1 representing the most abundant form produced by pathogenic mycobacteria. The direct role of SL1 in *Mycobacterium* pathogenicity remains unclear (Rousseau *et al.*, 2003; Kumar *et al.*, 2007). However, *mmpL8* knock-out mutants of *Mtb* have been shown to attenuate bacterial virulence in mouse models (Converse *et al.*, 2003; Domenech *et al.*, 2004). Additionally, *Mtb* sft0 mutants showed a better survival than wild-type *Mtb* strains in human macrophages but not in mice, suggesting that SL-1 negatively regulates the intracellular growth of *Mtb* (Gilmore *et al.*, 2012).

PDIMs are found in various *Mycobacterium* species and composed of mycocerosic fatty acids (Daffé and Laneelle, 1988; Daffé *et al.*, 1988). PDIMs have been described to play a role in *Mtb* virulence (Goren, Brokl and Schaefer, 1974; Cox *et al.*, 1999). Rousseau *et al.* have shown that a down regulation of PDIM induces production of high levels of TNF-α and IL-6 by macrophages and DCs in mice (Rousseau *et al.*, 2004). Moreover, PDIMs are important for the maintenance of cell envelope permeability and architecture involved in *Mtb* virulence (Camacho *et al.*, 2001). The presence of PDIMs at the bacterial surface can aide escape from macrophage recognition (Astarie-Dequeker *et al.*, 2009; Quigley *et al.*, 2017), mask PAMPs (Rousseau *et al.*, 2004), and prevent macrophage recruitment (Cambier *et al.*, 2014).

PIMs are glycoconjugates and represent the major components of the mycobacterial cell envelope. They are precursors of LM, LAM and mannan capped lipoarabinomannan (ManLAM). Different forms of PIMs are described depending on the degree of the mannosylation and acylation (Boonyarattanakalin *et al.*, 2008). PIMs play a crucial role in bacterial growth and survival (Haites *et al.*, 2005; Fukuda *et al.*, 2013; Yang *et al.*, 2013). Interactions between mycobacteria PIM derivatives and the host result in delay of phagosome maturation (Fratti *et al.*, 2001; Vergne, Chua and Deretic, 2003; Welin *et al.*, 2008) and modulation of the immune response. Mannoside caps associated to PIMs can be recognised by phagocytic receptors such as C-type lectins, including MR and DC-SIGN (Koppel *et al.*, 2004; Pitarque *et al.*, 2005; Driessen *et al.*, 2009). Additionally, LM has been described

as a TLR2 and TLR4 ligands, modulating anti- and pro-inflammatory responses against the bacteria (Vignal *et al.*, 2003; Quesniaux *et al.*, 2004; Gilleron *et al.*, 2006; Doz *et al.*, 2007; Puissegur *et al.*, 2007).

The proportions of lipids present within the mycobacterial cell wall can vary between the *Mycobacterium* strains and with changed properties (Guenin-Macé, Siméone and Demangel, 2009; Daffé, Crick and Jackson, 2014). However, variation in lipid compositions inside *Mtb* species can occur and impact on their pathogenicity. It has been shown that different clinical *Mtb* strains have been associated with important variations in immune response activation (Lin, Zhang and Barnes, 1998; Theus, Cave and Eisenach, 2005; Theus *et al.*, 2007; Mvubu *et al.*, 2018). In order to measure and compare the impact of total lipid extracts from different *Mycobacterium* and *Mtb* strains, we developed liposomes which contained *Mycobacterium* total lipid extracts. These liposomes are artificial vesicles composed of a mix of PC and cholesterol and used as the experimental foundation in our assays. In many cases, liposomes have been used as a carrier for various applications in pharmacology, including for diagnostic purposes, therapeutic treatments of cancer and use in vaccine technologies (Akbarzadeh *et al.*, 2013). In the context of TB, the interest of using liposomes for vaccination strategies is important and well described in the literature (Sprott *et al.*, 2004; Rosenkrands *et al.*, 2005; Cardona, 2006; Homhuan *et al.*, 2007; Kawasaki *et al.*, 2014; Khademi *et al.*, 2018). In our system, liposomes have been used as a carrier for total lipids from *Mycobacterium* without addition of any adjuvants allowing for the study the immunogenic properties of lipids extracts alone.

The first section of Chapter 2 focusses on characterising the generated liposomes by analysing their compositions and physical properties by TLC and NanoSight technology, respectively (**Part II.** *Section i.*). The second part of the Chapter is dedicated to studying the impact *Mycobacterium* liposomes have on modulating immune responses by studying the influence of BCG, *M. smegmatis*, *Mtb* H37Rv, HN878, CDC1551 and EU127 liposomes on stimulating macrophages, DCs and $CD4^+$ T cells *in vitro* (**Part II.** *Section ii.*) To characterise the activation and the immune responses induced by cells, Luminex® assays have been performed allowing for the simultaneous quantification of the cytokines listed below:

- GM-CSF, M-CSF and G-CSF growth factors implicated in the innate immune response;
- IL-1α, IL-1β, IL-6, IL-8, MIP-1α and MIP-2α implicated in the innate immune response and cell recruitment;
- IL-15 implicated in T cells proliferation and survival;

- IFN-α, IFN-β, IFN-γ, I-TAC, IP-10, MIG and RANTES involved in the adaptive immune response and T cell recruitment;
- IL-12 23p40, IL-12p70, IL-18, IL-23 and TGF-β involved in the adaptive immune response and T cell activation;
- IL-10, IL-27 and TGF-β involved in inducing anti-inflammatory responses.

Furthermore, the study of the impact of liposomes on DCs has been complemented with flow cytometry analyses to measure expression of cellular markers.

II. Results

i. Liposome generation and characterisation

Unilamellar liposomes were generated as described in Chapter 1 **Part I.** *Section ii.***.** Briefly, total lipid extracts from *Mycobacterium* strains (listed in Chapter 1 **Part I.** *Section i.c)*) were mixed together with PC and cholesterol following the ratio 0.6PC:0.2Ch:0.2*Mycobacterium*. After evaporating solvents and obtaining a dry lipid film of the mix, liposomes were obtained by hydration and a sonication step. We characterised 0.8PC:0.2Ch, BCG and *Mtb* H37Rv liposomes generated by NanoSight technology (Figure 2.1 and Figure 2.2) and TLC (Figure 2.3).

We visualised liposome particles using NanoSight NS300 optics and software (Figure 2.1 and Figure 2.2). 0.8PC:0.2Ch, BCG and *Mtb* H37Rv liposomes were compared. Two batches of BCG liposomes were tested in order to validate the technique of liposome generation and its reproducibility. Additionally, three different preparations of 0.8PC:0.2Ch liposomes were generated and tested: 0.8PC:0.2Ch liposomes calibrate at 100nm with the Extruder system, 0.8PC:0.2Ch liposomes calibrate at 200nm with the Extruder system and 0.8PC:0.2Ch obtained from a single sonication step. The calibrate 0.8PC:0.2Ch liposome preparations were used here as particle size controls.

We observed that the mean size obtained for 0.8PC:0.2Ch 100nm liposomes (Figure 2.1 **A.**) was 140.8nm with a unique peak around 140nm from the distribution curve. For 0.8PC:0.2Ch liposomes calibrate at 200nm **B.**, we observed a mean size higher at 182.9nm but with a presence of three peaks between 100 and 200nm from the distribution curve (Figure 2.1). The heterogenous populations of liposomes observed for 0.8PC:0.2Ch calibrating at 200nm

could be explained by the process of sonication that allows for the production of 100nm and 200nm unilamellar liposomes. The additional extrusion step at 200nm after sonication doesn't impact on the population distribution. From these controls, we validated the NanoSight analyses to characterise the size of *Mycobacterium* liposomes and allow for visualisation. 0.8PC:0.2Ch liposomes generated with a single step of sonication **C.** showed a mean size of 171.4nm with heterogenous populations. For the two batches of BCG **D.** and **E.**, we obtained larger sizes at 221.3 and 229nm respectively. The two different preparations of BCG liposomes showed close size values and distributions, validating the reproducibility of the liposome generation technique. Similarly, H37Rv liposomes **F.** we observed a mean size of 201.7nm higher than the 0.8PC:0.2Ch preparation. However, the incorporation of *Mycobacterium* lipids into liposome BCG and H37Rv could explain why these particles appeared bigger than 0.8PC:0.2Ch liposomes.

When comparing particle concentrations, we observed similar order values between liposome preparations included between 0.6-2x10^{12} particles per ml. Images of particle liposomes in solutions are represented Figure 2.2.

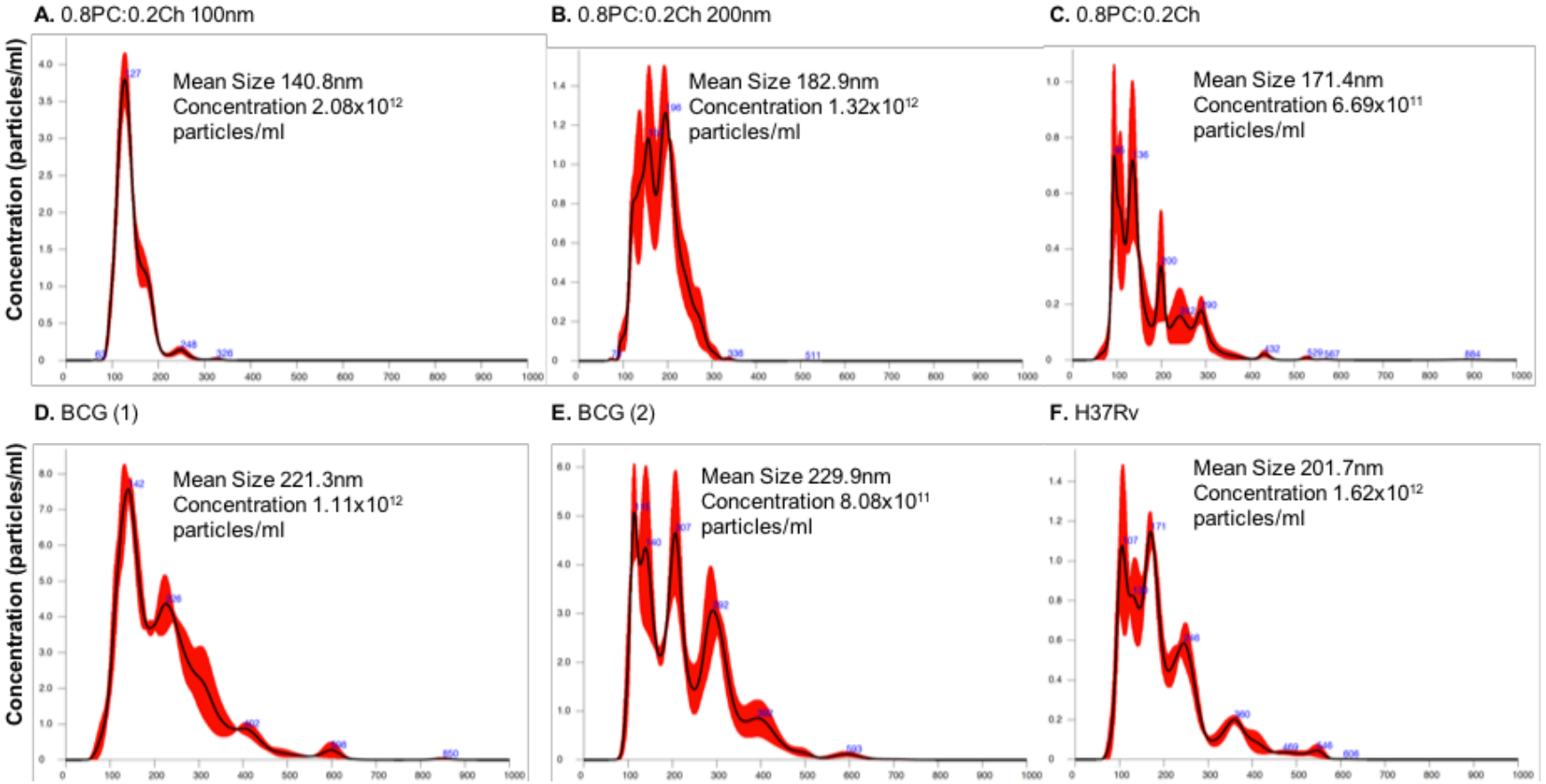

Figure 2.1 : NanoSight analyses of 0.8PC:Ch0.2, BCG and H37Rv liposomes

2. 0.8PC:0.2Ch liposomes generated with Extruder system at 100nm size, **B.** 0.8PC:0.2Ch liposomes generated with Extruder system at 200nm size and **C.** 0.8PC:0.2Ch, **D.** BCG batch n°1, **E.** BCG batch n°2 and **F.** H37Rv liposomes made with by sonication without Extruder step, were analysed on NanoSight NS300. Liposome suspensions were diluted 1:1000-1:2000 in PBS, and three 60sec videos were recording at camera level 13. Post-acquisition were setting with a minimum threshold 7, automatic blur and automatic minimum expected particle size. The data shown are form one experiment

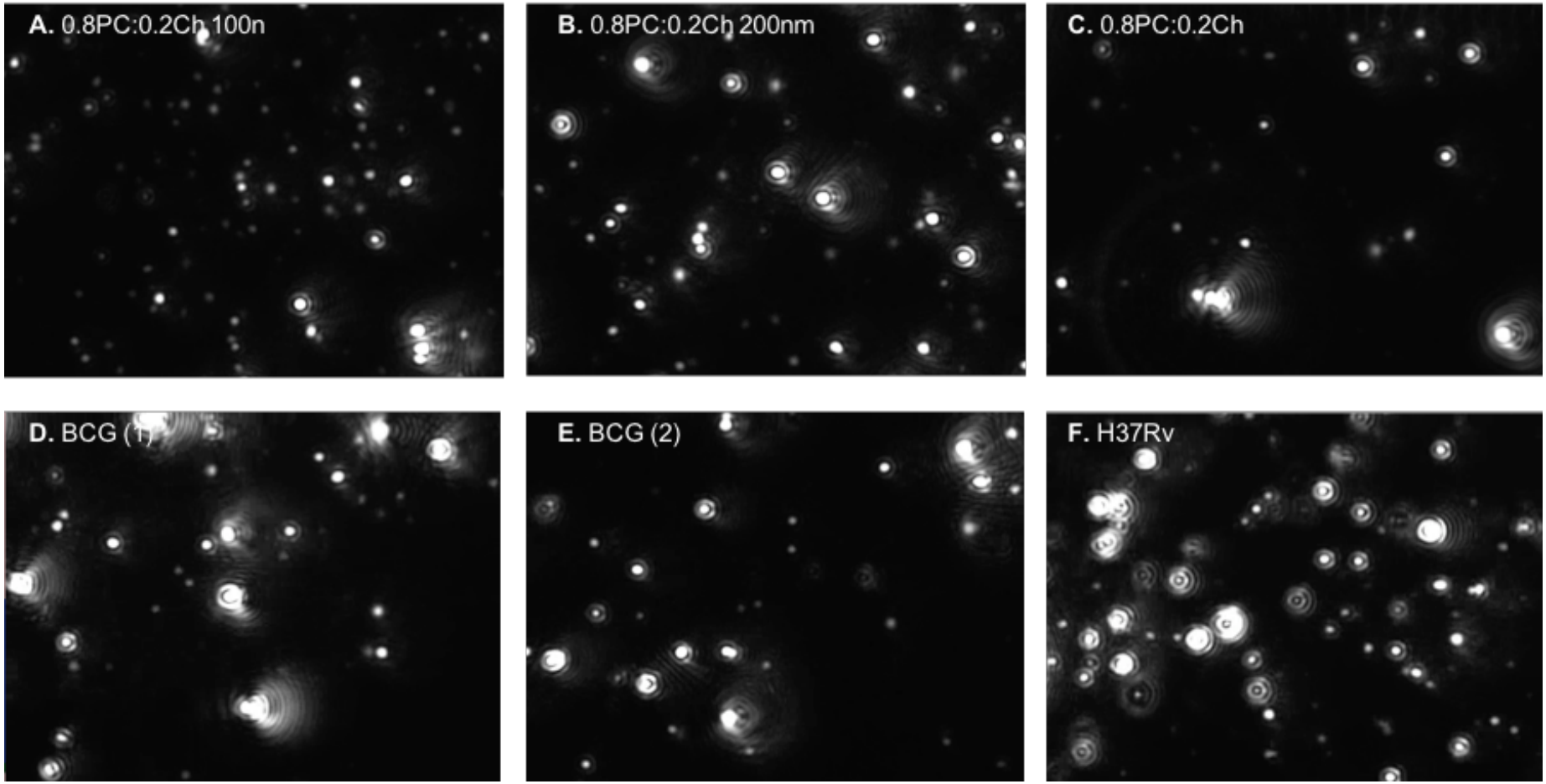

Figure 2.2 : Imaging of 0.8PC:Ch0.2, BCG and H37Rv liposomes from NanoSight analyses

Imaging from NanoSight analyses of **A.** 0.8PC:0.2Ch liposomes generated with Extruder system at 100nm size, **B.** 0.8PC:0.2Ch liposomes generated with Extruder system at 200nm size and **C.** 0.8PC:0.2Ch, **D.** BCG batch n°1, **E.** BCG batch n°2 and **F.** H37Rv liposomes made with by sonication without Extruder step. The data shown are from one experiment.

After visualisation of *Mycobacterium* liposome particles, 0.8PC:0.2Ch, BCG (two batches) and H37Rv liposomes in solution were separated on a silica membrane with 60:16:2 $CHCl_3$:MeOH:H_2O solvent in parallel of TDM, PDIM, SL and PIMs lipids solutions (Figure 2.3).

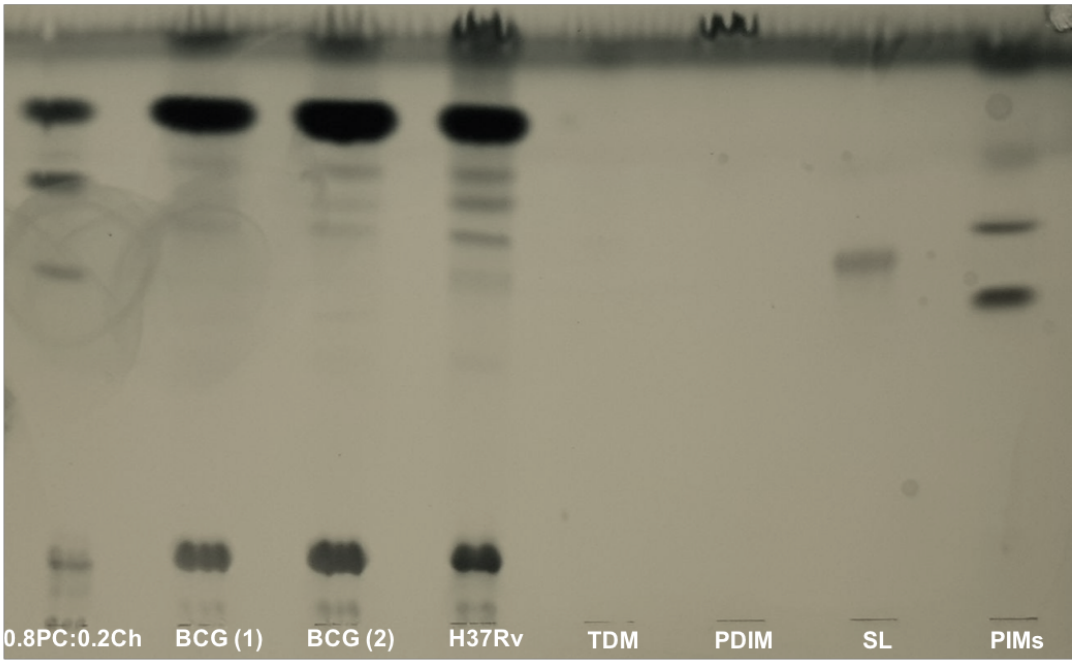

Figure 2.3 : TLC analyses of 0.8PC:Ch0.2, BCG and H37Rv liposomes

10µl of 0.8PC:0.2Ch, BCG batch n°1 (BCG 1), BCG batch n°2 (BCG 2) and H37Rv liposomes solution made in water were spotted and dried on a silica gel 60 F254 plate, in parallel of TDM, PDIM, SL and PIMs solutions. Samples separation occurred in 60:16:2 $CHCl_3$:MeOH:H_2O solvent and visualised by staining with molybdophosphoric acid (MPA) and charring. The data shown are from one experiment performed by Dr A. Bhatt, University of Birmingham.

We observed that the three types of liposomes tested showed specific TLC profiles. 0.8PC:0.2Ch, BCG and H37Rv liposomes shared in common 5 lines that could correspond to the migration of PC and cholesterol present in all the liposome preparations. Also, the two BCG batches showed exactly the same lipid separation profiles. BCG batches presented differences from H37Rv liposome lipid separations. Comparing lipid separation of BCG and H37Rv liposomes with TDM, SL, PDIM and PIMs lipid solution migration, we observed the presence of SL, PDIM and PIMs lipids in these liposomes. However, between BCG and H37Rv we observed variation in the intensity of lipid bands suggesting that SL, PDIM and PIMs are present in higher proportion in H37Rv than BCG liposomes. Unfortunately, we were not able to visual TDM in this assay.

From the TLC analyses we were able to conclude that the integration of specific *Mycobacterium* lipids into the liposomes compared to 0.8PC:0.2Ch control and the

homogeneity between preparations strongly validated the technique of liposome generation used in these studies.

From TLC and NanoSight analyses we validated the *Mtb* liposome generation technique to be utilised in the *in vitro* assays.

ii. Influence of Mycobacterium *liposomes on activating immune cells and cytokine production*

a) Activation of macrophages in presence of Mycobacterium *Liposomes*

In order to measure the impact of glycolipids from *Mycobacterium* strains on the immune response, we investigated the influence of BCG, *M. smegmatis*, *Mtb* H37Rv, HN878, CDC1551 and EU127 liposomes on stimulating MDM immune responses. *Mycobacterium* liposomes were incubated for 18h with macrophages isolated from healthy donors and the supernatants collected to be analysed by Luminex® technology (Figure 2.4). LPS was used as a positive control and 0.8PC:0.2Ch liposomes as a negative control.

We observed that BCG, *M. smegmatis* and *Mtb* H37Rv liposomes, activated the production of the pro-inflammatory cytokines IL-6, IL-8, IL-23, IL-10, IP-10 and TNF-α compared to MDM which did not receive any stimuli. Additionally, EU127 liposomes trended to activate IL-23 and TNF-α production in supernatant, but at a lower degree compared to BCG, *M. smegmatis* and H37Rv. Interestingly, all the *Mtb* liposomes demonstrated a trend towards up-regulating production of IL-15, RANTES and IL-12p40. Conversely, HN878 liposomes showed a trend towards down-regulating production of M-CSF and TGF-β3 as well as CDC1551 and EU127 and production of the anti-inflammatory cytokine IL-10. The positive control LPS showed the capacity to strongly activate production of a large number of the pro-inflammatory cytokines and chemokines, such as IL-6, IL-8, IL-23, MIP-1α, IL-10, IP-10, I-TAC, TNF-α, IL-15, RANTES and IL-12 23p40 and to down-regulate TGF-β1 and 2. MDM responses to LPS validated the assays as did the results with the negative control 0.8PC:0.2Ch liposomes which did not have any significant impact on MDM activity.

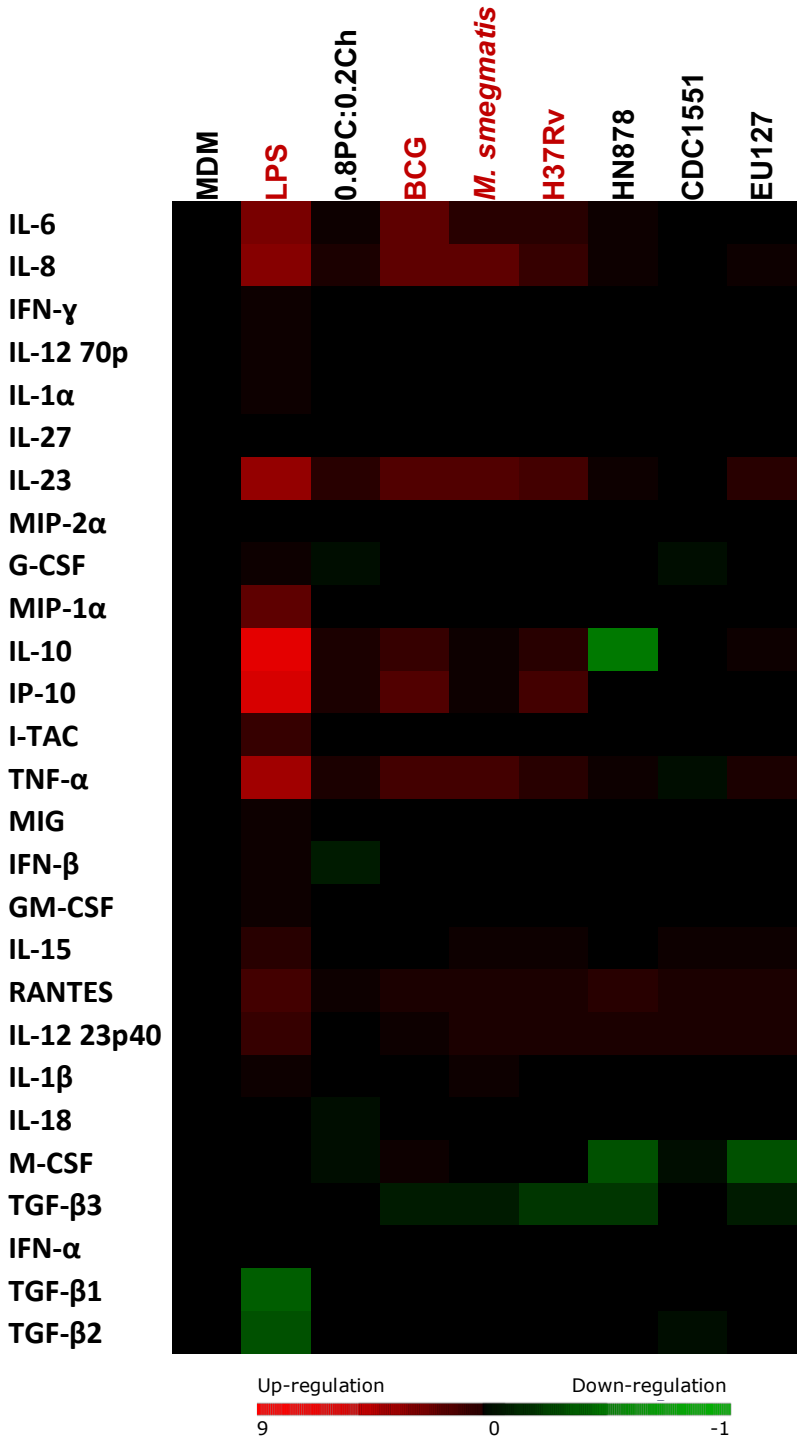

Figure 2.4 : Influence of **Mycobacterium** *liposomes on MDM cytokine production*

Human blood monocytes were isolated from buffy coats by Ficoll gradient centrifugation and a subsequent CD14 selection step using the MACS cell separation system. From $CD14^+$ isolation, MDMs were generated from 7 days of culture. On day 7, 10^6 cells/ml were harvested in 96-well plate and incubated with 5mg/ml LPS or 40µg/ml of 0.8PC:0.2Ch, BCG, *M. smegmatis*, H37Rv, HN878, CDC1551 and EU127 liposomes for 18h. The supernatant was harvested for Luminex® analyses. Luminex results are represented by Heat Map Clusters of the Log2 of liposomes treatment/MDM baseline ratio. An increase of cytokine production in the supernatant is represented in red, a diminution of cytokine production depict in green and no change shown as black. For the data shown, n=3 replicates using cells isolated from one donor.

These observations suggest that *Mycobacterium* liposomes could differentially modulate macrophage immune responses. CDC1551, EU127 and HN878 lipids appeared not to be able to activate MDM response as much as BCG, *M. smegmatis* and *Mtb* H37Rv that induced a heightened response from macrophages.

b) *Activation of iDCs in presence of* Mycobacterium *liposomes*

To further investigate on the influence of *Mycobacterium* liposomes on inducing immune responses, we studied the impact of BCG, *M. smegmatis*, *Mtb* H37Rv, HN878, CDC1551 and EU127 liposomes on iDCs activation. For this purpose, *Mycobacterium* liposomes were incubated for 18h with iDCs. The expression of specific markers of DC activation CD86, CD80, CD40, DC-SIGN and HLA-II, were measured on the cell surface by flow cytometry (Figure 2.5 and Appendixes 6, 7, 8). Additionally, Luminex® measurements were determined utilising the corresponding supernatants (Figure 2.6). LPS and Poly(I:C) were used as positive controls for iDCs activation and 0.8PC:0.2Ch as a negative control.

When comparing the impact of *Mtb* liposomes on modulating the percentage of DCs expressing the CD86 marker (Figure 2.5 **A**), we observed that the presence of *M. smegmatis*, H37Rv and HN878 increased CD86 expression to 71.3, 61.7 and 92.1%, respectively compared to 51.7% in iDCs that did not receive any stimuli. Concerning the CD80 marker, we observed that *M. smegmatis*, H37Rv and HN878 liposomes induced iDC expression of CD80 to 80.0, 76.5 and 97.4%, respectively compared to 72.7% in unstimulated cells. We did not observe any influence of 0.8PC:0.2Ch liposomes on CD86 and CD80 cell surface expression, suggesting that the impact of *M. smegmatis*, H37Rv and HN878 liposomes observed on DCs were due to *Mycobacterium* lipids integrated into liposomes. Also, we observed that the presence of BCG and CDC1551 liposomes did not impact on CD86 and CD80 expression. For CD40, DC-SIGN and HLA-II markers, we did not observe differences on percentage of expression in DC populations (Appendix 9), indicating that all the cells studied were expressing these markers. However, we were able to analyse the MFI for these conditions and determine differences in the proportion of each marker (Figure 2.5 **B**). We did not observe any significant influence of any *Mycobacterium* liposome on CD40 expression compared to LPS and Poly(I:C), which both increased MFI to 598 and 521, respectively, compared to 252 MFI for the unstimulated iDC population. Concerning DC-SIGN, the activation of iDCs resulted in a decrease of expression on the cell surface. We observed that HN878 liposomes strongly down regulated DC-SIGN expression to 392 MFI similar to LPS (384

MFI) and Poly(I:C) (456 MFI). Additionally, *M. smegmatis*, H37Rv and EU127 liposomes showed a trend towards decreasing DC-SIGN cell expression to 498, 501 and 510 MFI, respectively, compared to 577 MFI for iDCs. For the HLA-II marker, we observed that HN878 liposomes induced expression to 492 MFI comparable to LPS and Poly(I:C) with 598 and 555 MFI values, respectively. The presence of *M. smegmatis* demonstrated a trend towards increasing HLA-II expression to 230, compared to 122 MFI for iDCs alone. However, we observed that the presence of BCG and CDC1551 liposomes did not influence the expression of DC-SIGN and HLA-II significantly. The negative control 0.8PC:0.2Ch did not impact on the expression of CD40, DC-SIGN and HLA-II markers. From these observations we could conclude that the influence of *M. smegmatis*, H37RV, HN878 and EU127 on iDC activation were due to the presence of liposome glycolipids.

In conclusion, lipids from HN878 activate the maturation of iDCs to mDCs as shown by inducing the expression of CD86, CD80 and HLA-II and the reduction of DC-SIGN expression. Also, *M. smegmatis* glycolipids present on liposomes, appeared to activate iDCs with a less powerful effect compared to HN878 liposomes. Similarly, *Mtb* H37RV and EU127 lipids demonstrated a trend towards activating iDCs with lower CD86 expression and down-regulation of DC-SIGN receptor expression. However, glycolipids from BCG and CDC1551 did not activate maturation of iDCs in this assay.

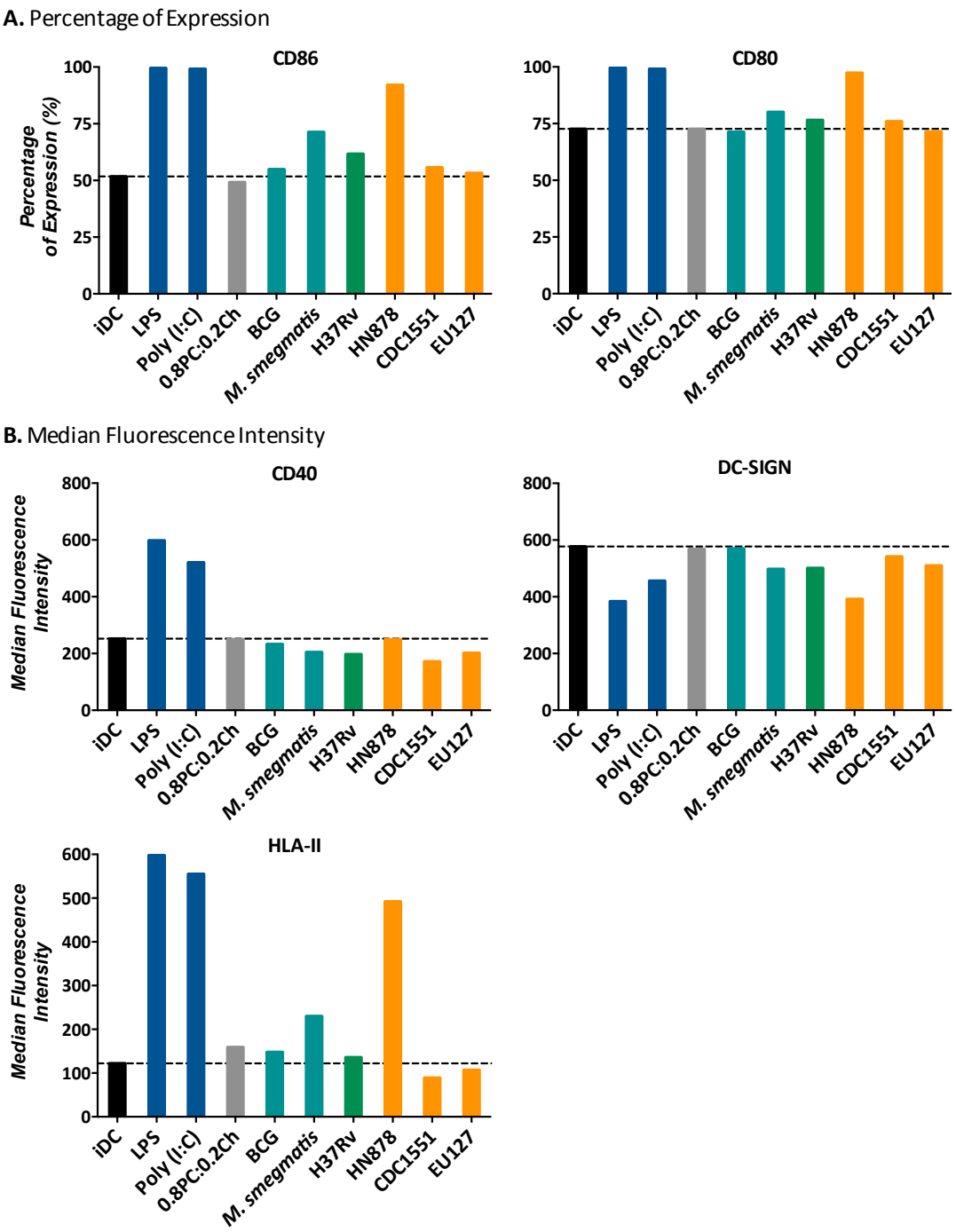

Figure 2.5: Activation of iDCs by* Mycobacterium *liposomes – FACS Analyses

Human blood monocytes were isolated from buffy coats by using Ficoll gradient centrifugation and a subsequent CD14 selection step using the MACS cell separation system. Purified monocytes were differentiated into iMDDCs in the presence of IL-4 and GM-CSF, 70ng/ml and 50ng/ml respectively. On day 6, $0.5x10^6$ iDCs were harvested and incubated with 20µg/ml Poly(I:C), 5mg/ml LPS or 100µg/ml 0.8PC:0.2Ch, BCG, *M. smegmatis*, H37Rv, HN878, CDC1551 and EU127 liposomes for 18h. Then the cells were stained with antibodies against CD80, CD86, CD40, HLA-II and DC-SIGN receptors and **A.** percentage of expression or **B.** The median fluorescence Intensity are measured for each condition after cell fixation with PFA by FACS analyses. The data shown are representative of two independent experiments using cells isolated from two different donors.

Concerning Luminex® analyses of supernatants (Figure 2.6), we observed that the two positive controls LPS and Poly(I:C) induced similar responses from iDCs *via* production of a large number of pro-inflammatory cytokines including IL-6, IL-8, IL-12 70p, IL-23, MIP-2α, G-CSF, MIP-1α, IL-10, IP-10, TNF-α, IFN-β, IL-15, RANTES and IL-12 23p40. Interestingly, the presence of the *Mtb* HN878 liposomes demonstrated a trend towards activating iDCs in a similar way, with an increase in production of IL-6, IL-8, MIP-1α, IL-10, IP-10, TNF-α, IL-15, RANTES and IL-12 23p40, correlating with the flow cytometry analyses. With the negative control 0.2PC:0.8Ch we observed a general reduction in cytokines production, suggesting that the liposome composition of PC and cholesterol might have an impact on iDCs. BCG and *M. smegmatis* liposomes showed a trend towards mimicking 0.8PC:0.2Ch impact, indicating that BCG and *M. smegmatis* glycolipids did not influence iDCs maturation. However, for *M. smegmatis* these observations were not correlated with the flow cytometry analyses whereby *M. smegmatis* showed an induction in CD-86, CD80 and HLA-II expression. Interestingly, *Mtb* H37Rv, CDC1551 and EU127 liposomes showed less impact on the decrease of IL-1α, IL-27, IP-10, TNF-α, GM-CSF and IL-12 23p40, indicating a possible activation of these cytokines produced when compared to the negative control. For the H37Rv and EU127 liposomes this observation correlated with the flow cytometry analysis which suggests a partial activation of iDCs, but not observed with CDC1551.

In conclusion, flow cytometry and Luminex® analysis indicated that *Mycobacterium* liposomes are able to activate iDCs differentially. Glycolipids from *Mtb* HN878 integrated into liposomes, are able to induce a strong pro-inflammatory response from DCs and activate them. Additionally, lipids from *Mtb* H37Rv and EU127 induced partial maturation of iDCs and inflammatory response. However, BCG, *M. smegmatis* and CDC1551 lipids presented in liposomes were not able to activate iDCs.

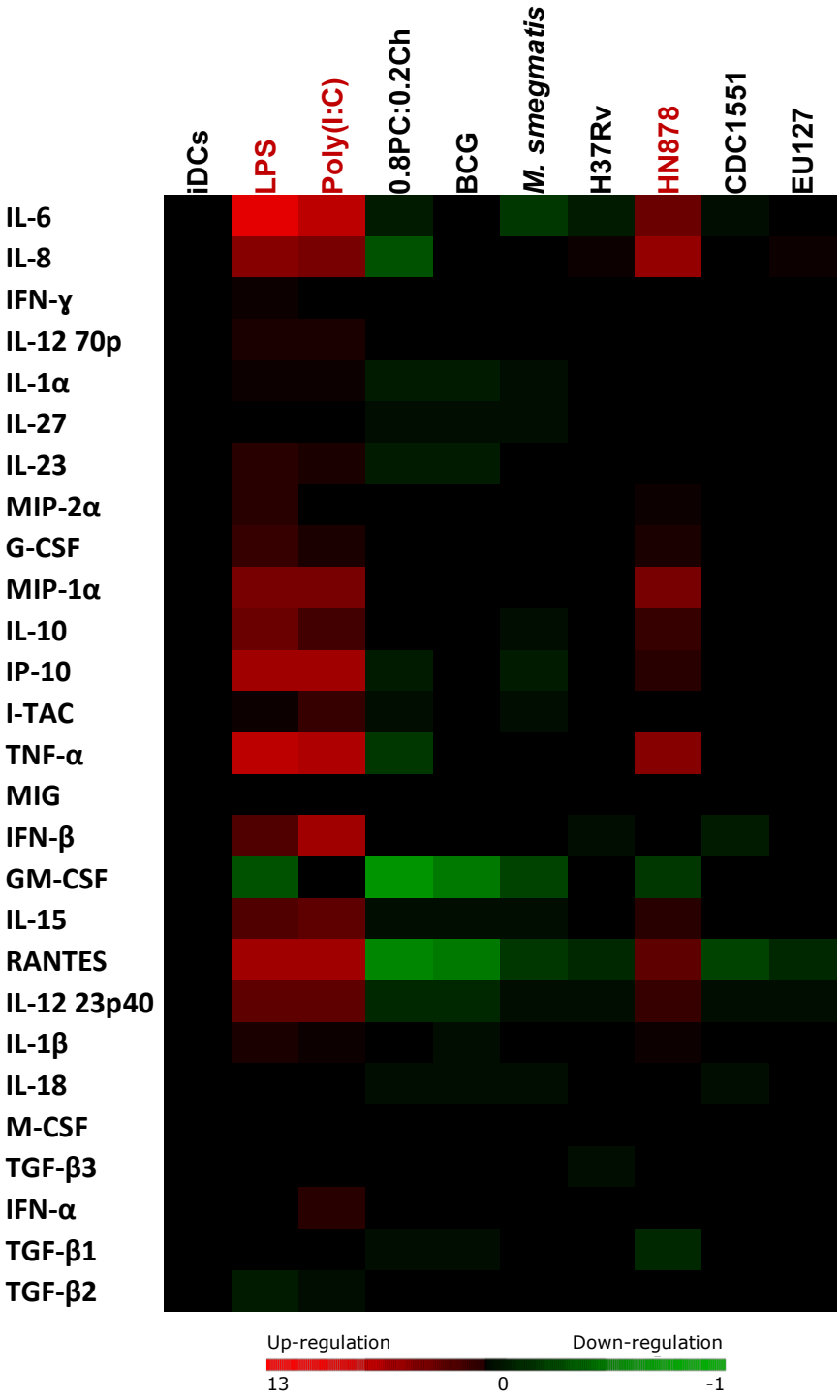

Figure 2.6 : Influence of **Mycobacterium** *liposomes on iDC cytokines production*

Human blood monocytes were isolated from buffy coats by using Ficoll gradient centrifugation and a subsequent CD14 selection step using the MACS cell separation system. Purified monocytes were differentiated into iMDDCs in the presence of IL-4 and GM-CSF, 70ng/ml and 50ng/ml respectively. On day 6, $0.5x10^6$ iDCs were harvested and incubated with 20µg/ml Poly(I:C), 5mg/ml LPS or 100µg/ml 0.8PC:0.2Ch, BCG, *M. smegmatis*, H37Rv, HN878, CDC1551 and EU127 liposomes for 18h. Then the supernatant from each condition were harvested for Luminex® analyses. Luminex results are represented by Heat Map Clusters of the Log2 of liposomes treatment/iDCs baseline ratio. An increase of cytokine production in the supernatant is represented in red, a diminution of cytokine production depict in green and no change shown as black. For the data shown, n=3 using cells isolated from one donor.

c) Activation of iDCs in presence of H37Rv liposome: role of SL1

We then characterised the maturation of iDCs induced by *Mtb* H37Rv and the implication of SL1 as its role in *Mtb* pathogenesis is not well described. For this purpose an H37Rv mutant papA1Δ was utilised. Polyketide associated-protein-1 (papA1) is an acetyltransferase enzyme present on the cytoplasmic side of the plasma membrane of *Mtb* and is involved in biogenesis of SL1. papA1Δ mutants result in the absence of SL1 on the mycobacterial cell wall. Liposomes with total lipids from H37Rv papA1Δ have been generated and tested in parallel to liposomes containing papA1Δ lipids complemented with soluble SL1. As described above liposomes were incubated for 18h with iDCs and the expression of specifics markers of DC activations CD80, CD40, DC-SIGN and HLA-II were then measured on the cell surface by flow cytometry (Figure 2.7 and Appendixes 10, 11, 12). 0.8PC:0.2Ch liposomes were used as a negative control and LPS and Poly(I:C) as positive controls for iDC maturation.

We observed that H37Rv liposomes induced expression of the CD80 marker on DCs to 58.0% compared to 33.6% for iDCs that had not been stimulated with liposomes (Figure 2.7 **A**). However, papA1Δ liposomes were shown to activate expression of CD80 to a lesser extent, with expression measured at 43.3%. Interestingly, liposomes containing papA1Δ total lipid complemented with soluble SL1 induced expression of CD80 at a similar level to H37Rv, with 55.5% DCs expressing CD80. LPS and Poly(I:C) both increase expression of CD80 to 99.0% of cells expressing the marker whilst 0.8PC:0.2Ch liposomes did not influence CD80 expression (38.7%), as expected. Altogether these observations suggest that SL1 is involved in the activation of CD80 expression during iDC maturation, induced by *Mtb* H37Rv. As described previously, we were not able to measure differences on the percentage of expression in DC populations for the CD40, DC-SIGN or HLA-II markers (Appendix 13), but we analysed MFI to determine the difference in proportion of each marker within the expressing cell population (Figure 2.7 **B**). We observed that H37Rv, papA1Δ and papA1Δ + SL1 liposomes similarly activated CD40 expression on iDCs to 224, 237 and 209 MFI, respectively compared to 167 for iDCs and 171 MFI for 0.8PC:0.2Ch liposomes. Also, LPS and Poly(I:C) strongly induced CD40 expression with 600 and 655 MFI measurements, respectively. These results suggest that SL1 is not involved in modulating CD40 expression during iDCs maturation induced by H37Rv. Concerning DC-SIGN, we observed that H37Rv and papA1Δ complemented with SL1 showed comparable MFI values obtained at 696 and 684 MFI, respectively. However, the presence of papA1Δ liposomes did not induce reduction of DC-SIGN expression with 721 MFI compared to iDCs with a 732 MFI.

The two positive controls significantly reduced DC-SIGN expression on DCs to 449 MFI for LPS and 468 MFI for Poly(I:C). However, the negative control liposome 0.8PC:0.2Ch also decreased DC-SIGN expression to 693 MFI, therefore we couldn't conclude on the specific role of SL1 modulating DC-SIGN expression. Finally, for HLA-II we observed that H37Rv liposomes induced expression to 582 MFI compared to 437 MFI for iDCs with no stimulation. Interestingly, papA1Δ and papA1Δ + SL1 liposomes did not activate HLA-II expression. LPS and Poly(I:C), as expected, induced high expression of HLA-II with 1,024 and 964 MFI measured, respectively compared to 429 MFI for 0.8PC:0.2Ch. These results suggest that SL1 is not involved in modulating HLA-II expression during iDCs maturation with H37Rv liposomes.

In conclusion, H37Rv lipids integrated into liposomes could partially activate iDCs by inducing the expression of CD80, CD40 and HLA-II markers and SL1 is likely involved in iDCs maturation by activating expression of CD80.

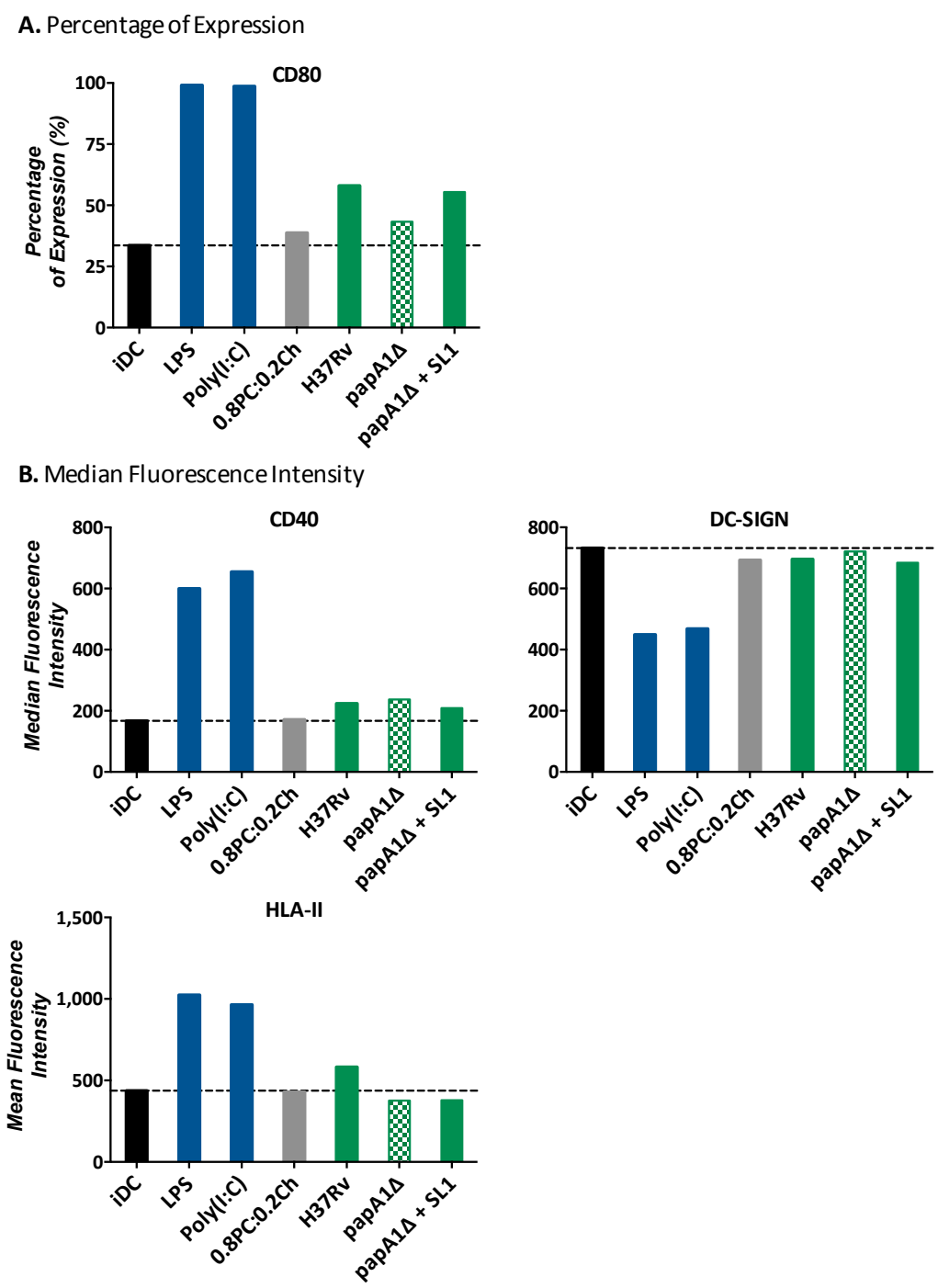

Figure 2.7 : Activation of iDCs by H37Rv - Role of SL1

Human blood monocytes were isolated from buffy coats by using Ficoll gradient centrigugation and a subsequent CD14 selection step using the MACS cell separation system. Purified monocytes were differentiated into iMDDCs in the presence of IL-4 and GM-CSF, 70ng/ml and 50ng/ml respectively. On day 6, $0.5x10^6$ iDCs are harvested and incubated with 20µg/ml Poly(I:C), 5mg/ml LPS or 100µg/ml 0.8PC:0.2Ch, H37Rv, papA1Δ, papA1Δ+SL1 liposomes for 18h. Then the cells stained with antibodies against CD80, CD40, HLA-II and DC-SIGN receptors and **A.** percentage of expression or **B.** the median fluorescence intensity are measured for each condition after cell fixation with PFA by FACS analyses. The data shown are form one experiment using cells isolated from one donor.

d) Co-culture of iDCs and CD4+T cells in presence of liposomes

Finally, in order to characterise the influence of *Mycobacterium* liposomes on the induction of immune responses, we analysed the cytokine production in iDCs and $CD4^+$ T lymphocytes co-cultures *in vitro* in the absence and presence of liposomes. iDCs and $CD4^+$ T cells were incubated for 7 days with *Mycobacterium* liposomes and the supernatants were collected for Luminex® analyses (Figure 2.8). LPS was used as a positive control, however, 0.8PC:0.2Ch couldn't be used as a negative control in this assay as the liposomes were found to be toxic to $CD4^+$ T cells (Appendix 14).

In the context of iDCs and $CD4^+$ T cell co-culture, the presence of LPS induced a global activation in production of several pro-inflammatory cytokines, including IL-6, IL-8, IFN-γ, IL-1α, IL-23, MIP-1α, IL-10, IP-10, TNF-α and IL-1β. Compared to the positive control, only *Mtb* H37Rv liposomes demonstrated a trend towards activating production of IL-8, MIP-1α and IL-15. Indeed, for all the other liposomes, BCG, HN878, CDC1551 and EU127, we observed that their presence in the context of iDCs/$CD4^+$ T cell co-cultures showed a trend towards decreasing production of a number of pro-inflammatory cytokines including MIP-1α. Additionally, H37Rv induces a decrease in IL-10, GM-CSF and M-CSF production. Interestingly, all the studied *Mtb* strains demonstrated a trend towards decreasing production of IP-10 and MIG.

In conclusion, H37Rv liposomes demonstrated a trend towards stimulating expression of pro-inflammatory cytokines from co-cultured iDCs and $CD4^+$ T cells. Conversely, EU127, CDC1551 and HN878 liposomes showed a trend towards decreasing pro-inflammatory responses whilst BCG did not induce any specific responses. From this observation we can conclude that H37Rv lipids can modulate and activate immune responses within co-cultured cells.

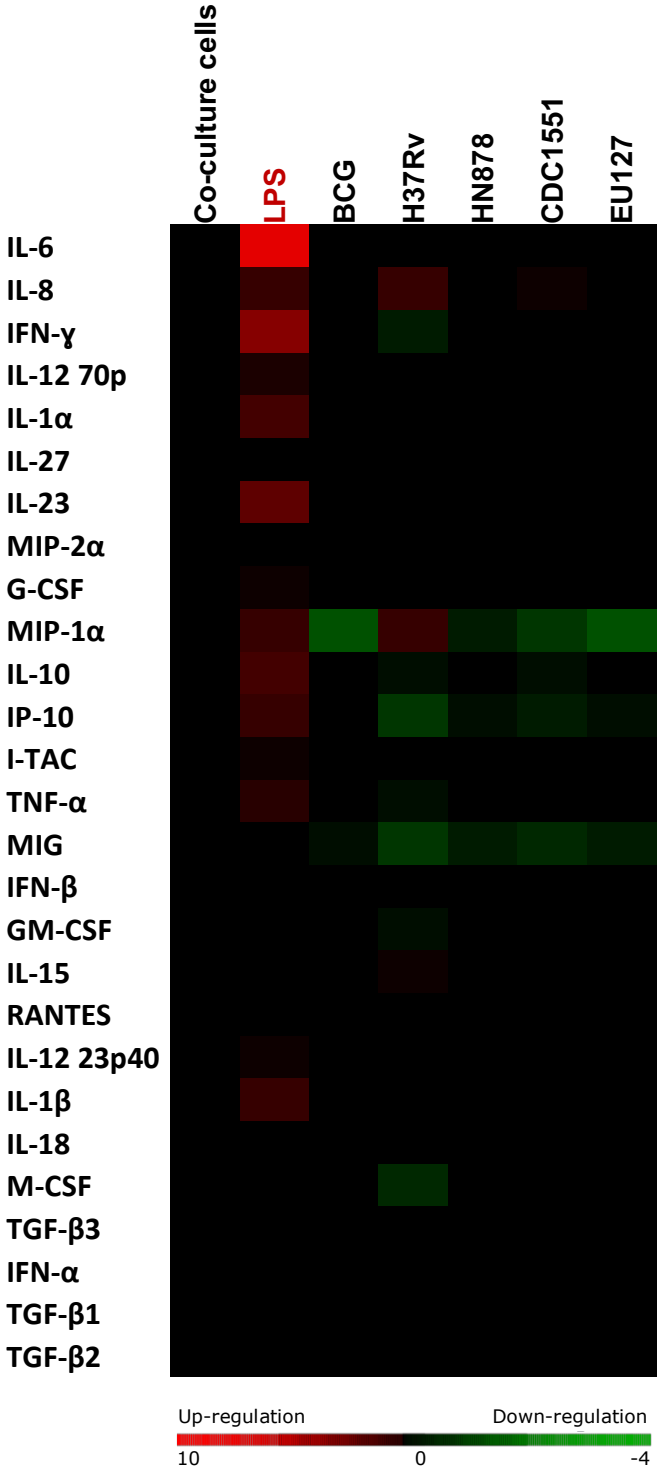

Figure 2.8 : Influence of* Mycobacterium *liposomes on CD4⁺T and iDCs co-culture cytokine production

In a 96-well plate $2x10^4$ iDCs were placed in culture with $2x10^5$ $CD4^+$ T lymphocytes per well and incubated with 5mg/ml LPS or 40µg of BCG, H37Rv, HN878, CDC1551 and EU127 liposomes. At day 4, the supernatant from each condition were harvested for Luminex® analyses. Luminex results are represented by Heat Map Clusters of the Log2 of liposomes treatment/cells baseline ratio. An increase of cytokine production in the supernatant is represented in red, a diminution of cytokine production depict in green and no change shown as black. For the data shown, n=3 using cells isolated from one donor.

III. Conclusion

From the characterisation and analyses of liposomes performed by TLC and NanoSight technologies, we validated our technique of liposome generation. Indeed, liposomes produced with BCG total lipids, showed consistency in sizes, concentrations (Figure 2.1 and 2.2) and composition from two preparation batches. Additionally, liposomes showed specific compositions depending on the origin of the *Mycobacterium* lipids as we were able to visualise the presence of PDIM, SL and PIMs integrated into BCG and H37Rv liposomes at different proportions (Figure 2.3). However, theses analyses need to be followed up and confirmed by mass spectrometry which will inform the exact chemical composition of the generated liposomes. This will enable for the identification of the specific lipid compositions of each studied *Mycobacterium* strain and provide for quantification of lipid incorporation into liposomes.

From analysing the influence of *Mycobacterium* liposomes on modulating immune responses, the results demonstrate various impacts depending on the origin of the *Mtb* strain being studied and also on the immune cells utilised (summarised Table 2.1). For macrophages, we showed that BCG, *M. smegmatis* and *Mtb* H37Rv were able to activate macrophage by inducing production of pro-inflammatory cytokines (Figure 2.4). These results suggest that BCG, *M. smegmatis* and H37Rv liposomes can induce innate immune responses within MDM *via* TNF-α production through activating IL-6, IL-8, MIP-1α, IL-10 and IL-12 expression and where *Mtb* EU127 showed the capacity to induce partial activation of MDM. Interestingly, in our *in vitro* assays all the liposomes induced production of IL-15, RANTES and IL-12p40. Concerning iDCs maturation, we observed that HN878 liposomes activated differentiation of iDCs by expression of CD80, CD86 and HLA-II surfaces markers and by induction of expression of a large number of pro-inflammatory cytokines including IL-12 and chemokines (Figures 2.5 and 2.6). Additionally, H37Rv and EU127 liposomes showed the capacity to activate iDCs but to a lower extent compared to HN878. Conversely, BCG, *M. smegmatis* and CDC1551 liposomes did not exhibit any impact on iDC maturation.

H37Rv liposomes are able to induce immune responses from MDM and iDCs, where in both assays H37Rv liposomes induced production of different cytokines and where the MDM response is stronger than seen with iDCs (no clear induction of cytokines production in this case). These results suggest that H37Rv lipids are able to activate immune responses from MDM and partially from iDCs, potentially through engaging different receptors expressed on

the different cell types. From H37Rv total lipids, LAM, LM and PIM showed the capacity to induce IL-8 expression in macrophages, which are involved in neutrophil recruitment (Zhang, Broser, *et al.*, 1995; Riedel and Kaufmann, 1997; Ameixa and Friedland, 2002; Krupa *et al.*, 2015). The induction of IL-8 in our *in vitro* assays could be due to the presence of LAM, LM or PIMs integrated within H37Rv liposomes. IL-23 has been described to be produced during *Mtb* infection and to be involved in T cell proliferation and differentiation (Khader *et al.*, 2005). Our results suggest that glycolipids integrated into H37Rv liposomes are implicated in IL-23 production from MDM. Additionally, isolated PIM and ManLAM from the H37Rv strain were associated with induction of iDC maturation in the presence of LPS *in vitro* (Mazurek *et al.*, 2012), suggesting that PIM and ManLAM present on liposomes could be involved in the maturation of iDCs. Also, our assays suggest a role of SL-1 expressed by H37Rv in DC activation where SL1 induced CD80 expression during iDCs maturation (Figure 2.7). *Mtb* EU127 is a clinical strain where the lipids have shown the capacity to induce partial maturation of MDM and iDCs, similar to H37Rv liposomes. This result suggests that lipids expressed by EU127, as similarly found in H37Rv, can activate MDM and iDCs.

Interestingly, comparing the impact of BCG, *M. smegmatis*, HN878 and CDC1551 liposomes on MDM and iDCs assays, we observed different profiles of activation. BCG and *M. smegmatis* liposomes clearly induced activation of MDM similar to H37Rv. However, none of them were able to activate differentiation of iDCs. For HN878 liposomes, the opposite phenomenon was observed where HN878 strongly activated iDCs but not macrophages. This was similar for EU127 liposomes which showed a lower degree of MDM and iDCs activation comparable to H37Rv. The observed differences between the two experiments could be explained by the presence of cell types showing variant degrees of activation. The response of macrophages and iDCs is depending on the stimuli which can generate differences in the metabolism within the cells, therefore effecting the induced immune responses measured (Kelly and O'Neill, 2015).

Concerning the ability of BCG liposomes to induce iDCs maturation, Sprott *et al.* described in 2004 induction of pro-inflammatory cytokines from iDCs incubated with liposomes containing total polar lipids from BCG where mannose and/or palmitoylated-mannose are involved in TNF production, PIMs and LAM in IL-12 production and IL-6 in mice (Sprott *et al.*, 2004). Compared to our *in vitro* assays, Sprott *et al.* used liposomes containing ovalbumin on immunised mice and this could explain why we were not able to visualise maturation of iDCs with BCG liposomes in our system. Also the proportion of total lipids from BCG incorporated

within the liposomes could be too low to observe activation of the cells. However, lipids associated with liposomes from BCG and *M. smegmatis* were able to activate macrophages, similarly to H37Rv, suggesting that the same lipids present in BCG, *M. smegmatis* and H37Rv could be involved in MDM activation. In accordance with these results, *M. smegmatis* total lipids incorporated into liposomes, similar to our assays, have been associated with immunogenic properties in mice creating cross reactions against *Mtb* antigens and making *M. smegmatis* liposomes a good candidate for TB vaccination (de los Angeles García *et al.*, 2013).

For CDC1551 liposomes, we observe a trend towards activation of MDM with production of IL-15, RANTES and IL-12, but we did not observe any impact on iDC maturation. These results suggest that lipids from CDC1551 were partially able to activate of MDM but not DCs. However, the CDC1551 *Mtb* strain has been described to induce production *in vitro* and *in vivo* of pro-inflammatory cytokines. In infected animals, the production of cytokines was associated with a long term survival of the bacteria (Manca *et al.*, 1999). Our *in vitro* system might need to be optimised to observe similar results as already described. Indeed, higher concentrations of liposomes or different liposome compositions should be tested in order to reproduce these observations. A more indepth analysis and quantification of lipid incorporation within liposomes may shed light on the lack of observed stimulations.

Concerning HN878 liposomes, lipids from *Mtb* HN878 showed a strong capacity to activate iDCs compared to the other *Mtb* strains studied, but not MDM. HN878 is a virulent *Mtb* strain described to be able to reduce TH1 immune responses at the early stage of infection by production of type I IFNs (Manca *et al.*, 2001; Ordway *et al.*, 2007). However, in our *in vitro* system even if we observed a down regulation of pro-inflammatory cytokine production from MDM in the presence of HN878 liposomes, we were not able to visualise any augmentation in production of IFN-α/β as well as for iDCs despite a strong activation of cells.

From the analyses on MDN and DC activation we observed variations between *Mtb* strains in their ability to induce immune responses (Figures 2.4, 2.5 and 2.6). Additionally, with the *in vitro* assay on iDCs and $CD4^+$ T lymphocytes co-cultures, we observed significant differences on cytokines production profiles from the cells in response to the *Mtb* lipids integrated within liposomes (Figure 2.8).

Concerning *Mtb* H37Rv liposomes, we observed a pro-inflammatory response from iDCs (suggested by production of chemokines MIP-1α, IL-8 and production of cytokines IL-15) and $CD4^+$ T lymphocytes. These results suggest that incubation with H37Rv lipids promotes interactions between $CD4^+$ T lymphocytes and DCs, stimulating adaptive immune responses that induce T cell proliferation and differentiation. Interestingly, we did not observe any decrease in IFN-γ. This observation could be explained by testing supernatants on day 7 post-incubation with liposomes and not 18h as with MDM and iDCs and where the cytokine has been internalised and consumed by the cells. However, BCG, *Mtb* HN878, CDC1551 and EU127 demonstrated a trend towards down regulating pro-inflammatory cytokine production during co-culture. Because HN878 and EU127 showed the capacity to activate iDCs maturation, we can hypothesise that these results could be due to variations in the assays or because of the consumption of cytokines at day 7.

In this Chapter we described the ability of lipids from *Mtb* to induce differential immune responses, suggesting *Mtb* lipids from variant strains can differentially stimulate and modulate the types of innate and adaptive immune responses mounted in infection. The variation observed with the studied glycolipids could explain the variation observed in *Mtb* pathogenicity (Lin, Zhang and Barnes, 1998; Theus, Cave and Eisenach, 2005; Theus *et al.*, 2007; Guenin-Macé, Siméone and Demangel, 2009; Daffé, Crick and Jackson, 2014; Mvubu *et al.*, 2018). In the case of HIV-1 and *Mtb* co-infection, *Mtb* infection and recognition by the immune system can impact on HIV-1 infection where TB leads to the activation of immune responses, including activation of macrophages/DCs, recruitment of lymphocytes, co-receptors expression and production of pro-inflammatory cytokines. The variation in immune responses induced by *Mtb* lipids as observed in this Chapter could then modulate HIV-1 infection and subsequent replication (Chapters 3 and 4). The results presented here could be expanded upon by measuring the effects of *Mtb liposomes* on whole PBMC cultures as well as other purified cell populations. Furthermore, variant compositions of liposomes could be tested containing different concentrations of incorporated total lipid extracts or fractionated lipids such as LAM, LM or PIM.

Table 2.1 : Results Summary

Conditions	BCG	*M. smegmatis*	H37Rv	HN878	CDC1551	EU127
MDM 18h activation	↑ TNF-α ↑ IL-6/IL-15 ↑ IL-12 23p40/IL-23 ↑ IL-10 ↑ MIP-1α /RANTES/IL-8 ↓TGF-β3			↑ IL-12 23p40 ↑ RANTES ↓M-CSF ↓ IL-10 ↓TGF-β3	↑ IL-15 ↑ IL-12 23p40 ↑ RANTES	↑ TNF-α ↑ IL-15 ↑ IL-12 23p40 ↑ IL-23 ↑ IL-10 ↑ RANTES ↓M-CSF ↓TGF-β3
iDC 18h activation	-	-	(↑) GM-CSF (↑) TNF-α (↑) IL-1α/IL-15 (↑) IL-12 23p40 (↑) IL-23/IL-27 (↑) IP-10 ↑ Low expresson CD86, CD80 and HLA-II	↑ TNF-α ↑ IL-6/IL-15 ↑ IL-12 23p40 ↑ IL-10 ↑ MIP-1α/RANTES ↑ IL-8 ↑ IP-10 ↓ GM-CSF ↓TGF-β1 ↑ Expression CD86, CD80 and HLA-II	(↑) GM-CSF (↑) TNF-α (↑) IL-1α/IL-15 (↑) IL-12 23p40 (↑) IL-23/IL-27 (↑) IP-10	(↑) GM-CSF (↑) TNF-α (↑) IL-1α/IL-15 (↑) IL-12 23p40 (↑) IL-23/IL-27 (↑) IP-10 ↑ Low expression CD86
iDC/CD4⁺ T cells co-culture 7 days culture	↓ MIP-1α	-	↑ IL-15 ↑ MIP-1α/IL-8 ↓ IFN-γ ↓ GM-CSF/M-CSF ↓ IL-10	↓ MIP-1α/MIG ↓ IP-10		

Chapter 3: Impact of *Mycobacterium* liposomes on HIV-1 *cis*-infection

I. Introduction

Infection with *Mycobacterium tuberculosis* (*Mtb*) creates a favourable environment for HIV-1 infection and/or replication through activation and induction of immune responses. We described in Chapter 2, how *Mtb* lipids associated with liposomes can modulate immune responses and potentially influence HIV-1 infection. In this Chapter, we study specifically how *Mtb* antigens in the context of liposomes can impact directly on HIV-1 *cis*-infection.

Immune cells including $CD4^+$ T lymphocytes, monocytes/macrophages, and DCs are the main target cells of HIV-1. Virus enters target cells by initially binding to the CD4 receptor molecule mediated by the viral surface glycoprotein Env. Following conformational changes, the gp120 sub-unit interacts with the co-receptor(s) CCR5 and/or CXCR4 to facilitate entry through membrane fusion and injection of the capsid into the cell. After entry, the capsid containing two copies of the HIV-1 genome is uncoated thereby releasing the viral RNA molecules into the cell cytoplasm. The process of reverse transcription results in viral RNA being copied into dsDNA. The dsDNA molecule is then translocated to the nucleus where it is integrated into the host genome. After integration, transcription regulatory factors including Sp, NF-κB, C/EBP, NFAT or AP-1 bind to the HIV-1 LTR-region to promote gene expression resulting in viral protein translation and viral assembly to generate new virions and completing the viral life-cycle (Lawn, Butera and Folks, 2001; Maartens, Celum and Lewin, 2014).

It was previously discussed that recognition of *Mtb* components by various cell-types within the immune system can activate PRR as well as intracellular signalling pathways. TB thereby creates a favourable environment for infection and/or replication HIV-1 through the modification/translocation of transcription factors and the resultant enhancement of HIV-1 LTR activity. In this context, *Mtb* has been described to increase HIV-1 replication in co-infected macrophages *in vitro* (Zhang, Nakata, *et al.*, 1995b; Goletti *et al.*, 1996; Lawn *et al.*, 2001; Hoshino *et al.*, 2002; Ranjbar *et al.*, 2009). TLR2 and TLR4 expression within immune

cells in HIV-1 patients infected with *Mtb* is up-regulated in comparison to HIV-1 patients not co-infected (Hernández *et al.*, 2012). TLR2 stimulation with soluble *Mtb* factors was shown to induce HIV-LTR transactivation, but also with TLR9 co-stimulation (Equils *et al.*, 2003). PIM_6 *in vitro* induces HIV-1 replication minimally and depending on TLR2 signalling (Rodriguez *et al.*, 2013). Bafica *et. al*. have demonstrated that there is a TLR2 dependant induction of HIV-1 in an HIV-1-transgenic mouse model (Bafica *et al.*, 2003). Moreover, *Mtb*-TLR engagement stimulates post-transcriptional modifications of C/EBP proteins, which in turn promotes C/EBP-dependent activation of the HIV-1 LTR. The *Mtb* proline-proline-glutamic acid (PPE) protein Rv1168c (PPE17) increases HIV-1 LTR transcription in monocyte/macrophage infected cells. The interaction between LRR motifs 11–15 of PPE17 and TLR2 leads to the downstream activation of NF-κB resulting in HIV-1 LTR transactivation (Bhat *et al.*, 2012). *Mtb* cell wall components rich in carbohydrate-containing molecules, such as PIMs, LM, LAM, polysaccharides or glycoproteins (19 kDa, 45 kDa and 38 kDa antigens), can interact with C-type lectin receptors expressed by DCs and macrophages and induce NF-κB pathways (Tailleux *et al.*, 2003; Geijtenbeek *et al.*, 2003; Koppel *et al.*, 2004; Neyrolles, Gicquel and Quintana-Murci, 2006; Driessen *et al.*, 2009; Geurtsen *et al.*, 2009; Gringhuis *et al.*, 2009; Ehlers, 2010; Falvo *et al.*, 2011; Lugo-Villarino *et al.*, 2011; Philips and Ernst, 2012). *Mtb* strains differ with regards to the cell wall composition which can differentially alter HIV-1 replication and disease progression profiles in HIV-1/*Mtb* co-infected individuals. Indeed, *in vitro* infection of PBMC from healthy donors has shown that HIV-1 replication is increased in the presence of antigens from the CDC1551 *Mtb* strain relative to viral replication in the presence of antigens from the HN878 strain. This observation is associated with increased levels of transcription and nuclear translocation of the p65 subunit of the transcription factor NF-κB by CDC1551 compared to HN878 (Ranjbar *et al.*, 2009).

PRR activation by *Mtb* antigens induces production of cytokines and chemokines by immune cells which can regulate the immune responses induced against bacteria. These pro-inflammatory cytokines lead to different mechanisms which influence HIV-1 infection. *Mtb* infection is able to induce expression of NF-κB/transcription factors, recruitment/activation of immune cells, expression of co-receptors CCR5 and CXCR4 as well as modulate cell contacts that enhance HIV-1 infection and replication. An increase of TNF-α, IL-6, and IFN-γ expression levels, found *in vivo* at the site of *Mtb* infection, can up-regulate HIV-1 expression patterns *in vitro* (Garrait *et al.*, 1997; Canaday *et al.*, 2009). The *Mtb* strains CDC155 and HN878, which can induce HIV-1 infection and replication, have been associated with increased levels of TNF and IL-6 expression patterns (Ranjbar *et al.*, 2009). High levels of the

MCP-1 protein were found in HIV-1/TB co-infected subject's pleural fluid and its neutralisation resulted in inhibition of *Mtb*-induced HIV-1 gag/pol mRNA transcription (Mayanja-Kizza *et al.*, 2009). Moreover, the balance between pro-inflammatory and anti-inflammatory cytokines plays a role on *Mtb*-HIV-1 regulation. Indeed, the neutralisation of endogenous IL-10 and TGF-β (with a negative effect on HIV-1 infection) augmented the up-regulation of *Mtb*-HIV-1 replication (Goletti *et al.*, 1998; Chetty *et al.*, 2014). The activation of signalling pathways by *Mtb* antigen can up-regulate the transcription of a wide range of host genes involved with cellular receptor expression patterns, improving HIV-1 entry and cell contacts. For example, the MCP-1 protein is an inflammatory CC chemokine permitting recruitment of $CCR2^+$ monocytes/macrophages and $CD4^+$ T lymphocytes. It is found at high levels in TB/HIV-1 co-infected patient's pleural fluid, suggesting that MCP-1 recruits HIV-1 permissive monocytes/macrophages and $CD4^+$ T lymphocytes to the site of infection and thereby promotes new rounds of HIV-1 replication. Furthermore, MCP-1 can induce HIV-1 co-receptor CXCR4 expression, CD4 helper T cell (Th0) polarisation in Th2 and IL-4 induction and CXCR4 expression on resting $CD4^+$ T lymphocytes: all enhancing HIV-1 infection (Wahid Ansari, Kamarulzaman and Schmidt, 2013). Hoshino *et. al.* documented that TB induces CXCR4 expression in alveolar macrophages increasing HIV-1 entry (Hoshino *et al.*, 2004). In 2002, they demonstrated that cell contacts between alveolar macrophages and activated $CD4^+$ T lymphocytes reduces inhibitory C/EBPβ expression and activates NF-κB thereby increasing HIV-1 replication (Hoshino *et al.*, 2002). Additionally in 2007, Hoshino *et. al.* described similar observations concerning direct contact between activated polymorphonuclear neutrophils and macrophages. Indeed, contact between these cells, stimulates HIV-1 replication and LTR transcription, and down-regulates inhibitory C/EBPβ in alveolar macrophages during pulmonary TB (Hoshino *et al.*, 2007).

The direct influence of *Mtb* antigens on HIV-1 $CD4^+$ T lymphocyte infection is less described and understood. In this Chapter, we studied the impact of *Mtb* liposomes on HIV-1 *cis*-infection using two different *in vitro* approaches. The first describes (**Part II.** *Section i.*) the pseudo-typed viral particle system, where we aim to understand if any interaction or interference occurs on HIV-1 entry and infection *via* co-receptors CCR5 or CXCR4 in the presence of *Mtb* antigens associated into liposomes. Following this strategy, HIV-1 pseudo-typed virus particles X4 or R5 produced by co-transfection of 293T were used to infect TZM-bl or GHOST cell lines that expressed reporter proteins enabling to monitor for infectivity specific to HIV-1: GFP expression for GHOST and luciferase activity for TZM-bl cells. The second aim was to describe the impact on *Mtb* liposomes on HIV-1 replication in $CD4^+$ T

lymphocytes (**Part II.** *Section ii.*). For that, fully replicative competent HIV-1 was utilised. Infections were performed on $CD4^+$ T lymphocytes from healthy donors and monitored for replication by measuring p24 production, HIV-1 DNA quantification and cytokine production.

II. Results

i. Influence of Mycobacterium *liposomes on HIV-1* cis*-infection – Pseudo-typed viral particle System*

a) Optimisation

Before studying the impact of *Mtb* liposomes on HIV-1 *cis*-infection, an optimisation of the experimental system to be utilised was required. GHOST cell lines expressing co-receptors CXCR4 or CCR5 were used to determinate the optimum concentration of virus required to detect infection and to control for virus envelope (Env) expression of HIV-1 pseudo-typed virus particles by monitoring virus tropism. HIV-LAI (HIV-1 X4, recognising co-receptor CXCR4) were tested on GHOST $CXCR4^+$ cells and HIV-JR-FL (HIV-1 R5, recognising co-receptor CCR5) on GHOST $CCR5^+$ cells in parallel to HIV-VSVg that possesses a neutral tropism and can infect all cell lines studied (Figure 3.1. **A**).

We observed that the percentage of infected GHOST $CXCR4^+$ cells expressing GFP is higher for HIV-VSVg infection than HIV-1 X4: 20-45% infected cells for HIV-VSVg compared to 3-12% for HIV-1 X4 (Figure 3.1 **A(1)**). Similar results were observed for HIV-1 R5 virus where HIV-VSVg infects 18-44% of GHOST $CCR5^+$ and HIV-1 R5 3-12% (Figure 3.1 **A(2)**). Furthermore, HIV-VSVg presented closer values of percentages of infected GHOST $CXCR4^+/CCR5^+$ cells (Figure 3.1 **A(3)**). HIV-VSVg was used as a positive control to validate the infection conditions. The higher infectivity observed with HIV-VSVg can be explained by the broad tropism of the virus that doesn't require specific co-receptor recognition as is the case for HIV-1 X4 and HIV-1 R5 infection. Importantly, we observed higher numbers of infected cells with higher dose of virus input: for instance, the percentage of GHOST $CXCR4^+$ cells expressing GFP is 3% with 2ng of HIV-1 X4 increasing to 12% with 8ng of virus input. This result suggests that 8ng is necessary to obtain good detection of infection (Figure 3.1 **A**). However, the efficacy of infections on GHOST cells expressing both receptors CXCR4 and CCR5 is lower than GHOST cells expressing single co-receptors. Indeed, the percentage of infected cells obtained with 8ng of HIV-1 X4 or HIV-1 R5 is around 5% corresponding to a decrease of more than 50% of infectivity compared to GHOST cells expressing single receptors where we observed 12% of

infection (Figure 3.1 **A(3)**). For these reasons a different cell line (TZM-bl,) was used for further analyses of liposomes. This cell line, like GHOST CXCR4^{+}/CCR5^{+}, expresses both co-receptors and produces luciferase upon HIV-1 infection, providing a more sensitive method of detection. We can visualise TZM-bl infections with 8ng of HIV-1 X4, HIV-1 R5 or HIV-VSVg (Figure 3.1 **B**). HIV-VSVg provided 2x10^{6} relative light units (RLU), reaching the maximum limit of detection of the luminescence reading and validated conditions of the assay. For HIV-1 X4 and HIV-1 R5 we observed 1.5x10^{6} and 0.5x10^{6} RLU, respectively, and these values are sufficient to visualise HIV-1 infection. In conclusion, the infection conditions and virus compositions were validated to further study the impact of *Mtb* liposomes on HIV-1 infection and/or replication.

A. Optimisation of HIV-1 pseudo-virus infection on GHOST cell lines

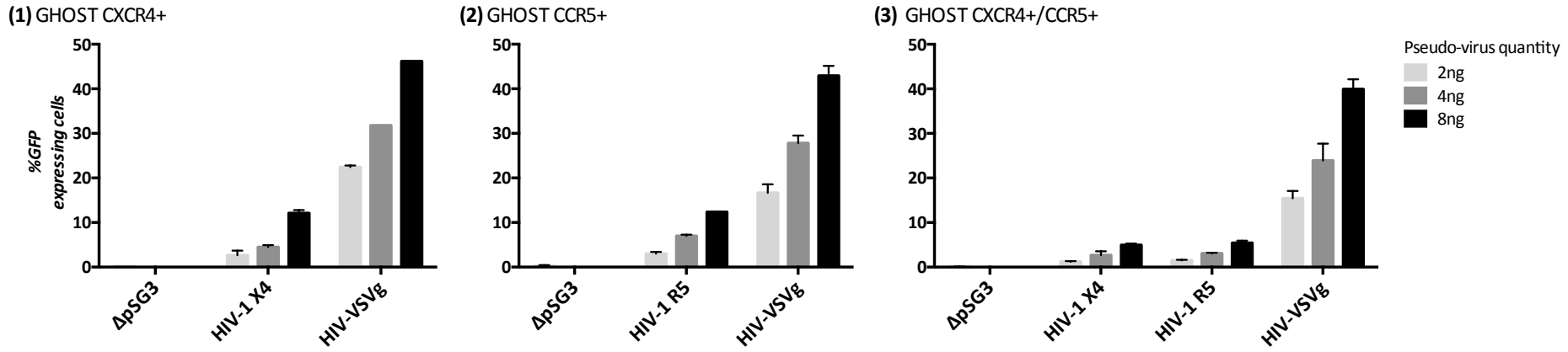

B. HIV-1 pseudo-virus infection on TZM-bl cells

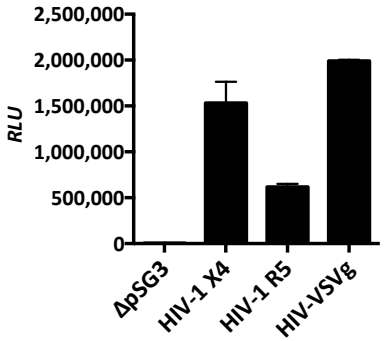

Figure 3.1 : Optimisation of HIV-1* cis*-infection on GHOST and TZM-bl cell lines

A. 3x10^4 GHOST cells and **B.** TZM-bl cells per well were seeded in 96-well plates. After 24h, the cells were infected with 2ng, 4ng or 8ng virus. Cells were infected with pSG3-LAI (HIV-1 X4), pSG3-JF-FL (HIV-1 R5), pSG3-VSVg (HIV-VSVg) or pSG3Δenv (ΔpSG3) virus. 48h after infection, **A.** cells were fixed in PFA to measure GFP expression by flow cytometry and **B.** cells were lysed to measure luciferase activity with RLU. For the data shown, n=2.

b) *Influence of* Mycobacterium *liposomes on modulating pseudo-typed virus infection*

Before introducing total lipids from *Mtb* strains into liposomes and monitoring the effects on HIV-1 infection with pseudo-typed virus particles, it was important to control the influence of liposome composition on target cells and infection. The viability of TZM-bl cells were tested in the presence of liposomes composed of PC or a mix of PC and cholesterol (0.8PC:0.2Ch). TZM-bl cells were incubated with increasing quantities of liposomes and monitored for viability after 48 h. We observed for all different conditions that liposomes do not affect cell viability, which remains around 90% for all concentrations tested (Figure 3.2).

Figure 3.2 : Viability of TZM-bl with liposomes

$3x10^4$ TZM-bl cells were seeded in 96-well plates, and incubated after 24h incubation with 1000, 100, 10 and 1ng of PC or 0.8:0.2Ch liposomes. After 48h of incubation, the cells were washed and fixed in PFA to determine cell viability by flow cytometry. For the data shown, n=2.

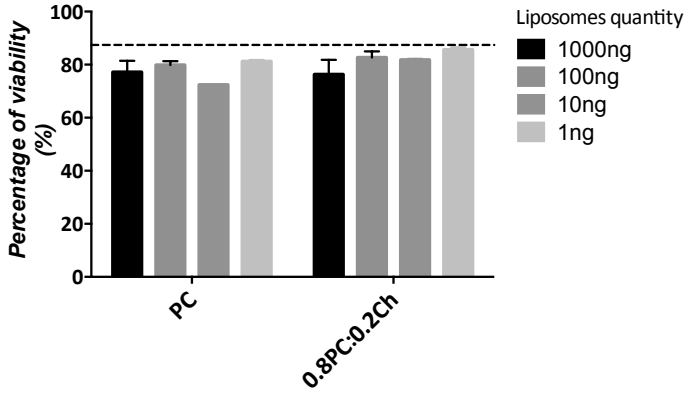

To control for the influence of liposome composition on HIV-1 infection, TZM-bl cells were infected with HIV-JR-FL (HIV-1 R5) in the presence of liposomes generated with different proportions of cholesterol: PC, 0.9PC:0.1Ch, 0.8PC:0.2Ch, 0.6PC:0.2Ch (Figure 3.3). Two different conditions were tested: **A.** liposomes were added to cells at the same time as virus and **B.** liposomes were incubated with cells 30min prior to infection. In comparison to the cells infected with virus alone (used here as reference=1), co-incubation with liposomes demonstrated no effect on HIV-1 *cis*-infection. Indeed, infection with 1ng or 100ng of liposome did not affect the level of infection with either method. For 0.6PC:0.4Ch, we observed a slight increase in HIV-1 R5 infectivity with 100ng liposomes. In conclusion, liposome compositions were chosen at a 0.6PC:0.2Ch:0.2*Mtb* ratio to build liposomes incorporating *Mtb* total lipids.

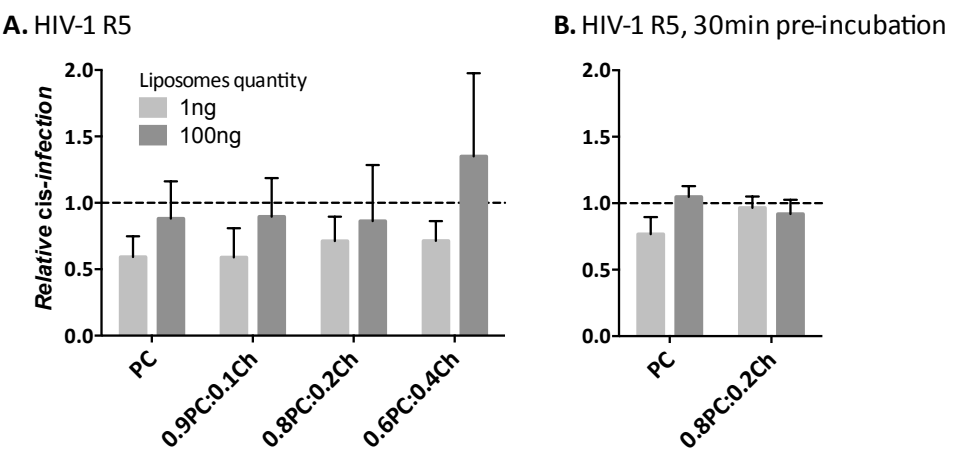

Figure 3.3 : Influence of liposomes without* Mycobacterium *lipids on HIV-1* cis*-infection

$3x10^4$ TZM-bl cells per well were seeded in 96-well plates. After 24h, the cells were infected with 8ng of pSG3-JF-FL (HIV-1 R5) and pSG3Δenv (ΔpSG3) where **A.** virus input with 1 or 100ng of liposomes at the same time or **B.** 1 or 100ng of liposomes added to TZM-bl cells 30min prior to adding virus. Liposomes tested: PC, 0.9PC:0.1Ch, 0.8PC:0.2Ch and 0.6PC:0.4Ch. 48h post-infection cells were lysed and luciferase activity measured (RLU). ΔpSG3 is used as a negative control and the infectivity of the virus alone as reference. For the data shown, n=4.

The impact of *Mtb* liposomes containing BCG, *M. smegmatis*, H37Rv, HN878, CDC1551 and EU127 glycolipids on TZM-bl HIV-LAI (HIV-1 X4) and HIV-BAL (HIV-1 R5) *cis*-infection were subsequently studied (Figure 3.4.). As described above, liposomes were either **A.** or **C.** added to cells at the same time as virus or **B.** and **D.** pre-incubated with TZM-bl before virus input. For both viruses, the reference used is the value of TZM-bl *cis*-infection in the presence of 0.2PC:0.8Ch liposomes. For HIV-1 X4 and HIV-1 R5, under both conditions, we did not observe any significant impact of *Mtb* liposomes on TZM-bl *cis*-infection.

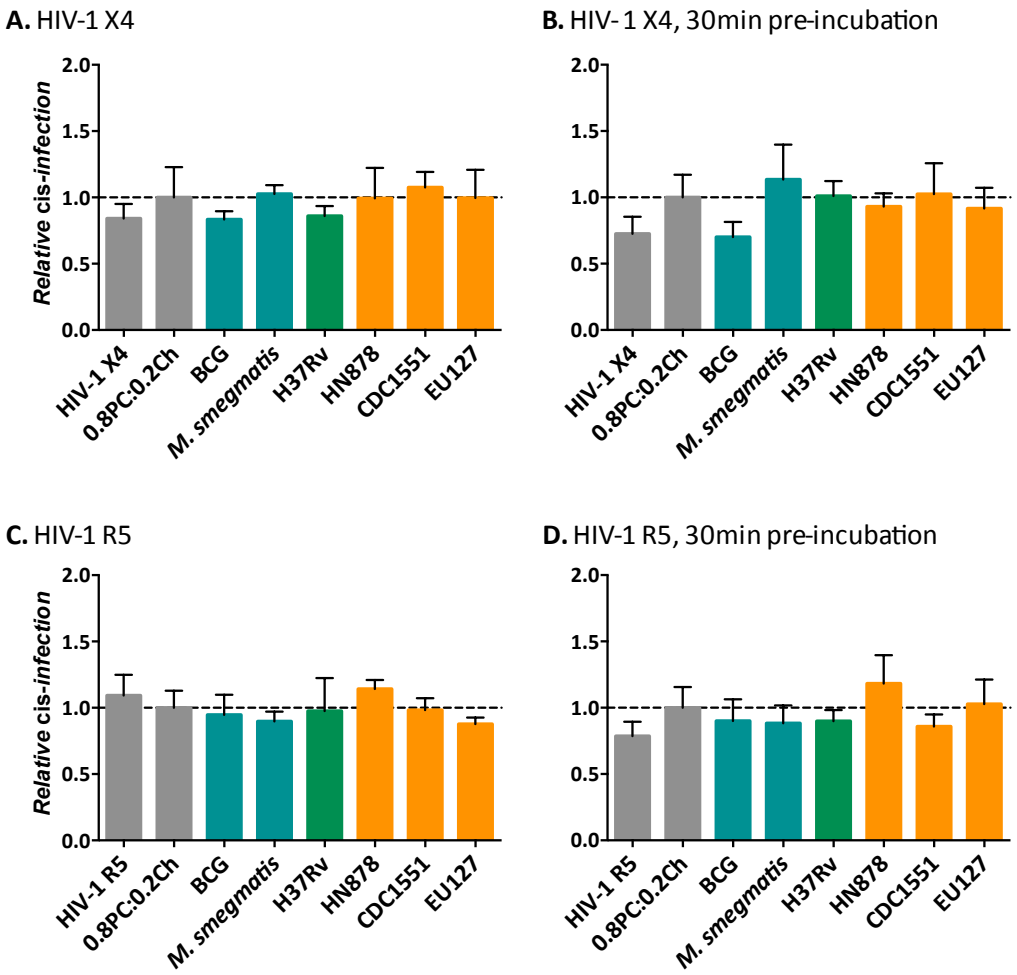

Figure 3.4 : Influence of* Mycobacterium *liposomes on HIV-1* cis*-infection

One day prior to infection, $3x10^4$ TZM-bl cells per well were seeded in 96-well plates. After 24h, the cells were infected with 8ng of **A. B.** pSG3-LAI (HIV-1 X4), **C. D.** pSG3-BAL (HIV-1 R5) and pSG3Δenv (ΔpSG3) where **A.** and **C.** virus input with 100ng of liposomes at the same time or **B.** and **D.** 100ng of liposomes added to TZM-bl cells 30min prior to adding virus. Liposomes tested: 0.8PC:0.2Ch, BCG, *M. smegmatis*, H37Rv, HN878, CDC1551 and EU127. 48h after infection cells were lysed to measure luciferase activity (RLU). 0.8PC:0.2Ch is used here as a negative control and reference. For the data shown, n=3.

ii. Influence of liposomes on HIV-1 cis*-infection – Replicative System*

a) Optimisation

We optimised *cis*-infection of $CD4^+$ T lymphocytes utilising two HIV-1 replicative competent strains; LAI-YFP (HIV-1 X4) and BAL-GFP (HIV-1 R5) (Figure 3.5). Lymphocytes isolated from healthy donors were infected with variant concentrations of both viruses. Infections were monitored over 14 days by measuring HIV-1 capsid p24 production and analysing percentages of $CD4^+$ cells expressing YFP (LAI) or GFP (BAL) by flow cytometry.

Four different concentrations of HIV-1 X4 LAI-YFP virus were tested (Figure 3.5): 40, 200, 1000, and 3000 $TCID_{50}$/ml. **(1)** At day 7 post-infection, for all viral inputs, we observed a peak of infected cells expressing YFP at 0.9, 2.1, 3.8 and 5.0%, respectively. At day 10 and 14 infection levels declined for 1000 and 3000 $TCID_{50}$/ml to 3.4%. The proportion of cells expressing YFP increased for the 40 and 200 $TCID_{50}$/ml input concentrations at day 10 to 2.5% and 3.0%, respectively. At day 14 a plateau was reached for 40 $TCID_{50}$/ml and a decline in infected cells to 2.0% for 200 $TCID_{50}$/ml was observed. Concerning p24 production Figure 3.5 **A(2)**, a progressive increase was observed over time. The 40 $TCID_{50}$/ml condition provided a clear increase in p24 production where the values increased from 1.5ng/ml at day 4 to 141.20ng/ml at day 10. For 200 $TCID_{50}$/ml input, we observed a similar replication profile, p24 concentration at day 4 post-infection of 9.9ng/ml increasing to 165.5ng/ml and 227.5ng/ml at day 7 and 10 respectively. For 1000 and 3000 $TCID_{50}$/ml, a plateau was reached at day 7 post-infection with 232.89ng/ml and 366.24ng/ml p24 measured respectively. To measure the impact of liposomes on $CD4^+$ T lymphocyte HIV-1 infection, we elected to use 200 $TCID_{50}$/ml input for HIV-1 X4 LAI-YFP virus and to monitor until day 7 post-infection.

For HIV-1 R5 BAL-GFP (Figure 3.5 **B**) three concentrations of virus input were tested: 500, 1000 and 3000 $TCID_{50}$/ml. When we measured the proportion of infected cells expressing GFP overtime by flow cytometry analyses **(1)**, a peak of 0.7% infected cells was observed at day 10 for all the conditions with a decline to 0.4% at day 14. For p24 production we observed an increase over time for all conditions tested **(2)**. A peak was observed at day 7 post-infection with p24 levels increasing from 40.96ng/ml at day 4 to 165.4ng/ml at day 7 for 500 $TCID_{50}$/ml; 26.57ng/ml to 167.21ng/ml for 1000 $TCID_{50}$/ml; and 34.2ng/ml to 303.22 for 3000 $TCID_{50}$/ml. For all three concentrations of BAL-GFP tested the p24 levels decreased at day 10 to 155.45, 135.90, and 132.01ng/ml, respectively. The low level of fluorescence measured for BAL-GFP virus indicated that p24 measurements would be a better indicator of replication. Based on the p24 analysis we chose to utilise 500 $TCID_{50}$/ml as the standard concentration of HIV-1 R5 BAL-GFP with monitoring replication over 7 days.

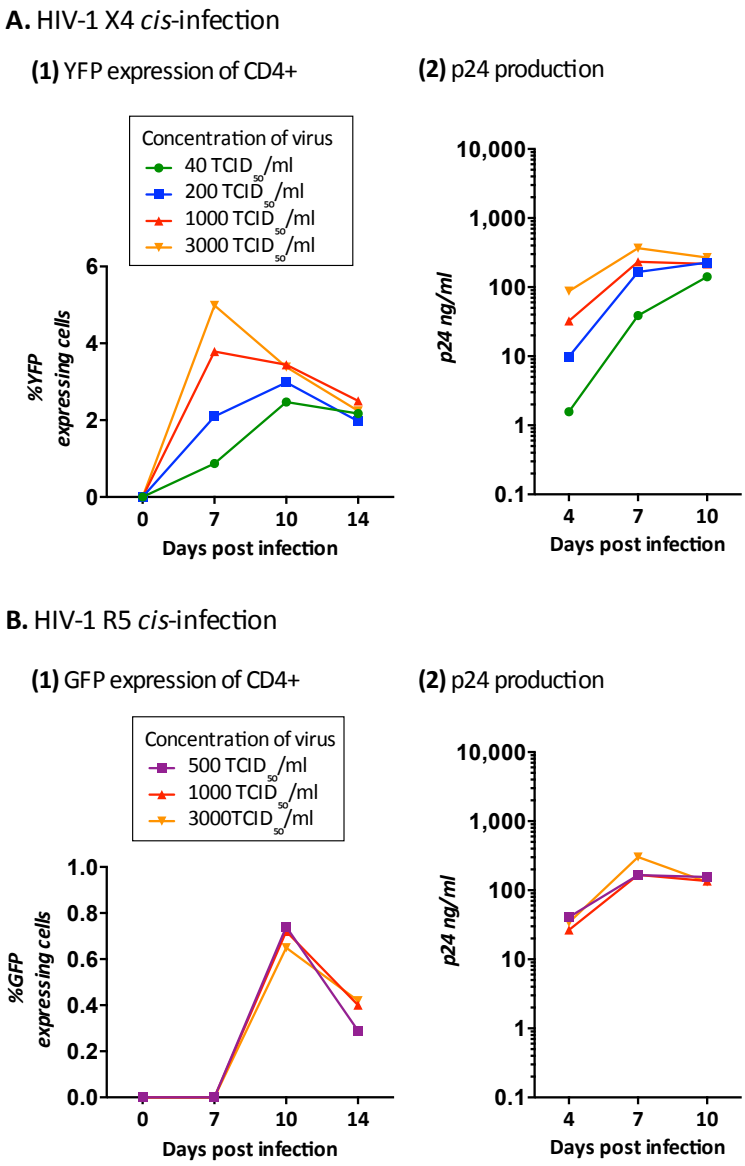

Figure 3.5 : Optimisation of HIV-1* cis*-infection on CD4⁺ T lymphocytes

$2x10^5$ CD4⁺ enriched T lymphocytes per well were seeded and incubated with **A.** 40, 200, 1000 or 3000 $TCID_{50}$/ml LAI-YFP (HIV-1 X4) or **B.** 500, 1000, 3000 $TCID_{50}$/ml BAL-GFP (HIV-1 R5) in 96-well plate. At day 4, 7 and 10 HIV-1 capsid p24 was determined in the supernatant by p24 ELISA **(2)** and at day 7, 10, and 14 the percentage of infected cells was measure by flow cytometry **(1)** (YFP expression for LAI and GFP expression for BAL). The data shown are from one experiment using cells isolated from one donor.

b) Influence of Mycobacterium *liposomes on HIV-1* cis*-infection*

We studied the effects that liposomes expressing variant *Mtb* strain glycolipids had on influencing HIV-1 *cis*-infection of CD4⁺ T lymphocytes. Viral p24 production was determined at two time points following infection (day 4 and 7) and with different forms of HIV-1 DNA being quantified at day 7: total HIV-1 DNA, 2-LTR circular form HIV-1 DNA and integrated

proviral HIV-1 DNA. Selected cytokine and chemokine levels were quantified on the corresponding culture supernatant at day 7 using the Luminex® assay.

Viral p24 production and HIV-1 DNA quantification analyses from HIV-1 X4 $CD4^+$ T lymphocyte *cis*-infections in the presence of *Mtb* liposomes were compared (Figure 3.6). In the supernatant **A.**, at day 4 post-infection **(1)**, we observed significant differences in p24 production during HIV-1 X4 infection, increasing from 12.48ng/ml (virus alone) to 18.04ng/ml in the presence of HN878 liposomes (P value =0.0286, Mann Whitney test). For all other liposomes tested no significant differences were observed in p24 production at day 4. BCG and H37Rv liposomes trended to decrease p24 concentration to 7.56 and 7.16ng/ml, respectively compared to the virus alone. At day 7 post-infection there was no significant difference in the level of p24 production with any of the liposomes. However, BCG liposomes demonstrated a trend towards decreasing p24 production by 2.4 fold whilst CDC1551 liposomes showed a trend towards activating p24 production by 1.9 fold (Figure 3.6 **A(2)**).

When analysing HIV-1 DNA quantification levels (Figure 3.6 **B**), we observed an increase in total HIV-1 DNA content **(1)** in the presence of LPS and CDC1551 liposomes to 6.9 log10 copies/10^6 cells compared to 6.74 with virus alone. Also, the presence of BCG liposomes demonstrated a decreasing trend in the number of total HIV-1 DNA copies to 6.45 log10 copies/10^6 cells. For 2-LTR HIV-1 DNA **(2),** BCG and EU127 liposomes decreased the number of 2-LTR by 4.04 (P value =0.0411, Mann Whitney test) and 4.07 (P value =0.0022, Mann Whitney test) log10 copies/10^6 cells compared to 4.39 with virus alone. H37Rv liposomes demonstrated a trend towards decreasing 2-LTR HIV-1 DNA to 4.2 log10 copies/10^6 cells. When comparing the quantification of integrated HIV-1 DNA levels **(3)**, we did not observe any significant differences. Nevertheless, we observed overall a similar trend of *Mtb* liposomes impacting on total HIV-1 DNA quantification. Indeed, from these analyses, we could conclude that LPS, HN878 and CDC1551 showed a trend towards increasing HIV-1 X4 replication, and conversely BCG, H37Rv and EU127 liposomes showed a trend towards inhibiting virus replication. Those observations are partially correlated with p24 production at day 4 and day 7. Finally, no differences were observed in proportions between total HIV-1 DNA, 2-LTR and integrated DNA quantity (Appendix 15) and no toxic effect of the *Mycobacterium* liposomes tested were observed in this assay (Appendix 16).

A. p24 production

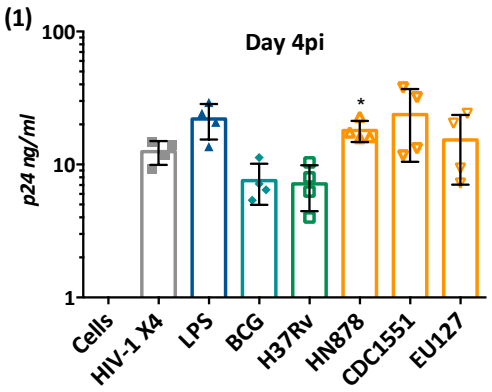

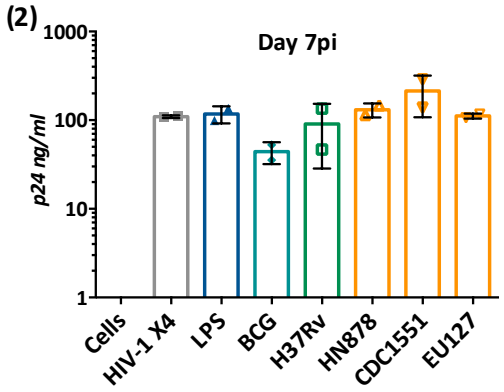

B. DNA quantification

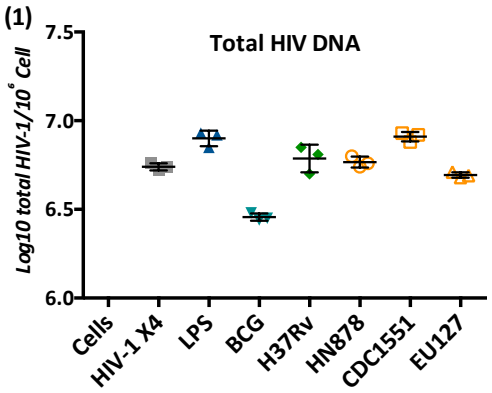

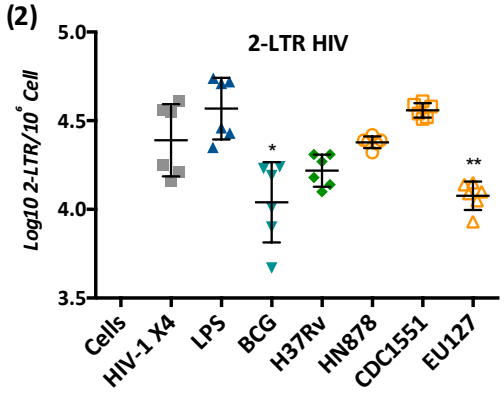

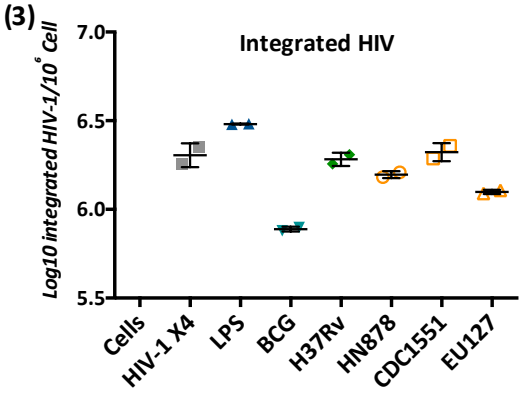

Figure 3.6 : Influence of* Mycobacterium *liposomes on HIV-1 X4 CD4⁺ T lymphocytes infection

$2x10^5$ $CD4^+$ enriched T lymphocytes per well were seeded and infected with 200 $TCID_{50}$/ml LAI-YFP (HIV-1 X4) in a 96-well plate. Then, 40µg of *Mycobacterium* liposomes BCG, H37Rv, HN878, CDC1551, EU127, or 100ng/ml of LPS was added. **A.** At **(1)** day 4 (n=4) and **(2) day** 7 post-infection (n=2), HIV-1 capsid p24 was determined in supernatant by ELISA. **B.** represents log10 HIV-1 DNA quantification determinate by PCR relative to the total number of $CD4^+$ cells day 7 post-infection with **(1)** total number of HIV-1 DNA (n=3), **(2)** number of HIV-1 2-LTR (n=6) and **(3)** number of integrated HIV (n=2). The data shown are from one experiment using cells isolated from one donor.

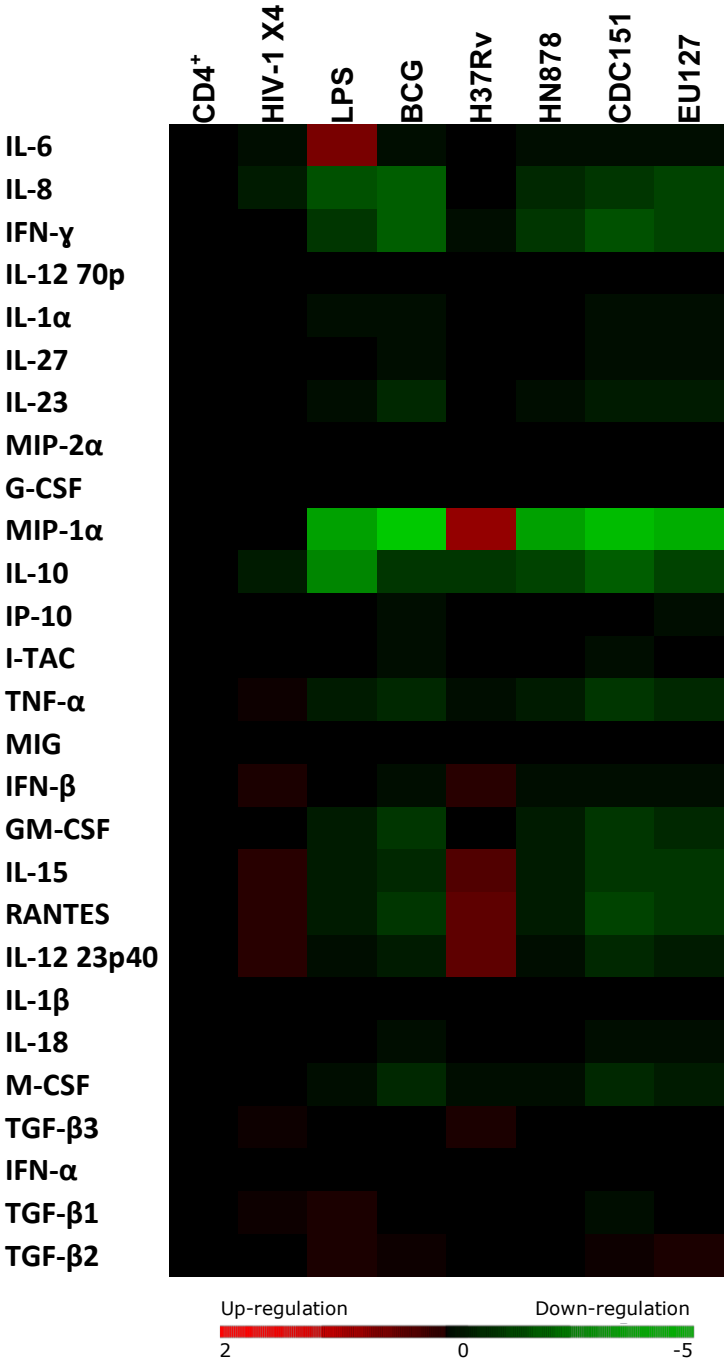

Figure 3.7 : Influence of* Mycobacterium *liposomes on HIV-1 X4 CD4+ T lymphocytes infection - Luminex®

$2x10^5$ $CD4^+$ enriched T lymphocytes per well were seeded and infected with 200 $TCID_{50}$/ml LAI-YFP (HIV-1 X4) in a 96-well plate. Then, 40µg of *Mycobacterium* liposomes BCG, H37Rv, HN878, CDC1551, EU127, or 100ng/ml of LPS was added. At day 7 post-infection, supernatants were collected for Luminex® analyses. Luminex results are represented by Heat Maps Cluster of the Log2 of liposomes treatment/cells baseline ratio. An increase of cytokine production in the supernatant is represented in red, a diminution of cytokine production depict in green and no change shown as black. For the data shown, n=3 using cells isolated from one donor.

When comparing the cytokine production during HIV-1 X4 $CD4^+$ T cell infection in the presence of liposomes, we observed that the virus alone induced a specific response from the cells characterised by induction of TNF-α, IFN-β, IL-15, RANTES, IL-12 23p40, TGF-β3 and TGF-β1 production and a decrease of IL-8 and IL-10 (Figure 3.7). Interestingly, we observed similar cytokine profiles in presence of liposomes H37Rv but at higher concentration. These observations suggest that H37Rv liposomes increase the viral response from $CD4^+$ cells. Additionally, H37Rv liposomes seemed to induce MIP-1α production compared to virus alone. For the remainder, LPS, BCG, HN878, CDC1551 and EU127, a global down-regulation of pro-inflammatory cytokine and chemokine production was observed indicating a decrease in the inflammatory response from infected cells. Only the presence on LPS during HIV-1 X4 *cis*-infection demonstrated a trend towards inducing IL-6 production. When we compared these observations with analyses of HIV-1 X4 replication we observed that *Mtb* liposomes demonstrated a trend towards up-regulating HIV-1 X4 infection such as with LPS, HN878 and CDC1551 and which shared similar $CD4^+$ T cells cytokine production profiles. However, BCG and EU127 that showed the same cytokine pattern as HN878 and CDC1551, presented a trend towards inhibiting HIV-1 replication. Also, H37Rv liposomes, which demonstrated a trend towards down-regulating HIV-1 X4 replication, we observed pro-inflammatory responses similar to the virus alone. All together, these observations suggest that different mechanisms are involved in the influence of *Mtb* liposomes on modulating HIV-1 X4 replication.

The influence of *Mtb* liposomes on HIV-1 R5 *cis*-infection of $CD4^+$T lymphocytes on p24 production and total HIV-1 DNA content is represented in Figure 3.8. For p24 production **A.**, we observed at day 4 **(1)** that LPS and CDC1551 liposomes enhanced p24 production in supernatant by 2.3 (P value =0.0286, Mann Whitney test) and 3.0 (P value = 0.0286, Mann Whitney test) fold respectively. Also, we observed that EU127 liposomes demonstrated a trend towards activating p24 production by 1.9 fold. Conversely, the presence of H37Rv liposomes decreased p24 concentration by 2.2 fold (P value = 0.0286, Mann Whitney test). At day 7 post-infection we observed a trend towards an increase of p24 production in the presence of LPS, CDC1551 and EU127 liposomes by 2.6, 3.4 and 2.3 fold, respectively (Figure 3.8 **A(2)**). Concerning the influence of liposomes on HIV-1 DNA quantification **(**Figure 3.8 **B**) we observed that only the H37Rv liposome showed a trend towards decreasing total HIV-1 DNA **(1)** to 6.71 compared to 6.99 log10 copies/10^6 cells for HIV-1 R5 alone. On HIV-1 2-LTR circular HIV-1 DNA **(2)**, LPS, HN878 and CDC1551 liposomes significantly increased the number of HIV-1 copies to 4.57 (P value =0.0411, Mann Whitney test), 4.53 (P value =0.0368,

Mann Whitney test) and 4.79 (P value =0.0022, Mann Whitney test) log10 copies/10^6 cells, respectively. We also observed that EU127 liposomes demonstrated a trend towards increasing the number of 2-LTR copies to 4.51 log10 copies/10^6 cells. For integrated HIV-1 proviral DNA levels **(3)**, no significant differences were observed, but we did observe a similar trend when we compared the 3 graphs together. LPS, H878, CDC1551 and EU127 liposomes appeared to activate HIV-1 R5 replication and H37Rv liposomes showed a trend towards blocking replication. These observations from the DNA quantification analyses were correlated with p24 production overtime. Finally, no differences were observed in the proportions between total HIV-1 DNA, 2-LTR and integrated DNA quantity (Appendix 15) and no toxic effect of the *Mycobacterium* liposomes tested were observed in this assay (Appendix 16).

The analyses of the cytokine production by $CD4^+$ T cells during HIV-1 R5 infection in the presence of *Mtb* liposomes presented, as for X4 virus, a specific response from infected cells characterised by induction of MIP-1α, IP-10, TNF-α, IL-15, RANTES, IL-12 23p40, TGF-β3 and TGF-β2 and a decrease of IL-10 production (Figure 3.9). H37Rv liposomes followed the same pattern of cytokine production observed with virus alone but with higher concentrations. Also, the presence of H37Rv showed a trend towards up-regulating production of IL-8 and IFN-β. Conversely, the presence of LPS, BCG, HN878, CDC1551 and EU127 showed a decrease of $CD4^+$ T cell inflammatory cytokine production with the exception of IP-10 that was up-regulated. These observations indicate that these liposomes modulate $CD4^+$ T cell responses during infection with HIV-1 R5 where a down-regulation of $CD4^+$ T cell pro-inflammatory responses is associated with up-regulation of HIV-1 R5 replication and an increase of pro-inflammatory responses associates with a down-regulation of HIV-1 R5 replication.

A. p24 production

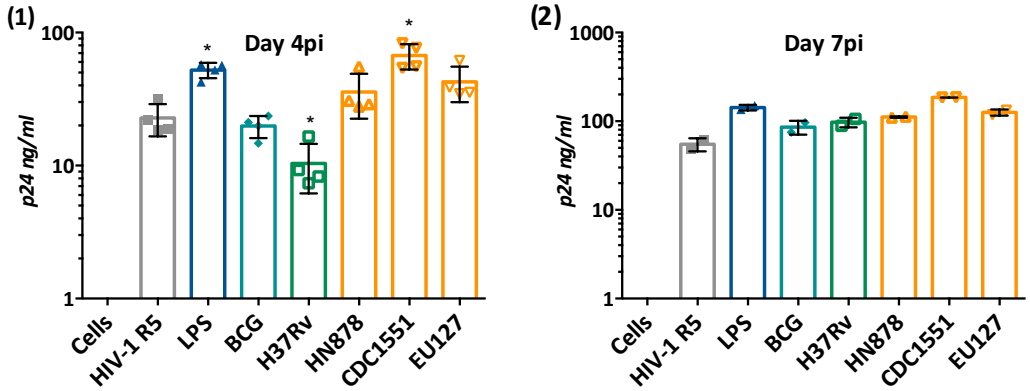

B. DNA quantification

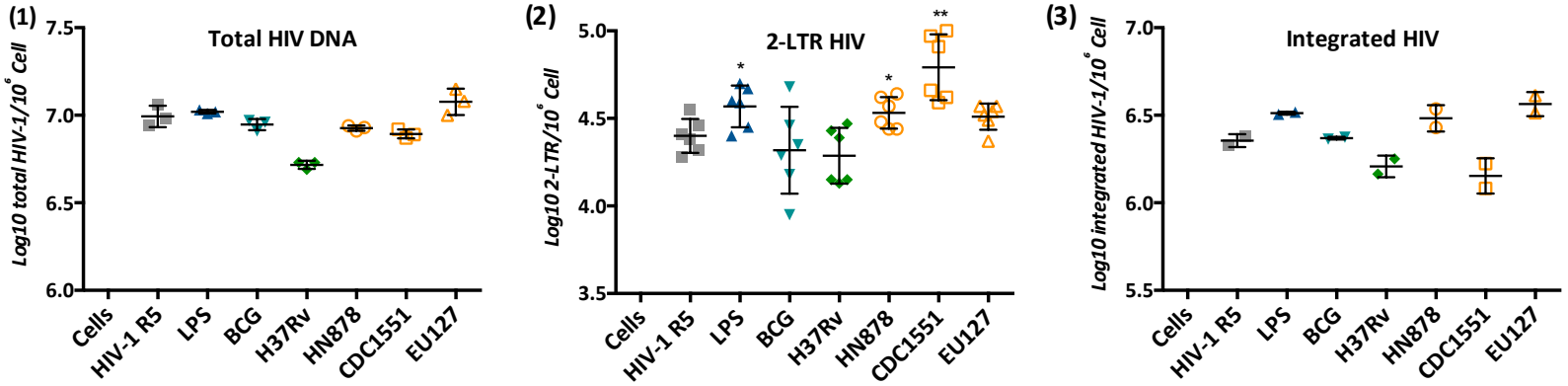

Figure 3.8 : Influence of* Mycobacterium *liposomes on HIV-1 R5 CD4⁺ lymphocytes infection

$2x10^5$ $CD4^+$ enriched T lymphocytes per well were seeded and infected with 500 $TCID_{50}$/ml BAL-GFP (HIV-1 R5) in a 96-well plate. Then 40µg of *Mycobacterium* liposomes BCG, H37Rv, HN878, CDC1551, EU127, or 100ng/ml of LPS was added. **A.** At Day 4 (n=4) **(1)** and 7 (n=2) **(2)** post-infection, HIV-1 capsid p24 was determined in supernatant by ELISA. **B.** represents log10 HIV-1 DNA quantification determined by PCR relative to the total number of $CD4^+$ cells at day 7 post-infection with **(1)** total number of HIV-1 DNA (n=3), **(2)** number of HIV-1 2-LTR (n=6) and **(3)** number of integrated HIV (n=2). The data shown are from one experiment using cells isolated from one donor.

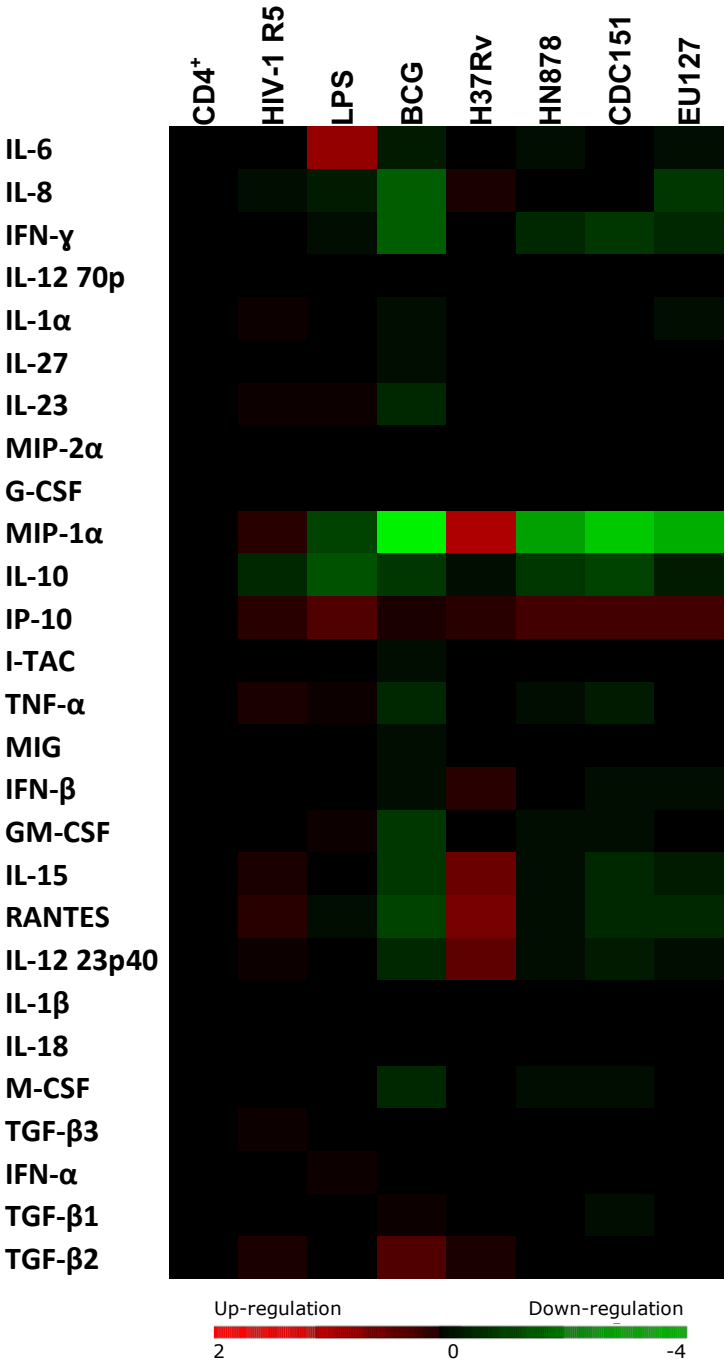

Figure 3.9 : Influence of* Mycobacterium *liposomes on HIV-1 R5 CD4+ lymphocytes infection

$2x10^5$ $CD4^+$ enriched T lymphocytes per well were seeded and infected with 500 $TCID_{50}$/ml BAL-GFP (HIV-1 R5) in a 96-well plate. Then 40µg of *Mycobacterium* liposomes BCG, H37Rv, HN878, CDC1551, EU127, or 100ng/ml of LPS was added. At day 7 post-infection, supernatants were collected for Luminex® analyses. Luminex results are represented by Heat Maps Cluster the Log2 of liposomes treatment/cells baseline ratio. An increase of cytokine production in the supernatant is represented in red, a diminution of cytokine production depict in green and no change shown as black. The data shown are form one experiment with n=3 using cells isolated from one donor.

The pro-inflammatory responses from infected cells with HIV-1 X4 or R5 presented some similarities with the production of TNF-α, IL-15, RANTES, IL-12 23p40 and TGF-β3, suggesting activation of same anti-viral mechanisms. Additionally, when comparing the influence of *Mtb* liposomes on HIV-1 X4 and HIV-1 R5 replication, we observed some variations. For both viruses, *Mtb* H37Rv liposome appeared to block *cis*-infection of $CD4^+$ T lymphocytes demonstrated a trend towards increasing the anti-viral response from infected $CD4^+$ T cells. Additionally LPS, HN878 and CDC1551 showed a trend towards activating HIV-1 replication associated with a down-regulation of the pro-inflammatory response. However, BCG liposomes blocked replication of HIV-1 X4 but not HIV-1 R5 virus. Additionally, EU127 liposomes demonstrated a trend towards lowering HIV-1 X4 replication and conversely showed a trend towards activating HIV-1 R5 *cis*-infection. BCG and EU127 showed in both virus infections a down regulation of pro-inflammatory responses from $CD4^+$ T infected cells.

In conclusion, we observed that liposomes representing variant *Mtb* strains were shown to induce differences in HIV-1 *cis*-infection of $CD4^+$ T lymphocytes. This impact can also be variable depending on the tropism of the virus and is not solely influenced by the *Mtb* pathogenic strain being tested.

III. Conclusion

From the approach studying *cis*-infection of TZM-bl cells with HIV-1 pseudo-typed virus particles in the presence of *Mtb* liposomes we observed that none of the glycolipids from *Mtb* strains H37Rv, HN878, CDC1551 and EU127 and non-pathogenic strains BCG and *M. smegmatis*, influenced HIV-1 X4 or HIV-1 R5 infectivity (Figure 3.4). The bacterial glycolipid antigens presented on liposomes therefore did not interfere with HIV-1 entry to target cells *via* either the CCR5 or CXCR4 co-receptor. Interestingly, when studying HIV-1 replicative competent viruses large differences were observed when comparing both the *Mtb* strains being tested and the co-receptor usage profile of the virus strains (CCR5 or CXCR4) (Figures 3.6 and 3.8), observable also when considering the cytokine profiles produced during infection (summarised in Table 3.1).

Concerning the non-pathogenic BCG strain, liposomes blocked HIV-1 *cis*-infection on $CD4^+$ T lymphocytes by reducing HIV-1 replication. Indeed, we observed a decrease in p24 production at day 4 and day 7 post-infection with HIV-1 X4, correlating with a decrease in HIV-1 DNA copies at day 7 (both for total HIV-1 DNA and 2-LTR forms). Nevertheless, BCG

glycolipids did not demonstrate the same effect for HIV-1 R5 infectivity. However, for both viruses BCG glycolipids presented by liposomes reduced pro-inflammatory responses from infected $CD4^+$ T lymphocytes. Additionally, EU127 (*Mtb* strain isolated from clinical samples) showed the opposite effect when comparing HIV-1 X4 and HIV-1 R5 infections. For X4 virus we described that EU127 liposomes demonstrated a trend towards lowering p24 production at day 7 post-infection, reducing HIV-1 replication. Conversely, we observed activation of HIV-1 R5 replication (both p24 and HIV-1 DNA levels). As observed for BCG liposomes, EU127 decreased pro-inflammatory responses in $CD4^+$ T cells with both virus infections. From this observation, EU127 *Mtb* strains may therefore have the potential to modulate viruses found early in infection, including during the acute stages of infection in patients and when viral loads are typically high. The differences observed between virus tropisms may be due to variation in cell types being infected as well as cell activation profiles.

The pathogenic CDC1551 *Mtb* liposome demonstrated the induction of heightened HIV-1 replication for both R5 and X4 viruses. For HN878, the observations were less clear but demonstrated a trend towards activating HIV-1 *cis*-infection with both virus strains. CDC1551 and HN878 are both *Mtb* pathogenic strains and where CDC1551 induced a strong pro-inflammatory response and where HN878 is deemed to be more lethal (Manca *et al.*, 1999, 2001; Ordway *et al.*, 2007). Additionally, CDC1551 has been described to significantly increase IL-6 and TNF levels in context of HIV-1 X4 PBMC infection compared to HN878 (Ranjbar *et al.*, 2009). In our *in vitro* assays, our results showed the opposite effect where HN878 and CDC1551 demonstrated a trend towards decreasing pro-inflammatory responses in $CD4^+$ T cells, with both X4 and R5 viruses. Additionally, up-regulation of HIV-1 replication was not correlated with high levels of TNF-α and IFN-γ as expected (Garrait *et al.*, 1997; Canaday *et al.*, 2009). Ranjbar *et al.* used in their assays *Mtb* bacteria and PBMCs from PPD^+ patient that could explain the variations observable. However, from these observations we could conclude that different mechanisms are involved in the modulation of HIV-1 replication in $CD4^+$ T cells in the presence of HN878 and CDC1551 lipids *in vitro*. However, IP-10 is a chemokine described to up-regulate HIV-1 infection (Lane *et al.*, 2003). In case of HN878, CDC1551 and EU127 liposomes, the increase in IP-10 production could activate HIV-1 R5 replication.

Table 3.1 : Luminex Results Summary

Conditions	BCG	H37Rv	HN878	CDC1551	EU127
$CD4^+$ T cells HIV-1 X4 *cis*-infection Day 7 post-infection	↓ TNF-α/IFN-γ ↓ IFN-β ↓ M-CSF/GM-CSF ↓ IL-15/IL-18 ↓ IL-12 23p40/IL-23 ↓ MIP-1α/RANTES/IL-8 ↓ TGF-β1/2	↑ IFN-β ↑ IL-15 ↑ IL-12 23p40 ↑ MIP-1α/RANTES/IL-8 ↑ TGF-β3 ↓ M-CSF	↓ TNF-α/IFN-γ ↓ IFN-β ↓ M-CSF/GM-CSF ↓ IL-15 ↓ IL-12 23p40/IL-23 ↓ MIP-1α/RANTES/IL-8		
	Block virus replication		**Increase virus replication**		**Block virus replication**
$CD4^+$ T cells HIV-1 R5 *cis*-infection Day 7 post-infection	↑ TGF-β2 ↓ TNF-α/IFN-γ ↓ IFN-β ↓ M-CSF/GM-CSF ↓ IL-15 ↓ IL-12 23p40/IL-23 ↓ MIP-1α/RANTES/IL-8 ↓ MIG/I-TAC ↓ TGF-β3	↑ IFN-β ↑ IL-15 ↑ IL-12 23p40 ↑ IL-10 ↑ MIP-1α/RANTES/IL-8 ↑ IP-10 ↓ TNF-α	↑ IP-10 ↓ TNF-α/IFN-γ ↓ IFN-β ↓ M-CSF/GM-CSF ↓ IL-15 ↓ IL-12 23p40 ↓ MIP-1α/RANTES/IL-8 ↓ TGF-β1/2/3		
	-	**Block virus replication**	**Increase virus replication**		

Concerning H37Rv liposomes, we demonstrated that H37Rv significantly reduces HIV-1 X4 and R5 *cis*-infection. These observations suggest that H37Rv glycolipids block $CD4^+$ T lymphocyte infection. The variation between the glycolipid components on each *Mtb* strain could explain the differences that we observed in our assays. Interestingly, H37Rv liposomes induce in both cases similar pro-inflammatory responses comparable to virus alone but to higher levels suggesting that H37Rv lipids up-regulate responses from infected cells. Furthermore, the chemokines MIP-1α and RANTES, known to inhibit viral entry of HIV-1 R5 (Cocchi *et al.*, 1995; Trkola *et al.*, 1998), were produced at higher concentrations in the supernatant during HIV-1 X4 and R5 $CD4^+$ T cell infection. This observation suggests that the H37Rv liposomes blocking effect on HIV-1 R5 replication could be due to an inhibition of virus entry as described by (Hoshino *et al.*, 2004) on macrophages and mediated *via* the blocking of the CCR5 receptor by its natural ligands.

To further investigate and better understand the impact of *Mtb* glycolipids on modulating HIV-1 infections, *in vitro* infections of HIV-1 X4 and R5 virus on macrophages, DCs and PBMC cultures could be realised in parallel in order to characterise sub-cellular population effects and interactions between cells. Additionally, transformed cell lines expressing specific markers of signalling pathways, such a TLRs, NF-κB could be used to identify mechanisms involved with liposomes modulating HIV-1 replication. Finally, liposomes containing lipids from *Mtb* strains only could be designed and used in order to characterise any specific roles towards affecting HIV-1 infections.

From the work presented the direct role of *Mtb* glycolipids on modulating HIV-1 $CD4^+$ T cells *cis*-infection remains un-clear but we demonstrate differential impacts of liposomes depending on *Mtb* strains as well as virus tropism. Several articles in the literature have described the modulation of HIV-1 replication by altering expression of several transcriptions factors differentially expressed following the activation of specific cell signalling pathways. However, the system of infection monitored here is different to those utilised in most studies cited in the literature. In the present Chapter we analysed the direct impact *Mtb* glycolipids exerted on HIV-1 *cis*-infection, in the next Chapter we focus on a second mechanism of HIV-1 infection: *trans*-infection

Chapter 4: Impact of *Mycobacterium* liposomes on HIV-1 *trans*-infection

I. Introduction

Dendritic cells play a major role in controlling pathogen infections. Micro-organisms entering mucosal tissues are captured by DCs and their antigens processed for presentation to the immune system. The cells migrate to lymph nodes for presentation to naïve lymphocytes and activate a cascade of reactions driving the adaptive immune response. HIV-1 recognition by DCs induces strong $CD4^+$ and $CD8^+$ T lymphocyte responses (Cameron, Forsum, *et al.*, 1992; Larsson *et al.*, 2002; Zhao *et al.*, 2002; Frank *et al.*, 2003; Jones, McDonald and Canaday, 2007). However, DCs have also been shown to capture virus and subsequently present infectious virus particles to target $CD4^+$ T lymphocytes, thereby enhancing infection through the classic CD4 and co-receptor mediated pathway (Cameron, Freudenthal, *et al.*, 1992; Cameron *et al.*, 1994; Dong *et al.*, 2007; J. T. Kim *et al.*, 2018). The mechanism of *trans*-infection occurs in the infectious synapse where high concentration of HIV-1 from DCs are in contact with $CD4^+$ T lymphocytes enriched in co-receptor expression (Sallusto *et al.*, 1995; Gummuluru, KewalRamani and Emerman, 2002; McDonald *et al.*, 2003; Turville *et al.*, 2004; Garcia *et al.*, 2005). Different receptors have been described to be involved with *trans*-infection, such as the mannose receptor (Sallusto *et al.*, 1995; Turville *et al.*, 2002) and the C-type lectin receptor DC-SIGN (Geijtenbeek *et al.*, 2000; Turville *et al.*, 2003; Moris *et al.*, 2006; van Montfort *et al.*, 2007), which both capture virus by interaction with the HIV-1 gp120 envelope protein. Siglec, expressed mainly on mature DCs (mDCs), can capture HIV-1 *via* interactions with ganglioside GM3 localised on the virus membrane and allow for *trans*-infection (Bobardt *et al.*, 2003; de Witte *et al.*, 2007; Puryear *et al.*, 2012; Izquierdo-Useros *et al.*, 2014; Akiyama *et al.*, 2015). Immature DCs (iDCs) and mature DCs (mDCs) are both able to facilitate HIV-1 *trans*-infection. Unlike iDC, mDC are not infectable with HIV-1 but are more efficient at supporting virus *trans*-infection (Granelli-Piperno *et al.*, 1998; Sanders *et al.*, 2002; Izquierdo-Useros *et al.*, 2014).

Different parameters can alter the mechanism of HIV-1 *trans*-infection. Naarding *et al.* described that Lewis X containing molecules, present in human milk, can inhibit HIV-1 transfer to $CD4^+$T lymphocytes specific to DC-SIGN by binding the receptor and blocking viral interactions (Naarding *et al.*, 2005). They further demonstrated that bile salt-stimulated lipase (BSSL), a Lewis X containing glycoprotein present in human milk, can alter HIV-1 capture-transfer *via* DC-SIGN (Naarding *et al.*, 2006; Stax *et al.*, 2011). It was also identified that molecular polymorphisms in BSSL could associate with the strength of inhibition and was further shown that these could also associate with parameters associated with HIV-1 disease progression. Mucin 6 (MUC6) present in seminal plasma has also been identified to inhibit DC-SIGN mediated *trans*-infection (Stax *et al.*, 2009). Collectively, these findings indicate that host proteins within bodily secretions and plasma have the potential to bind DC-SIGN and block HIV-1 *trans*-infection, thereby interfering with either viral transmission and/or subsequent disease progression.

As explained in the Introduction, Chapter 2 and Chapter 3, *Mtb* components such as PIMs, LM, LAM, polysaccharides and glycoproteins can interact with C-type lectin receptors and potentially interfere with HIV-1 capture and transfer. In this Chapter, the aim was to study the influence of *Mtb* glycolipids associated with liposomes on HIV-1 *trans*-infection.

As described in Chapter 3, we utilised the pseudo-typed virus particle system in parallel with the HIV-1 replicative system to study the effects of *Mtb* carrying liposomes in modulating HIV-1 *trans*-infection. *Trans*-infection experiments were performed using different cell-types including Raji-DC-SIGN cells as well as iDCs and mDCs from healthy donors. The Raji-DC-SIGN cell line cannot be infected with HIV-1, but can support capture-transfer of the virus due to expression of DC-SIGN. Both iDCs and mDCs transfer HIV-1 as explained. The TZM-bl cell line, expressing CD4 and the CCR5 and CXCR4 co-receptors were used as the target cell for the pseudo-typed virus system (**Part II.** *Sections i. and ii.*) and $CD4^+$ T lymphocytes for the replicative system (**Part II.** *Sections iii. and iv.*).

II. Results

i. *Influence of liposomes on HIV-1* trans-*infection – Pseudo-typed virus particle System*

a) *HIV-1* trans-*infection on TZM-bl via Raji-DC-SIGN*

To be able to study the impact of liposomes on HIV-1 *trans*-infection the system was optimised. First, we selected an HIV-1 R5 virus strain that demonstrated sufficient capture and transfer of virus to TZM-bl *via* Raji-DC-SIGN cells (Figure 4.1). We compared *trans*-infection of two HIV-1 R5 strains from different origin: JR-FL and BAL. For HIV-1 R5 JR-FL we observed that the efficacy of *trans*-infection was lower when compared to BAL (Figure 4.1 **A**), indeed BAL virus provided RLU values 10 times higher than for JR-FL pseudo-typed virus particles even with the two viruses showing similar infectivity of TZM-bl cells (Figure 4.1 **B**) with RLU values around 600,000 each. From this observation, HIV-1 R5 BAL virus was selected for use in further experiments.

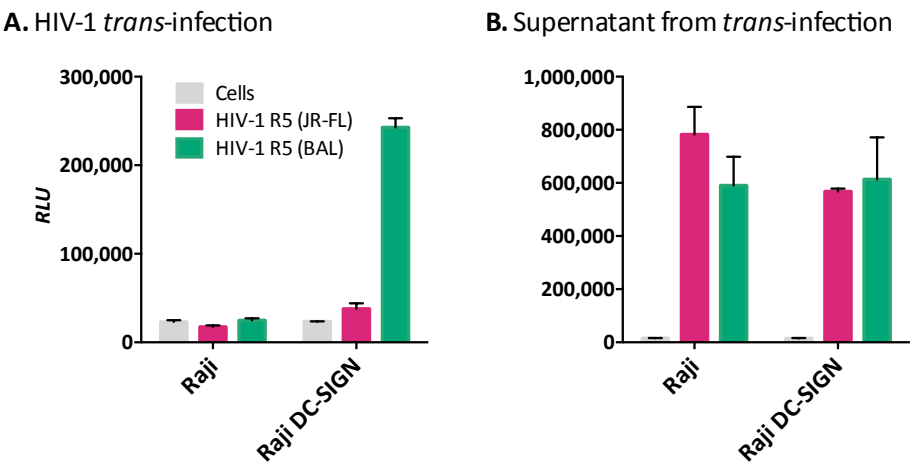

Figure 4.1 : Optimisation of HIV-1 R5 pseudo-virus trans-infection on TZM-bl via Raji DC-SIGN

$0.5x10^6$ of Raji and Raji-DC-SIGN cells were incubated 2h with HIV-1 pseudo-typed virus: particles 20ng pSG3-JR-FL (pink) or pSG3-BAL (green). **A.** After capture the cells were washed and co-cultured with TZM-bl cells. The luciferase activity (RLU) was read after 48h. **B.** After capture and before Raji and Raj-DC-SIGN cells were washed, the supernatant (15µL) was kept to infect directly the TZM-bl cells. After 48h incubation luciferase activity (RLU) was determined. For the data shown, n=2.

To measure the influence of *Mtb* antigens on HIV-1 *trans*-infection via DC-SIGN, liposomes containing *Mtb* incorporated glycolipids were incubated with Raji-DC-SIGN before capture of HIV-1 (Figure 4.2). The results represent the influence liposomes have on HIV-1 X4 **A.** and R5 **B.** *trans*-infection. The efficacy of capture-transfer of HIV-1 has been normalised for the value

of *trans*-infection in the presence of liposomes 0.2PC:0.8Ch not containing incorporated *Mtb* glycolipids (negative control). The *Mtb* pathogenic strain, H37Rv, significantly blocked *trans*-infection of HIV-1 X4 virus *via* DC-SIGN by 2.9 fold (P value< 0.0001, Mann Whitney test) (Figure 4.2**A**). Conversely, HN878 slightly increased efficacy of *trans*-infection by 1.16 fold (P value= 0.0012, Mann Whitney test) whilst CDC1551 did not affect HIV-1 X4 *trans*-infection. The *Mtb* clinical strains EU127, Ex30 and EU111 provided a different impact on *trans*-infection. EU127 blocked capture and transfer of HIV-1 X4 to 0.74 relative efficacy of transfer (P value= 0.0001, Mann Whitney test) compared to the negative control 0.8PC:0.2Ch liposomes. On the contrary, Ex30 and EU111 liposomes did not influence HIV-1 *trans*-infection.

Concerning the non-pathogenic mycobacterial strains BCG and *M. smegmatis*, we observed a strong effect for BCG, which decreased 2.5 fold DC-SIGN mediated *trans*-infection (P value< 0.0001, Mann Whitney test). *C. glutamicum* was tested here as it is a micro-organism described with a membrane composition comparable to *Mycobacterium*, but *M. smegmatis* and *C. glutamicum* did not impact HIV-1 capture-transfer. *M. chelonae* and *M. marinum* are both non-pathogenic mycobacterial strains that under specific conditions could both create opportunistic infections with strong damage to the infected host. Here, we observed that these two strains blocked the efficacy of HIV-1 X4 *trans*-infection *via* DC-SIGN by 1.4 fold (P value< 0.0001 and P value= 0.0004 respectively, Mann Whitney test). *S. aureus* which is a common co-infection observed in HIV-1 patients did not affect HIV-1 X4 capture-transfer. Interestingly, both viruses exhibited similar profiles to *Mycobacterium* liposomes (Figure 4.2). Generally, we observed a similar trend for HIV-1 X4 **A.** and HIV-1 R5 **B.**. *Mtb* H37Rv, with *Mtb* EU127, BCG, *M. chelonae* and *M. marinum* liposomes significantly decreasing DC-SIGN mediated HIV-1 *trans*-infection with a decrease of 2.9 (P value< 0.0001, Mann Whitney test), 1.4 (P value< 0.0001, Mann Whitney test), 2.1 (P value< 0.0001, Mann Whitney test), 1.4 (P value < 0.0001, Mann Whitney test) and 1.6 (P value< 0.0001, Mann Whitney test) respectively. Contrary to HIV-1 X4, CDC1551 increased virus capture-transfer by 1.2 fold (P value= 0.0313, Mann Whitney test) but which was not observed for HN878. We did observe the same phenomena with *M. smegmatis*, where HIV-1 R5 virus *trans*-infection was increased 1.4 fold (P value= 0.0034, Mann Whitney test). Concerning the clinical *Mtb* strains Ex30 and EU111, we observed that EU111 significantly reduced capture-transfer significantly by 1.1 fold (P value= 0.04, Mann Whitney test). Variations observed on HN878 and EU111 liposomes impact on HIV-1 X4 and R5 trans-infection *via* DC-SIGN may be explained by experimental variation. Indeed, in the case of HIV-1 R5, even though HN878 liposomes did

not significantly affect *trans*-infection, there was a consistent trend towards heightened capture-transfer.

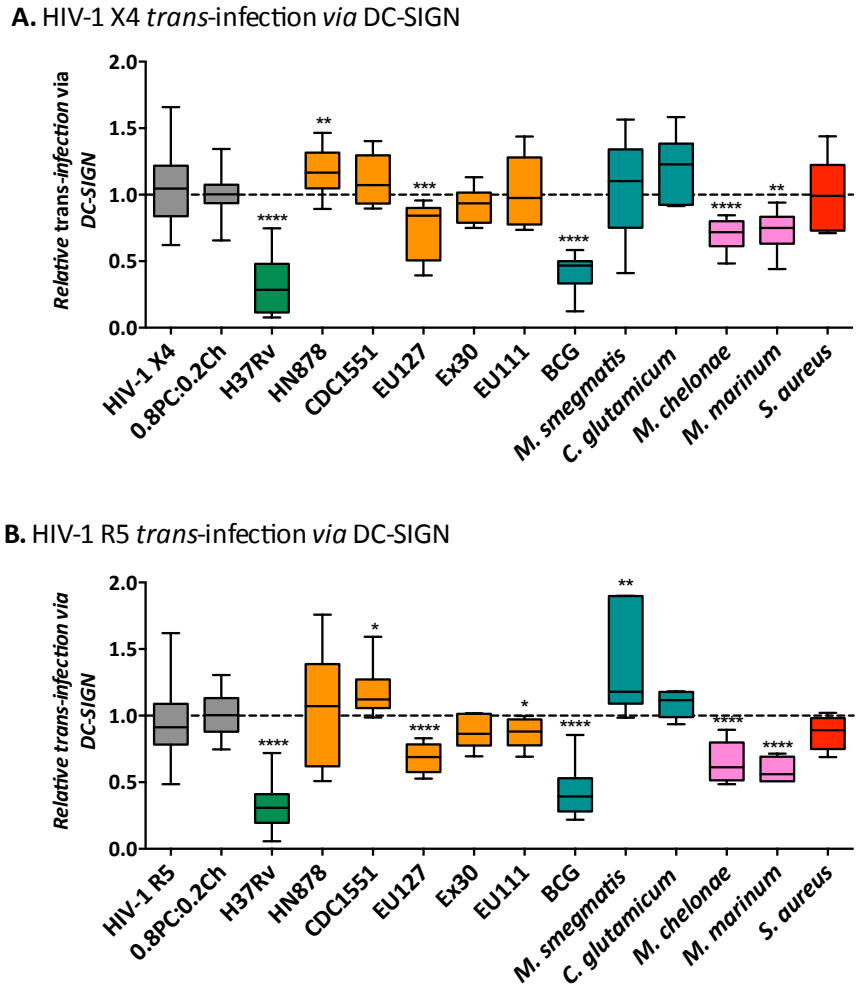

Figure 4.2 : HIV-1 trans-infection on TZM-bl via Raji-DC-SIGN with* Mycobacterium *liposomes

0.5x10^6 of Raji-DC-SIGN cells were pre-incubated for 30min with 100µg of liposomes or 50µl of media. Then the cells were incubated 2h with HIV-1 pseudo-typed virus: **A.** 12.5ng pSG3-LAI (HIV-1 X4) or **B.** 20ng pSG3-BAL (HIV-1 R5). After capture the cells were washed and co-cultured with TZM-bl cells. The luciferase activity (RLU) was read after 48h. 0.8PC:0.2Ch liposome was used here as a negative control and reference. Data are represented in boxplot where the box extends from the 25th and 75th percentiles, the median is plotted at the line in the middle of the box, the whiskers represents the minimum and maximum value and where n≥3.

The *Mycobacterium* glycolipid liposomes including H37Rv, EU127, BCG, *M. chelonae* and *M. marinum* could potentially recognise DC-SIGN thereby blocking HIV-1 *trans*-infection to target cells. Importantly, we have observed an array of impacts *Mycobacterium* glycolipids can have on *trans*-infection, dependent on the strain being tested. Additionally, similar trends were observed between HIV-1 R5 and X4 strains of virus. These results indicate that

different *Mtb* strains possess the ability to differentially effect DC-SIGN mediated capture-transfer.

b) HIV-1 trans-*infection* via *DCs on TZM-bl*

We next tested the impact of *Mycobacterium* liposomes on *trans*-infection of HIV-1 *via* DCs, the physiological relevant cell-types mediating HIV-1 capture-transfer. As described above with Raji-DC-SIGN, DCs were pre-incubated with liposomes before capture-transfer of virus. HIV-1 X4 and R5 *trans*-infection were tested mediated by DCs at different stages of maturation: iDCs (Figure 4.3) and mDCs (Figure 4.4).

Interestingly, *Mtb* H37Rv, EU127, Ex30 and EU111 liposomes reduced HIV-1 X4 *trans*-infection *via* iDC by 1.9 (P value= 0.0003, Mann Whitney test), 1.8 (P value= 0.0003, Mann Whitney test), 2.9 (P value= 0.0008, Mann Whitney test) and 2.1 (P value= 0.0008, Mann Whitney test) fold, respectively (Figure 4.3 **A**) compared to the negative control. For *Mtb* HN878, we observed a trend towards increased *trans*-infection and *Mtb* CDC1551 heightened *trans*-infection by 1.3 fold (P value= 0.0022). For non *Mtb* liposomes (BCG) we observed a decrease in HIV-1 R4 *trans*-infection *via* iDCs by 1.7 fold (P value= 0.0010, Mann Whitney test), but no significant changes were observed for *M. smegmatis*, *C. glutamicum*, *M. chelonae* and *M. marinum.* Conversely, *S. aureus* liposomes increased HIV-1 capture-transfer by 1.4 fold (P value= 0.0238, Mann Whitney test) compared to the negative control (0.8PC:0.2Ch).

Concerning the HIV-1 R5 strain, as observed with HIV-1 X4 the *Mtb* H37Rv and EU127 liposomes decreased *trans*-infection by 2.0 (P value< 0.0001, Mann Whitney test) and 1.7 fold (P value= 0.0009, Man Whitney test), respectively (Figure 4.3**B**). HN878 demonstrated again a trend towards increasing HIV-1 capture-transfer when compared to the negative control (0.8PC:0.2Ch), opposed to CDC1551 which increased the effect by 1.7 fold (P value= 0.0139, Mann Whitney test). Ex30 and EU111 *Mtb* liposomes did not affect HIV-1 R5 t*rans*-infection *via* iDCs. Interestingly, BCG, *C. glutamicum*, *M. chelonae* and *M. marinum* liposomes decreased HIV-1 R5 capture-transfer *via* iDCs of 1.3 (P value= 0.0345, Mann Whitney test), 1.6 (P value= 0.0408, Mann Whitney test), 1.6 (P value= 0.0087, Mann Whitney test) and 1.6 (P value< 0.0001, Mann Whitney test) fold, respectively. Conversely, the *M. smegmatis* liposome blocked transfer by 1.7 fold (P value= 0.0090, Mann Whitney test). *S. aureus*,

contrary to what was observed with HIV-1 X4, did not impact on HIV-1 R5 *trans*-infection *via* iDCs when compared to the negative control.

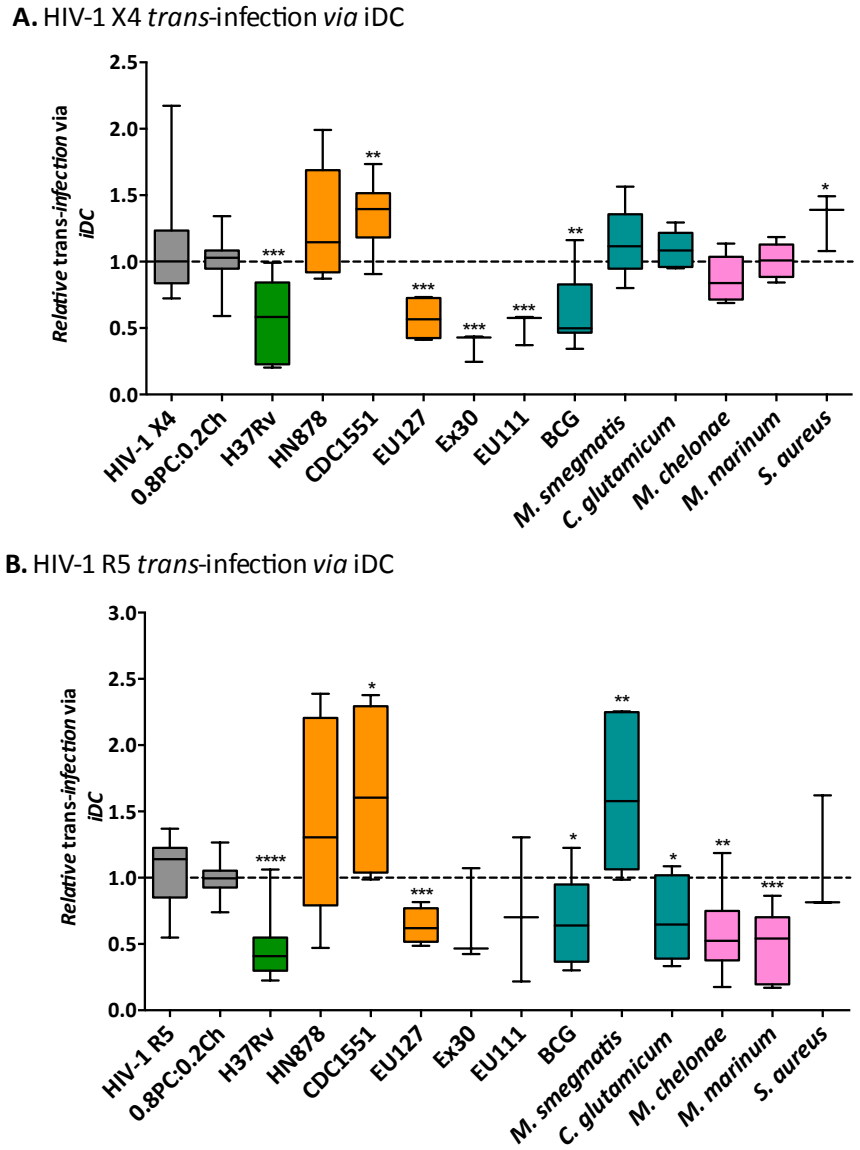

Figure 4.3 : HIV-1* trans*-infection on TZM-bl cells* via *iDC with* Mycobacterium *liposomes

Human blood monocytes were isolated from buffy coats using Ficoll gradient and a subsequent CD14 selection step using the MACS system. Purified monocytes were differentiated into iDCs in the presence of IL-4 and GM-CSF, 70ng/ml and 50ng/ml respectively. On day 6, the phenotype of the cultured iDCs was confirmed by flow cytometry and $0.5x10^6$ iDCs was pre-incubation for 30min with 100µg of liposomes or 50µl of media. The cells were then incubated 2h with HIV-1 pseudo-typed virus: **A.** 12.5ng pSG3-LAI (HIV-1 X4) or **B.** 20ng pSG3-BAL (HIV-1 R5). After capture the cells were washed and co-cultured with TZM-bl cells. The luciferase activity (RLU) was read after 48h. 0.8PC:0.2Ch liposome was used here as a negative control and reference. Data are represented in boxplot where the box extends from the 25th and 75th percentiles, the median is plotted at the line in the middle of the box, the whiskers represents the minimum and maximum value and where n≥3. For the data shown, the experiment has been performed using cells isolated from on at least two different donors.

The observations from Figure 4.2 and Figure 4.3 are similar. Indeed, in both situations *Mtb* H37RV, *Mtb* EU127 and BCG liposomes significantly blocked both HIV-1 X4 and R5 *trans*-infection. The similarity in results between HIV-1 *trans*-infection *via* DC-SIGN receptor and *via* iDCs indicates that the blocking effect of *Mtb* liposomes *via* iDCs is likely due to the interaction of glycolipids with the DC-SIGN receptor. Additionally, *Mtb* CDC1551, *Mtb* HN878 and *M. smegmatis* trended to increase HIV-1 capture-transfer for both HIV-1 strains in both assays. In this case, glycolipids from those specific strains may signal through binding DC-SIGN and activate expression of other receptors.

The impact *Mtb* liposomes have on influencing HIV-1 *trans*-infection *via* mDCs is shown in Figure 4.4. Isolated iDCs were maturated with poly (I:C) for 18h before being pre-incubated with liposomes prior to performing virus capture-transfer assay. Variation between donors was observed, explaining for the high standard deviations observed, however trends were observed when comparing the different *Mtb* strains. None of the *Mtb* liposomes were shown to impact HIV-1 *trans*-infection, but for HN878, one mDCs donor did exhibit heightened transfer of HIV-1 X4 by 2.5 fold and which seemed to follow a trend of activation (Figure 4.4 **A**). For non TB liposomes, BCG and *C. glutamincum* significantly blocked *trans*-infection by 1.2 (P value= 0.0075, Mann Whitney test) and 1.7 (P value= 0.0075, Mann Whitney test) fold, respectively. As observed for the *Mtb* HN878 liposomes, *M. smegmatis* and *M. marinum*, trends were observed towards increased HIV-1 X4 capture-transfer *via* mDCs with one specific donor showing an increase of 1.5 and 2.9 fold, respectively. Interestingly, the same donor increased *trans*-infection of HIV-1 X4 *via* mDCs in the presence of HN878 and *M. marinum* liposomes, and another donor for *M. smegmatis* liposomes. Additionally, we observed that *S. aureus* increased *trans*-infection by 1.14 fold (P value= 0.0438, Mann Whitney test).

The *Mtb* H37Rv liposome, opposed to HIV-1 X4 *trans*-infection *via* mDCs, was shown to significantly block HIV-1 R5 capture-transfer by 1.3 fold (P value= 0.0020, Mann Whitney test) (Figure 4.4 **B**). The same observation was found for *Mtb* CDC1551 which decreased transfer by 1.6 fold when compared to the negative control (P value= 0.0002, Mann Whitney test). Concerning non-TB liposomes, BCG, *C. glutamicum*, *M. chelonae* and *S. aureus*, were shown to significantly decrease HIV-1 R5 *trans*-infection *via* mDCs by 1.5 (P value= 0.0019; Mann Whitney test), 2.05 (P value= 0.0002, Mann Whitney test), 2.6 (P value< 0.0001, Mann Whitney test) and 1.5 fold (P value= 0.0033, Mann Whitney test), respectively.

A. HIV-1 X4 *trans*-infection *via* mDC

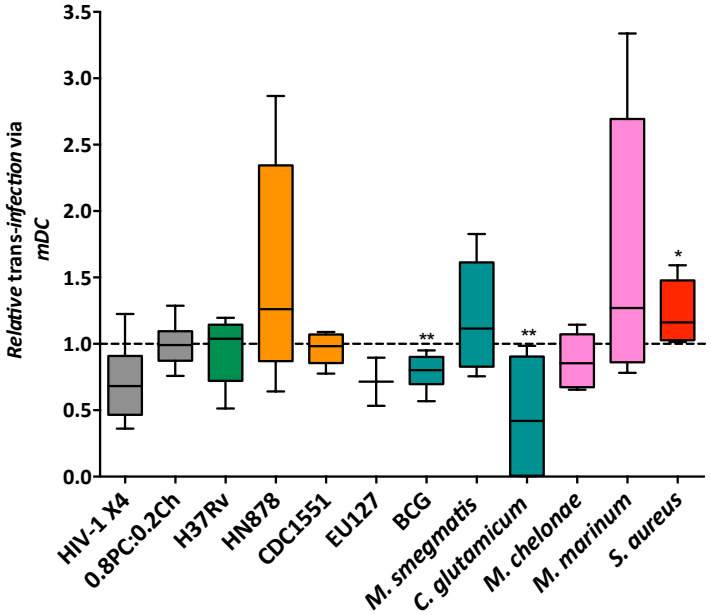

B. HIV-1 R5 *trans*-infection *via* mDC

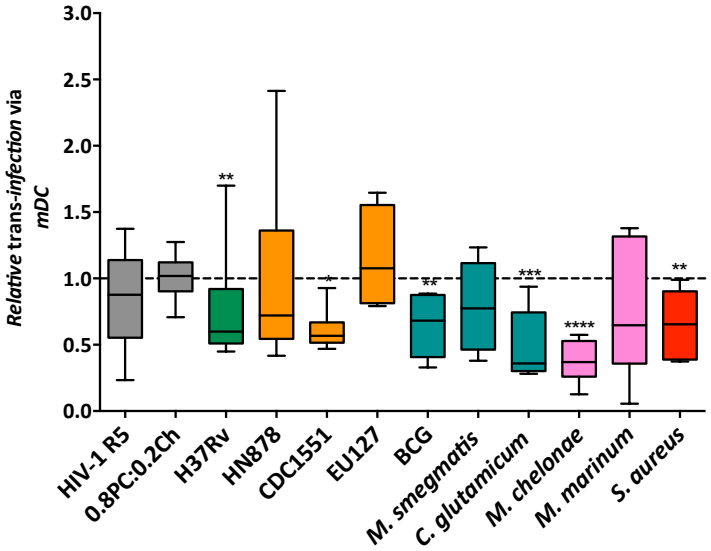

Figure 4.4 : HIV-1* trans-*infection on TZM-bl cells* via *mDC with* Mycobacterium *liposomes

Human blood monocytes were isolated from buffy coats by using Ficoll gradient and a subsequent CD14 selection step using the MACS system. Purified monocytes were differentiated into iDCs in the presence of IL-4 and GM-CSF, 70ng/ml and 50ng/ml respectively. On day 6, iDC are differentiated in the presence of 20µg/ml Poly(I:C), On day 7, the phenotype of the cultured mDCs were confirmed by flow cytometry and $0.5x10^6$ mDCs was pre-incubation during 30min with 100µg of liposomes or 50µl of media. Then the cells were incubated 2h with HIV-1 pseudo-typed virus: **A.** 12.5ng pSG3-LAI (HIV-1 X4) or **B.** 20ng pSG3-BAL (HIV-1 R5). After capture the cells were washed and co-cultured with TZM-bl cells. The luciferase activity was read after 48h. 0.8PC:0.2Ch liposome was used as a negative control and reference. Data are represented in boxplot where the box extends from the 25th and 75th percentiles, the median is plotted at the line in the middle of the box, the whiskers represents the minimum and maximum value and where n≥3. For the data shown, the experiment has been performed using cells isolated from at least two different donors.

Generally we observed variations on the impact of *Mtb* liposomes on HIV-1 X4 and R5 *trans*-infection *via* mDCs compared to iDCs. Indeed, for iDCs mediated virus capture-transfer we observed a clear impact of liposomes on transfer with no variation between blood donors and when compared to mDCs. Additionally, we observed some variations of liposomes when comparing the X4 and R5 strains of HIV-1. These observations suggest that receptors other than DC-SIGN are likely involved when considering mDCs HIV-1 *trans*-infection compared to iDCs.

We further investigated the involvement of the DC-SIGN receptor on influencing HIV-1 *trans*-infection *via* iDC and mDCs (Figure 4.5). For this purpose mannan was included in our experiments as a DC-SIGN receptor antagonist. As described for the *Mtb* liposome assays Raji-DC-SIGN, iDCs and mDCs were pre-incubated with mannan prior to HIV-1 capture-transfer to TZM-bl with two concentrations tested.

Figure 4.5 : HIV-1* trans*-infection on TZM-bl cells in presence of mannan

0.5x10^6 Raji-DC-SIGN, iDCs and mDCs were pre-incubation for 30min with 20µg/ml, 2mg/ml of mannan or 50µl of media. The cells were then incubated for 2h with 12.5ng pSG3-LAI HIV-1 X4 pseudo-typed viral particles. After capture the cells were washed and co-cultured with TZM-bl cells. The luciferase activity was read after 48h. RLU from condition of capture-transfer without mannan is used here as a reference for each cell types. The data shown are representative of one experiment using cells isolated from one donor with n=3.

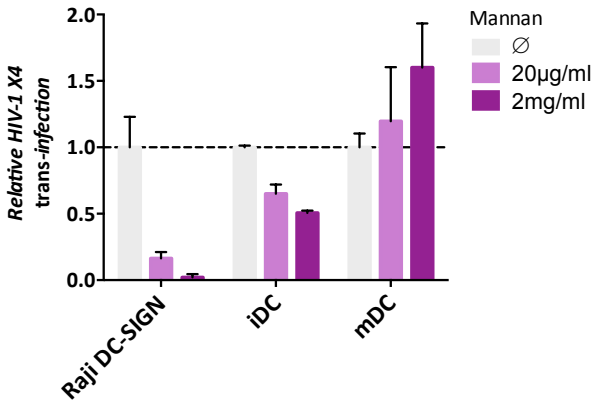

We observed that Raji-DC-SIGN HIV-1 X4 *trans*-infection of TZM-bl cells is strongly inhibited with both concentrations of mannan tested. Indeed the efficacy of transfer decreased to 0.16 with 20µg/ml and was totally inhibited with 2mg/ml of mannan compared to virus alone. For iDCs, capture-transfer was found to be partially blocked by mannan in a dose dependant way: where with 20µg/ml the efficacy was reduced by 1.5 fold and to 2.0 fold with 2mg/ml. Blocking DC-SIGN receptor with mannan on iDCs seems not to fully inhibit HIV-1 *trans*-infection. Concerning capture-transfer *via* mDCs, we did not observe any inhibition to HIV-1 X4 capture-transfer but an increase was observed with 2mg/ml by 1.6 fold.

It can be concluded that DC-SIGN recognition from antagonists such as mannan can decrease HIV-1 *trans*-infection *via* iDCs (Figure 4.5). Conversely, on mDCs the DC-SIGN antagonist could even be seen to increase HIV-1 *trans*-infection at the higher concentration. Those observations confirm our hypothesis that glycolipids from *Mtb* H37Rv, *Mtb* EU127 and BCG strains can recognise the DC-SIGN receptor on iDCs and block HIV-1 *trans*-infection.

ii. Characterisation of H37Rv lipids involved on HIV-1 trans-*infection modulation – Pseudo-typed virus particles System*

As described previously, we observed that *Mtb* H37Rv glycolipids integrated within liposomes can interact with the DC-SIGN receptor and block HIV-1 *trans*-infection *via* iDC. In this section, we characterised specifically the *Mtb* H37Rv impact on HIV-1 *trans*-infection *via the* DC-SIGN receptor.

We compared the influence of *Mtb* H37Rv liposomes with variant H37Rv strains from different origins to better understand the biology behind the effects observed (Figure 4.6). The main H37Rv strain that was used in all assays is from William Jacobs (Albert Einstein College of Medicine). We compared this H37Rv strain with H37Rv MA originally from Chris Sassetti (University of Massachusetts) on HIV-1 *trans*-infection *via* Raji-DC-SIGN and iDCs. As described previously, Raji-DC-SIGN and iDCs were pre-incubated with liposomes prior to capture-transfer of virus to TZM-bl cells. Interestingly, *Mtb* H37Rv MA did not block Raji-DC-SIGN HIV-1 *trans*-infection compared to H37Rv (Figure 4.6 **A**). Indeed, for both viruses HIV-1 X4 and R5, the efficacy of capture-transfer in the presence of H37Rv MA liposomes was at 1.09 and 0.98, respectively compared to 0.35 (P value= 0.0004, Mann Whitney test) and 0.22 (P value= 0.0004, Mann Whitney test) in the presence of H37Rv. For HIV-1 X4 virus we observed that H37Rv MA blocked *trans*-infection *via* iDCs by 2.6 fold compared to HIV-1 R5 where H37Rv MA did not show any impact (Figure 4.6 **B**). From this observation, we conclude that H37Rv and H37Rv MA have different effects on HIV-1 *trans*-infection *via* DC-SIGN. This discrepancy is most likely due to differences in the glycolipid composition of the liposomes generated from the two H37Rv strains.

Figure 4.6 : Comparison between H37Rv and H37Rv MA

$0.5x10^6$ **A.** Raji-DC-SIGN (n≥6) and **B.** iDCs (n=3, using cells isolated from one donor) were pre-incubated for 30min with 100µg of 0.8PC:0.2Ch, H37Rv, H37Rv MA liposomes or 50µl of media. The cells were then incubated 2h with HIV-1 pseudo-typed virus: **(1)** 12.5ng pSG3-LAI (HIV-1 X4) or **(2)** 20ng pSG3-BAL (HIV-1 R5). After capture the cells were washed and co-cultured with TZM-bl cells. The luciferase activity was read after 48h. 0.8PC:0.2Ch liposome is used here as a negative control and reference. Data are represented in boxplot where the box extends from the 25th and 75th percentiles, the median is plotted at the line in the middle of the box, the whiskers represents the minimum and maximum value.

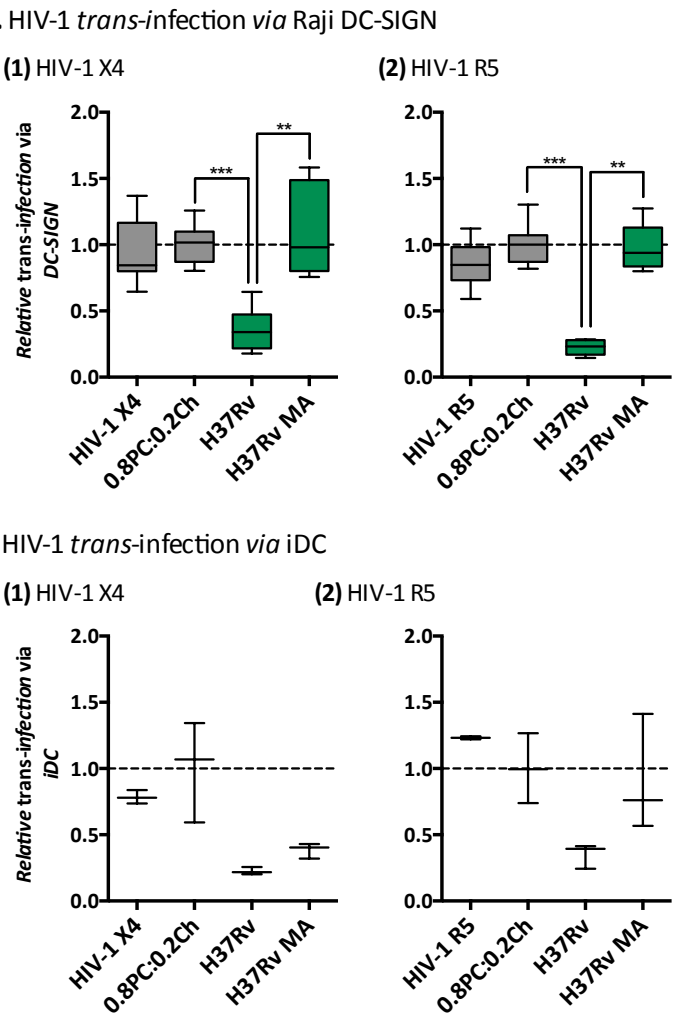

We therefore aimed to identify and characterise glycolipids from H37Rv that influence specifically HIV-1 *trans*-infection *via* DC-SIGN interactions (Figures 4.7 and 4.8). H37Rv total lipid extract was fractionated as described in Chapter 1 **Part I.** *Section i.b)*. The H37Rv lipid fractionation was visualised by TLC allowing a partial identification of some components as PDIM, SL, TDM, TMM, PL and PIMs present on fractions (Figure 4.7).

The H37Rv fractions obtained were then associated into liposomes and analysed to characterise the impact on HIV-1 X4 **A.** and R5 **B.** *trans*-infection *via* DC-SIGN. On HIV-1 X4 *trans*-infection (Figure 4.8 **A**), we observed that Fractions 2 and 4 strongly inhibited capture-transfer by 6.3 and 4.9 fold, respectively. For Fraction 1 and 5, we observed some weaker inhibition, Fraction 1 decreased the efficacy by 1.4 and Fraction 5 by 1.7 fold compared to the negative control (0.8PC:0.2Ch liposomes). Fraction 3 and 6, conversely, did not show any modulation of HIV-1 X4 *trans*-infection *via* DC-SIGN. Interestingly, for Fraction 7 and 8 we observed an increase by 2.4 and 2.3 fold, respectively. Concerning HIV-1 R5 similar

observations were obtained for HIV-1 X4 (Figure 4.8 **B**). Indeed, Fractions 2 and 4 totally inhibited HIV-1 R5 *transfer via* the DC-SIGN receptor to 0.06 and 0.15, respectively, compared to 0.23 for H37Rv liposomes containing total lipids. Fraction 5 decreased capture-transfer by 1.5 fold. For Fractions 1, 3 and 7 the impact of HIV-1 R5 is not clear due to high variations observed between values produced in triplicate, but these fractions demonstrated a trend towards not impacting on *trans*-infection *via* DC-SIGN, with relative values of 0.8, 0.79 and 0.8 observed, respectively. Interestingly Fractions 6 and 8 showed a trend towards decreasing capture-transfer by 1.6 and 1.4 fold, respectively.

PDIM and SL are both present in Fraction 2 (Figure 4.7) with the inhibition of Fraction 2 (for HIV-1 X4 and R5 *trans*-infection) *via* DC-SIGN suggesting interactions between PDIM and/or SL resulted in blocking virus capture (Figure 4.8). In addition, TDM is present within Fractions 4 to 7, with a decrease in concentration through fractionation: TDM is present at higher concentrations in Fraction 4 compared to Fraction 7 (Figure 4.7). The inhibition of Fraction 4 on capture-transfer of HIV-1 suggests that the presence of TDM could interact with DC-SIGN and block HIV-1 recognition(Figure 4.8). This conclusion is supported by the fact that Fraction 5 can still inhibit DC-SIGN mediated *trans*-infection but the effect is lost when the concentration of TDM is lower in Fractions 6 and 7 (dose dependant effect). TMM, PL and PIM present in Fraction 5, 6, 7 and 8 (Figure 4.7), showed in our assays no clear impact on HIV-1 *trans*-infection *via* DC-SIGN with variations of impact of Fractions 7 and 8 based on HIV-1 tropism observed (Figure 4.8).

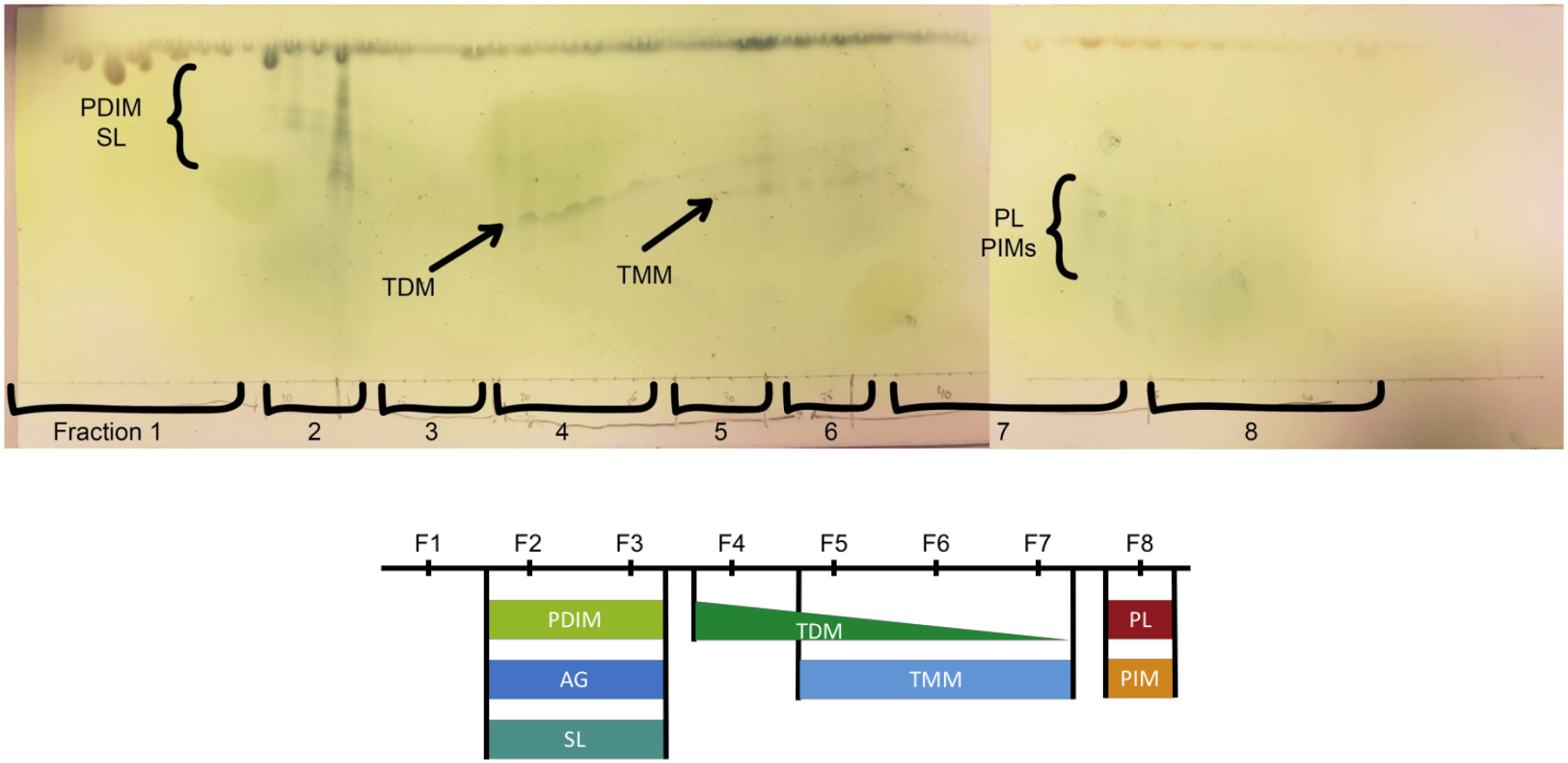

Figure 4.7 : TLC analyses of H37Rv Fractions

TLC of H37Rv's fractions occurred from H37Rv total lipid extract in 60:16:2 $CHCl_3$:MeOH:H_2O solvent and visualised by staining with MPA and charring. Fractions (1-9) were pooled as Fraction 1, (10-13) pooled as Fraction 2, (14-18) pooled as Fraction 3, (19-27) pooled as Fraction 4, (28-32) pooled as Fraction 5, (33-36) pooled as Fraction 6, (37-44) pooled as Fraction 7, and (45-63) pooled as Fraction 8. The data shown are from one experiment performed by Dr A. Bhatt, University of Birmingham..

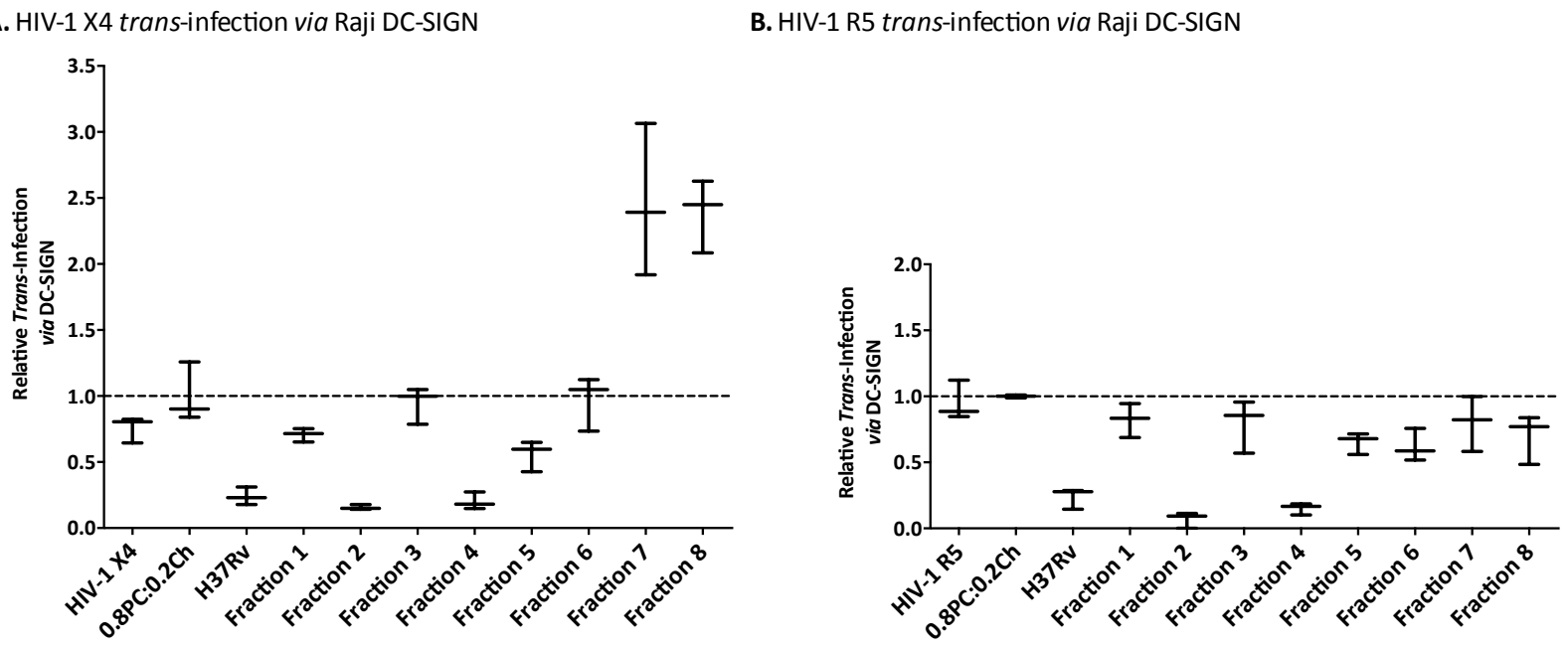

Figure 4.8 : Impact of H37Rv Fractions on HIV-1* trans*-infection

H37Rv Fractions 1 to 8 have been integrated into liposomes following the ratio 0.6PC:0.2Ch:0.2Fraction. $0.5x10^6$ Raji DC-SIGN were pre-incubated during 30min with 100µg liposomes or 50µl of media. The cells were then incubated for 2h with HIV-1 pseudo-typed virus **B.** 12.5ng pSG3-LAI (HIV-1 X4) **C.** 20ng pSG3-BAL (HIV-1 R5). After capture the cells were washed and co-cultured with TZM-bl cells. The luciferase activity was read after 48h. 0.8PC:0.2Ch liposome is used here as a negative control and reference. Data are represented in boxplot where the box extends from the 25th and 75th percentiles, the median is plotted at the line in the middle of the box, the whiskers represents the minimum and maximum value and where n=3.

We further investigated the potential role of PDIM and SL1 from *Mtb* H37Rv on affecting HIV-1 *trans*-infection (Figure 4.9). For this purpose the H37Rv mutant papA1Δ was used. As described in Chapters 2 **Part II.** *Section ii.c)*, liposomes with total lipids from H37Rv papA1Δ (missing SL1) were generated in parallel to liposomes with papA1Δ lipids complemented with soluble SL1. Additionally, liposomes containing soluble PDIM lipids were generated and tested.

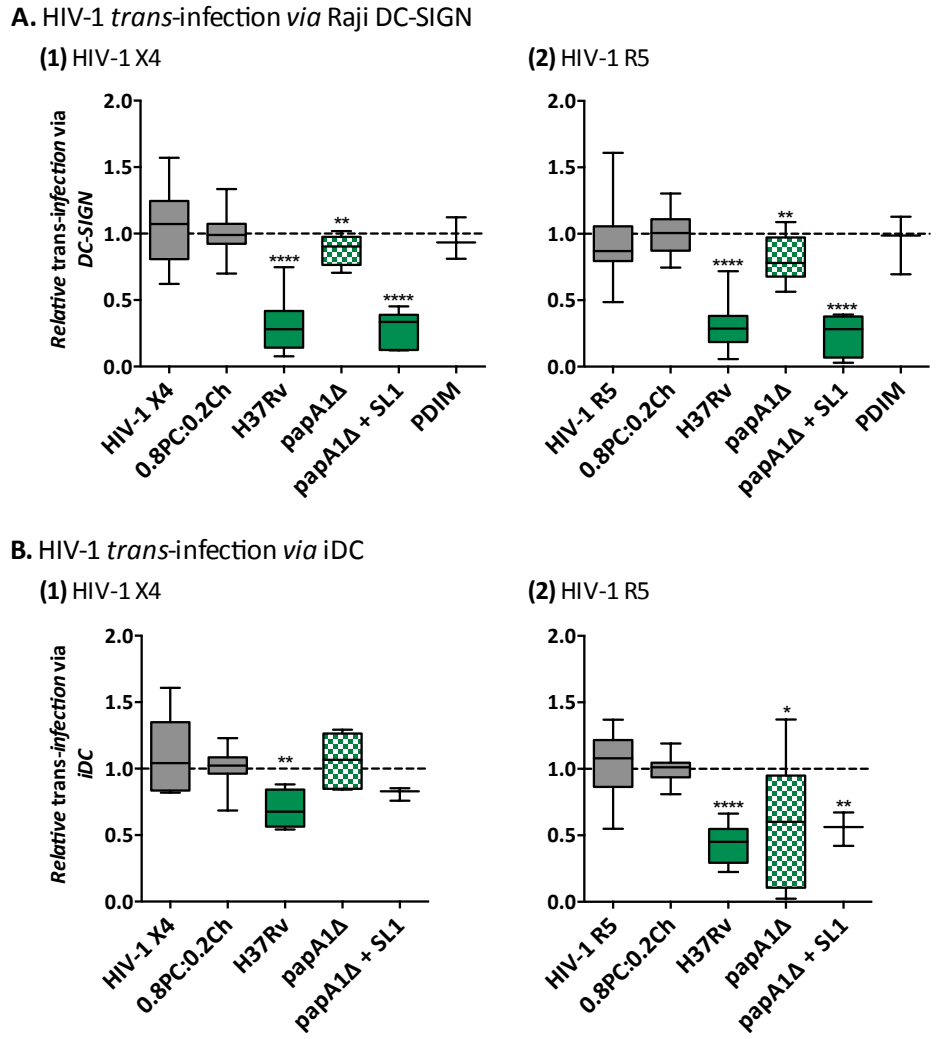

Figure 4.9 : Role of SL1 and PDIM lipids on HIV-1* trans*-infection

$0.5x10^6$ **A.** Raji-DC-SIGN (n≥3) and **B.** iDCs (n≥3 on cells isolated from two donors, excepted for the papA1Δ + SL1 condition which utilised cells isolated form one donor) were pre-incubated for 30min with 100µg liposomes or 50µl of media. The cells were then incubated for 2h with HIV-1 pseudo-typed virus: **(1)** 12.5ng pSG3-LAI (HIV-1 X4) or **(2)** 20ng pSG3-BAL (HIV-1 R5). After capture the cells were washed and co-cultured with TZM-bl cells. The luciferase activity was read after 48h. 0.8PC:0.2Ch liposome is used here as a negative control and reference. Data are represented in boxplot where the box extends from the 25th and 75th percentiles, the median is plotted at the line in the middle of the box, the whiskers represents the minimum and maximum value.

We observed that papA1Δ liposomes decreased slightly HIV-1 X4 **(1)** and R5 **(2)** *trans*-infection *via* DC-SIGN but with much lower effect when compared to H37Rv liposomes (Figure 4.9**A**). Indeed, in the presence of papA1Δ liposomes the efficacy of capture-transfer decreased to 0.8 (X4 P value= 0.0053, R5 P value= 0.0030, Mann Whitney test) compared to 0.3 for H37Rv for both virus strains (X4 and R5 P value<0.0001, Mann Whitney test), respectively. Interestingly, liposomes composed of papA1Δ total lipids complemented with SL1 were shown to cause strong inhibition of 3.4 fold for HIV-1 X4 (P value< 0.0001, Mann Whitney test) and 4.1 for HIV-1 R5 (P value< 0.0001, Mann Whitney test) *trans*-infection, respectively. This result indicates that SL1 expressed on H37Rv binds the DC-SIGN receptor, blocking HIV-1 *trans*-infection *via* this C-type lectin. Concerning PDIM, the liposomes containing soluble PDIM did not significantly impact on either HIV-1 X4 or R5 virus *trans*-infection *via* DC-SIGN.

When further investigating the impact of SL1 and PDIM on HIV-1 *trans*-infection *via* iDCs (Figure 4.9**B**), a similar trend was observed as with Raji-DC-SIGN capture-transfer (Figure 4.9**A**). For HIV-1 X4, papA1Δ did not impact on *trans*-infection compared to H37Rv which decreased the efficacy by 1.4 fold (P value =0.0176, Mann Whitney test). Liposomes complemented with SL1 did not show a significant influence on HIV-1 X4 *trans*-infection but showed a trend towards decreasing the effect by 1.2 fold. Regarding HIV-1 R5, we observed differences with papA1Δ on modifying virus capture-transfer, but which seemed to inhibit to a lesser extent compared to H37Rv: with papA1Δ decreasing transfer by 1.6 fold (P value= 0.0279, Mann Whitney test) compared to 2 for H37Rv (P value< 0.0001, Mann Whitney test). When papA1Δ liposomes were complemented with SL1 we observed less variation and a decrease of HIV-1 R5 *trans*-infection *via* iDCs by 1.8 fold (P value= 0.0036, Mann Whitney test). From those observations we could conclude that SL1 from H37Rv can be recognised by the DC-SIGN receptor expressed on iDCs and thereby decreasing HIV-1 capture-transfer *to* TZM-bl cells.

iii. Influence of liposomes on HIV-1 trans-infection - Replicative System

a) Optimisation

HIV-1 *trans*-infection *via* iDCs to $CD4^+$ lymphocytes within a replicative system was optimised before studying the effects of *Mtb* liposomes on HIV-1 replication. As explained previously in Chapter 3 **Part II.** *Section ii.a)*, two HIV-1 strains were tested; HIV-1 X4 LAI-YFP and HIV-1 R5

BAL-GFP, with infection being monitored over 14 days by measuring HIV-1 capsid p24 production and analysing percentage of $CD4^+$ infected cells expressing YFP (LAI) or GFP (BAL) by flow cytometry. The optimisation of the system for *trans*-infection using the replicative system is shown (Figure 4.10).

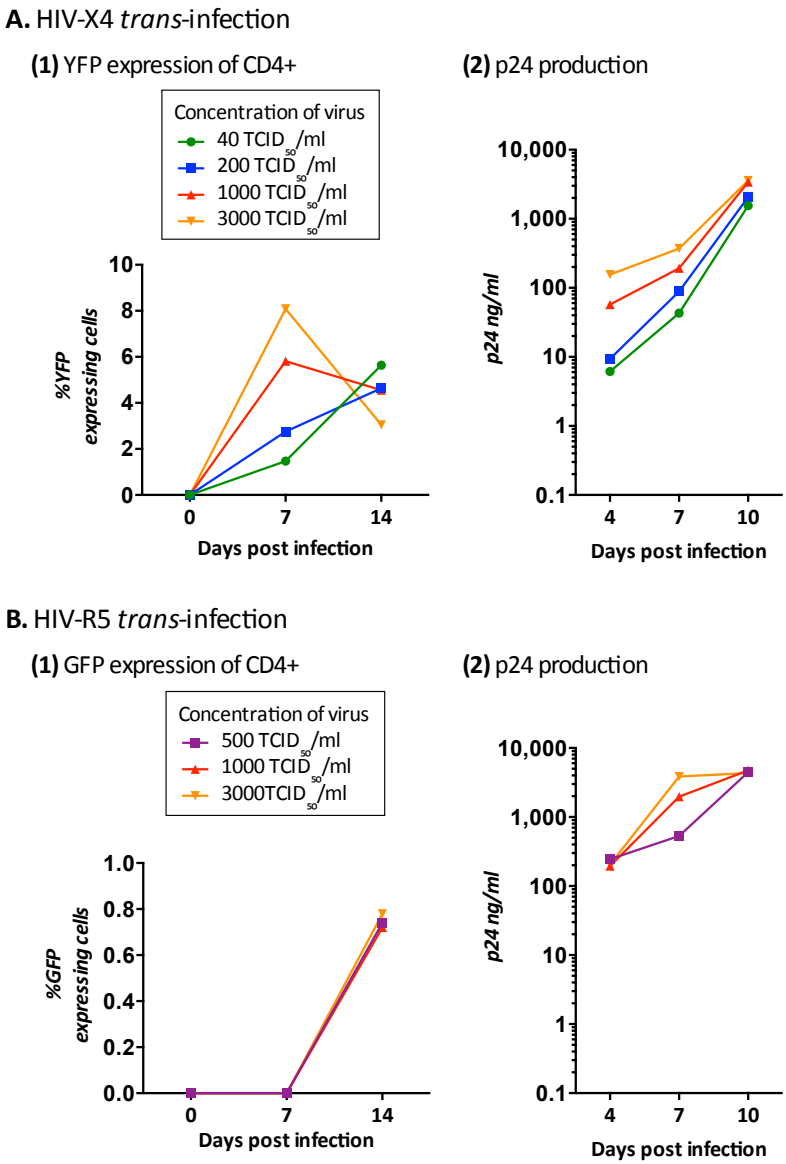

Figure 4.10 : Optimisation of HIV-1* trans*-infection using $CD4^+$ T cells

Human blood monocytes were isolated from buffy coats using Ficoll gradient and a subsequent CD14 selection step using the MACS system. Purified monocytes were differentiated into iDCs in the presence of IL-4 and GM-CSF, 70ng/ml and 50ng/ml respectively. On day 6, the phenotype of the cultured iDCs cells was confirmed by flow cytometry and $2x10^4$ iDCs were incubated 30min with **A.** 40, 200, 1000, 3000 $TCID_{50}$/ml LAI-YFP (HIV-1 X4) or **B.** 500, 1000, 3000 $TCID_{50}$/ml BAL-GFP (HIV-1 R5) virus. After capture the cells were washed and co-cultured with $2x10^5$ $CD4^+$ enriched T-lymphocytes. At day 4, 7 and 10 HIV-1 capsid p24 was determined in the supernatant by ELISA, and at day 7, 10, and 14 the percentage of infected cells was measure by FACS (YFP expression for LAI, and GFP expression for BAL). The data shown is from one experiment using cells isolated from one donor.

Four titres of HIV-1 X4 were tested: 40, 200, 1000 and 3000 $TCID_{50}$/ml (Figure 4.10 **A.**). Regarding YFP expression by infected cells **(1)**, we observed at day 7 a peak of infected cells for 1000 and 3000 $TCID_{50}$/ml LAI-YFP concentrations with 5.8% and 8.09% cells expressing YFP, respectively. This number decreased overtime to 4.55 and 3.05%, respectively at day 14 post-infection. For 40 and 200$TCID_{50}$/ml titres, the peak of infected cells was obtained at day 14 with 5.6 and 4.6% cells expressing YFP. Concerning p24 production in supernatant **(2)**, for all four conditions we observed a gradual increase in p24 production overtime from day 4 to day 10 post-infection rising from 6.1 to 1551.9ng/ml for 40 $TCID_{50}$/ml, 9.4 to 2058.6ng/ml for 200 $TCID_{50}$/ml, 57.3 to 3401.9ng/ml for 1000 $TCID_{50}$/ml and 155.4 to 3583.6ng/ml for 3000 $TCID_{50}$/ml. As for the HIV-1 *cis*-infection assays (Chapter 3) we decided to use 200 $TCID_{50}$/ml for HIV-1 X4 LAI-YFP titres and to stop the experiment at day 7 post-infection for the capture-transfer assay.

Next three concentrations of BAL-GFP 500, 1000 and 3000$TCID_{50}$/ml were tested (Figure 4.10 **B**). As observed Chapter 3 **Part II.** *Section ii.a)* for $CD4^+$ T lymphocytes *cis*-infection, measuring the proportion of infected cells by flow cytometry with percentage cells expressing GFP was not a good read-out for our assays. Indeed **(1)**, the percentage of infected cells reached only 0.7% of infected cells at day 14 post-infection. Conversely, when reading p24 production in the supernatant **(2)** we observed a gradual rise in p24 overtime. The p24 concentration increased from 245.0 at day 4 to 4475.8ng/ml at day 10 for 500 $TCID_{50}$/ml, 194.9 to 4753.8ng/ml for 1000 $TCID_{50}$/ml and 206.7 to 4345.9ng/ml for 3000 $TCID_{50}$/ml. We therefore chose to use 500 $TCID_{50}$/ml as a standard titre for HIV-1 R5 BAL-GFP infections and to complete *trans*-infection experiments at day 7 post-infection.

b) Influence of Mycobacterium *liposomes on HIV-1 trans-infection*

We studied the effects that *Mtb* glycolipid liposomes have on HIV-1 X4 and R5 *trans*-infection *via* iDCs to $CD4^+$ T lymphocytes where *Mtb* liposomes were present during capture-transfer of virus. The p24 production was determined at day 4 and 7 post-infection, and HIV-1 DNA content was quantified at day 7 (total HIV-1 DNA, 2-LTR circular DNA and integrated DNA). Cytokine and chemokine expression levels were monitored in culture supernatant at day 7 using the Luminex® assay.

The influence of *Mtb* liposomes present during virus capture-transfer on HIV-1 X4 *trans*-infection *via* iDCs to $CD4^+$ lymphocytes is shown (Figure 4.11 and 4.12). The condition of capture-transfer with virus alone was used as a reference.

Monitoring p24 at day 4 post-infection LPS, BCG, H37Rv, HN878, CDC1551 and EU127 demonstrated significant decreases in HIV-1 replication, by 1.3, 2.2, 2.4, 1.4, 1.7 and 2.2 fold (P values= 0.0286, Mann Whitney test), respectively (Figure 4.11 **A(1)**). The strongest effect was observed for BCG, H37Rv and EU127 liposomes. The same phenomenon was observed at day 7 post-infection **(2)** where BCG, HN878, CDC1551 and EU127 demonstrated a trend towards decreasing p24 production by between 1.2-1.3 fold for each. The presence of H37Rv liposomes did not have a significant impact on capture-transfer. We observed an increase (Figure 4.11 **B**) in total HIV-1 copy numbers **(1)** in the presence of LPS to 7.7 log10 copies per 10^6 cells compared to 7.3 for virus alone. *Mtb* HN878 liposomes present during capture-transfer of HIV-1 X4 showed a trend towards increasing HIV-1 replication with 7.5 log10 copies per 10^6 cells measured. The 2-LTR circular DNA copy numbers **(2)** indicated that the presence of BCG and CDC1551 log10 copy numbers per cell were reduced by 4.9 compared to 5.1 for virus alone. In addition, LPS demonstrated a trend towards increasing HIV-1 2-LTR copy numbers to 5.2. Concerning the HIV-1 integrated DNA form **(3)**, we did not observe any significant impact of liposomes on modulating copy numbers. When observing ratios between quantity of HIV-1 total DNA, 2-LTR and integrated forms, no differences where noticed (Appendix 19, right panels). Finally, no toxic effects of the liposomes tested were observed in this assay when comparing cell concentration for each condition (Appendix 20).

It can be concluded, taking the results together, that *Mtb* HN878 and LPS showed a trend towards increasing HIV-1 X4 *trans*-infection when liposomes were present during capture-transfer, thereby heightening virus replication. BCG, H37Rv, CDC1551 and EU127 liposomes, on the contrary, appear to exert no significantly impact on HIV-1 X4 *trans*-infection *via* iDCs to $CD4^+$ T lymphocytes.

A. p24 production

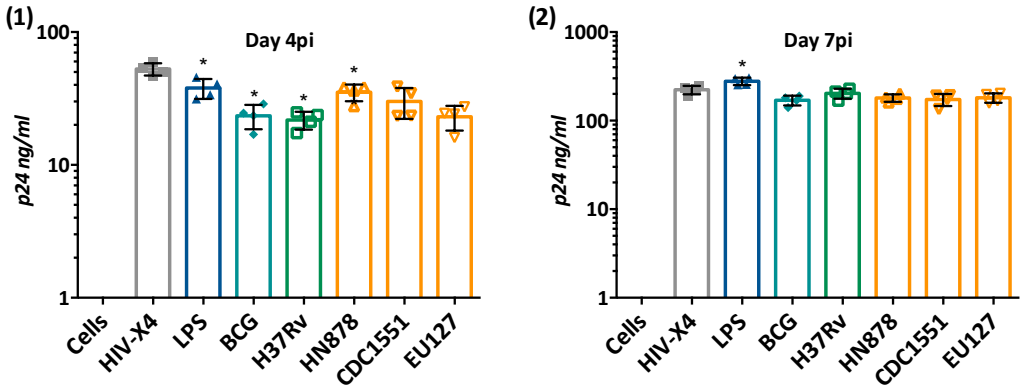

B. DNA quantification

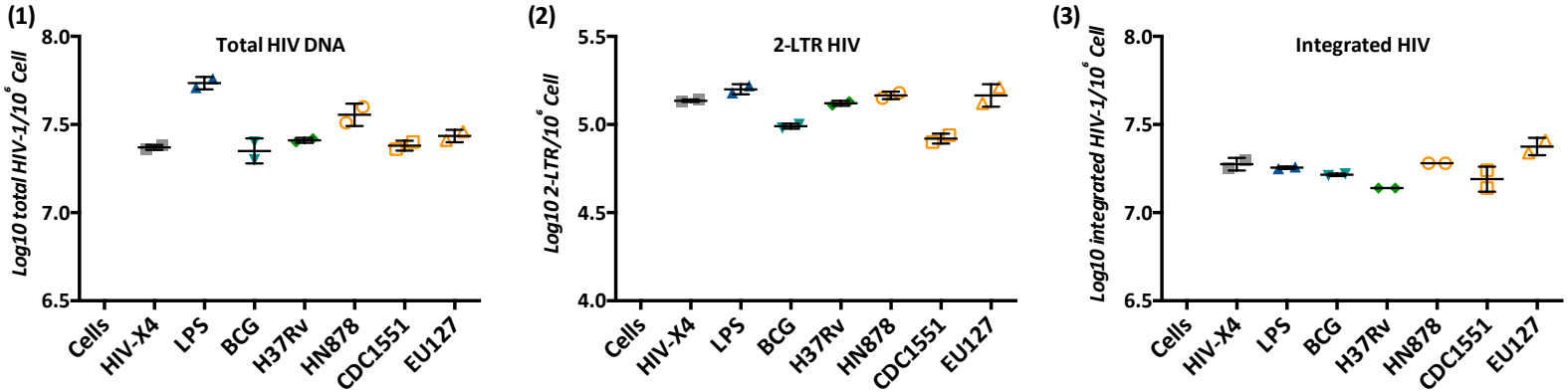

Figure 4.11 : Influence of* Mycobacterium *liposomes on HIV-1 X4* trans*-infection

$8x10^4$ iDCs were pre-incubated with 100µg of *Mycobacterium* liposomes *or* 100ng/ml of LPS for 30min. The cells were incubated 30min with 200 $TCID_{50}$/ml LAI-YFP (HIV-1 X4), washed then co-cultured with $CD4^+$ enriched T lymphocytes in 96-well plate. Finally 40µg of the same *Mycobacterium* liposomes or 100ng/ml of LPS was added per well. **A.** Concentration of total HIV-1 capsid p24 was determined in the supernatant by ELISA at **(1)** day 4 (n=4) and **(2)** day 7 (n=4)post-infection. **B.** represents log10 HIV-1 DNA quantification determined by PCR relative to the total number of cells at day 7 post-infection with **(1)** total HIV-1 DNA quantification (n=2), **(2)** number of HIV-1 2-LTR (n=2) and **(3)** number of integrated HIV (n=2). The data shown are representative of one experiment using cells isolated from one donor.

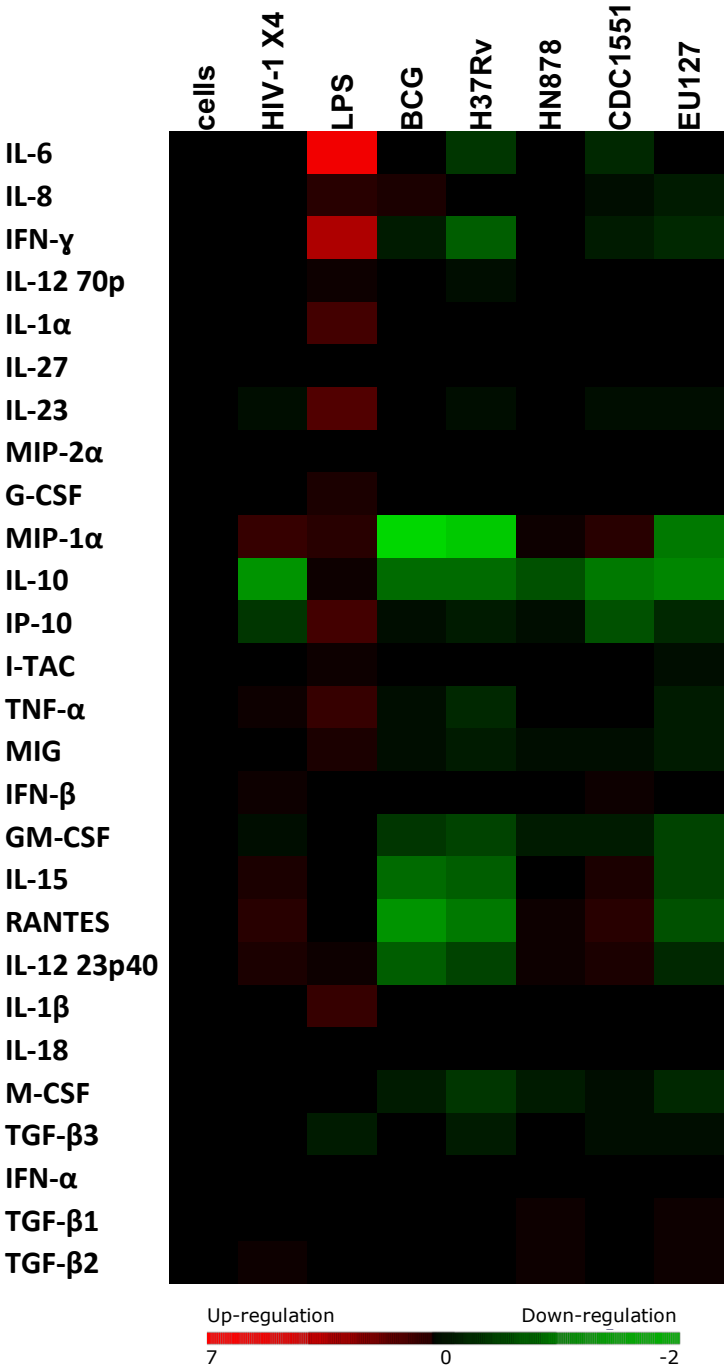

Figure 4.12 : Influence of* Mycobacterium *liposomes on HIV-1 X4* trans*-infection – Luminex®

8x10^4 iDCs were pre-incubated with 100µg of *Mycobacterium* liposomes *or* 100ng/ml of LPS for 30min. The cells were incubated 30min with 200 $TCID_{50}$/ml LAI-YFP (HIV-1 X4), washed then co-cultured with $CD4^+$ enriched T lymphocytes in 96-well plate. Finally 40µg of the same *Mycobacterium* liposomes or 100ng/ml of LPS was added per well. At day 7 post-infection, supernatants were collected for Luminex® analyses. Luminex results are represented by Heat Maps Cluster of the Log2 of liposomes treatment/MDM baseline ratio. An increase of cytokine production in the supernatant is represented in red, a diminution of cytokine production depict in green and no change shown as black. For the data shown, n=3 using cells isolated from one donor.

From Luminex® assays (Figure 4.12), Heat Map analyses revealed that HIV-1 X4 *trans*-infection enhanced production of MIP-1α, TNF-α, IFN-γ, IFN-β, IL-15, RANTES, IL-12 23p40 and TGF-β2 compared to the non-infected cells, and induced a reduction of IL-23, IL-10, IP-10 and GM-CSF. The liposomes HN878 and CDC1551 followed globally the same pattern observed with virus alone, suggesting that they did not impact on the immune response induced within the infected cells. LPS showed the capacity to induce a strong production of numerous pro-inflammatory cytokines such as IL-6, IL-8, IL-1α, IL-23, G-CSF, IP-10, TNF-α, MIG and IL-1β compared to virus alone. However, the presence of BCG, H37Rv and EU127 liposomes during *trans*-infection showed a different profile of cytokine production compared to the virus alone and LPS. Indeed, for these conditions we observed a decrease in IFN-γ, MIP-1α, TNF-α, MIG, IL-15, RANTES, IL-12 23p40, M-CSF and TGF-β3 cytokines. This result suggests that these liposomes influenced the infected cells immune response.

Depending on the *Mtb* strains studied we observed different impacts on HIV-1 X4 *trans*-infection and cytokine production. When comparing analyses from Figures 4.11 and 4.12, we could conclude that HN878 and LPS demonstrated a trend towards activating HIV-1 X4 *trans*-infection *via* the different mechanisms that allow for activation of the immune response favourable for virus infection. Indeed, LPS showed a trend towards activating many pro-inflammatory cytokines, whereas HN878 did not seem to change the immune response from the infected cells compared to *trans*-infection with virus alone. Conversely, liposomes showing influences on cytokine production from infected cells did not influence HIV-1 X4 replication.

The influence of *Mtb* liposomes on HIV-1 R5 capture-transfer is shown (Figures 4.13 and 4.14). The *trans*-infection of virus alone, as above, was used as a reference. At day 4 post-infection the presence of LPS and HN878 significantly increased p24 production in the supernatant by 1.6 and 1.2 respectively (P value= 0.02686, Mann Whitney test) (Figure 4.13 **A(1)**). However, we additionally observed a trend towards increased replication with H37Rv (1.3 fold) and EU127 (1.2 fold). At day 7 post infection only EU127 stimulation showed a significant impact on p24 production with an increase of 1.3 fold (P value= 0.02686, Mann Whitney test) compared to virus alone (Figure 4.13 **A(2)**).

A. p24 production

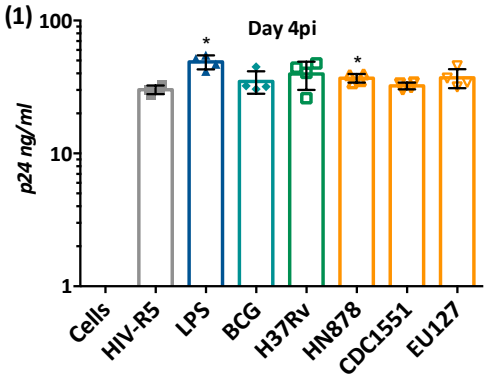

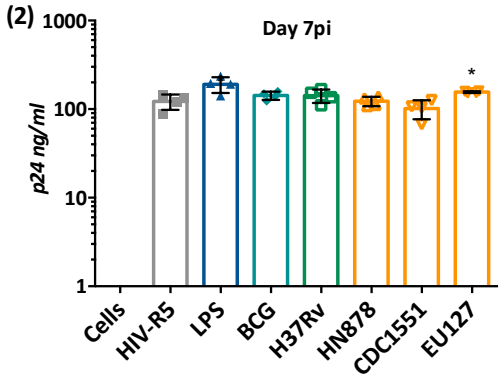

B. DNA quantification

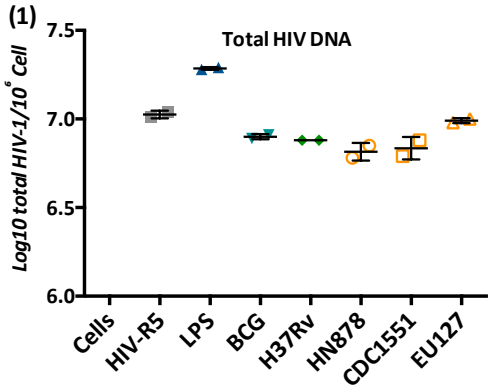

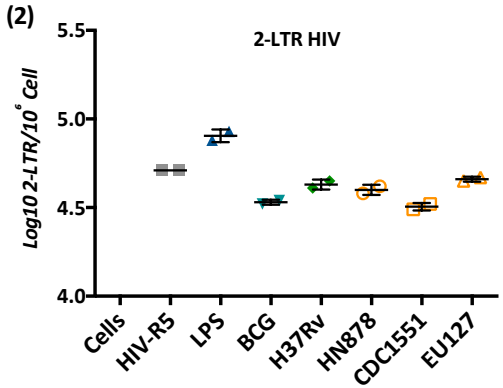

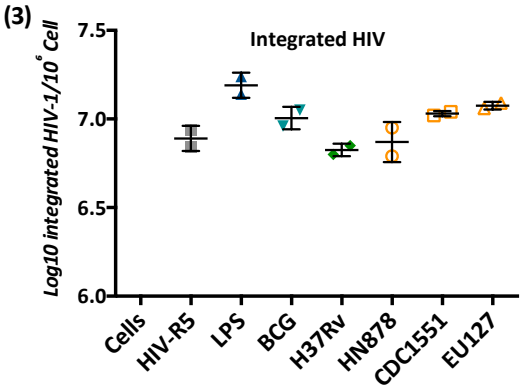

Figure 4.13 : Influence of* Mycobacterium *liposomes on HIV-1 R5* trans*-infection

$8x10^4$ iDCs were pre-incubated with 100µg of *Mycobacterium* liposomes for 30min or 100ng/ml of LPS. The cells were incubated 30min with 500 $TCID_{50}$/ml BAL-GFP (HIV-1 R5) and washed before co-culturing with $CD4^+$ enriched T lymphocytes in 96-well plate. Finally 40µg of the same *Mycobacterium* liposomes *or* 100ng/ml of LPS was added per well. **A.** Concentration of total HIV-1 capsid p24 was determinate in the supernatant by ELISA at **(1)** day 4 (n=4) and **(2)** day 7 (n=4) post-infection. **B.** represents log10 HIV-1 DNA quantification determined by PCR relative to the total number of CD4+ cells at day 7 post-infection with **(1)** total HIV-1 DNA quantification (n=2), **(2)** number of HIV-1 2-LTR (n=2) and **(3)** number of integrated HIV (n=2). The data shown are representative of one experiment using cells isolated from one donor.

The observation concerning p24 production did not totally correlate with HIV-1 DNA quantification levels (Figures 4.13 **B**). Total HIV-1 DNA copy numbers **(1)** increased in the presence of LPS to 7.2 log10 copies per 10^6 cells from 7 for virus alone. However, BCG, H37Rv, HN878 and CDC1551 demonstrated a trend towards decreasing the copy number to 6.9 and 6.8 log10 copies per 10^6 cells. Concerning HIV-1 2-LTR DNA forms **(2)**, the presence of LPS showed a trend in increasing numbers to 4.9 log10 copies per 10^6 cells. As observed for total DNA quantifications BCG, H37Rv, HN878, CDC1551 and EU127 demonstrated a trend in decreasing the number of 2-LTR copies to 4.5, 4.6, 4.6, 4.5 and 4.6 log10 copies per 10^6 cells, respectively compared to 4.7 for virus alone. For integrated HIV-1 DNA copies **(3)** we observed a similar trend with LPS, where levels increased to 7.1 log10 copies per 10^6 cells compared to 6.8 for virus alone. However, the influence of BCG, H37Rv and HN878 liposomes were not clear due to a high degree of variation between duplicates. Interestingly, CDC1551 and EU127 demonstrated a trend towards increasing the levels of integrated HIV-1 copies to 7 copies. When observing ratios between quantity of HIV-1 total DNA, 2-LTR and integrated forms, no differences where noticed (Appendix 19, right panels). Finally, no toxic effect of the liposomes tested were observed in this assay (Appendix 20).

In conclusion, LPS increased HIV-1 R5 *trans*-infection *via* iDCs to $CD4^+$T lymphocytes and showed increased viral replication, however none of the *Mtb* liposomes demonstrated an impact on HIV-1 R5 *trans*-infection.

Concerning the cytokines produced during HIV-1 R5 *trans*-infection (Figure 4.14), we observed that infection with virus alone induced specific production profiles compared to the uninfected cells. Indeed, HIV-1 R5 *trans*-infection induced a decrease in production of IFN-γ, MIP-1α, TNF-α, IL-15, RANTEs and IL-12 23p40. LPS presence influenced infected responses by inducing production of a large pro-inflammatory response. Interestingly, BCG, H37Rv and EU127 liposomes showed a trend similar for virus alone, however some variations can be observed. BCG liposomes induced stronger inhibition of MIP-1α, IL-15, RANTEs and IL-12 23p40 compared to virus alone. Additionally, BCG induced a decrease in IL-10, IFN-β, GM-CSF and M-CSF whereas H37Rv inhibited IL-6 and MIG. The presence of EU127 liposomes during R5 *trans*-infection seemed to induce production of IL-6, IL-8, IL-10, IP-10 and IL-1β. These results suggest that BCG, H37Rv and EU127 influenced immune responses within infected cells. For HN878 and CDC1551 there was a trend observed towards altering cytokine profiles within infected cultures. Indeed, for both liposomes we observed less impact on cytokine production compared to non-infected cells. HN878 liposomes provided an increase

of IL-8 and IP-10 production whereas CDC1551 induced a decrease in IFN-γ, IL-10 and M-CSF production.

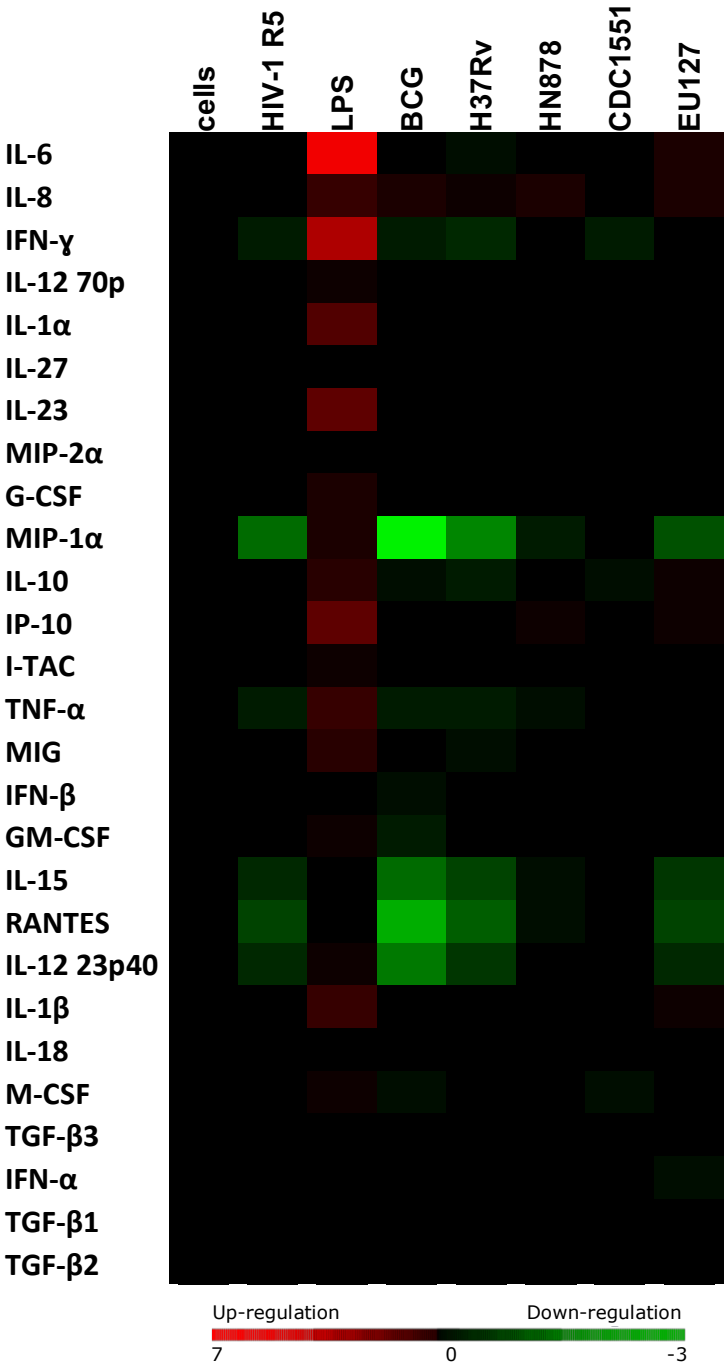

Figure 4.14 : Influence of* Mycobacterium *liposomes on HIV-1 R5* trans*-infection - Luminex®

8x10^4 iDCs were pre-incubated with 100µg of *Mycobacterium* liposomes *or* 100ng/ml of LPS for 30min. The cells were incubated 30min with 500 $TCID_{50}$/ml BAL-GFP (HIV-1 R5), washed then co-cultured with $CD4^+$ enriched T lymphocytes in 96 well plate. Finally 40µg of the same *Mycobacterium* liposomes or 100ng/ml of LPS was added per well. At day 7 post-infection, supernatants were collected for Luminex® analyses. Luminex results are represented by Heat Maps Cluster of the Log2 of liposomes treatment/MDM baseline ratio. An increase of cytokine production in the supernatant is represented in red, a diminution of cytokine production depict in green and no change shown as black. For the data shown, n=3 using cells isolated from one donor.

When comparing the impact of liposomes on HIV-1 R5 *trans*-infection on replication (Figure 4.13) and the cytokines production (Figure 4.14) analyses, we observed that the origin of *Mtb* strains influences differentially HIV-1 R5 *trans*-infection *via* iDCs to $CD4^+$T lymphocytes. LPS, CDC1551 and EU127 showed a trend towards enhancing HIV-1 R5 replication. The mechanisms behind this observation might be different since variant cytokine production profiles were observed as with HIV-1 non-infected cultures. Additionally, from HIV-1 X4 and R5 *trans*-infection, we observed different impacts of liposomes, where HN878 up-regulates replication of HIV-1 X4 but no HIV-1 R5 or CDC1551 and EU127 up-regulates HIV-1 R5 but not HIV-1 X4. Also, the cytokines profiles obtained by both infections were slightly different where HIV-1 X4 showed a stronger capacity to induce pro-inflammatory cytokine production compared to HIV-1 R5. The presence of liposomes therefore induced some variations on the immune response from infected cells depending of the virus being tested.

iv. Influence of Mycobacterium *liposomes on co-culture – Replicative System*

To understand the impact of *Mtb* glycolipids on HIV-1 infection and pathogenicity, the strategy selected was to study *cis*- and *trans*-infection separately. Indeed, we tested in Chapter 3, the impact of *Mtb* liposomes on HIV-1 *cis*-infection and in this Chapter the focus is studying liposome influence on HIV-1 *trans*-infection. For both experimental systems we utilised two different systems: the pseudo-typed virus particle system and the replicative system. In this section we studied a more physiologically relevant system, ie addressing the impact *Mtb* liposomes have on HIV-1 infections where iDCs and $CD4^+$ T lymphocytes are co-cultured together. In this setting, HIV-1 *cis*- and *trans*-infection occur simultaneously. We studied the impact of liposomes on influencing HIV-1 X4 (Figures 4.15), and HIV-1 R5 (Figure 4.17) replication. As previously described, infections were monitored by measuring p24 production at day 4 and 7 post-infection as well as HIV-1 DNA quantifications (total HIV DNA, 2-LTR, and integrated HIV) and Luminex® quantifications at day 7.

A. p24 production

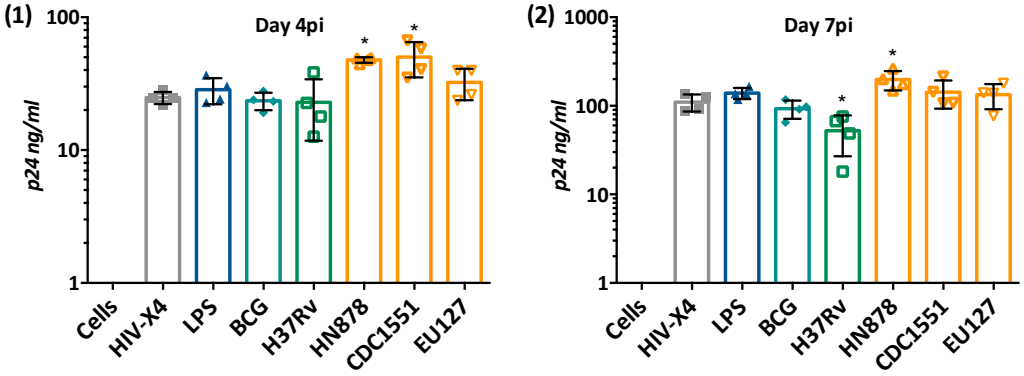

B. DNA quantification

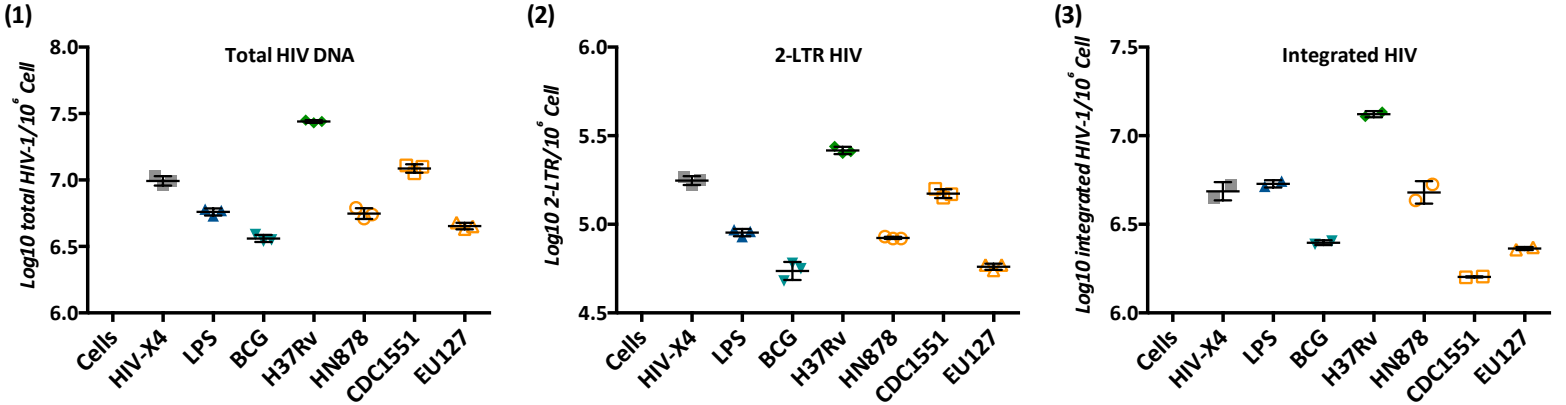

Figure 4.15 : Influence of* Mycobacterium *liposomes on HIV-1 X4 infections - co-culture iDC and CD4⁺T cells

In a 96-well plate, 2x10⁴ iDCs were placed in culture with 2x10⁵ CD4⁺ T lymphocytes and infected with 200 $TCID_{50}$/ml LAI-YFP (HIV-1 X4). 40µg of *Mycobacterium* liposomes or 100ng/ml of LPS was added. **A.** Concentration of total HIV-1 capsid p24 was determined in the supernatant by ELISA at **(1)** day 4 (n=4) and **(2)** day 7 (n=4) post-infection. **B.** represents log10 HIV-1 DNA quantification determinate by PCR relative to the total number of CD4+ cells at day 7 post-infection with **(1)** total HIV-1 DNA quantification (n=3), **(2)** number of HIV-1 2-LTR (n=3) and **(3)** number of integrated HIV (n=2). The data shown are from one experiment using cells isolated from one donor.

When HN878 and CDC1551 liposomes were present during co-culture the p24 production with HIV-1 X4 significantly increased by 1.9 and 2.0 fold (P values= 0.0286, Mann-Whitney test), respectively (Figure 4.15 **A(1)**). None of the other conditions demonstrated any impact on infection. At day 7 post-infection H37Rv decreased p24 production by 2.0 fold (P value= 0.0286, Mann-Whitney test) compared to virus alone (Figure 4.15 **A(2)**). Conversely, HN878 increased p24 production by 1.7 fold (P value= 0.0286, Mann-Whitney test). Concerning HIV-1 DNA quantification, we observed a clear profile of *Mtb* liposomes impacting on HIV-1 replication (Figure 4.15 **B.**). For total HIV-1 DNA **(1)**, LPS, BCG, HN878 and EU127 decreased the number of copies to 6.7, 6.5, 6.7 and 6.6 log10 copies per 10^6 cells compared to 6.9 copies for the virus alone. Conversely, H37Rv and CDC1551 increased HIV-1 DNA to 7.4 and 7 log10 copies per 10^6 cells, respectively. A similar profile was observed for 2-LTR circular DNA levels **(2)**, indeed, LPS, BCG, HN878 and EU127 decreased the number of copies to 4.9, 4.7, 4.9 and 4.7 log10 copies per 10^6 compared to 5.2 for virus alone. *Mtb* H37Rv increased 2-LTR copies to 5.4, but CDC1551 decreased the levels to 5.1 copies. For integrated HIV-1 DNA levels **(3)**, H37Rv increased HIV-1 copy numbers to 7.1 log10 copies per 10^6 cells from 6.6 for virus alone. However, CDC1551 decreased HIV-1 DNA integration to 6.2 copies. LPS and HN878 did not demonstrate any influence on HIV DNA-1 integration but BCG and EU127 showed a trend towards reducing levels to 6.3 log10 copies per 10^6 cells. When observing ratios between quantity of HIV-1 total DNA, 2-LTR and integrated forms, no differences where observed (Appendix 21). Finally, no toxic effect of the liposomes tested were observed in this assay (Appendix 22). Overall, we can conclude that BCG, HN878 and EU127 appear to reduce HIV-1 X4 replication, whilst H37Rv and CDC1551 showed a trend towards activating virus production and replication on iDC/$CD4^+$ T cell co-culture *in vitro*.

From the Luminex® analyses on iDC/$CD4^+$ T cell co-cultures infected with HIV-1 X4 (Figure 4.16) we observed that virus alone induced production of TGF-β1 and 2, and decreased IL-10 production. The presence of LPS induced production of a large number of pro-inflammatory cytokines. Additionally, H37Rv, HN878, CDC1551, EU127 similarly enhanced production of cytokines compared to virus alone. However, compared to LPS, different cytokines were expressed such as MIP-1α, IFN-β, GM-CSF, IL-15 for H37Rv and decreased MIG for H37Rv, HN878, CDC1551 and EU127. Additionally, the presence of BCG and EU127 during HIV-1 X4 infection demonstrated a decrease in MIP-1α production. These results suggest that *Mtb* liposomes induced different responses in infected cell populations compared to infection without stimuli. These observations suggest that the mechanisms involved might be different for BCG liposomes compared to H37Rv, HN878, CDC1551 and EU127.

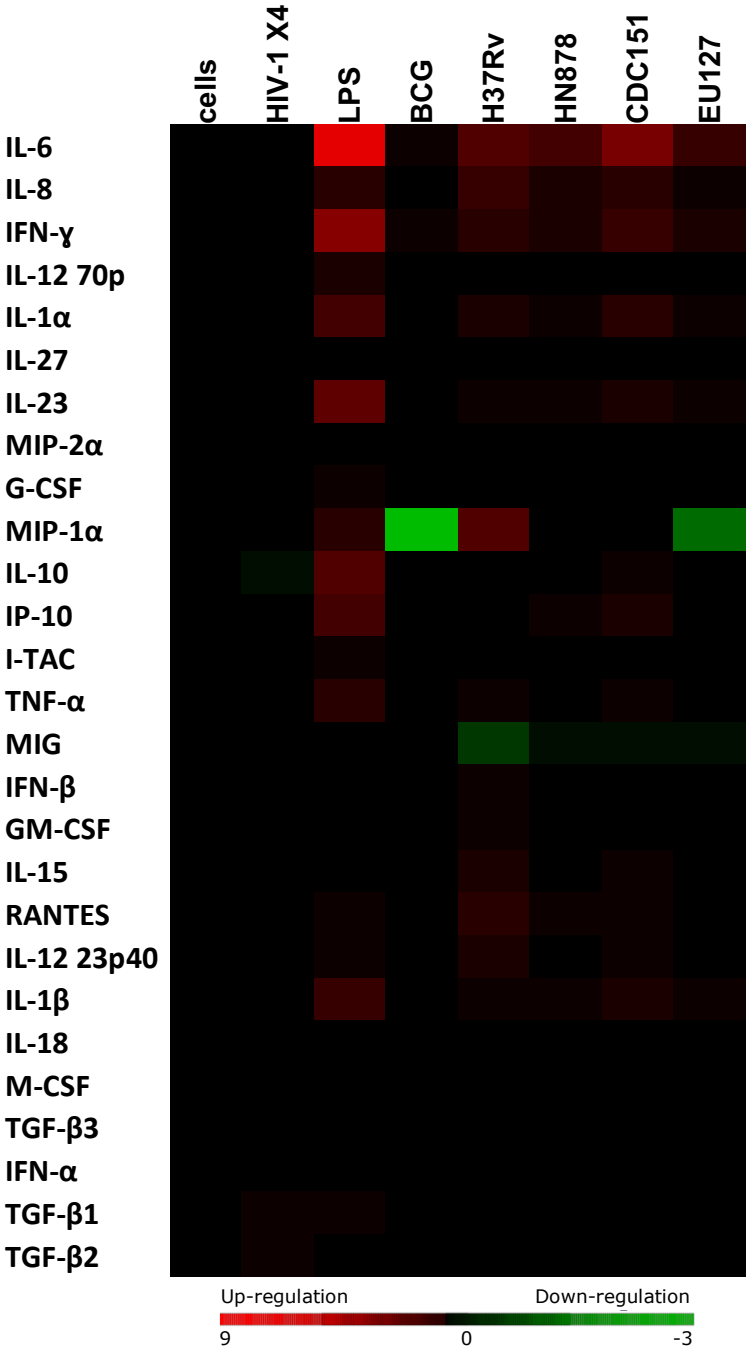

Figure 4.16 : Influence of* Mycobacterium *liposomes on HIV-1 X4 infections - co-culture iDC and CD4⁺T cells - Luminex®

In a 96-well plate, $2x10^4$ iDCs were placed in culture with $2x10^5$ $CD4^+$ T lymphocytes and infected with 200 $TCID_{50}$/ml LAI-YFP (HIV-1 X4). 40µg of *Mycobacterium* liposomes or 100ng/ml of LPS was added. At day 7 post-infection, supernatants were collected for Luminex® analyses. Luminex results are represented by Heat Maps Cluster of the Log2 of liposomes treatment/MDM baseline ratio. An increase of cytokine production in the supernatant is represented in red, a diminution of cytokine production depict in green and no change shown as black. For the data shown, n=3 using cells isolated from one donor.

Interestingly, when we compared Luminex results with the impact of liposomes on modulating HIV-1 X4 replication we observed some variations. Indeed, BCG, HN878 and EU127 demonstrated a trend towards inhibiting HIV-1 X4 replication in iDC/$CD4^+$ T cell co-cultures. However, cytokine production induced by infected cells were found to differ for the three liposomes tested suggesting that BCG, HN878 and EU127 blocked HIV-1 X4 replication by different mechanisms which were modulated by immune responses induced in HIV-1 infected cultures. Additionally, H37Rv and CDC1551 demonstrated a trend towards increasing HIV-1 X4 replication. This associated with heightened activation of pro-inflammatory cytokine production compared to HN878 and EU127, similar to LPS. These results suggest that H37Rv and CDC1551 created a favourable environment for HIV-1 replication, but conversely LPS showed a trend towards decreasing HIV-1 X4 replication. We can conclude that strong activation of the pro-inflammatory response with LPS can down-modulate HIV-1 X4 replication.

The impact of *Mtb* liposomes on modulating HIV-1 R5 infection when $CD4^+$ T cells and iDCs are co-cultured are shown Figures 4.17. At day 4 post-infection LPS and H37Rv decreased p24 production to 10.5ng/ml and 10.3ng/ml (P values= 0.0286, Mann-Whitney test) compared to 28.9ng/ml for virus alone (Figures 4.17 **A(1)**). For the other liposomes no effects were observed. At day 7 post-infection BCG, H37RV, CDC1551 and EU127 decreased p24 production to 61.2, 35.1, 51.9 and 60.2ng/m,l respectively (P values= 0.0286, Mann-Whitney test) compared to 109.3ng/ml for HIV-1 R5 alone (Figures 4.17 **A(2)**).

When analysing total HIV-1 DNA quantification it was observed that for all liposomes an increase in copy numbers was observed (Figure 4.17 **B(1)**). Indeed, LPS increased total HIV-1 DNA to 7.1 log10 copies per 10^6 cells, BCG 6.9 copies, H37Rv to 6.9 copies and EU127 to 7 copies compared to 6.8 log10 copies per 10^6 cells with the control. The stronger effects were observed with HN878 and CDC1551 which increased HIV-1 DNA production to 7.4 and 7.5 log10 copies per 10^6 cells, respectively. Interestingly, we observed that HN878 and CDC1551 significantly increased the copy numbers of HIV-1 2-LTR **(2)** to 5.5 and 5.6 log10 copies per 10^6 cells compared to 5.1 copies for virus alone. LPS, BCG, and EU127 did not show any influence on the 2-LTR copy number but H37Rv decreased the number of copies to 5 log10 copies per 10^6 cells. Relating to virus integration **(3)**, LPS and H37Rv increased integrated DNA levels to 6.9 log10 copies per 10^6 compared to 6.8 copies for virus alone. HN878 and CDC1551 showed again the strongest effects with an increase to 7.3 copies. When observing ratios between quantity of HIV-1 total DNA, 2-LTR and integrated forms, no differences where

observed (Appendix 21). Finally, no toxic effect of the *Mycobacterium* liposomes tested were observed in this assay (Appendix 22). Taking the results together, we can conclude that HN878 and CDC1551 liposomes showed a strong trend towards increasing HIV-1 production and replication in our system. The action of BCG, H37Rv and EU127 liposomes showed lesser effects on modulating HIV-1 replication.

We next compared cytokine production during HIV-1 R5 infection of iDC/$CD4^+$ co-cultures (Figure 4.18) and compared infected and uninfected responses. HIV-1 R5 infection induced production of IFN-γ, IL-23, IL-10, IP-10, TNF-α, MIG, GM-CSF and IFN-α, and decreased TGF-β3 in the absence of liposomes. Liposomes additionally induced production of IL-10, IP-10 and TNF-α suggesting that production of these cytokines is associated with viral infection. Furthermore, we observed some variations where liposomes were able to induce differential cytokine production in infected populations, such as IL-8 and decrease M-CSF production. These observations suggest that *Mtb* liposomes were able to induce differential immune responses from infected cells compared to virus alone, depending on the *M* strain. LPS alone showed the capacity to induce a strong pro-inflammatory response with up-regulation of various cytokines and reduction of IL-8 production.

When comparing HIV-1 R5 replication (Figure 4.17) and cytokine production (Figure 4.18), we can conclude that the up-regulation observed with HN878 and CDC1551 liposomes in association with HIV-1 R5 replication is due to the creation of a favourable environment for viral expansion. Indeed, HN878 and CD1551 induced different cytokine production profiles. Whereas with BCG, H37Rv and EU127 liposomes, the modulation of immune responses observed in the infected co-cultures had no impact on HIV-1 R5 replication.

Differing cytokine/chemokine Luminex profiles were observed when comparing the effects of the variant liposomes on HIV-1 X4 and R5 virus replication in the iDCs/$CD4^+$ T lymphocyte co-culture system. For HIV-1 X4, H37Rv clearly increased HIV-1 production and replication, whereas BCG, HN878 and EU127 demonstrated a trend towards decreasing infection. Conversely, HIV-1 R5 was shown to increase in the presence of HN878 and CDC1551 liposomes. We have therefore observed variations in immune profiles induced in co-cultures infected with either an HIV-1 R5 or X4 strain and which can be influenced by exposure to *Mtb* liposomes in a strain dependent manner.

A. p24 production

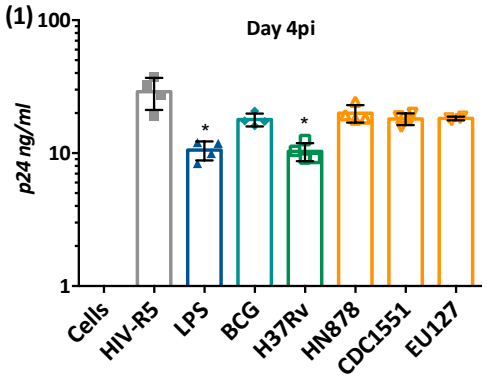

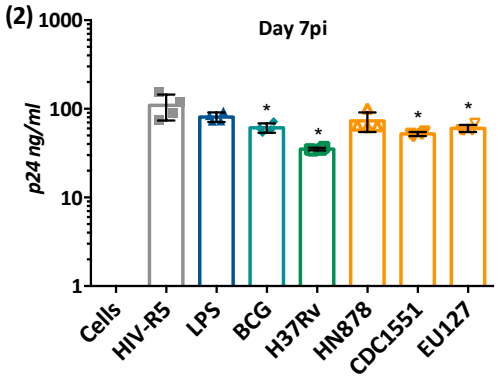

B. DNA quantification

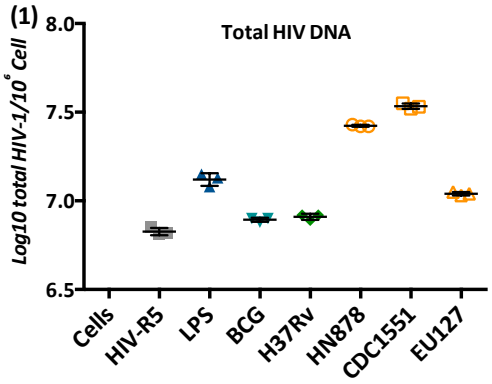

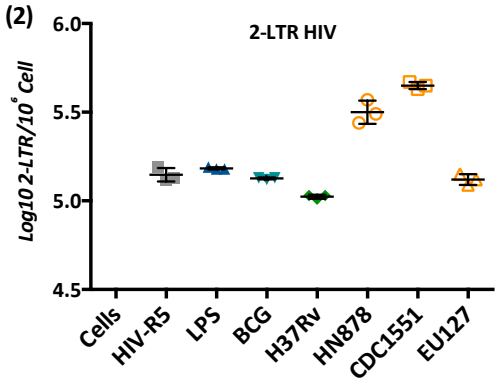

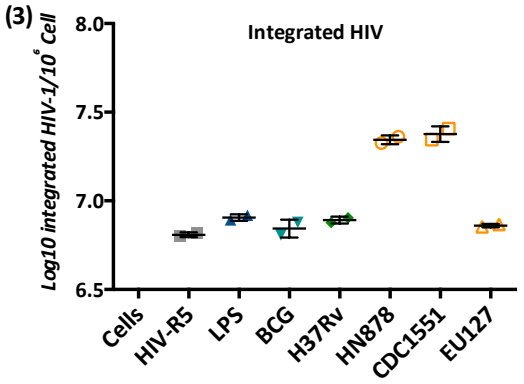

Figure 4.17 : Influence of liposomes on HIV-1 R5 infections - co-culture iDC and CD4⁺ T cells

In a 96-well plate, $2x10^4$ iDCs were placed in culture with $2x10^5$ $CD4^+$ T lymphocytes and infected with 200 $TCID_{50}$/ml LAI-YFP (HIV-1 X4). 40µg of *Mycobacterium* liposomes or 100ng/ml of LPS was added. **A.** Concentration of total HIV-1 capsid p24 was determinate in the supernatant by ELISA at **(1)** day 4 (n=4) and **(2)** day 7 (n=4) post-infection. **B.** represents log10 HIV-1 DNA quantification determinate by PCR relative to the total number of CD4+ cells at day 7 post-infection with **(1)** total number of HIV-1 DNA (n=3), **(2)** number of HIV-1 2-LTR (n=3) and **(3)** number of integrated HIV (n=2). The data shown are form one experiment using cells isolated from one donor.

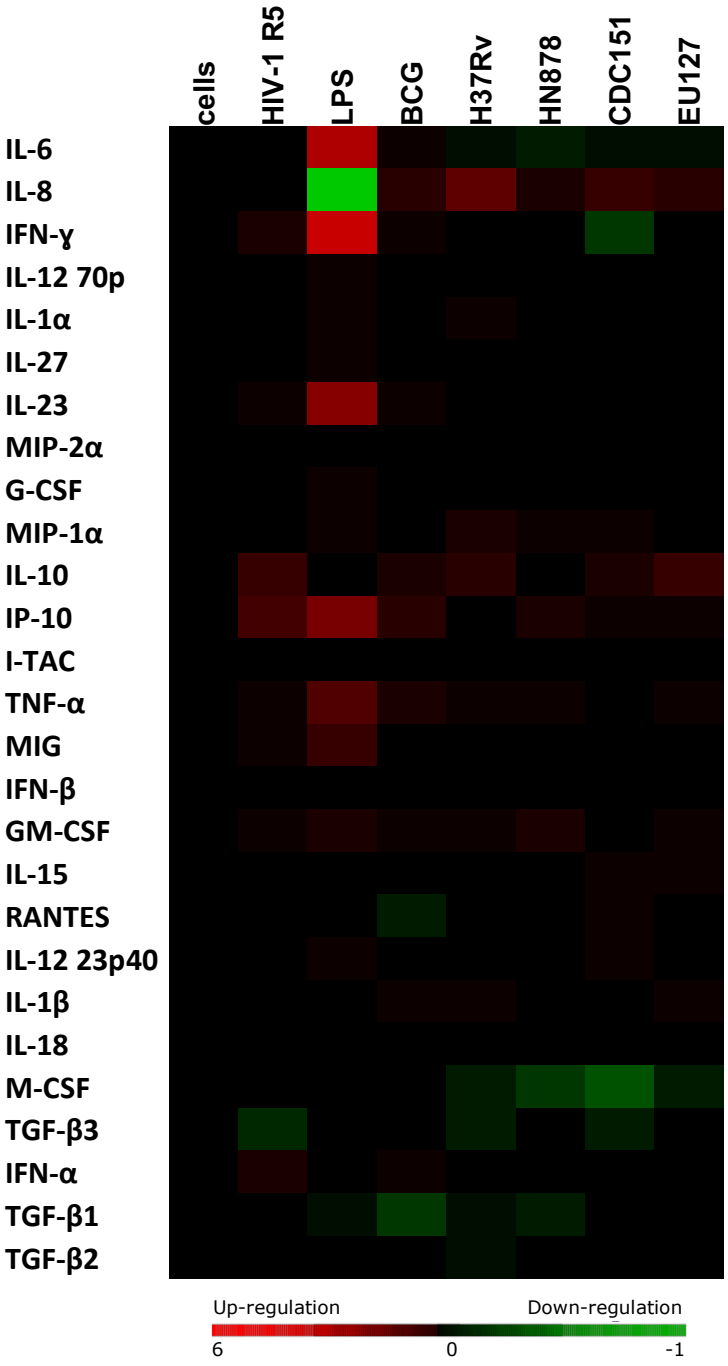

Figure 4.18 : Influence of liposomes on HIV-1 R5 infections - co-culture iDC and CD4⁺ T cells - Luminex®

In a 96-well plate, $2x10^4$ iDCs were placed in culture with $2x10^5$ $CD4^+$ T lymphocytes and infected with 500 $TCID_{50}$/ml BAL-GFP (HIV-1 R5). 40µg of *Mycobacterium* liposomes or 100ng/ml of LPS was added. At day 7 post-infection, supernatants were collected for Luminex® analyses. Luminex results are represented by Heat Maps Cluster of the Log2 of liposomes treatment/MDM baseline ratio. An increase of cytokine production in the supernatant is represented in red, a diminution of cytokine production depict in green and no change shown as black. For the data shown, n=3 using cells isolated from one donor.

III. Conclusion

The initial section to this Chapter focussed on studying the impact liposomes carrying *Mtb* glycolipids exerted on HIV-1 *trans*-infection. The approach utilising pseudo-typed virus particles demonstrated how glycolipids from variant *Mtb* strains can differentially modulate *trans*-infection *via* the DC-SIGN receptor, through studying Raji-DC-SIGN cells. H37Rv, EU127, BCG, *M. chelonae* and *M. marinum* glycolipids showed the capacity to block HIV-1 X4 and R5 *trans*-infection *via* DC-SIGN compared to HN878, CDC1551, EX30, EU111, *M. smegmatis*, *C. Glutamicum* and *S. Aureus* (Figure 4.2). When comparing the effect on iDCs mediated *trans*-infection, we observed similar results for H37Rv, BCG and EU127, suggesting that on iDC the DC-SIGN receptor is the main component being blocked by the *Mtb* glycolipids (Figure 4.3). Various components from *Mtb* have been described to interact with DC-SIGN receptors such as Man-LAM, LM, arabinomannan, glycoproteins, PIM_6 and α-glucan (Lugo-Villarino *et al.*, 2011), suggesting their implication on the phenomena observed in HIV-1 *trans*-infection *via* iDCs . Variation in lipid proportions in *Mycobacterium* cell walls could explain the variation observed in our *Mtb* strains tested. However, HN878, CDC1551 and *M. smegmatis* showed a trend towards enhancing iDC mediated *trans*-infection of $CD4^+$ T cells, suggesting others receptors than DC-SIGN may be involved in promoting the process. Interestingly, when analysing the effects utilising mDCs stimulated with Poly(I:C), we observed some differential effects. Indeed, *Mtb* HN878 and *M. marinum* showed a trend towards up-regulating *trans*-infection (mainly with HIV-1 X4 virus) (Figure 4.4). This observation implies that receptors other than DC-SIGN are involved. The finding that mannan similarly did not impact on blocking *trans*-infection (Figure 4.5) supports the concept that other more diverse receptors are involved as mannan binds a wide-array of C-type lectins.

The sialic acid binding Ig-like lectin 1 (Siglec-1), expressed on DCs, has been identified to be involved in HIV-1 *trans*-infection. Pino *et al.*, described that this molecule is responsible for HIV-1 capture by IFN-α-activated DCs (Pino *et al.*, 2015). The maturation of the DCs with Poly(I:C) induced production IFN-α (Avril *et al.*, 2009) and could activate expression of Siglec-1 on the cell surface. By interactions with Siglec-1, glycolipids from HN878 or *M. marinum* could thereby enhance HIV-1 *trans*-infection. Further studies with H37Rv allowed us to further characterise the implication of SL1, TDM, PIM and PDIM lipids on modulating DC-SIGN mediated HIV-1 capture-transfer. The analyses of lipid fractions (Figure 4.8) from total H37Rv cell wall components revealed the interaction of SL1, TDM and PDIM with DC-SIGN, since they potently blocked HIV-1 *trans*-infection. Interestingly, PIM which is known to

interact with DC-SIGN, did not show strong inhibition in our *in vitro* system. However, the role of SL1 in DC-SIGN mediated *trans*-infection was confirmed with using total lipid extract from H37Rv mutants delated of SL1 (papA1Δ), where liposomes associated with lipids from the mutant complemented with purified SL1 showed again a decrease in HIV-1 *trans*-infection with Raji-DC-SIGN cells (Figure 4.9). The Interaction of SL1 and TDM with DC-SIGN has not been described in the literature and studying these interaction further would lead to a better understanding of the molecular interactions leading to the block. Conversely, the role of PDIM in DC-SIGN mediated *trans*-infection is less clear. Indeed, analyses on HIV-1 capture-transfer from two H37Rv strains with different origins revealed variant effects and where H37Rv, H37Rv MA did not block HIV-1 *trans*-infection *via* DC-SIGN (Figure 4.6). Compared to H37Rv MA, H37Rv is mutated in the PDIM biosynthesis genes through regular passaging in mice, resulting in loss in bacterial virulence (Ioerger *et al.*, 2010). Liposomes specifically containing PDIM lipid did not show the capacity to block HIV-1 *trans*-infection *via* DC-SIGN, suggesting that high levels of expression of PDIM at the cell wall could mask SL1 interactions with DC-SIGN.

When analysing the influence of *Mtb* liposomes on HIV-1 *trans*-infection on $CD4^+$ T cells *via* iDCs with replicative competent viruses (summarised in Table 4.1), we observed differences to the observations made using the pseudo-typed virus particle system. BCG liposomes that demonstrated the capacity of blocking HIV-1 *trans*-infection *via* DC-SIGN recognition, did not significantly impact on HIV-1 X4 or R5 replication on $CD4^+$ T cells following *trans*-infection *via* iDCs. The same phenomenon occurs for *Mtb* H37Rv and EU127 liposomes. It is possible that when HIV-1 replication was monitored either *via* p24 production or HIV-1 DNA quantification the initial effects on capture-transfer were lost at days 4 and 7. It is important to notice that additional *in vitro* assays were performed where liposomes were only pre-incubated with iDCs (similar to the pseudo-typed viral particle system) before HIV-1 X4 and R5 *trans*-infection onto $CD4^+$ T cells (presented Appendixes 17, 18, 19 and 20). We did not observe any significant impact of *Mtb* glycolipids on HIV-1 X4 and R5 replication, supporting the loss of the initial effect. Interestingly, only HN878 liposomes showed the capacity to up-regulate iDC mediated HIV-1 X4 *trans*-infection in the pseudo-typed and replicative system. This observation suggests that similar mechanisms and receptors (Siglec-1 or MR) could be involved in the enhancement of HIV-1 replication by HN878 glycolipids.

During HIV-1 X4 *trans*-infection, *Mtb* liposomes induced a global down-regulation of the pro-inflammatory cytokine production compared to virus alone. These results suggest either a

down-regulation of the immune activation from infected iDCs and $CD4^+$ T cells during infection in presence of liposomes, or either the induction of pro-inflammatory cytokines followed by their subsequent consumption by the cells over time, therefore being removed from the culture supernatant. Interestingly, HN878 liposomes demonstrated less down-regulation of pro-inflammatory responses than other liposomes tested which correlated with an increase in HIV-1 replication. Concerning HIV-1 R5 *trans*-infection, the impact of the liposomes were more diverse and demonstrated differences compared to HIV-1 X4 infection. Indeed, H37Rv did not modulate cytokine responses from HIV-1 R5 infected cells compared to BCG which showed a trend towards increasing the down-regulation of cytokine production initiated by infection. HN878, CDC1551 and EU127 presented a trend toward activation of pro-inflammatory cytokines, suggesting a positive stimulation of the immune response from infected iDCs/$CD4^+$ T cell. However, even if liposomes demonstrated a trend towards inhibiting or activating the immune response from infected cells, it did not impact on HIV-1 R5 *trans*-infection *in vitro*.

The *in vitro* system of iDC/$CD4^+$ T cell co-culture system, a more physiologically relevant scenario, revealed totally different results from the *cis*-infection assays (Chapter 3) and *trans*-infection. Indeed, whereas *Mtb* H37Rv liposomes showed a trend towards inhibiting HIV-1 X4 and R5 virus and did not impact on *trans*-infection to $CD4^+$ T cells, enhanced HIV-1 X4 replication in co-culture. The up-regulation of HIV-1 X4 replication is associated with a significant increase in pro-inflammatory responses, compared to HIV-1 R5 infection, with notable production of TNF-α, IL-1, IL-6 and IFN-γ, which have all been described to enhance LTR transcription (Falvo *et al.*, 2011). Similar to H37Rv, CDC1551 induced production of these cytokines in HIV-1 X4 co-culture infections and which associated with an increase in HIV-1 replication. BCG and EU127 liposomes, as for HN878, trended to impact less on pro-inflammatory cytokine production and block HIV-1 X4 replication. These observations suggest that production of TNF-α associated with IL-6 and IL-1 production and can modulate HIV-1 X4 LTR activation. However, HN878 and CDC1551 showed the capacity to activate HIV-1 R5 replication, but in this case, without production of TNF-α, suggesting other mechanism could be involved.

We have observed from *cis*-, *trans*-infection and co-culture assays, that virus tropism can alter the impact of the *Mtb* liposomes on infection. One explanation could be that *Mtb* glycolipids could interfere with HIV-1 X4 or R5 viral entry. The *cis*-infection results using pseudo-typed viral particles suggests otherwise as *Mtb* liposomes did not demonstrate

reduction in infectivity. This could be confirmed using the viral replicative system and testing entry inhibitors specific for blocking R5 or X4 virus. Importantly, the interactions between iDCs and $CD4^+$ T cells are essential for the course of infection and the pro-inflammatory response induced. Indeed, depending of the assay tested differing panels of cytokines were produced which have variant impacts on HIV-1 infection. Future work should focus on better understanding DC responses to *Mtb* glycolipids and the impact on HIV-1 *cis*- and *trans*-infection with *in vitro* HIV-1 infection using naïve T cells co-cultured with iDCs or mDCs as well as iDCs incubated with *Mtb* glycolipids. Depending of the *in vitro* system designed, variations could be expected in cellular responses which could modulate HIV-1 infection (Kedzierska and Crowe, 2001). Indeed, while most of the studies report that *Mtb* can up-regulate infection in macrophages (Zhang, Nakata, *et al.*, 1995a; Mancino *et al.*, 1997), others described the opposite effect (Goletti *et al.*, 2004).

Overall the results presented in this Chapter have revealed that the strain origin of *Mtb* induce considerable variations on HIV-1 infection by increasing or decreasing replication.

Table 4.1 : Luminex Results summary

Conditions	BCG	H37Rv	HN878	CDC1551	EU127
$CD4^+$ T cells HIV-1 X4 *cis*-infection Day 7 post-infection	↓ TNF-α/IFN-γ ↓ IFN-β ↓ M-CSF/GM-CSF ↓ IL-15/IL-18 ↓ IL-12 23p40/IL-23 ↓ MIP-1α/RANTES/IL-8 ↓ TGF-β1/2	↑ IFN-β ↑ IL-15 ↑ IL-12 23p40 ↑ MIP-1α/RANTES/IL-8 ↑ TGF-β3 ↓ M-CSF	↓ TNF-α/IFN-γ ↓ IFN-β ↓ M-CSF/GM-CSF ↓ IL-15 ↓ IL-12 23p40/IL-23 ↓ MIP-1α/RANTES/IL-8		
	Block virus replication		**Increase virus replication**		**Block virus replication**
$CD4^+$ T cells HIV-1 R5 *cis*-infection Day 7 post-infection	↑ TGF-β2 ↓ TNF-α/IFN-γ ↓ IFN-β ↓ M-CSF/GM-CSF ↓ IL-15 ↓ IL-12 23p40/IL-23 ↓ MIP-1α/RANTES/IL-8 ↓ MIG/I-TAC ↓ TGF-β3	↑ IFN-β ↑ IL-15 ↑ IL-12 23p40 ↑ IL-10 ↑ MIP-1α/RANTES/IL-8 ↑ IP-10 ↓ TNF-α	↑ IP-10 ↓ TNF-α/IFN-γ ↓ IFN-β ↓ M-CSF/GM-CSF ↓ IL-15 ↓ IL-12 23p40 ↓ MIP-1α/RANTES/IL-8 ↓ TGF-β1/2/3		
	-	**Block virus replication**	**Increase virus replication**		

Table 4.8 continued

Conditions	BCG	H37Rv	HN878	CDC1551	EU127
$CD4^+$ T cells HIV-1 X4 *trans*-infection Day 7 post-infection	↓ TNF-α/IFN-γ ↓ IFN-β ↓ M-CSF ↓ IL-15 ↓ IL-12 23p40 ↓ MIP-1α/RANTES/MIG	↓ TNF-α/IFN-γ ↓ IFN-β ↓ M-CSF ↓ IL-6/IL-15 ↓ IL-12 23p40/IL-12 70p ↓ MIP-1α/RANTES/MIG ↓ TGF-β3	↑ TGF-β1 ↓ TNF-α ↓ IFN-β ↓ M-CSF ↓ IL-15 ↓ MIP-1α/MIG	↓ TNF-α/IFN-γ ↓ M-CSF ↓ IL-6 ↓ IL-8/MIG ↓ TGF-β2/3	↑ TGF-β1 ↓ TNF-α/IFN-γ ↓ IFN-β ↓ M-CSF ↓ IL-15 ↓ IL-12 23p40 ↓ MIP-1α /RANTES/IL-8 MIG/I-TAC ↓ TGF-β3
	-	-	**Increase virus replication**	-	-
$CD4^+$ T cells HIV-1 R5 *trans*-infection Day 7 post-infection	↑ IL-8 ↓ IFN-β ↓ M-CSF/GM-CSF ↓ IL-15 ↓ IL-12 23p40 ↓ IL-10 ↓ MIP-1α/RANTES	↓ IFN-γ ↓ IL-10 ↓ MIG	↑ IFN-γ ↑ IL-15 ↑ IL-12 23p40 ↑ MIP-1α/RANTES/IL-8 ↑ IP-10 ↓ IL-12 23p40	↑ TNF-α ↑ IL-15 ↑ IL-12 23p40 ↑ MIP-1α/RANTES ↓ M-CSF ↓ IL-10	↑ TNF-α/IFN-γ ↑ IL-6/IL-1β ↑ IL-10 ↑ IL-8 ↑ IP-10 ↓ IFN-α
	-	-	-	-	-

Table 4.1 continued

Conditions	BCG	H37Rv	HN878	CDC1551	EU127
iDCs/CD4⁺ T co-culture HIV-1 X4 Day 7 post-infection	↑ IL-10 ↓ MIP-1α ↓ TGF-β1/2	↑ TNF-α/IFN-γ ↑ IFN-β ↑ GM-CSF ↑ IL-6/IL-1α/IL-1β/IL-15 ↑ IL-12 23p40/IL-23 ↑ IL-10 ↑ MIP-1α/RANTES/IL-8 ↓ MIG ↓ TGF-β1/2	↑ IFN-γ ↑ IL-6/IL-1α/IL-1β ↑ IL-23 ↑ IL-10 ↑ RANTES/IL-8 ↑ IP-10 ↓ MIG ↓ TGF-β1/2	↑ TNF-α/IFN-γ ↑ IL-6/IL-1α/IL-1β/IL-15 ↑ IL-12 23p40/IL-23 ↑ IL-10 ↑ RANTES/IL-8 ↑ IP10 ↓ MIG ↓ TGF-β1/2	↑ IFN-γ ↑ IL-6/IL-1α/IL-1β ↑ IL-23 ↑ IL-10 ↓ MIP-1α/MIG ↓ TGF-β1/2
	Block virus replication	No clear role	**Block virus replication**	**Increase virus replication**	**Block virus replication**
iDCs/CD4⁺ T co-culture HIV-1 R5 Day 7 post-infection	↑ IL-1β ↑ IL-8 ↑ TGF-β3 ↓ IFN-γ ↓ RANTES/MIG ↓ TGF-β1	↑ IL-1β ↑ MIP-1α/IL-8 ↓ IFN-γ/IFN-α ↓ M-CSF ↓ MIG ↓ IP-10 ↓ TGF-β1/2	↑ MIP-1α/IL-8 ↑ TGF-β3 ↓ IFN-γ/IFN-α ↓ M-CSF ↓ IL-6 ↓ IL-10 ↓ MIG ↓ TGF-β1	↑ IL-15 ↑ MIP-1α/RANTES/IL-8 ↑ IL-12 23p40 ↓TNF-α/IFN-γ/IFN-α ↓ GM-CSF/M-CSF ↓ IL-10 ↓ MIG ↓ IP-10 ↓ TGF-β1	↑ IL-1β/IL-15 ↑ IL-8 ↑ TGF-β3 ↓ IFN-γ/IFN-α ↓ M-CSF ↓ MIG ↓ IP-10
	-	-	**Increase virus replication**	**Increase virus replication**	-

Chapter 5: Exosomes Isolation and impact on HIV-1 infection

I. Introduction

Extracellular vesicles (EVs) is a generic term referring to vesicles secreted into the extracellular environment by cells. It includes a variety of vesicle populations characterised by their cell origin, biogenesis, function or biophysical properties. Generally, vesicles range in size between 150 to 1,000nm and are secreted from the plasma membrane, budding as ectosomes, shedding vesicles, micro-vesicles as well as micro-particle. The term exosomes typically refers to vesicles with a size ranging from 30 to 100nm and which possess an endosomal origin (Gould and Raposo, 2013; Raposo and Stoorvogel, 2013; Colombo, Raposo and Théry, 2014; Iraci *et al.*, 2016). The content of EVs varies depending on the cells from which they originate and can include the incorporation of functional proteins, lipids or RNAs. Once the components of EVs are released, they can either influence the local micro-environment or either spread in the circulation. EVs can be detected in various biological fluids such as blood, urine, saliva, amniotic fluid, ascites, bronchoalveolar lavage, synovial fluid, semen and breast milk. A large range of functions have been associated with EVs in cancer, signalling, immunity, pathogenesis and infection (Théry, Ostrowski and Segura, 2009; Mathivanan, Ji and Simpson, 2010; Bobrie *et al.*, 2011; Colombo, Raposo and Théry, 2014; Anderson, Kashanchi and Jacobson, 2016; Iraci *et al.*, 2016). In viral diseases, EVs containing viral particles, virus-derived nucleic acids (genomes, cellular and viral mRNAs, miRNAs) or proteins can have effects on both infection and disease outcome. Indeed, vesicles containing viral components/products can possess a route for viral transmission and provide protection against immune recognition (Delabranche *et al.*, 2012; Wurdinger *et al.*, 2012; Hossain and Norazmi, 2013; Alenquer and Amorim, 2015; Chahar, Bao and Casola, 2015; Meckes, 2015; Schwab *et al.*, 2015; Anderson, Kashanchi and Jacobson, 2016; Petrik, 2016; van Dongen *et al.*, 2016).

In the case of HIV-1 infection, the cargos present in EVs isolated from infected cells can include viral components and suggests a role of EVs in facilitating virus replication and

pathogenicity (Kadiu *et al.*, 2012; Arenaccio, Chiozzini, Columba-Cabezas, Manfredi and Federico, 2014a; Madison and Okeoma, 2015; Hildreth, 2017). For example, the viral protein Nef can be incorporated into EVs (McNamara *et al.*, 2018) and once released the EVs have been reported to be able to trigger apoptosis of T cells (Muratori *et al.*, 2009; Lenassi *et al.*, 2010), activate HIV-1 replication (Arenaccio, Chiozzini, Columba-Cabezas, Manfredi, Affabris, *et al.*, 2014) or promote inflammation (Lee *et al.*, 2016). HIV-1 RNA molecules have also been shown to be encased in EVs (Columba Cabezas and Federico, 2013) as TAR elements (miRNA) and have been found in EVs isolated from HIV^+ patients and are believed to be involved in enhancement of HIV-1 replication and the induction of pro-inflammatory cytokine responses (Narayanan *et al.*, 2013; Sampey *et al.*, 2015). Additionally, EVs containing HIV-1 components have been hypothesised to play a role in HIV *trans*-infection *via* DCs and thereby influence viral transmission (Wiley and Gummuluru, 2006; Izquierdo-Useros *et al.*, 2010; Hildreth, 2017; Kulkarni and Prasad, 2017).

Concerning *Mtb* infection, EVs produced from infected macrophages have been described to regulate the activity of uninfected macrophages and thereby promote immune evasion or other important host defence mechanisms. Various mycobacterial components have been reported to be incorporated into EVs such as lipoproteins, lipoglycans, LAM, LM, PIMs as well as antigens (Beatty *et al.*, 2000; Athman *et al.*, 2015; Lee *et al.*, 2015; Gupta and Rodriguez, 2018). These elements incorporated within EVs can contribute to the inhibition of the maturation of phagosomes (LAM) or influence macrophage antigen presentation (Singh *et al.*, 2011; Kruh-Garcia, Wolfe and Dobos, 2015; Athman *et al.*, 2017; Gupta and Rodriguez, 2018; Li *et al.*, 2018). However, they have also been described to activate immune responses (Bhatnagar *et al.*, 2007; Giri and Schorey, 2008; Singh *et al.*, 2012; Kruh-Garcia, Wolfe and Dobos, 2015; Athman *et al.*, 2017; Gupta and Rodriguez, 2018).

HIV-1 and *Mtb* have common target cells: namely MDM and DCs. In the context of co-infection, the role of EVs on influencing HIV-1 infectivity is not well understood. The aim was to investigate whether secreted EVs from plasma of HIV-1/*Mtb* co-infected patients could alter the infection and/or replication capacity of either pathogen within the co-infected host. Under this perspective we aimed in this chapter to determine whether EVs could be successfully isolated form plasma material. Numerous methodologies are currently available using EVs properties such as size, density, ultracentrifugation (UC), microfiltration, gel filtration or based on interactions between the molecules exposed on EVs surface and microfluidic technologies (Théry *et al.*, 2006; Baranyai *et al.*, 2015; Lobb *et al.*, 2015; Nordin

et al., 2015; Taylor and Shah, 2015; Hong *et al.*, 2016; Konoshenko *et al.*, 2018). We specifically focused on testing whether UC and gel filtration technologies could be used in isolating EVs from plasma.

II. Results

i. Optimisation of EVs isolation from plasma by centrifugation

Isolation of EVs by differential centrifugation is a common and efficient method previously used and well described. The technique is based on utilising the differential density found between cells, cell debris, apoptotic bodies, aggregates of biopolymers and EVs that are separated with successive centrifugation steps using variant acceleration rates (Théry *et al.*, 2006; Baranyai *et al.*, 2015; Lobb *et al.*, 2015; Taylor and Shah, 2015; Konoshenko *et al.*, 2018). We tested two different protocols: one at small scale using 2ml of plasma diluted in PBS and a second technique using 20ml of diluted plasma.

The isolation of EVs using the small scale protocol (2ml of diluted plasma) is represented in Figure 5.1 **A**. The plasma was first centrifuged for 5min to remove cell debris and apoptotic bodies. The supernatant from the first centrifugation was then centrifuge a second time to isolate the EVs present in the pellet, which was resuspended in PBS. The pellet **(1)** and the supernatant **(2)**, collected from the second centrifugation, were then tested in the HIV-1 X4 Raji-DC-SIGN *trans*-infection assay using TZM-bl cells as the reporter cell of infection (pseudo-typed viral particle system) (Figure 5.1 **B**). Gradual dilutions of pellet and supernatant were tested and compared in the *trans*-infection assay with the results being compared to reference virus alone. We observed that the presence of pellet prior to virus capture by Raji-DC-SIGN cells significantly decreased efficacy of DC-SIGN *trans*-infection by 50% (P value= 0.004, Mann-Whitney test). For the pellet dilutions we observed a loss of the inhibitory effect through augmentation of dilutions. Pellet dilution 1/10 showed a trend towards decreasing the HIV-1 *trans*-infection by 20% and dilution 1/100 not showing any significant impact (down 10%). However, interestingly the higher dilution 1/1000 inhibited DC-SIGN capture-transfer efficacy by 50% (P value= 0.0095, Mann-Whitney test) as seen with the non-diluted resuspended pellet.

Figure 5.1 : Isolation of EVs from Plasma by centrifugation

A. Schematic representation of EVs isolated by centrifugation. **B.** 50µl of **(1)** pellet resuspended in PBS (non-diluted, 1/10, 1/100 and 1/1000 dilution in PBS), **(2)** supernatant (non-diluted, 1/10, 1/100 and 1/1000 dilution in PBS) from centrifugation, was pre-incubated for 30min with $0.5x10^6$ of Raji-DC-SIGN. Then the cells were incubated 2h with 12.5ng pSG3-LAI HIV-1 X4. After the capture the cells were washed and co-cultured with TZM-bl cells. The luciferase activity was read after 48h. *Trans*-infection of the virus alone where Raji-DC-SIGN were pre-incubated with PBS, was used as a reference. For the data shown, n=8 using plasma isolated from one donor.

A. Isolation by centrifugation protocol

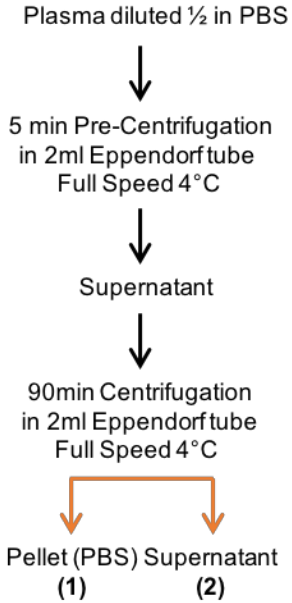

B. Impact on HIV-1 X4 *trans*-infection on TZM-bl *via* Raji DC-SIGN

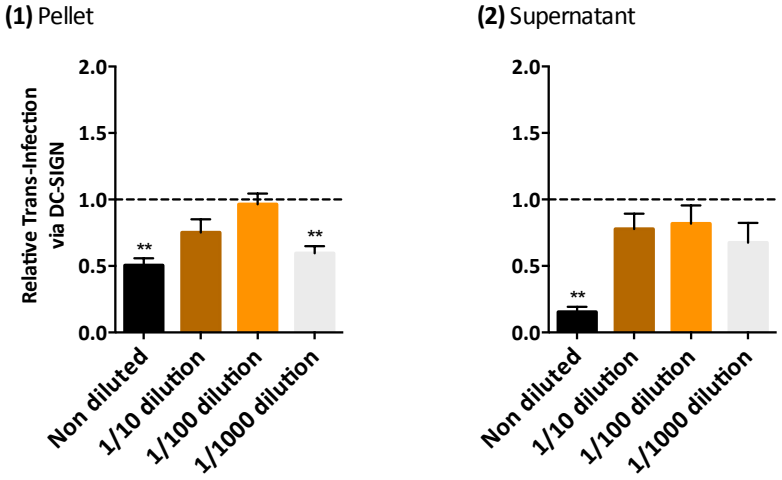

This result suggests that components present in the pellet can interact with virus binding the DC-SIGN receptor on Raji-DC-SIGN cells thereby blocking HIV-1 X4 *trans*-infection. However, it cannot specifically be determined whether the effect is mediated *via* the isolated EVs from the plasma or pelleted proteins/molecules. The presence of supernatant **(2)**, composed of contaminants from plasma, demonstrated an impact on the efficacy of DC-SIGN *trans*-infection: non-diluted supernatant decreased the efficacy by 85% (P value= 0.004, Mann-Whitney test). The effect observed was reduced with further dilution, where 1/10, 1/100 and 1/1000 reduced infection by 25%, 20% and 30%, respectively. This result suggests that components present in the supernatant interfere with HIV-1 X4 DC-SIGN *trans*-infection as observed in Appendix 23 when plasma was pre-incubated with Raji-DC-SIGN cells prior to capture of virus. From this centrifugation technique, the isolation of EVs from plasma was not optimum and did not allow for isolation of EVs from plasma components interfering with HIV-1 DC-SIGN *trans*-infection.

Secondly, we tested the isolation of EVs from a large volume of plasma (20ml). As described by Théry *et al.*, 2006 and represented (Figure 5.2 **A**), diluted plasma was first centrifuged at 10,000g for 30 min to eliminate cell debris, with the supernatant further centrifuged at 100,000g for 2h. The EVs are present in the pellet but contaminant proteins are eliminated at this stage through a second UC step using the same conditions. After the second centrifugation the pellet was resuspended in PBS. We subsequently tested the influence of the supernatant from the first UC, the supernatant as well as the pellet from the second UC on influencing HIV-1 X4 *trans*-infection *via* Raji-DC-SIGN **B.** and iDCs **C.** Figure 5.2.

It was observed that the supernatant **(1)** from the first UC step incubated prior to HIV-1 X4 capture by Raji-DC-SIGN cells decreased *trans*-infection efficacy by 76% (P value= 0.0286, Mann-Whitney test) (Figure 5.2 **B**), indicating that plasma strongly inhibits HIV-1 *trans*-infection. However, the pellet **(2)** and the supernatant **(3)** from the second UC step did not show any significant impact on HIV-1 X4 capture and transfer when they were present prior to virus capture. Indeed, in the presence of pellet resuspended in PBS, the efficacy of *trans*-infection *via* DC-SIGN was inhibited by only 12% thereby having no obvious effect on modulating HIV-1 *trans*-infection.

Figure 5.2 : Isolation of EVs from Plasma by ultra-centrifugation

A. Schematic representation of EVs isolation by ultra-centrifugation. **B.** Two plasma donors have been utilised. 50µl of **(1)** supernatant from the first centrifugation, **(2)** pellet or **(3)** supernatant from the second centrifugation step, was pre-incubated 30min with $0.5x10^6$ of Raji-DC-SIGN cells. Then the cells were incubated 2h with 12.5ng pSG3-LAI HIV-1 X4. After capture the cells were washed and co-cultured with TZM-bl cells. The luciferase activity was read after 48h. *Trans*-infection of the virus alone where Raji-DC-SIGN were pre-incubated with PBS, used here as reference (n=4) **C.** 50µl of **(1)** supernatant from the first centrifugation, **(2)** pellet or **(3)** supernatant from the second centrifugation step, was pre-incubated 30min with $0.5x10^6$ of iDCs isolated either from the same plasma (homologous) or from a different plasma donor (heterologous). The cells then were incubated 2h with 12.5ng pSG3-LAI HIV-1 X4, and after the capture, were washed and co-cultured with TZM-bl cells. The luciferase activity was read after 48h. *Trans*-infection of the virus alone where iDCs were pre-incubated with PBS, was used as reference (n=2). Cells were isolated from one donor.

A. Isolation by UC protocol

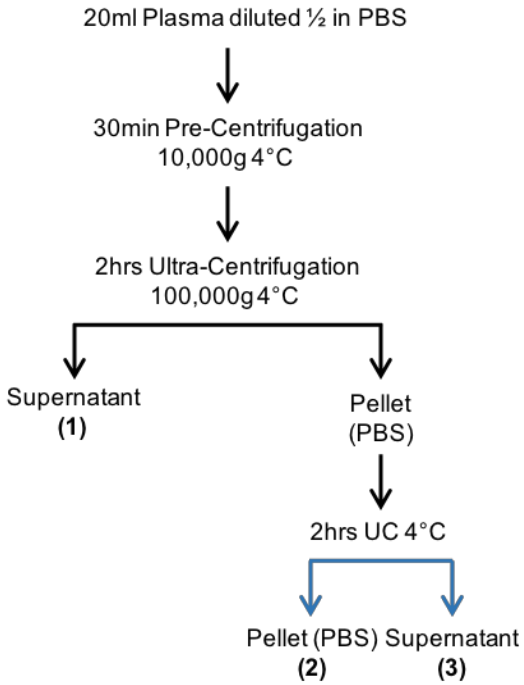

B. Impact on HIV-1 X4 *trans*-infection on TZM-bl *via* Raji DC-SIGN

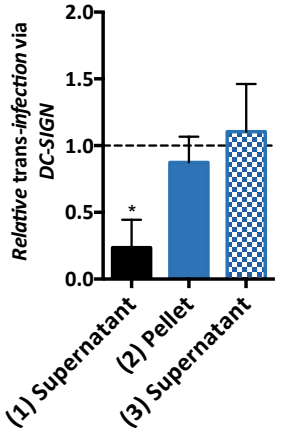

C. Impact on HIV-1 X4 *trans*-infection on TZM-bl *via* iDCs

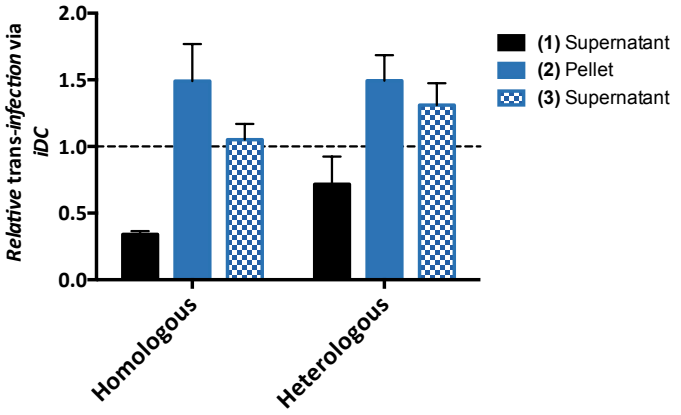

It was next tested whether there was any influence on HIV-1 X4 *trans*-infection *via* iDC rather than the Raji-DC-SIGN cell line (Figure 5.2 **C**), in this case the plasma was from either the same iDCs donor (homologous), or from a different donor (heterologous). As observed for Raji-DC-SIGN *trans*-infection, the presence of the supernatant **(1)** from the first centrifugation containing most of the contaminants from plasma, demonstrated a trend towards decreasing capture-transfer to TZM-bl to 65% for homologous and 28% for heterologous cells. Interestingly, the pellet **(2)** containing the EVs from the second UC step, showed a trend towards enhancing HIV-1 X4 *trans*-infection by 50% for both conditions. This result suggests that EVs from plasma could impact on HIV-1 *trans*-infection *via* iDCs. The supernatant **(3)** with less amounts of plasma contaminants from the second UC did not show any significant impact on virus capture-transfer where iDCs were from the same donor (1.05 relative efficacy), but where the EVs were from a different donor than the iDCs, the supernatant demonstrated an increase of 30% to *trans*-infection.

Compared to the initial technique of centrifugation, the second method, using higher amounts of plasma and UC speed, seemed to be more efficient at isolating EVs from plasma, and eliminated most of the contaminants that could impact on HIV-1 *trans*-infection. However, from the second technique the presence of EVs needs to be confirmed by further analyses through Western Blot and electronic microscopy analyses. The aim is to ultimately isolate EVs from plasma of patient infected with HIV-1 and/or *Mtb*. These samples need to be treated and processed within CL3 facilities. In order to eliminate the need of an ultra-centrifuge in CL3 facilities, the aim was to find an alternative and rapid technique for isolating EVs, such as through gel filtration.

ii. Optimisation of EVs isolation by Gel Filtration (SEC) form plasma

Gel filtration enables the separation of molecules regarding the component's size, not molecular weight (hydrodynamic radius). The SEC is composed of a matrix containing heteroporous beads in a cross-linked polymeric support packed into a column forming pores and tunnels. The separation of macromolecules occurs by differential exclusion or inclusion of the macromolecules as they pass through the column (Taylor and Shah, 2015; Konoshenko *et al.*, 2018). We tested two different methods of EVs isolation by gel filtration. The first one is a technique of gel filtration paired with a concentration step using Sephadex G-25 as matrix

for gel filtration (Figure 5.3). The second is a technique using a different matrix for the filtration, sepharose CL-2B previously described by Böing *et al.*, 2014 (Figure 5.4).

A scheme of the isolation protocol by gel filtration associated with the concentration step is depicted (Figure 5.3 **A**), where the following protocol was used: after a pre-centrifugation of the plasma to remove cells debris the supernatant was then passed through a Sephadex G-25 column. The filtrate obtained from the SEC containing EVs is then additionally concentrated using an Amicon 30KDa filter. Sephadex G-25 is a cross-linking dextan matrix with epichlorohydrin used to allow the separation of small peptides and proteins of 1-5KDa in size. It was used here to eliminate contaminants contained within the plasma. The volume of eluate was then concentrated and EVs were then isolated from the remaining proteins. The impact of the concentrate **(1)** and filtrate **(2)** (from filtration with Amicon 30KDa) on HIV-1 X4 DC-SIGN specific *trans*-infection was determined (Figure 5.3 **B**). The concentrate and the filtrate were pre-incubated with Raji-DC-SIGN cells prior to virus capture, where different dilutions of concentrate and filtrate were tested and the efficacy of HIV-1 X4 *trans*-infection determined, and where virus alone was used as the reference.

We observed that the presence of concentrate **(1)**, prior to HIV-1 X4 capture by Raji-DC-SIGN cells, was associated with a total inhibition of DC-SIGN *trans*-infection. This effect was shown to be dilution dependent: for 1/10 dilution, the relative *trans*-infection efficacy was 0.5 and for the 1/100 dilution was shown to be 0.82 (Figure 5.3 **B(1)**). This result suggests that elements of the concentrate, where the EVs are expected, can interact with Raji-DC-SIGN, inhibiting HIV-1 X4 *trans*-infection. However, the presence of filtrate **(2)** on HIV-1 X4 Raji-DC-SIGN mediated *trans*-infection was also associated of a decrease of capture-transfer with the effect again being lost through dilution. Non-diluted filtrate demonstrated a trend towards decreasing *trans*-infection efficacy by 60% but with 1/10 and 1/100 dilutions, the efficacy was partially restored to 0.80. The filter is composed of protein contaminants from the plasma that appeared to interfere with HIV-1 DC-SIGN *trans*-infection (as supported by Appendix 23). However, regarding its impact in HIV-1 *trans*-infection *via* Raji-DC-SIGN, some contaminants and components from plasma were still present on the EVs isolation concentrate affecting virus capture. From these observations we conclude that this protocol did not allow for optimum separation and isolation of EVs from plasma.

Figure 5.3 : Isolation of EVs from plasma by Gel Filtration and concentration

A. Schematic representation of EVs isolation by gel filtration and concentration. **B.** 50µl of **(1)** concentrate (non-diluted, 1/10 and 1/100 dilution in PBS), **(2)** filtrate (non-diluted, 1/10 and 1/100 dilution in PBS) from gel filtration, was pre-incubated 30min with $0.5x10^6$ of Raji-DC-SIGN cells. The cells were incubated 2h with 12.5ng pSG3-LAI HIV-1 X4. After capture the cells were washed and co-cultured with TZM-bl cells. The luciferase activity was read after 48h. *Trans*-infection of virus alone where Raji-DC-SIGN were pre-incubated with PBS was used here as a reference. For the data shown, n=4 using plasma isolated from one donor.

A. Isolation by gel filtration protocol

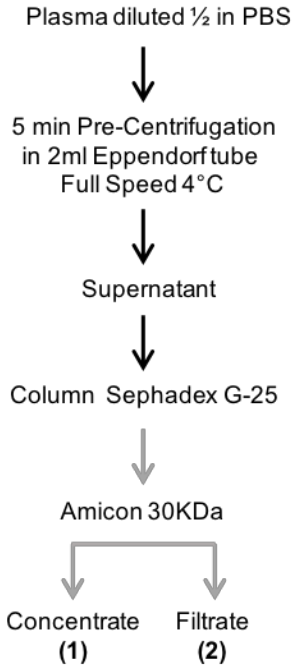

B. Impact on HIV-1 X4 *trans*-infection on TZM-bl *via* Raji DC-SIGN

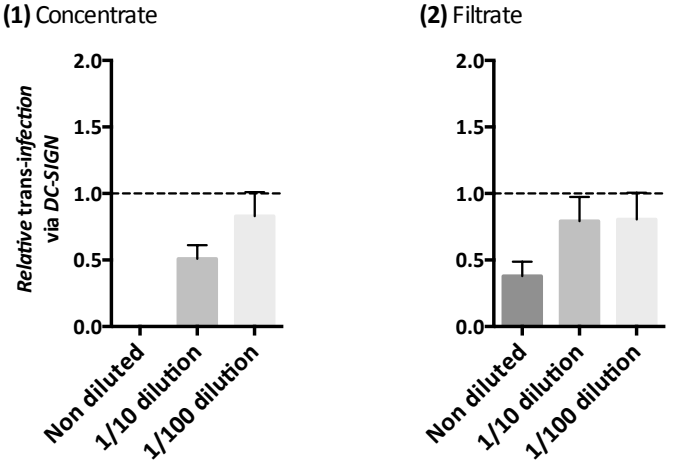

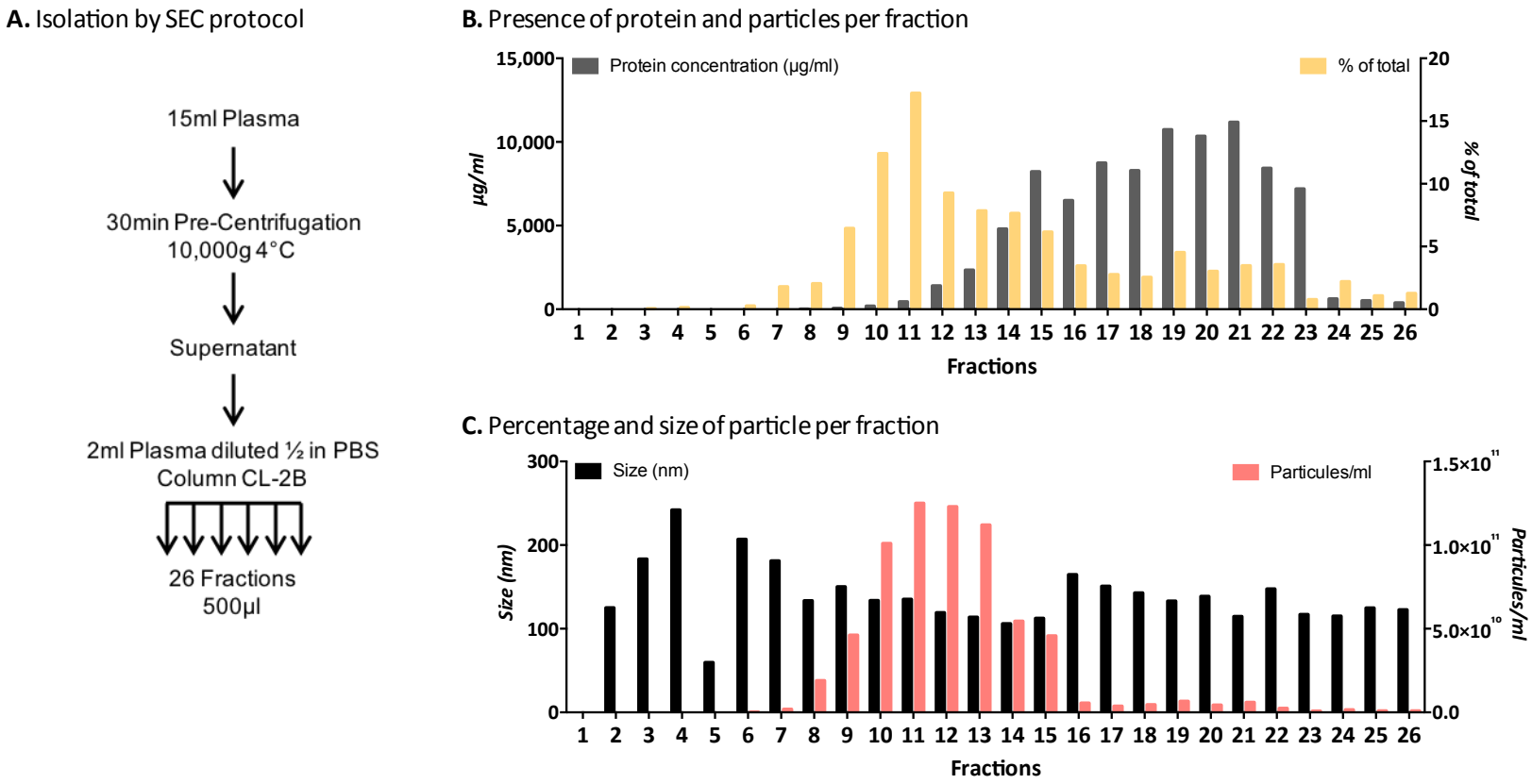

Figure 5.4 : Isolation of EVs from Plasma by SEC

A. Schematic representation of EVs isolation by SEC. **B.** Protein concentration (µg/ml) was measured in each fraction (Bradford assay). The percentage of particles present within fractions was determined by NanoSight and related to the total number of particles passed through the column. **C.** The mean size (nm) of particles present in each fractions and the concentration of particles were determinate by NanoSight. The data shown are representative of two experiments using plasma isolated from one donor.

The Sephadex G-25 matrix was switched to a sepharose CL-2B matrix as previously reported (Böing *et al.*, 2014; Muller *et al.*, 2014; Baranyai *et al.*, 2015; Hong *et al.*, 2016; Konoshenko *et al.*, 2018). This matrix is composed of cross-linked beads of agarose which is routinely used for isolation of DNA-protein complexes or virus isolation with a range of 70 - 40,000KDa. Plasma (15ml) was first pre-centrifuged at 10,000g for 30min to eliminate the cell debris, after which 2ml of supernatant was used as input on the CL-2B column and 26 fractions of 500µl were collected as described Böing *et al.*, 2014 (Figure 5.4 **A**).

To identify fractions where EVs were located and evaluate protein contaminations, protein and particle concentrations were analysed within the different fractions. Protein concentration was determined utilising the Bradford assay allowing for quantification of all proteins, and NanoSight analysis performed to visualise the EVs particles and identify their concentration and size. The concentration of proteins (grey) in µg/ml with regard to percentage of particles related to the total number of particles (yellow) is shown for each 26 fractions (Figure 5.4 **B**). We observed that elution of particles occurred early (from fraction 7 to 23). The elution of proteins happened later in the elution series from fraction 9. High concentrations (superiors to 2500 µg/ml), were observed from fractions 14 to 23. From these observations we identified that the higher proportion of particles with the least protein contamination being found in fractions 9 to 13. The particle sizes being isolated were found to be homogenous and ranged between 50 and 240nm in size. Also, Fractions 10, 11, 12 and 13 were identified to have the highest particle concentrations, ranging between 1 and $1.25x10^{11}$ particles per ml (Figure 5.4 **C**).

iii. Characterisation of EVs isolated by Gel Filtration

To characterise and control EVs isolation from SEC, Western Blot analysis was undertaken. This technique allows for the visualisation of EVs protein from various cells of origin. TSG-101 and CD63 are exosome markers both described to be highly enriched in EVs (Théry *et al.*, 2006; Böing *et al.*, 2014; Muller *et al.*, 2014; Baranyai *et al.*, 2015; Lobb *et al.*, 2015; Sampey *et al.*, 2015; Hong *et al.*, 2016; Konoshenko *et al.*, 2018). We visualised these markers through immunoblotting of the 26 fractions from SEC and where two different protocols were tested (Figure 5.5).

For Protocol 1, fractions 1-7 and 8-13 were pooled and concentrated using Amicon 3KDa filters (higher proportions of EVs expected in pool 8-13 as explain above). The samples were then denatured (in reduction conditions) and equalised for protein concentration by SDS-PAGE electrophoresis, transferred to PVDF membrane and visualised by Ponceau red staining (Figure 5.5 **A(1)**). We observed for Protocol 1, homogenous bands for each fraction, validating sample input and conditions of the electrophoresis and transfer. For pooled fractions 1-7, containing very low concentrations of EVs we did not visualise proteins. From TGS-101 immuno-blotting we observed a homogenous protein band profile for each fraction indicating unspecific binding of TSG-101 antibodies and no bands at 44KDa where TSG-101 was expected (Figure 5.5 **B(1)**). From this observation it can be concluded that the Protocol 1 immuno-blotting was not optimum to allow visualisation of TSG-101 from EVs.

In protocol 2 **(2)** samples from SEC isolation were prepared either in reducing (R) or non-reducing (NR) conditions. For Western Blot analysis samples were generally reduced in the presence of β-mercaptoethanol or dithiothreitol to disrupt peptide interactions. However, in some cases antibodies can't recognise the protein in the reduced form, which is the case for CD63 (Théry *et al.*, 2006), tested in this protocol. For this reason both R and NR conditions were tested. The SDS-PAGE and transfer were performed similar to Protocol 1. From Ponceau red staining of PVDF membrane it was observed that NR disrupted protein migrations compared to R condition (Figure 5.5 **A(2)**). Indeed, in NR condition protein migration was less linear than under R conditions. In Protocol 2, we tested visualisation of CD63 markers by immune-blotting (Figure 5.5 **B(2)**). Unfortunately, as for TSG-101, non-specific binding of the antibodies to protein was observed. As for Protocol 1, Protocol 2 needs to be optimised to allow visualisation of CD63 from EVs.

We were not able to control and visualise specifically the presence of EVs through SEC isolation by Western-blot analysis for detecting TSG-101 or CD63. However, from the NanoSight analysis and according to Böing *et al.*, 2014, we assumed that our final product of isolated EVs from SEC were present in fraction 9 to 13.

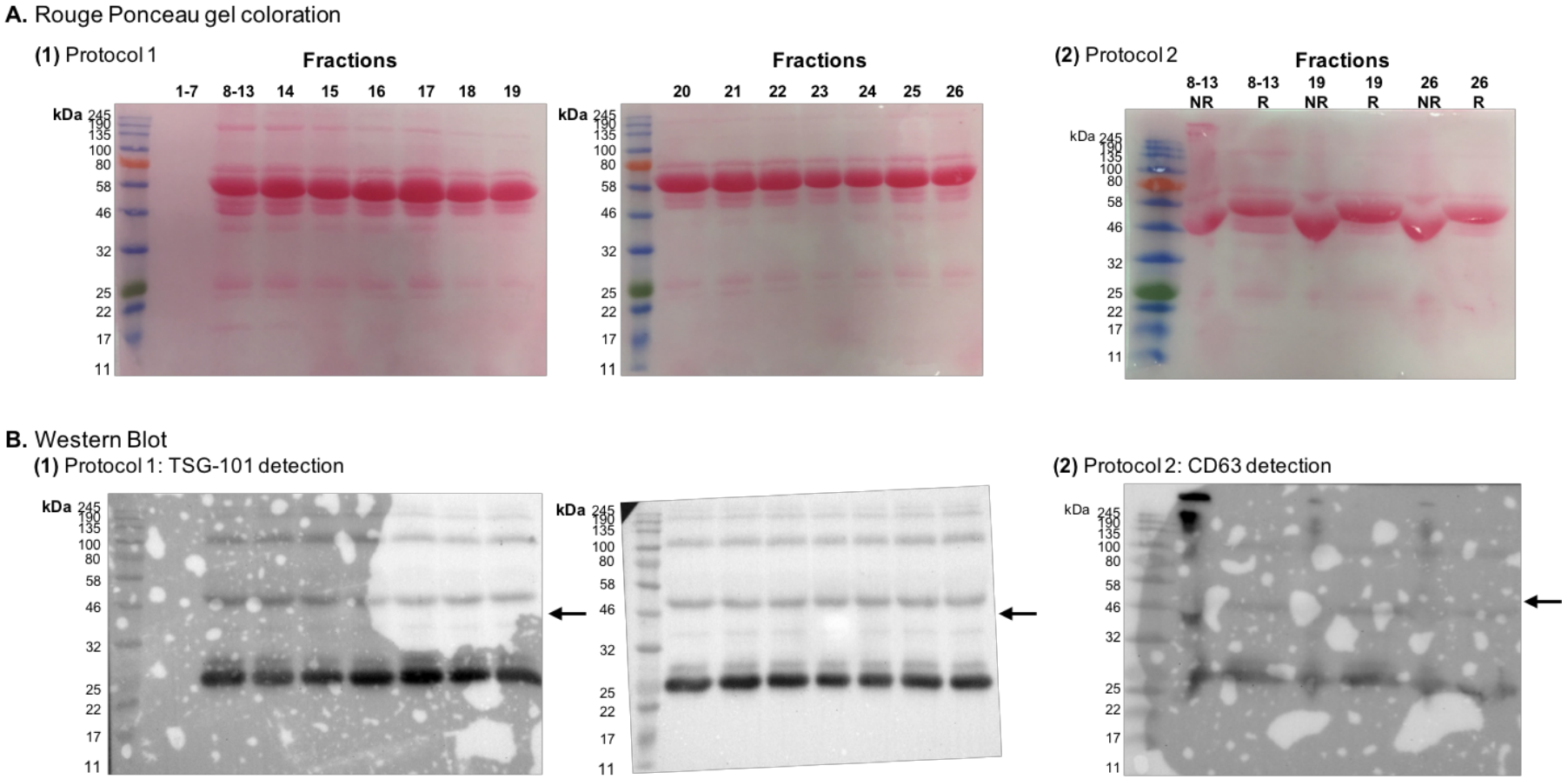

Figure 5.5 : Characterisation of EVs from plasma by Western Blot

A. Presence of proteins were shown on each Fractions by Ponceau red staining after SDS-PAGE with 13µg (20µl) per well. **(1)** Protocol 1, all samples were prepared in reduction condition and the electrophoresis performed at 100V for 1h30. **(2)** Protocol 2, the samples were prepared in non-reduction (NR) and reduction (R) conditions and the electrophoresis at 170V for 50min. **B. (1)** Protocol 1, detection of TSG-101 (arrow at 44kDa) and **(2)** Protocol 2, CD63 (arrow at 50-60kDa) were tested by immunoblotting. The data shown are representative of one experiment using plasma isolated from one donor.

iv. Influence of EVs from plasma on HIV-1 infection

EVs isolated from plasma by SEC gel filtration were analysed in HIV-1 infection assays. As described above, fractions 9 to 13 were identified as fractions containing EVs. For this reason, the fractions were pooled and tested in HIV-1 *cis*- **A.** and *trans*-infection **B.** assays utilising the pseudo-typed HIV-1 viral particle system (Figure 5.6).

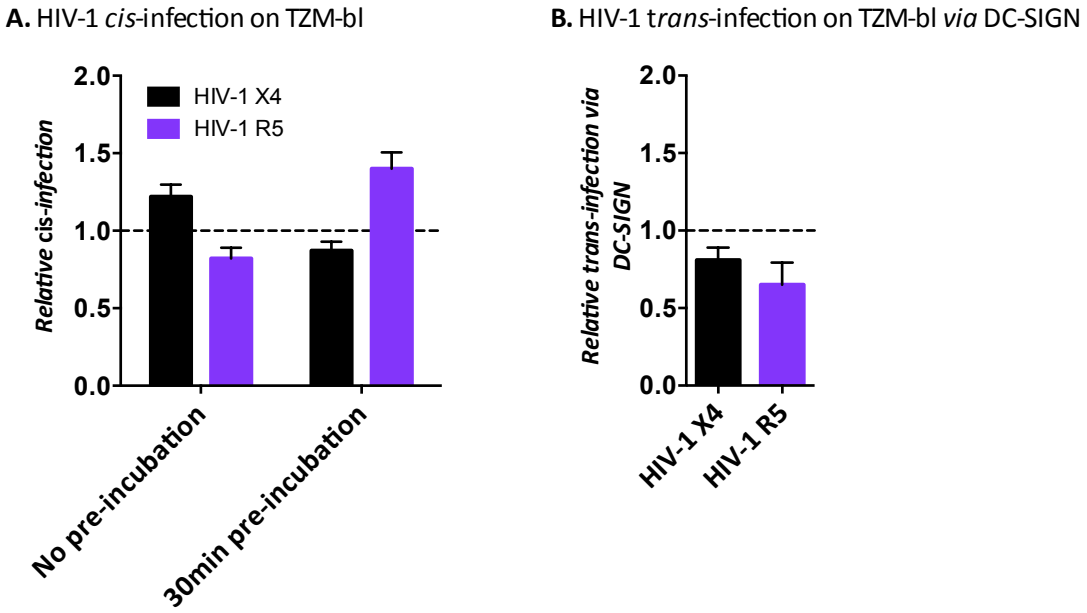

Figure 5.6 : Influence of EVs isolated from plasma on HIV-1 infections

A. One day prior to infection, $3x10^4$ TZM-bl cells per well were seeded in 96-well plates. After 24h, TZM-bl cells were infected with 8ng of pSG3-LAI (HIV-1 X4) and pSG3-BAL (HIV-1 R5) with 50µl of EVs isolated from plasma by SEC (pool fractions 9-13). In one case, EVs were incubated at the same time as virus and in the second case TZM-bl cells were pre-incubated for 30min prior to infection. 48h following infection cells were lysed to measure luciferase activity (RLU). *Cis*-infection of the virus alone is used as reference (n=3). **B.** 50µl of EVs isolated from plasma by SEC (pool fractions 9-13) $0.5x10^6$ of Raji-DC-SIGN cells. Cells were incubated 2h with 12.5ng pSG3-LAI (HIV-1 X4, black) or 25ng pSG3-BAL (HIV-1 R5, purple). After capture the cells were washed and co-cultured with TZM-bl cells. The luciferase activity was read after 48h. *Trans*-infection of virus alone with Raji-DC-SIGN that were pre-incubated with PBS, was used as the reference infection (n=3). The data shown are from one experiment using plasma isolated from one donor.

For the HIV-1 *cis*-infection assay, isolated EVs were either added at the same time as virus to target cells (TZM-bl) or were pre-incubated for 30min with cells before virus was added. *Cis*-infection with HIV-1 alone was used as the negative control and as the reference for this assay. When EVs were added at the same time as HIV-1 X4 to the target cells, we observed that the efficacy of *cis*-infection increased to 1.2. However, when TZM-bl cells were pre-incubated with EVs, *cis*-infection decreased to 0.8 efficacy compared to HIV-1 X4 alone. For HIV-1 R5 the opposite was observed where EVs added at the same time as virus decreased to 0.8 and when EVs were pre-incubated before HIV-1 R5 infection, we observed a 1.4 fold

increase compared to virus alone. From these observations, the impact of EVs isolated from plasma from healthy donors on HIV-1 *cis*-infection was different when comparing both virus phenotypes; however, these results did not reach statistical significance (Mann-Whitney test).

Concerning HIV-1 DC-SIGN mediated *trans*-infection EVs were incubated 30min with Raji-DC-SIGN cells prior virus capture (Figure 5.6 **B**). For both viruses, we observed that the presence of EVs from SEC demonstrated a trend towards decreasing DC-SIGN *trans*-infection efficacy to 0.8 for HIV-1 X4 and to 0.6 for HIV-1 R5 virus. This suggests that EVs isolated from plasma could reduce HIV-1 DC-SIGN mediated *trans*-infection, but again as for *cis*-infection, did not reach statistical significance (Mann-Whitney).

III. Conclusion

Multiple approaches are available to isolate EVs from biological fluids. In this Chapter the focus was to analyse two major methods, UC and gel filtration, to study the effects of EVs isolated from plasma on modulating HIV-1 infection.

We demonstrated that the elimination of contaminants from plasma is crucial to study the possible impact of EVs on HIV-1 *trans*-infection (Figure 5.1 and 5.2). Simple centrifugation of diluted plasma at 7,000g for 90min, did not allow for the separation of EVs from contaminating protein according to (Taylor and Shah, 2015; Konoshenko *et al.*, 2018). Indeed, our samples containing EVs (pellet resuspended in PBS) partially inhibited HIV-1 X4 DC-SIGN mediated *trans*-infection, as did the supernatant. In order to study the specific impact on HIV-1 infection it is crucial to purify EVs from the contaminants. The UC protocol described by Théry *et al.*, 2006 is a standard technique allowing for working with large volumes. Due to practical application (few consumables and reagents needed) many laboratories choose to use this method (Konoshenko *et al.*, 2018). Here it was shown that EVs isolated from healthy donors plasma by UC did not significantly affect HIV-1 X4 *trans*-infection mediated *via* DC-SIGN or iDCs. This result suggests that most of the contaminants from plasma were eliminated through the differential centrifugation steps as expected. However, the UC technique doesn't allow for optimum purification of EVs from contaminants found within plasma such as albumin (Baranyai *et al.*, 2015) and represents a long process that potentially damages the integrity of EVs (Lobb *et al.*, 2015).

To isolate and purify EVs from HIV-1/*Mtb*$^{+}$ patients using UC may well prove problematic due to the equipment range in CL3 facilities. Additionally, isolation of EVs from HIV-1 virions in HIV^{+} samples requires particular purification strategies due to a similar size and density of both types of particles, again providing a limitation to using this approach (Cantin *et al.*, 2008; Madison and Okeoma, 2015; Cheruiyot *et al.*, 2018). An iodixanol (Optiprep) gradient can be used but this approach again requires UC steps (Cheruiyot *et al.*, 2018).

The second method analysed involved the isolation of EVs by gel filtration. Two different types of matrix that separate EVs from plasma based on differential hydrodynamic radius of macromolecules were tested. Because of the high hydrodynamic radius of EVs compared to proteins, lipoproteins or protein complexes, purification from these elements is relatively simple (Taylor and Shah, 2015; Konoshenko *et al.*, 2018). We demonstrated that the column Sephadex G-25 did not allow for optimum purification of EVs from plasma (Figure 5.3). Indeed, the eluate containing EVs, which has been concentrated in an additional step, was shown to inhibit HIV-1 X4 DC-SIGN *trans*-infection. This result suggests that contaminating elements from plasma are still present in the eluate blocking viral capture-transfer. As Sephadex G-25 allowed separation of 1-5KDa range of proteins, the EVs were expected to be eluted at the early stages of the chromatography. However, collection of too large volumes during the assay could explain the presence of contaminants in the eluate. The elution of volume being too big could lead to the collection of the same molecules (eluting at early and late stages of the chromatography) in the same fraction and not allowing for efficient separation. Due to descriptions in the literature, it was decided to study another matrix, Sepharose CL-2B (Baranyai *et al.*, 2015; Hong *et al.*, 2016; Konoshenko *et al.*, 2018), and follow the published protocol Böing *et al.*, 2014. As described the fractions obtained by CL-2B SEC were analysed using NanoSight technology and the protein concentration assay. Similar observations were made to Bïong *et al.*, where particles with less protein contaminations were present in the pooled fraction 9 to 13. Sepharose CL-2B SEC is a relatively easy and rapid means of generating EVs from plasma (Figure 5.4).

To control for EV isolation and purification from SEC, Western Blot analyses of all the generated fractions was performed (Figure 5.5). Two EV specific markers, TGS-101 and CD63 were tested for being present in each fraction. Unfortunately, immunoblotting for either marker was inconclusive. Indeed we were not able to visualise specifically TSG-101 (44KDa) nor CD63 (50-60KDa) being present in EV fractions. For this assay antibodies were used as recommended by the manufacturer and as described in the literature (Baranyai *et al.*, 2015;

Lobb *et al.*, 2015). Optimisation of antibody concentrations to be utilised may be required and should be tested using cell lysates to control for sensitivity and specificity as these markers are present on cell membranes. Furthermore, other antibodies should be tested against other EV specific markers such as CD9 described to be present at high proportion in EVs (Théry *et al.*, 2006). The characterisation of isolated EVs by Western Blot analysis is essential to confirm their presence and could be used to control for their purity. Additionally, in the perspective of working in HIV-1/*Mtb*$^{+}$ patients, Western Blot analysis would represent a good method to characterise specific protein cargoes from HIV-1 and/or *Mtb* integrated to EVs.

NanoSight analysis did show isolation of particles as observed in Böing *et al.*, 2014, suggesting EVs were isolated as previously described. The impact of EVs isolated from plasma on HIV-1 *cis*- as well as *trans*-infection was tested (Figure 5.7). The results suggested that EVs isolated using CL-2B SEC did not significantly impact on HIV-1 X4 or R5 *cis*-infection nor *trans*-infection *via* DC-SIGN or iDCs.

The role EVs in infectious diseases and in modulating immunity is important. In the case of HIV-1 infection, multiple studies have described the ability of virus to use the exosomal pathway for cell infection and propagation. The convergence of HIV-1 replication and exosome biogenesis leads to the incorporation of viral proteins such as Nef, Env and Gag, or HIV-1 nucleic acids and microRNA into EVs (Kadiu *et al.*, 2012; Arenaccio, Chiozzini, Columba-Cabezas, Manfredi, Affabris, *et al.*, 2014; Madison and Okeoma, 2015; Hildreth, 2017). The similarities in biogenesis of exosomes and HIV-1 guides the Trojan exosomes hypothesis which suggests that virus uses exosome biogenesis to allow formation of infectious virions that don't require Env for cell entry (Gould, Booth and Hildreth, 2003; Madison and Okeoma, 2015). Furthermore, EVs produced from infected cells allowing for transfer of viral proteins could facilitate HIV-1 infection, such as the transfer of Nef between cells (Madison and Okeoma, 2015). As with HIV-1, many studies have described the fundamental role of EVs in influencing *Mtb* infections. Mycobacterial components can be detected in EVs which have the potential to modulate the immune response by regulating uninfected macrophage responses (Beatty *et al.*, 2000; Athman *et al.*, 2015; Lee *et al.*, 2015; Gupta and Rodriguez, 2018). In the context of co-infection, the role of EVs has not been described. It could be expected that EVs isolated from HIV-1/Mtb^{+} co-infected individuals could contain components from HIV-1 and/or *Mtb* and could therefore modulate either pathogens

infectivity and or replication cycle. The results presented here provide some indicators of how EVs can be isolated from plasma of such patients.

General conclusion and discussion

HIV-1 and *Mycobacterium* (*Mtb*) co-infection represents a serious diagnostic and therapeutic challenge, particularly in resource-limited settings. However, knowledge regarding the mechanisms of interactions between the two pathogens still needs to be characterised in order to develop preventive measures and treatment strategies against the two diseases separately or within a co-infection *scenario*. Limitations exist in access to effective drug therapies and the emergence of resistance. Improvements in drug access and simplified treatment regimens are urgently required (Anandaiah *et al.*, 2011; Kwan and Ernst, 2011).

I. Liposomes Technology

In order to describe and better understand the implication of *Mtb* glycolipids in HIV-1 infection in the context of co-infection, liposomes generated from various *Mtb* strains containing total lipids were developed. The artificial vesicle technology is largely established and used in pharmacology and in various vaccination strategies (Akbarzadeh *et al.*, 2013). The interest of using liposomes here is that the generation of liposomes allows a reorganisation of *Mtb* components close to the original mycobacteria cell wall. Additionally, proportions of individual glycolipids are representative and the use of soluble lipids solution is avoided. We demonstrated that generated liposomes are composed of *Mtb* specific glycolipid components.

II. Modulation of the immune response by *Mtb* glycolipids

We first described the influence of *Mtb* glycolipids on altering MDM, DC and $CD4^+$ T cell responses. In the *in vitro* systems developed, we observed a strong heterogeneity of *Mtb* liposome effects on modulating immune cells and this was found to be dependent on the cell types and *Mtb* strain of origin. *Mtb* component glycolipids, glycerol mono-mycolate, TDM, PIM, LAM and LM were previously known to modulate immune responses through engagements of PRRs pathways (Barnes *et al.*, 1992; Quesniaux *et al.*, 2004; Banaiee *et al.*, 2006; Andersen *et al.*, 2009). Differences in the proportion and composition of those lipids could modulate differentially immune responses from MDM and DC.

Mazurek *et al.* revealed the importance of ManLAM and PIMs in maturation of DCs during *Mtb* infection. Purified ManLAM from the H37Rv *Mtb* pathogenic strain induce stronger responses from iDCs compared to ManLAM isolated from BCG (*M. bovis* strain used for *Mtb* vaccination) (Mazurek *et al.*, 2012). In our system, we observed variant responses in iDC maturation in the presence of H37Rv and BCG glycolipids, supporting Mazurek's observations. This differential impact of ManLAM from H37Rv compared to BCG, could be explained by the differential structure of ManLAM (Torrelles *et al.*, 2008). The glycerol mono-mycolate from the mycobacteria cell wall have been described to activate DCs (Andersen *et al.*, 2009). Mazurek *et al.* revealed also that compared to ManLAM, soluble PIM can induce lower responses from iDCs (Mazurek *et al.*, 2012). However, some *Mtb* components can inhibit inflammatory responses, as found for glycolipids isolated from the HN878 *Mtb* strain that showed the capacity to strongly inhibit inflammatory responses from MDM (Reed *et al.*, 2004). Variations in the proportion of glycolipids being incorporated into liposomes could explain for the differences observed in MDM and DC induced responses. However, various studies support that ManLAM can indeed inhibit pro-inflammatory responses within DCs. Geijtenbeek *et al*. showed in 2003 that soluble *Mtb* ManLAM was not able to induce maturation of iDCs in their assays (Geijtenbeek *et al.*, 2003). Differences in ManLAM structure could explain the divergent impact of ManLAM on MDM and DC activation (Nigou *et al.*, 1997; Briken *et al.*, 2004; Pitarque *et al.*, 2005). Interestingly, co-cultures of iDCs with $CD4^+$ T cells in the presence of *Mtb* glycolipids, revealed a global down-regulation of pro-inflammatory responses. These observations are in correlation with the capacity of *Mtb* components to inhibit pro-inflammatory responses as mentioned above. The inhibition of immune responses observed from DCs and $CD4^+$ T cell co-culture, could be explained by the impairment of DC antigen presentation to T cells by alteration of CD1b, DC-SIGN and MR (Balboa *et al.*, 2010). PIM is associated with altering anti-inflammatory properties by inhibiting TLR activation (Doz *et al.*, 2009), such as observed with a 19kDa lipoprotein (Pai *et al.*, 2004). By the interaction with DC-SIGN receptor, PIM and ManLAM have been identified to impair DC maturation. However, the *Mtb* mutant lacking both glycolipids demonstrated that ManLAM and PIM interaction with DC-SIGN was not crucial for cytokine secretion *in vitro* and for immune protection *in vivo*. This suggests that other receptors such as MR could be involved in the anti-inflammatory responses as well as other *Mtb* components reviewed in (Ehlers, 2010).

III. Modulation of HIV-1 infection by *Mtb* glycolipids

Variations in glycolipid composition and proportions, depending on the *Mtb* strains, induce differential immune responses from MDM, DC and $CD4^+$ T cells in our *in vitro* culture systems. The influence of *Mtb* glycolipids were subsequently tested in the context of co-infection with HIV-1 X4 or R5 strains. In the three assays developed, we observed strong variations in *Mtb* glycolipid impact on HIV-1 infections depending on virus tropism and the culture system being tested. We aimed to identify whether *Mtb* components could directly affect HIV-1 *cis*-infection or *trans*-infection. From all the analyses, it can be concluded that *Mtb* glycolipids mainly regulate HIV-1 infection by modulation of the immune response induced from the infected cells. Indeed, in each case, the introduction of *Mtb* glycolipids to the culture systems infected with HIV-1 induced modifications to cytokine production compared to infected cells alone. DCs appeared to play a major role in this modulation of induced cytokine/chemokine responses. As explained above, *Mtb* glycolipids can modulate pro- or anti-inflammatory responses from DCs by interactions with PRRs such as DC-SIGN. Analyses of HIV-1 *trans*-infection, mediated *via* DC-SIGN, indicated that *Mtb* glycolipids from BCG, H37Rv or EU127 can interact with DC-SIGN and block viral capture and transfer. Additionally, we identified SL1 and TDM as potent antigens able to block DC-SIGN receptor mediated HIV-1 *trans*-infection. However, the role of DC-SIGN engagement by *Mtb* glycolipids in modulation of pro- or anti-inflammatory response from DCs remains unclear (Ehlers, 2010). Singh *et al.*, described that co-infection of DCs significantly reduced IFN-γ revealing impairment in antigen presentation (Singh *et al.*, 2016). In our co-culture assay, we observed a decrease in production of IFN-γ in HIV-1 R5 infections in the presence of *Mtb* glycolipids, suggesting that perturbation of DC antigen presentation occurred decreasing pro-inflammatory responses and HIV-1 R5 replication. However, Van Kooyk and Geijtenbeek described that an impairment in DC function by *Mtb* components could benefit virus replication by decreasing internalisation of the DC-SIGN receptor, leading to the enhancement of HIV-1 transmission *via trans*-infection (Van Kooyk, Appelmelk and Geijtenbeek, 2003), but the assays on HIV-1 *trans*-infection in CD4+ T cell co-cultures mediated by iDCs did not reveal a major impact of *Mtb* glycolipids on HIV-1 replication.

With HIV-1 X4 infections we observed a global activation of the pro-inflammatory response from CD4+ T cells and DCs, indicating that other mechanisms are involved in the inhibition of HIV-1 X4 virus replication. Nieto-Garai *et al.*, recently revealed how lipidomimetic compounds can alter HIV-1 fusion during viral entry (Nieto-Garai *et al.*, 2018). We could

hypothesise that *Mtb* glycolipids associated into liposomes could affect viral entry, however, our assays using pseudo-typed HIV-1 particles indicate that *Mtb* glycolipids do not interfere with HIV-1 *cis*-infection.

The up-regulation of the pro-inflammatory responses by *Mtb* glycolipids can result in enhancement of LTR transactivation (Bafica *et al.*, 2003; Equils *et al.*, 2003; Rodriguez *et al.*, 2013). This suggests that in co-culture assays, the up-regulation in pro-inflammatory responses induced by H37Rv and CDC1551 glycolipids is sufficient to promote and enhance replication of HIV-1 X4 strains. This was also observed for HN878 and CDC1551 glycolipids when monitoring HIV-1 R5 replication.

The difference of *Mtb* glycolipid impact between HIV-1 X4 and R5 tropism is intriguing and has major consequences for better understanding virus replication during disease. Our results suggest that *Mtb* glycolipids can differentially modulate immune activation, dependent on the *Mtb* strain and can also modulate HIV-1 replication differentially based on co-receptor usage. The findings that *Mtb* HN878 and CDC1551 up-regulate HIV-1 R5 replication could have a serious impact during primary infection, where viruses exclusively utilise the CCR5 co-receptor, whereas *Mtb* H37Rv could have more of a detrimental effect on enhancing HIV-1 infection during the chronic stage of infection in individuals where X4 viruses have emerged.

IV. Future perspectives

To identify and characterise precisely the modulation of *Mtb* components on the skewing of immune responses and HIV-1 infection a number of complementary research approaches need to be taken. First, the affect of liposome composition would need to be characterised further as some liposomes generated with only PC and cholesterol demonstrated T cell toxicity properties. Additionally, *Mtb* glycolipids should be integrated into liposomes separately, such as LAM, LAM, or PIM, in order to characterise their impact on altering immune responses and influencing HIV-1 replication individually. Additionally, HPLC analyses needs to be performed in order to better quantify and control *Mtb* glycolipid associations in liposomes. Concerning analyses of *Mtb* components on the immune response, assays should be performed using whole PBMC *in vitro* cultures to characterize sub-population effect and interactions between cells and in the context of HIV-1 infection or not. Transformed cell lines

expressing specific molecules of signalling pathways, such as TLRs, NF-κB should be tested to identify mechanisms involved in the induction of cellular responses and HIV-1 replication. To understand better the importance of DC responses induced by *Mtb* glycolipids on HIV-1 replication and the involvement of DC-SIGN receptor, *in vitro* HIV-1 infection could be developed using naïve T cells co-cultured with iDCs or mDCs as well as iDCs incubated with *Mtb* glycolipids. The involvement of the DC-SIGN receptor should be then investigated by using antagonists of DC-SIGN, thereby blocking its usage by HIV-1 or engagement with *Mtb* glycolipid antigen. To confirm the observations that *Mtb* glycolipids do not have any impact on viral entry, *in vitro* tests could be developed using HIV-1 replicative system in the absence or presence of HIV-1 specific entry inhibitors. This analysis could be complementary to *in vivo* studies using transgenic mice models used to study HIV-1 and/or TB infection.

Understanding of the role that EVs can play in modulating HIV-1 infection during co-infection with *Mtb* is important. EVs have been shown to influence diseases through modulating immune responses. In HIV-1 infection production of EVs are believed to associate with production of infectious viral particles that do not require Env for cell entry (Hildreth, 2017). However, the implication of EVs in the context of *Mtb* co-infection has not been described and could be involved more so in the modulation of the immune responses being induced by both pathogens in the context of co-infection.

The work presented here demonstrates that variant *Mtb* glycolipids antigens can differentially modulate HIV-1 infection. The characterisation of the *Mtb* components involved in this modulation represents a key point in better understanding the interactions between HIV-1 and *Mtb* and the role such interactions can have on influencing disease. Further elucidation of these pathogen interactions will undoubtedly lead to the design of new approaches and development of products aimed at limiting the detrimental effects observed during co-infection.

Appendixes

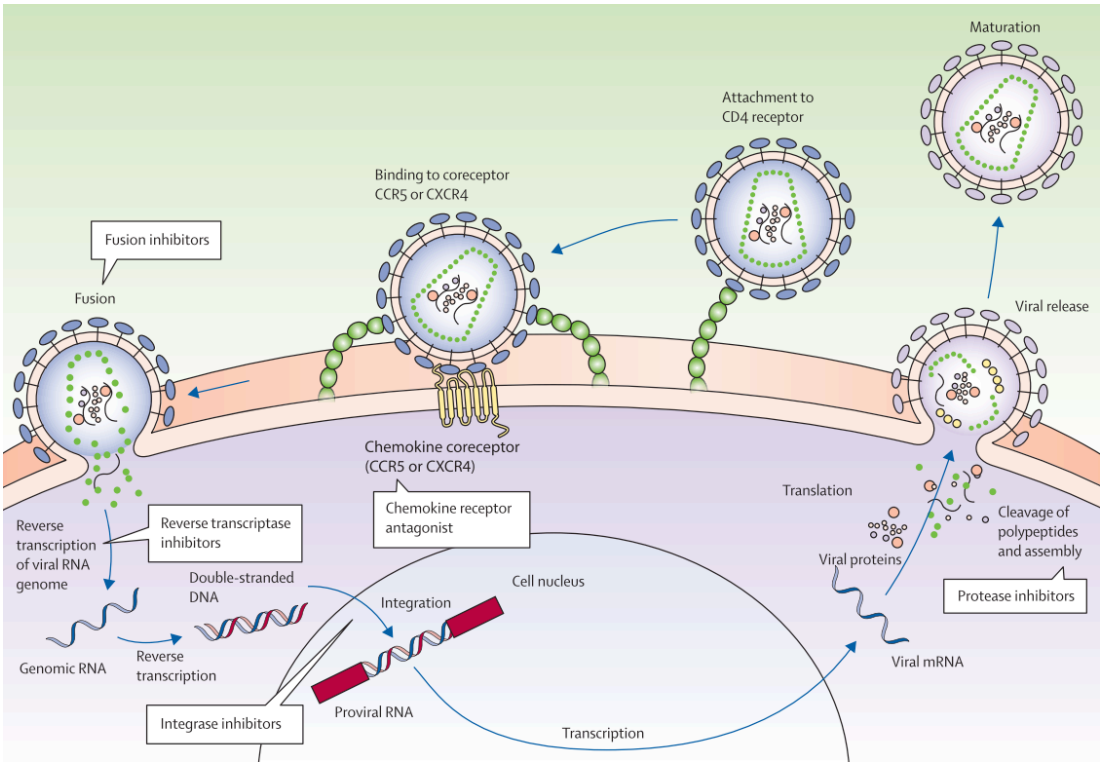

Appendix 1 : Steps of HIV-1 cycle

Adapted from (Maartens, Celum and Lewin, 2014)
First, virus attachment to target cells is initiated by binding to the CD4 receptor and co-receptor CCR5 and/or CXCR4. The fusion of the viral and cell membranes allows the entry of the capsid into the cells. The viral RNA genome is then reverse-transcribed into DNA in the cytoplasm and translocated to the nucleus for integration. The proviral DNA is then transcribed and subsequently translated to express the viral proteins required for production of immature virions containing two copies of viral genome. After budding of new virions, maturation occurs, allowing for the production of mature viral particles capable of infecting new cells. Antiretroviral therapy target specific phase of the viral life-cycle: viral entry with chemokine receptor antagonist (Maraviroc for CCR5) and fusion inhibitors FIs (Enfuvirtide); reverse transcription with nucleotide and non-nucleotide reverse transcription inhibitors NRTIs and NNRTIs; integration with integrase strand transfer inhibitors INSTIs and viral assembly with protease inhibitors PIs.

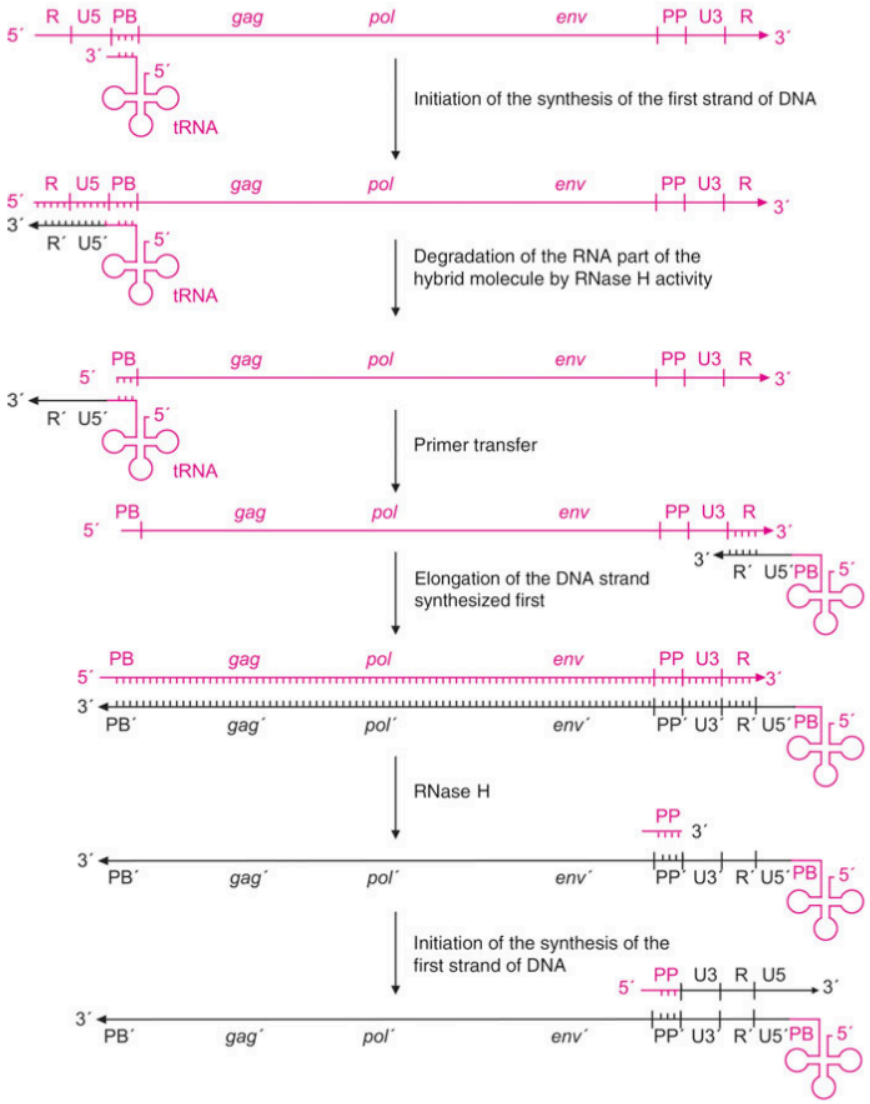

Appendix 2 : HIV reverse transcription

Adapted from (Modrow *et al.*, 2013)
RNA reverse transcription is initiated with binding of transfer RNA (tARN) on the primer binding site PB at the 5' end of the genome. RT allows for the generation of a minus stranded DNA molecule and degrades the complementary RNA by its RNase H activity. The DNA-tRNA hybrid subsequently produced is then transferred to the 3' end of the genome and used as a primer for the synthesis of the first DNA strand.

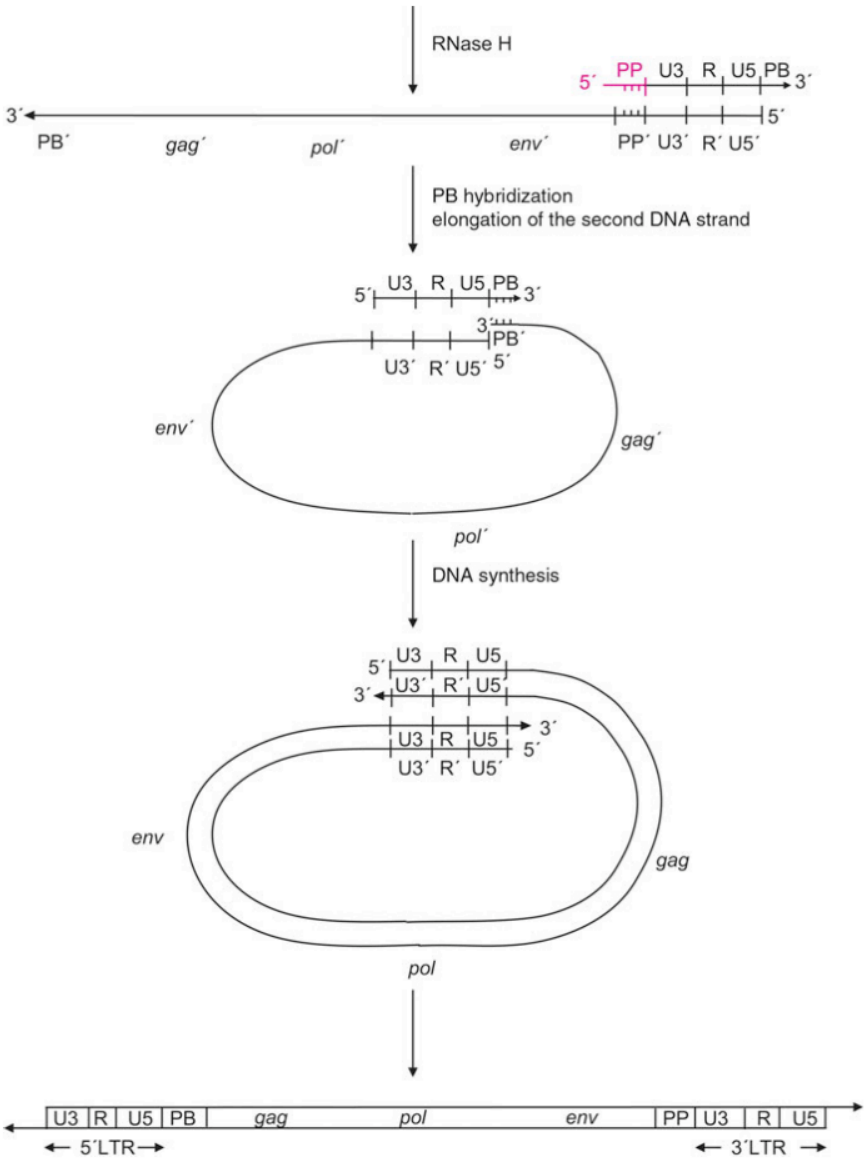

Appendix 2 continued

Adapted from (Modrow *et al.*, 2013)
The ssRNA molecule is degraded by RT, except the PP site that serves for priming synthesis the second DNA strand. After degradation of the tRNA, hybridisation at the PB site occurs and for elongation of the second DNA strand by RT and allowing for the generation of dsDNA and its LTRs (U3-R-U5).

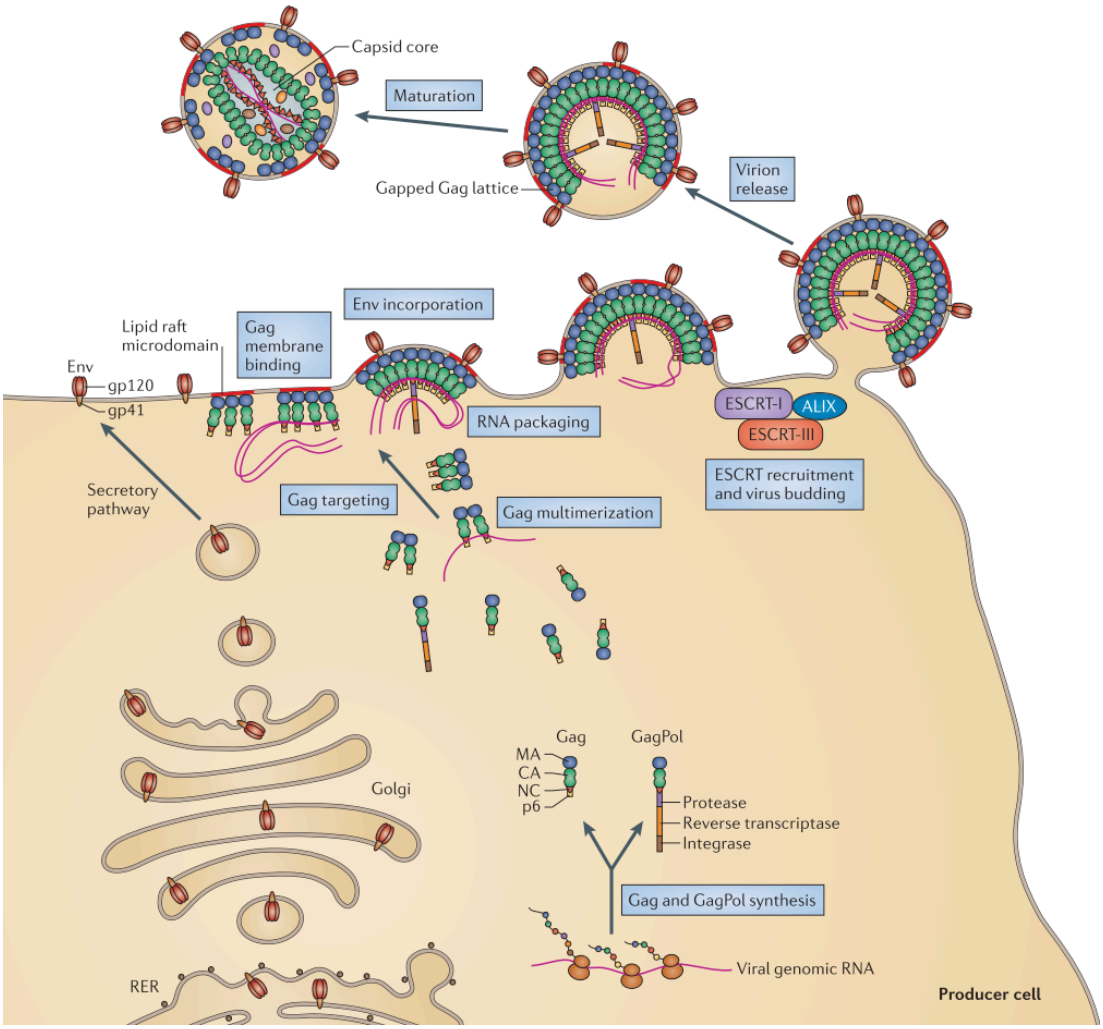

Appendix 3 : HIV particle assembly, budding and maturation

Adapted from (Freed, 2015)
The Env polyproteins are transported from the rough endoplasmic reticulum RER to lipid rafts within the cellular membrane *via* the typical secretory pathways. Gag and Gag-Pol precursors generate viral proteins involved in particle assembly. Gag precursors contain MA, CA, NC and p6 domains. Gag recruits the viral genomic RNA (by the NC domain) to migrate and multimerise (by the CA domain) at the plasma membrane under the same rafts. After incorporation of Env (by the MA domain), the endosomal sorting complex, required for transport (ESCRT-I), is recruited via the p6 domain catalysing membrane fission and completing the budding process. Additionally, the p6 protein of Gag additionally allows for recruitment of Vpr, Vif and Nef to associate with viral particles before budding. The particles released are immature until the protease p11 cleaves Gag and Gag-Pol into the appropriate structural proteins. Once maturation is complete the new viral particles are fully infectious and ready to start a new replicative cycle.

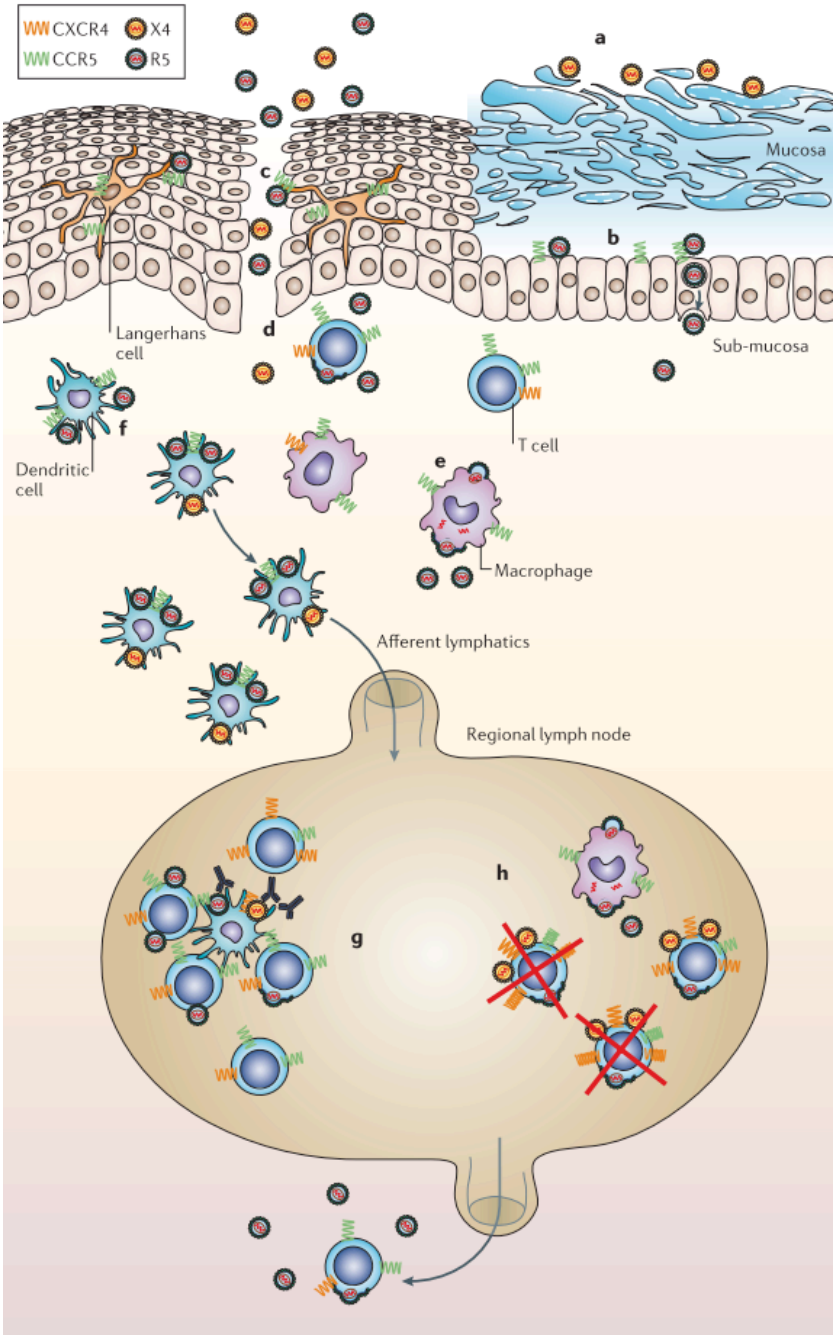

Appendix 4 : HIV-1 mucosal transmission

Adapted from (Margolis and Shattock, 2006)
a. Trapping and inactivation of X4 viruses by mucin and innate antiviral proteins. **b.** Transcytosis of viruses (preferentially R5 viruses). **c.** Infection of Langerhans cells expressing CCR5 co-receptor preferentially. **d.** R5 viruses might demonstrate preferential tropism for memory $CD4^+$ T cells. **e.** Infection of macrophages by R5 viruses **f.** Recognition of virus particles by DCs and migration of the cells to the lymph nodes. **g.** Presentation of viruses to naïve $CD4^+$ T lymphocytes and initiation of the cytotoxic response. **h.** HIV replication in the lymph node and cytotoxic response.

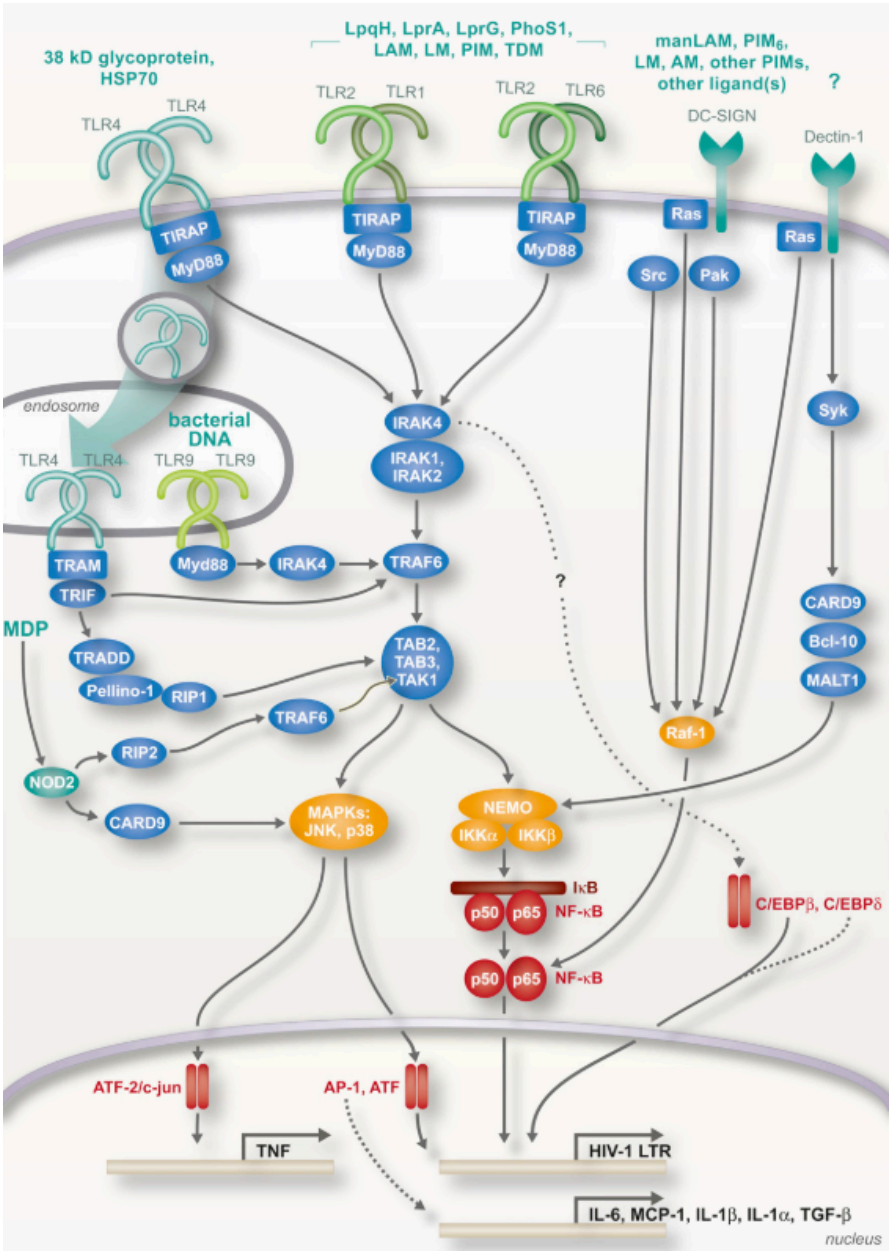

Appendix 5 : Signal transduction pathway activated by* Mtb *components

Adapted from (Falvo *et al.*, 2011)
Generalised intracellular cascades after engagement of Toll-like receptors (TLRs), C-type lectins, and NOD2 by the indicated ligands derived from *Mtb* in macrophages and DCs. Receptors are in green; adapter proteins and upstream kinases are in blue; downstream kinases are in orange; and transcription factors are in red. HIV-1 LTR and activated cytokines are indicated at the bottom. Translocation of TLR4 into the endosome after ligand engagement is indicated by the green arrow.

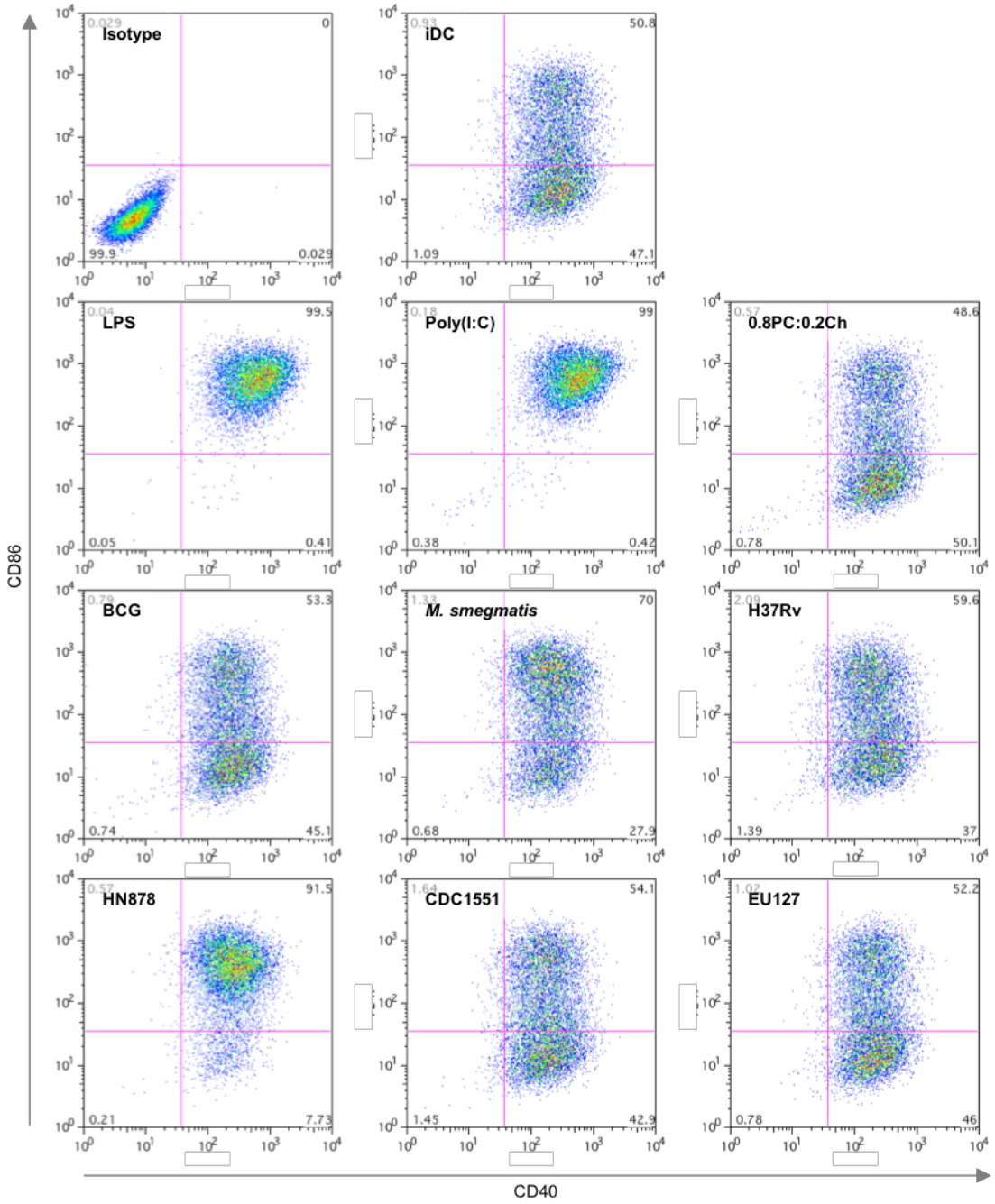

Appendix 6 : Flow Cytometry of iDCs in presence of Mycobacterium *liposomes: CD86/CD40 markers*

Human blood monocytes were isolated from buffy coats by using Ficoll gradient centrifugation and a subsequent CD14 selection step using the MACS cell separation system. Purified monocytes were differentiated into iMDDCs in the presence of IL-4 and GM-CSF, 70ng/ml and 50ng/ml respectively. On day 6, $0.5x10^6$ iDCs were harvested and incubated with 20µg/ml Poly(I:C), 5mg/ml LPS or 100µg/ml 0.8PC:0.2Ch, BCG, *M. smegmatis*, H37Rv, HN878, CDC1551 and EU127 liposomes for 18h. Then the cells were stained with CD-86-PE and CD40-APC antibodies. The data shown are representative of two independent experiments using cells isolated from two different donors.

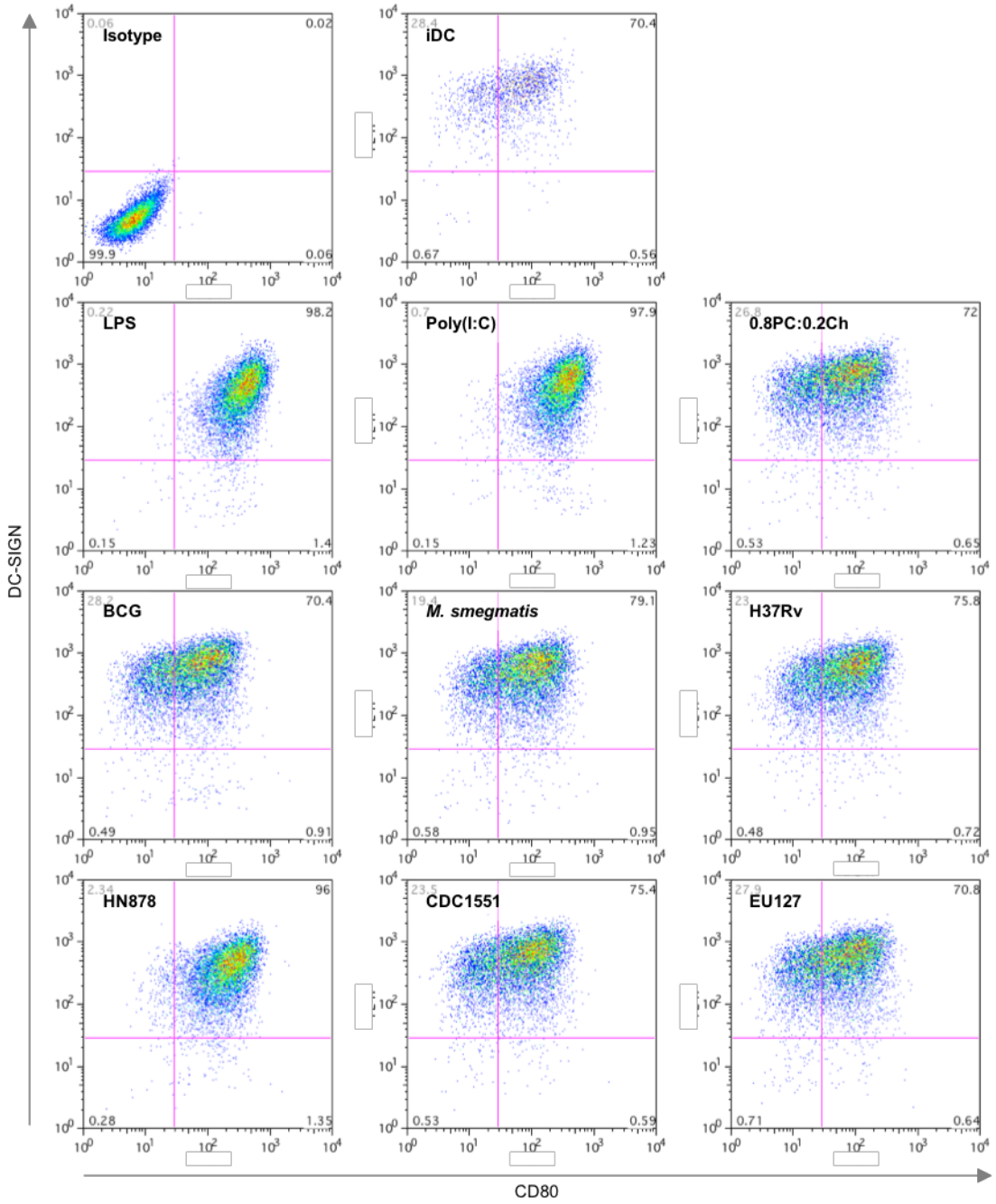

Appendix 7 : Flow Cytometry of iDCs in presence of* Mycobacterium *liposomes: DC-SIGN/CD80 markers

Human blood monocytes were isolated from buffy coats by using Ficoll gradient centrifugation and a subsequent CD14 selection step using the MACS cell separation system. Purified monocytes were differentiated into iMDDCs in the presence of IL-4 and GM-CSF, 70ng/ml and 50ng/ml respectively. On day 6, $0.5x10^6$ iDCs were harvested and incubated with 20µg/ml Poly(I:C), 5mg/ml LPS or 100µg/ml 0.8PC:0.2Ch, BCG, *M. smegmatis*, H37Rv, HN878, CDC1551 and EU127 liposomes for 18h. Then the cells were stained with DC-SIGN-PE and CD80-APC antibodies. The data shown are representative of two independent experiments using cells isolated from two different donors.

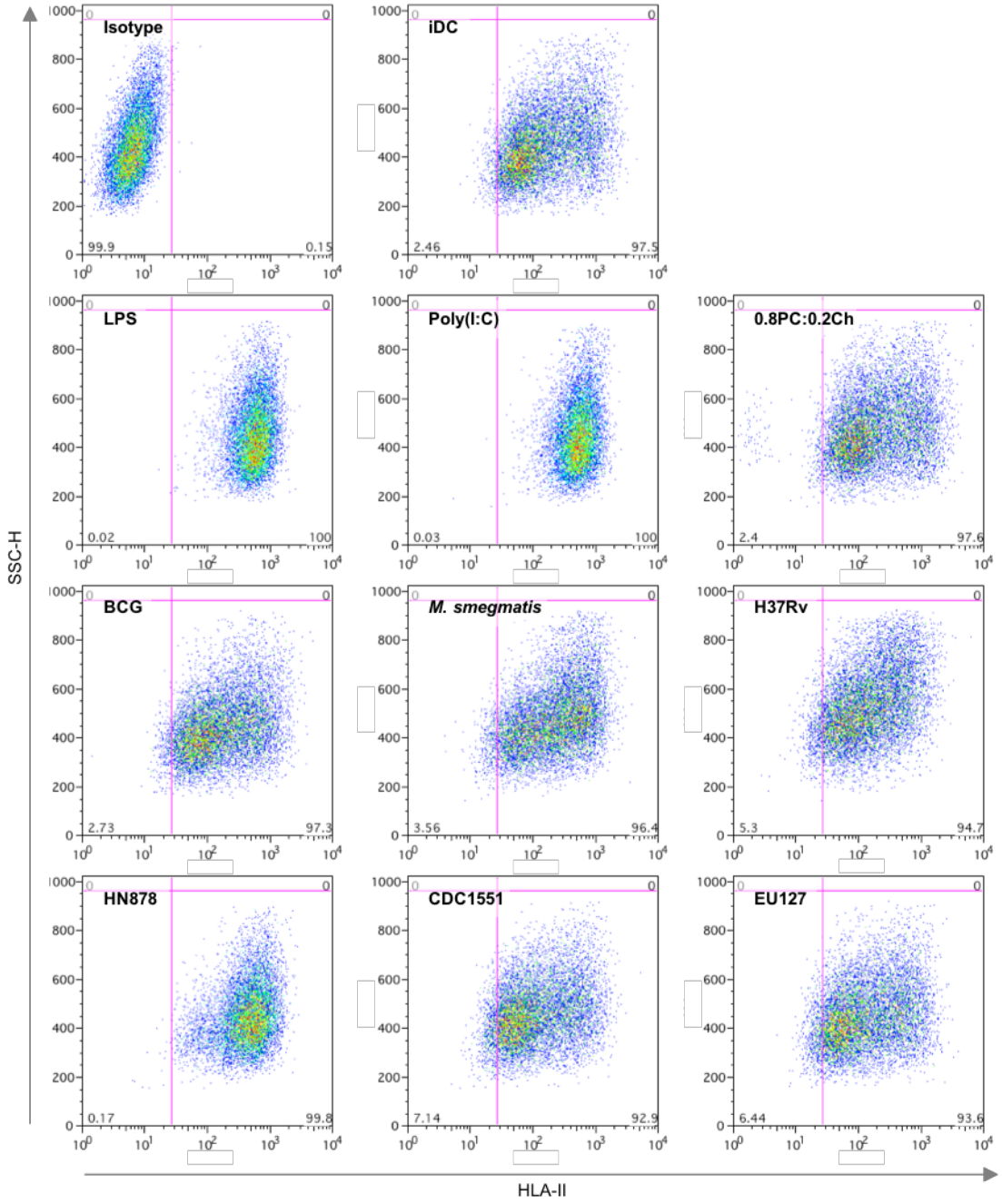

Appendix 8 : Flow Cytometry of iDCs in presence of Mycobacterium *liposomes: HLA-II marker*

Human blood monocytes were isolated from buffy coats by using Ficoll gradient centrifugation and a subsequent CD14 selection step using the MACS cell separation system. Purified monocytes were differentiated into iMDDCs in the presence of IL-4 and GM-CSF, 70ng/ml and 50ng/ml respectively. On day 6, 0.5×10^6 iDCs were harvested and incubated with 20µg/ml Poly(I:C), 5mg/ml LPS or 100µg/ml 0.8PC:0.2Ch, BCG, *M. smegmatis*, H37Rv, HN878, CDC1551 and EU127 liposomes for 18h. Then the cells were stained with HLA-II-APC antibody. The data shown are representative of two independent experiments using cells isolated from two different donors.

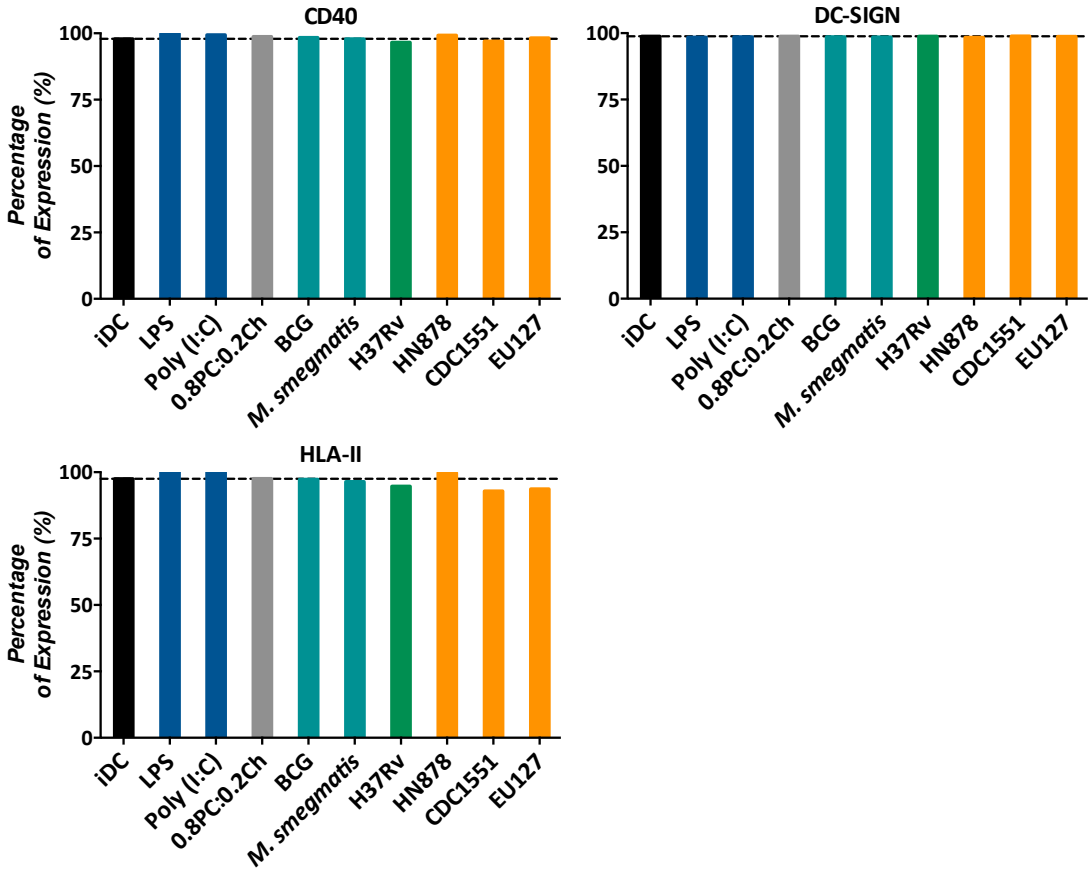

Appendix 9 : Activation of iDCs by Mycobacterium *liposomes*

Human blood monocytes were isolated from buffy coats by using Ficoll gradient centrifugation and a subsequent CD14 selection step using the MACS cell separation system. Purified monocytes were differentiated into iMDDCs in the presence of IL-4 and GM-CSF, 70ng/ml and 50ng/ml respectively. On day 6, $0.5x10^6$ iDCs were harvested and incubated with 20µg/ml Poly(I:C), 5mg/ml LPS or 100µg/ml 0.8PC:0.2Ch, BCG, *M. smegmatis*, H37Rv, HN878, CDC1551 and EU127 liposomes for 18h. Then the cells were stained with antibodies against CD80, CD86, CD40, HLA-II and DC-SIGN receptors and percentage of expression are measured for each condition after cell fixation with PFA by FACS analyses. The data shown are representative of two independent experiments using cells isolated from two different donors.

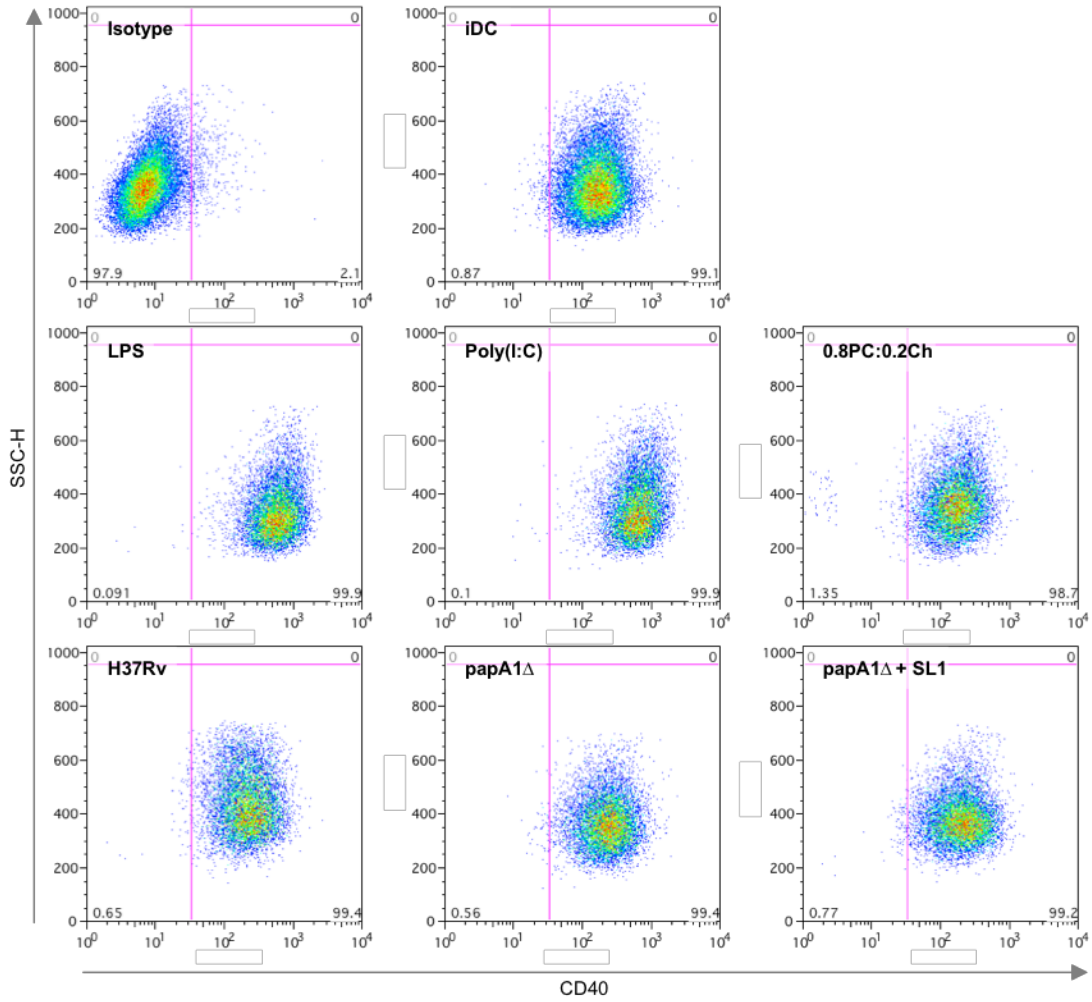

Appendix 10 : Flow Cytometry of iDCs in presence of H37Rv liposomes: CD40 marker

Human blood monocytes were isolated from buffy coats by using Ficoll gradient centrifugation and a subsequent CD14 selection step using the MACS cell separation system. Purified monocytes were differentiated into iMDDCs in the presence of IL-4 and GM-CSF, 70ng/ml and 50ng/ml respectively. On day 6, $0.5x10^6$ iDCs were harvested and incubated with 20µg/ml Poly(I:C), 5mg/ml LPS or 100µg/ml 0.8PC:0.2Ch, BCG, *M. smegmatis*, H37Rv, HN878, CDC1551 and EU127 liposomes for 18h. Then the cells were stained with CD40-APC antibody. The data shown are form one experiment using cells isolated from one donor.

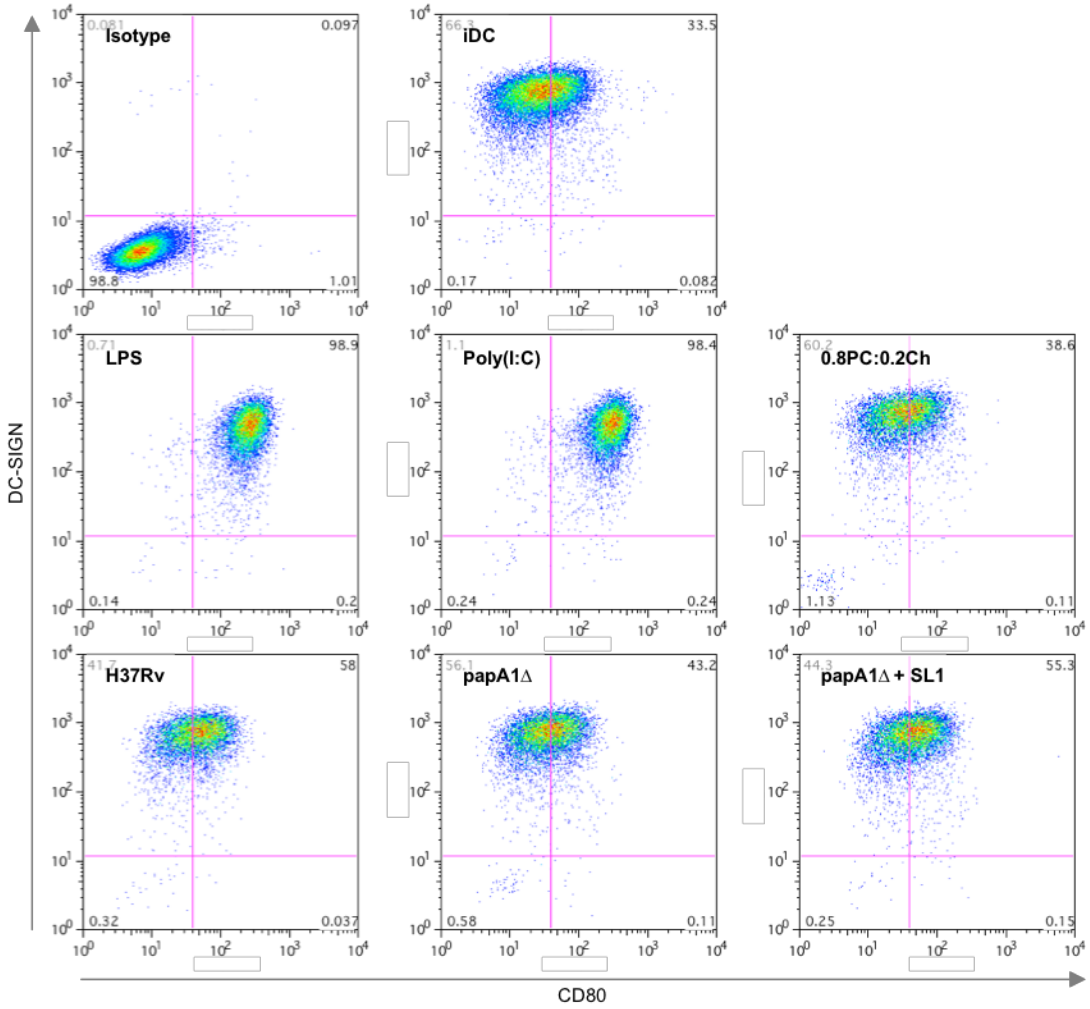

Appendix 11 : Flow Cytometry of iDCs in presence of H37Rv liposomes: DC-SIGN/CD80 markers

Human blood monocytes were isolated from buffy coats by using Ficoll gradient centrifugation and a subsequent CD14 selection step using the MACS cell separation system. Purified monocytes were differentiated into iMDDCs in the presence of IL-4 and GM-CSF, 70ng/ml and 50ng/ml respectively. On day 6, $0.5x10^6$ iDCs were harvested and incubated with 20µg/ml Poly(I:C), 5mg/ml LPS or 100µg/ml 0.8PC:0.2Ch, BCG, *M. smegmatis*, H37Rv, HN878, CDC1551 and EU127 liposomes for 18h. Then the cells were stained with DC-SIGN-PE and CD80-APC antibodies. The data shown are form one experiment using cells isolated from one donor.

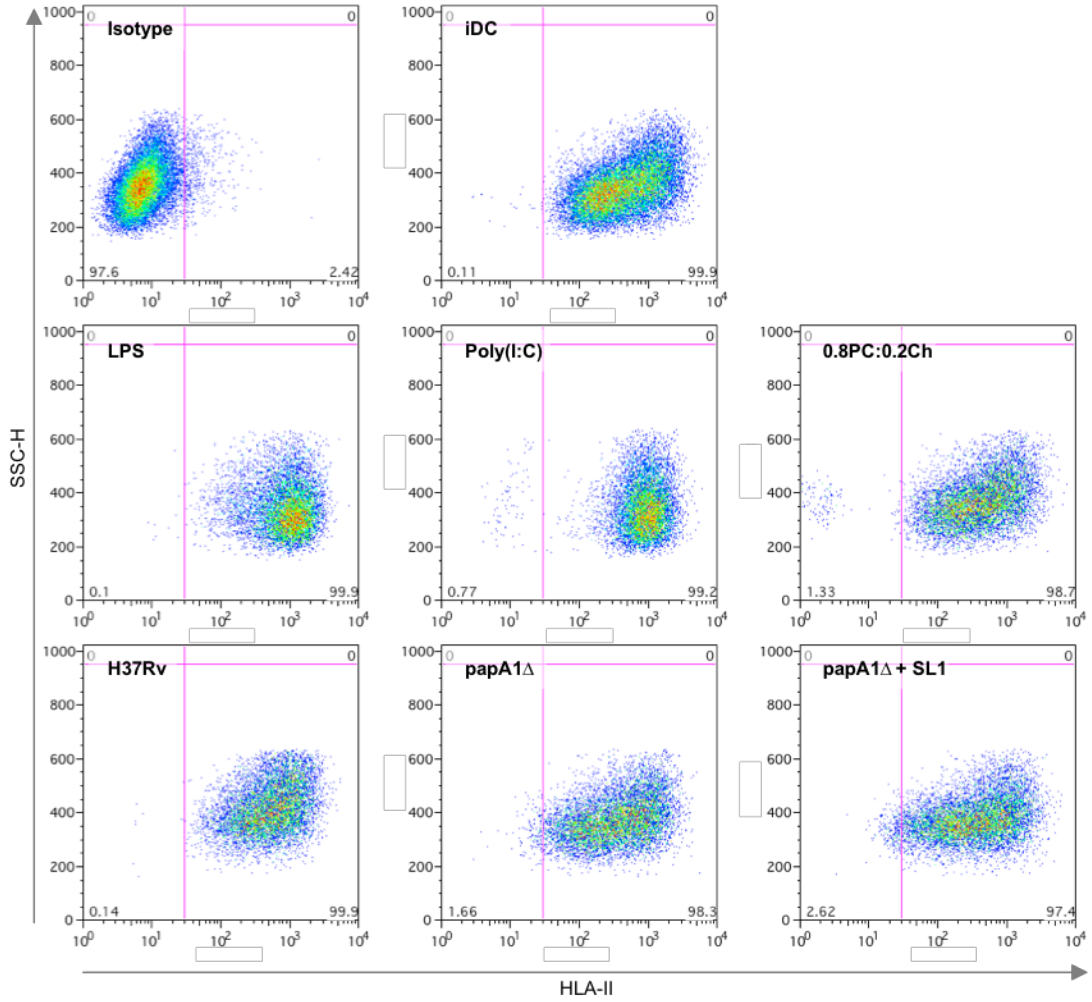

Appendix 12 : Flow Cytometry of iDCs in presence of H37Rv liposomes: HLA-II marker

Human blood monocytes were isolated from buffy coats by using Ficoll gradient centrifugation and a subsequent CD14 selection step using the MACS cell separation system. Purified monocytes were differentiated into iMDDCs in the presence of IL-4 and GM-CSF, 70ng/ml and 50ng/ml respectively. On day 6, $0.5x10^6$ iDCs were harvested and incubated with 20µg/ml Poly(I:C), 5mg/ml LPS or 100µg/ml 0.8PC:0.2Ch, BCG, *M. smegmatis*, H37Rv, HN878, CDC1551 and EU127 liposomes for 18h. Then the cells were stained with HLA-II-APC antibody. The data shown are form one experiment using cells isolated from one donor.

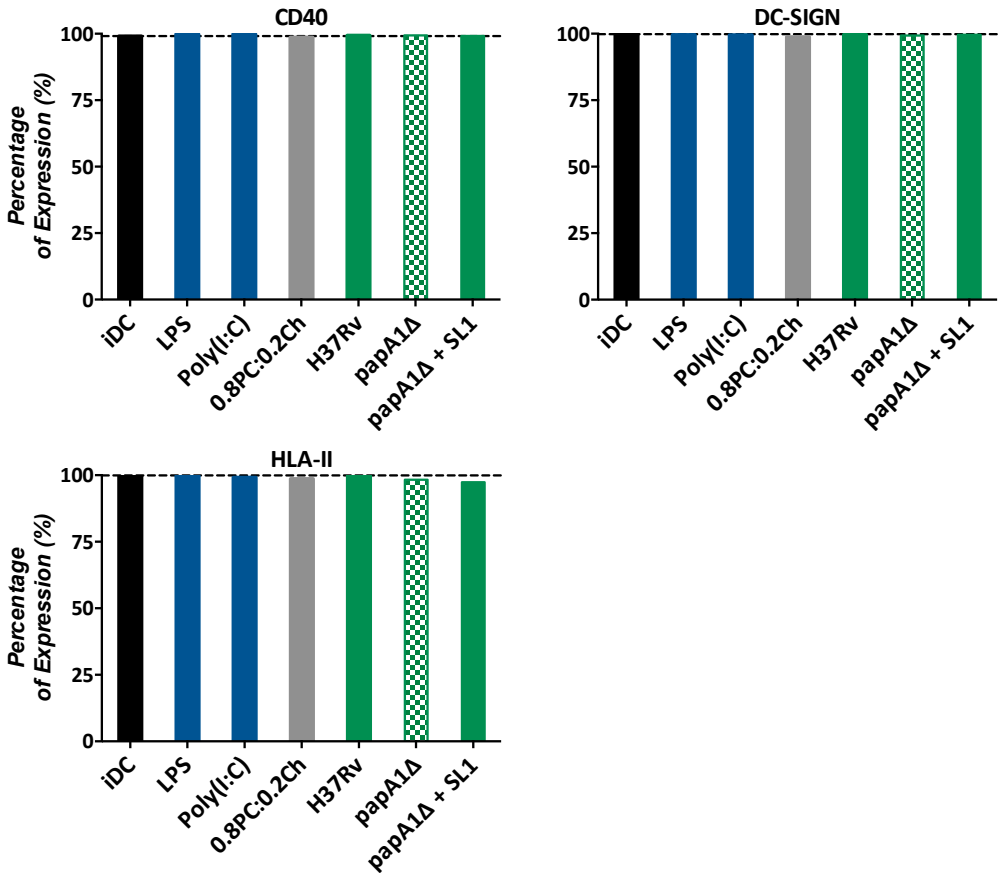

Appendix 13 : Activation of iDCs by H37Rv liposomes

Human blood monocytes were isolated from buffy coats by using Ficoll gradient centrifugation and a subsequent CD14 selection step using the MACS cell separation system. Purified monocytes were differentiated into iMDDCs in the presence of IL-4 and GM-CSF, 70ng/ml and 50ng/ml respectively. On day 6, $0.5x10^6$ iDCs are harvested and incubated with 20µg/ml Poly(I:C), 5mg/ml LPS or 100µg/ml 0.8PC:0.2Ch, H37Rv, papA1Δ, papA1Δ+SL1 liposomes for 18h. Then the cells stained with antibodies against CD80, CD40, HLA-II and DC-SIGN receptors and percentage of expression are measured for each condition after cell fixation with PFA by FACS analyses. The data shown are form one experiment using cells isolated from one donor.

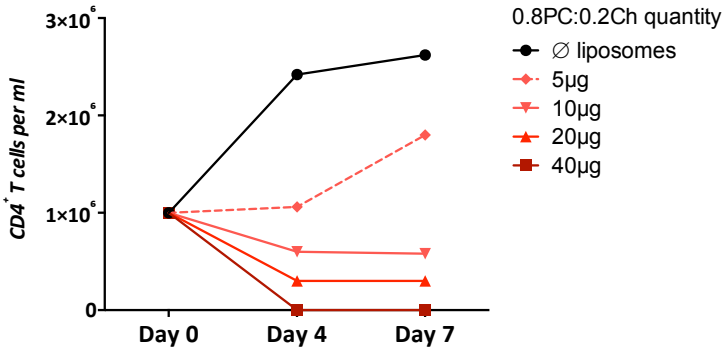

Appendix 14 : Toxicity of 0.8PC:0.2Ch liposomes on CD4⁺ T lymphocytes

In a 96-well plate, $2x10^5$ enriched $CD4^+$ T lymphocytes were seeded per well and incubated with 5, 10, 20 or 40µg of 0.8PC:0.2Ch liposomes. On days 4 and 7 the cells counts were determinate using trypan blue. The data shown are from one experiment using cells isolated from one donor.

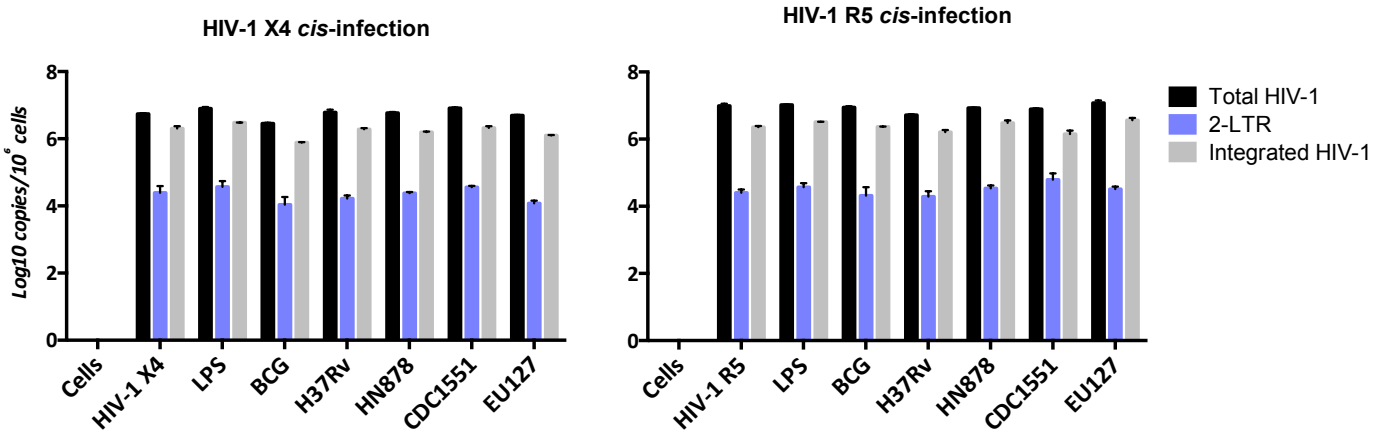

Appendix 15 : Comparison of HIV DNA copies during HIV-1* cis-*infection

$CD4^+$ enriched T lymphocytes ($2x10^5$ cells/well in 96-well plates) were infected with 200 $TCID_{50}$/ml LAI-YFP (HIV-1 X4, left) 500 $TCID_{50}$/ml BAL-GFP (HIV-1 R5, right) and 40µg of *Mycobacterium* liposomes BCG, H37Rv, HN878, CDC1551, EU127, or 100ng/ml of LPS. At day 7 post-infection, quantifications of HIV-1 DNA were determined by PCR and are represented here in log10 HIV-1 DNA copies relative to the total number of cells with total HIV-1 DNA (black, n=3), HIV-1 2-LTR (blue, n=3) and number of integrated HIV (grey, n=3). The data shown are from one experiment using cells isolated from one donor.

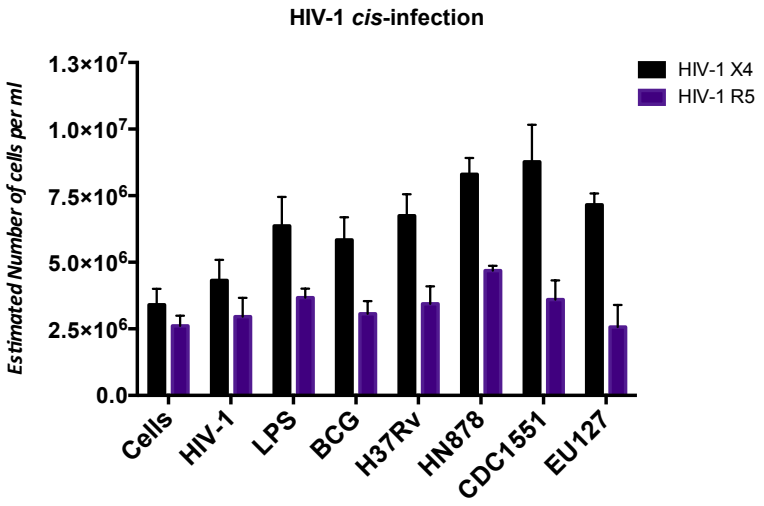

Appendix 16 : Toxicity of Mycobacterium *liposomes on CD4⁺ T lymphocytes during HIV-1* cis-*infection*

$CD4^+$ enriched T lymphocytes ($2x10^5$ cells/well in 96-well plates) were infected with 200 $TCID_{50}$/ml LAI-YFP (HIV-1 X4, black) or 500 $TCID_{50}$/ml BAL-GFP (HIV-1 R5, purple) and 40µg of Mycobacterium liposomes BCG, H37Rv, HN878, CDC1551, EU127, or 100ng/ml of LPS. At day 7 post-infection, the total number of cells were estimated by quantification of CD3 expression by PCR (n=3). The data shown are from one experiment using cells isolated from one donor.

A. p24 production

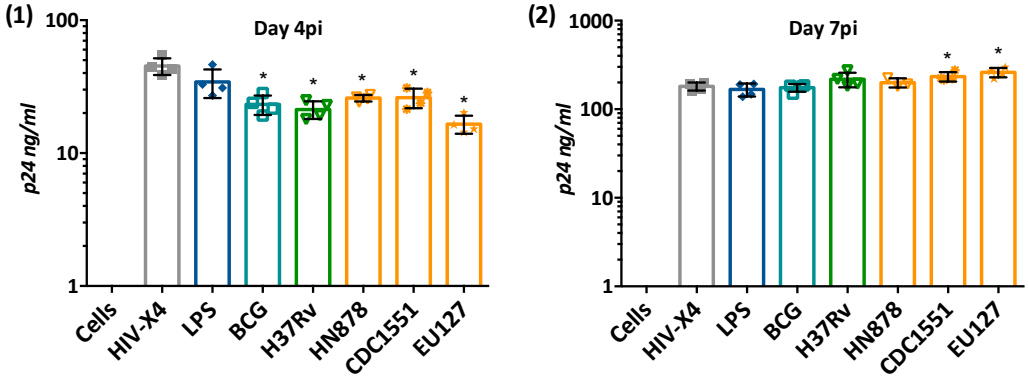

B. DNA quantification

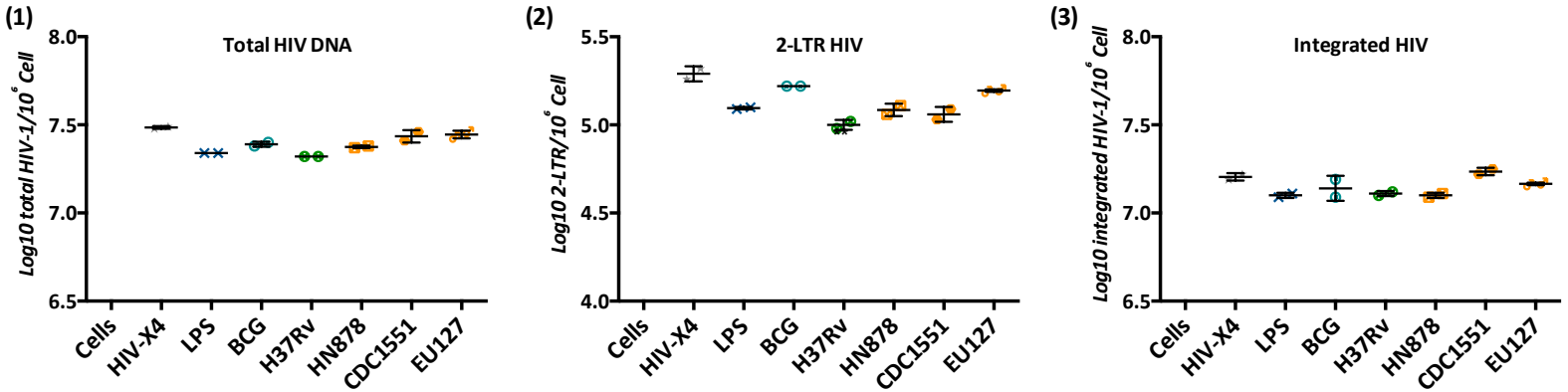

Appendix 17 : Influence of liposomes on HIV-1 X4 trans-infection - liposomes present during capture

8x10^4 iDCs were pre-incubated with 100µg of *Mycobacterium* liposomes or 100ng/ml of LPS for 30min. Then the cells were incubated 30min with 200 $TCID_{50}$/ml LAI-YFP (HIV-1 X4) and washed to be co-cultured with $CD4^+$ enriched T-lymphocytes. **A.** Concentration of total HIV-1 capsid p24 was determinate in the supernatant by ELISA at **(1)** day 4 (n=4) and **(2)** day 7 (n=4) post-infection. **B.** represents log10 HIV-1 DNA quantification determinate by PCR relative to the total number of cells at day 7 post-infection with **(1)** total HIV-1 DNA (n=2), **(2)** number of HIV-1 2-LTR (n=2) and **(3)** number of integrated HIV-1 (n=2). The data shown are from one experiment using cells isolated from one donor.

A. p24 production

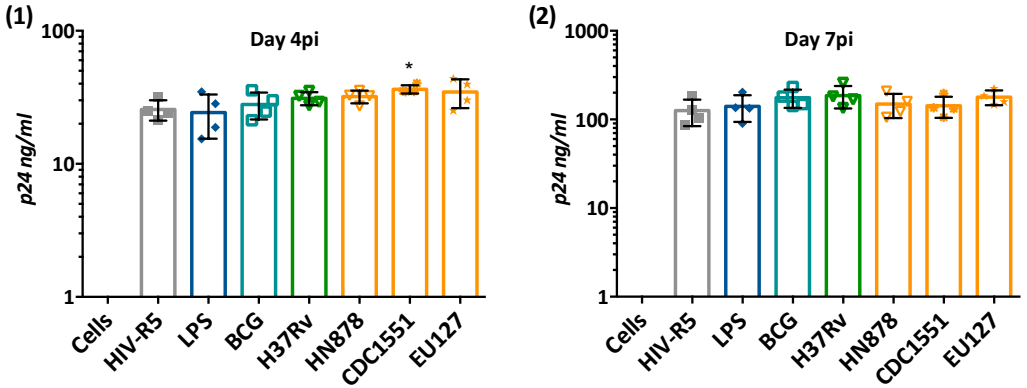

B. DNA quantification

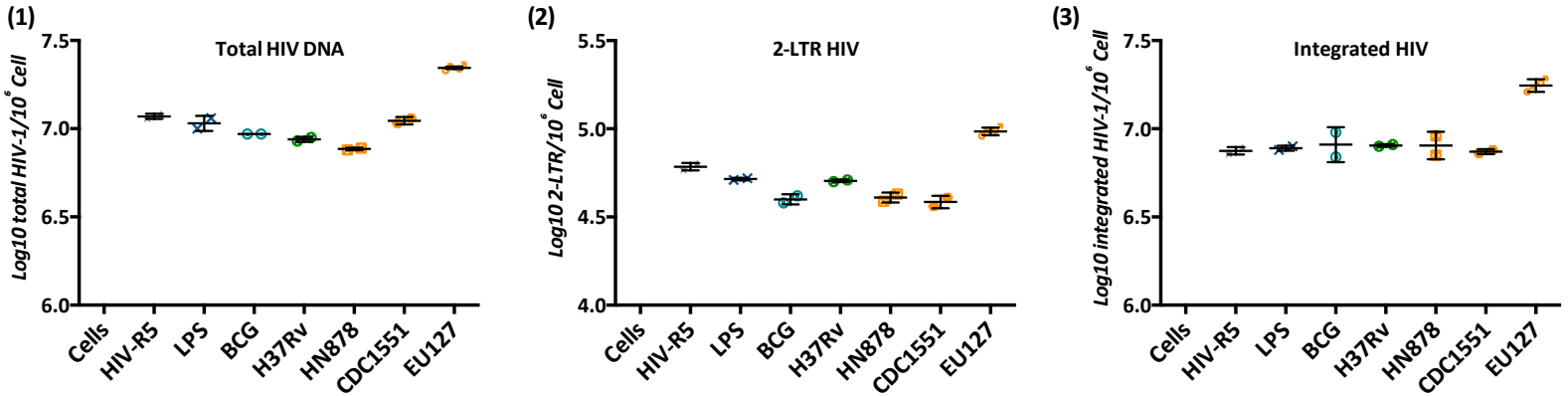

Appendix 18 : Influence of liposomes on HIV-1 R5 trans-infection - liposomes present during capture

$8x10^4$ iDCs were pre-incubated with 100µg of *Mycobacterium* liposomes or 100ng/ml of LPS for 30min. The cells were incubated 30min with 500 $TCID_{50}$/ml BAL-GFP (HIV-1 R5) and washed to be co-cultured with $CD4^+$ enriched T lymphocytes. **A.** Concentration of total HIV-1 capsid p24 was determined in the supernatant by ELISA at day 4 (n=4) **(1)** and day 7 (n=4) **(2)** post-infection. **B.** represents log10 HIV-1 DNA quantification determined by PCR relative to the total number of cells at day 7 post-infection with **(1)** total HIV-1 DNA quantification (n=2), **(2)** number of HIV-1 2-LTR (n=2) and **(3)** number of integrated HIV-1 (n=2). The data shown are from one experiment using cells isolated from one donor.

Appendix 19 : Comparison of HIV DNA copies during HIV-1 trans*-infection*

$8x10^4$ iDCs were pre-incubated with 100µg of Mycobacterium liposomes or 100ng/ml of LPS for 30min. The cells were incubated 30min with 200 $TCID_{50}$/ml LAI-YFP (HIV-1 X4) or 500 $TCID_{50}$/ml BAL-GFP (HIV-1 R5) and washed to be co-cultured with $CD4^+$ enriched T lymphocytes (left panel). Finally, when liposomes are present during capture and transfer (right panel), 40µg of the same *Mycobacterium* liposomes or 100ng/ml of LPS was added per well. At day 7 post-infection, quantifications of HIV-1 DNA were determined by PCR and are represented here in log10 HIV-1 DNA copies relative to the total number of cells with total HIV-1 DNA (black, n=2), HIV-1 2-LTR (blue, n=2) and number of integrated HIV (grey, n=2). The data shown are from one experiment using cells isolated from one donor.

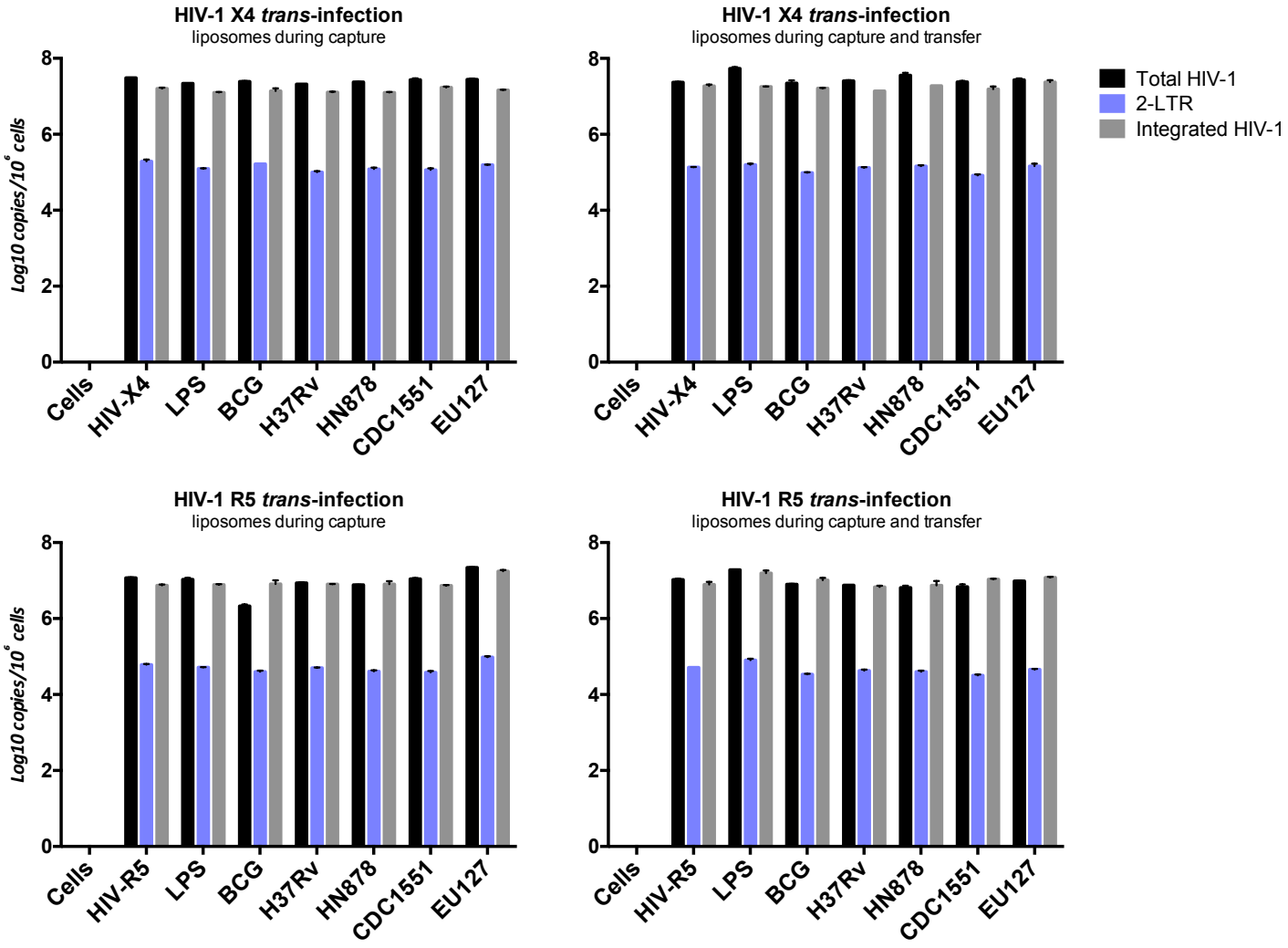

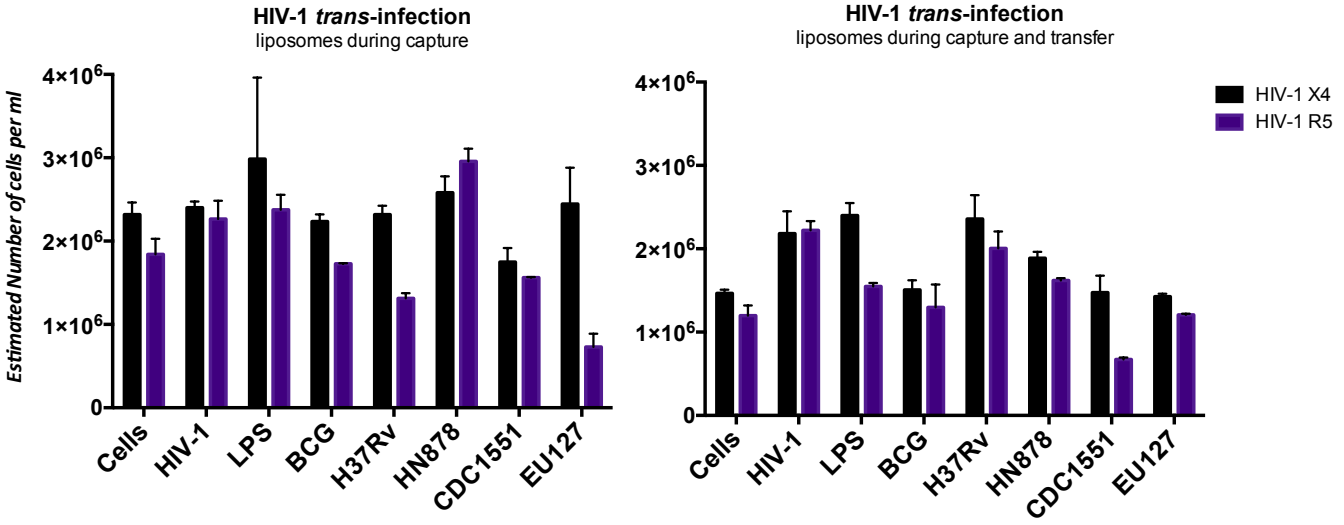

Appendix 20 : Toxicity of* Mycobacterium *liposomes on CD4⁺ T lymphocytes and iDCs during HIV-1* trans*-infection

$8x10^4$ iDCs were pre-incubated with 100µg of Mycobacterium liposomes or 100ng/ml of LPS for 30min. The cells were incubated 30min with 200 $TCID_{50}$/ml LAI-YFP (HIV-1 X4, black) or 500 $TCID_{50}$/ml BAL-GFP (HIV-1 R5, purple) and washed to be co-cultured with $CD4^+$ enriched T lymphocytes (left panel). Finally, when liposomes are present during capture and transfer (right panel), 40µg of the same Mycobacterium liposomes or 100ng/ml of LPS was added per well At day 7 post-infection, the total number of cells were estimated by quantification of CD3 expression by PCR (n=3). The data shown are from one experiment using cells isolated from one donor.

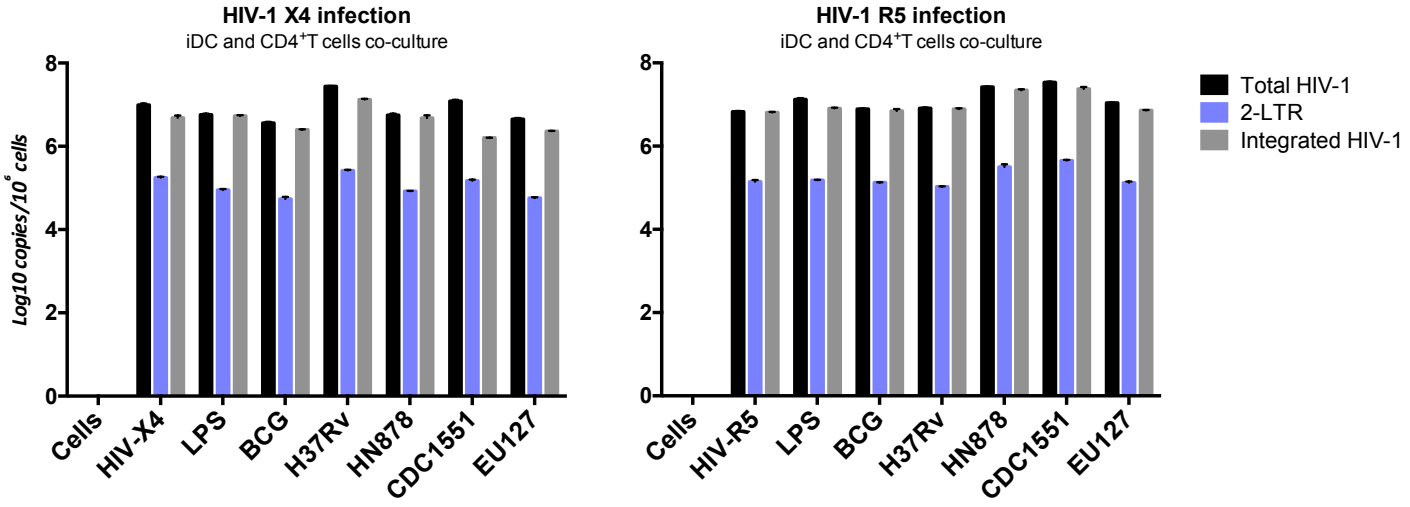

Appendix 21 : Comparison of HIV DNA copies during HIV-1 infections – co-culture iDCs and CD4⁺T cells

In a 96-well plate, $2x10^4$ iDCs were placed in culture with $2x10^5$ $CD4^+$ T lymphocytes and infected with 200 $TCID_{50}$/ml LAI-YFP (HIV-1 X4) or 500 $TCID_{50}$/ml BAL-GFP (HIV-1 R5). 40µg of *Mycobacterium* liposomes or 100ng/ml of LPS was added. At day 7 post-infection, quantifications of HIV-1 DNA were determined by PCR and are represented here in log10 HIV-1 DNA copies relative to the total number of cells with total HIV-1 DNA (black, n=3), HIV-1 2-LTR (blue, n=3) and integrated HIV-1 copies (grey, n=*3).* The data shown are from one experiment using cells isolated from one donor.

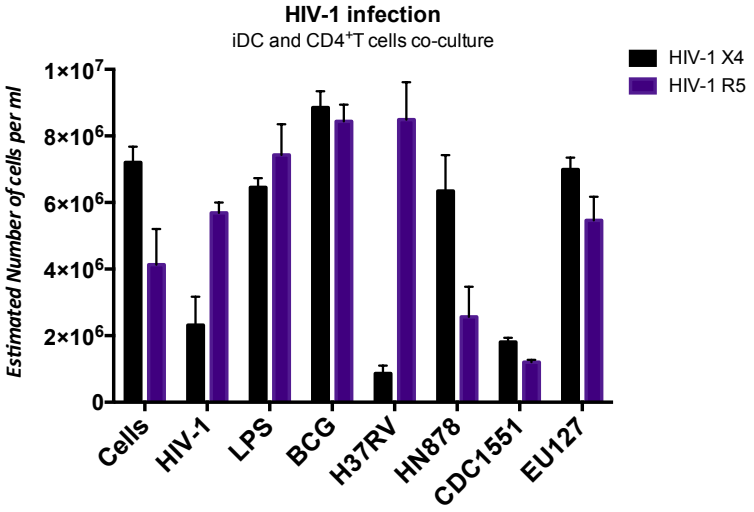

Appendix 22 : Toxicity of Mycobacterium *liposomes on CD4+ T lymphocytes and iDCs during HIV-1 infection – co-culture*

In a 96-well plate, $2x10^4$ iDCs were placed in culture with $2x10^5$ $CD4^+$ T lymphocytes and infected with 200 $TCID_{50}$/ml LAI-YFP (HIV-1 X4, black) or 500 $TCID_{50}$/ml BAL-GFP (HIV-1 R5, purple). 40µg of Mycobacterium liposomes or 100ng/ml of LPS was added. At day 7 post-infection, the total number of cells were estimated by quantification of CD3 expression by PCR (n=3). The data shown are from one experiment using cells isolated from one donor.

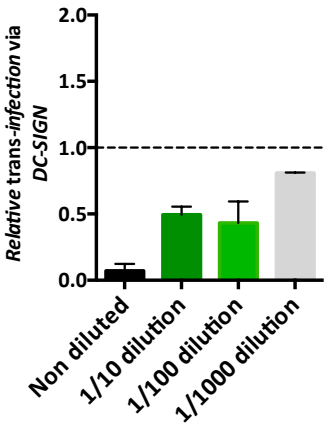

Appendix 23 : Influence of Plasma on HIV-1 X4 trans-*infection* via *DC-SIGN*

50µl of plasma were pre-incubated 30min with $0.5x10^6$ of Raji DC-SIGN. The cells were then incubated 2h with 12.5ng pSG3-LAI HIV-1 X4, and washed after the capture to be finally co-cultured with TZM-bl cells. The luciferase activity was red after 48h. Trans-infection of the virus alone where Raji DC-SIGN were pre-incubated with PBS, was used here as reference. For the data shown, n=2 using plasma isolated from one donor.

Bibliography

Akbarzadeh, A., Rezaei-Sadabady, R., Davaran, S., Joo, S. W., Zarghami, N., Hanifehpour, Y., Samiei, M., Kouhi, M. and Nejati-Koshki, K. (2013) 'Liposome: classification, preparation, and applications.', *Nanoscale research letters*. Nanoscale Research Letters, 8(1), p. 102. doi: 10.1186/1556-276X-8-102.

Akiyama, H., Ramirez, N.-G. P., Gudheti, M. V. and Gummuluru, S. (2015) 'CD169-mediated trafficking of HIV to plasma membrane invaginations in dendritic cells attenuates efficacy of anti-gp120 broadly neutralizing antibodies.', *PLoS pathogens*, 11(3), p. e1004751. doi: 10.1371/journal.ppat.1004751.

Alenquer, M. and Amorim, M. J. (2015) 'Exosome Biogenesis, Regulation, and Function in Viral Infection.', *Viruses*, 7(9), pp. 5066–83. doi: 10.3390/v7092862.

Alizon, S. and Magnus, C. (2012) 'Modelling the course of an HIV infection: insights from ecology and evolution.', *Viruses*, 4(10), pp. 1984–2013. doi: 10.3390/v4101984.

Altfeld, M. and Gale, M. (2015) 'Innate immunity against HIV-1 infection.', *Nature immunology*, 16(6), pp. 554–62. doi: 10.1038/ni.3157.

Alvarez-Jiménez, V. D., Leyva-Paredes, K., García-Martínez, M., Vázquez-Flores, L., García-Paredes, V. G., Campillo-Navarro, M., Romo-Cruz, I., Rosales-García, V. H., Castañeda-Casimiro, J., González-Pozos, S., Hernández, J. M., Wong-Baeza, C., García-Pérez, B. E., Ortiz-Navarrete, V., Estrada-Parra, S., Serafín-López, J., Wong-Baeza, I., Chacón-Salinas, R. and Estrada-García, I. (2018) 'Extracellular Vesicles Released from Mycobacterium tuberculosis-Infected Neutrophils Promote Macrophage Autophagy and Decrease Intracellular Mycobacterial Survival.', *Frontiers in immunology*, 9(1), p. 272. doi: 10.3389/fimmu.2018.00272.

Ambrose, Z. and Aiken, C. (2014) 'HIV-1 uncoating: connection to nuclear entry and regulation by host proteins.', *Virology*, 454–455, pp. 371–9. doi: 10.1016/j.virol.2014.02.004.

Ameixa, C. and Friedland, J. S. (2002) 'Interleukin-8 secretion from Mycobacterium tuberculosis-infected monocytes is regulated by protein tyrosine kinases but not by ERK1/2 or p38 mitogen-activated protein kinases.', *Infection and immunity*, 70(8), pp. 4743–6. doi: 10.1128/IAI.70.8.4743.

Anandaiah, A., Dheda, K., Keane, J., Koziel, H., Moore, D. a J. and Patel, N. R. (2011) 'Novel Developments in the Epidemic of Human Immunodeficiency Virus and Tuberculosis Coinfection', *American Journal of Respiratory and Critical Care Medicine*, 183(8), pp. 987–997. doi: 10.1164/rccm.201008-1246CI.

Andersen, C. S., Agger, E. M., Rosenkrands, I., Gomes, J. M., Bhowruth, V., Gibson, K. J. C., Petersen, R. V., Minnikin, D. E., Besra, G. S. and Andersen, P. (2009) 'A Simple Mycobacterial Monomycolated Glycerol Lipid Has Potent Immunostimulatory Activity', *The Journal of Immunology*, 182(1), pp. 424–432. doi: 10.4049/jimmunol.182.1.424.

Anderson, M. R., Kashanchi, F. and Jacobson, S. (2016) 'Exosomes in Viral Disease.', *Neurotherapeutics : the journal of the American Society for Experimental NeuroTherapeutics*. Neurotherapeutics, 13(3), pp. 535–46. doi: 10.1007/s13311-016-0450-6.

Angala, S. K., Belardinelli, J. M., Huc-Claustre, E., Wheat, W. H. and Jackson, M. (2014) 'The cell envelope glycoconjugates of Mycobacterium tuberculosis.', *Critical reviews in biochemistry and molecular biology*, 49(5), pp. 361–99. doi: 10.3109/10409238.2014.925420.

Arenaccio, C., Anticoli, S., Manfredi, F., Chiozzini, C., Olivetta, E. and Federico, M. (2015) 'Latent HIV-1 is activated by exosomes from cells infected with either replication-competent or defective HIV-1', *Retrovirology*. BioMed Central, 12(1), pp. 1–17. doi: 10.1186/s12977-015-0216-y.

Arenaccio, C., Chiozzini, C., Columba-Cabezas, S., Manfredi, F., Affabris, E., Baur, A. and Federico, M. (2014) 'Exosomes from human immunodeficiency virus type 1 (HIV-1)-infected cells license quiescent CD4+ T lymphocytes to replicate HIV-1 through a Nef- and ADAM17-dependent mechanism.', *Journal of virology*, 88(19), pp. 11529–39. doi: 10.1128/JVI.01712-14.

Arenaccio, C., Chiozzini, C., Columba-Cabezas, S., Manfredi, F. and Federico, M. (2014) 'Cell activation and HIV-1 replication in unstimulated CD4+ T lymphocytes ingesting exosomes from cells expressing defective HIV-1.', *Retrovirology*, 11(1), p. 46. doi: 10.1186/1742-4690-11-46.

Arhel, N., Genovesio, A., Kim, K.-A., Miko, S., Perret, E., Olivo-Marin, J.-C., Shorte, S. and Charneau, P. (2006) 'Quantitative four-dimensional tracking of cytoplasmic and nuclear HIV-1 complexes.', *Nature methods*, 3(10), pp. 817–24. doi: 10.1038/nmeth928.

Astarie-Dequeker, C., Le Guyader, L., Malaga, W., Seaphanh, F.-K., Chalut, C., Lopez, A. and Guilhot, C. (2009) 'Phthiocerol dimycocerosates of M. tuberculosis participate in macrophage invasion by inducing changes in the organization of plasma membrane lipids.', *PLoS pathogens*, 5(2), p. e1000289. doi: 10.1371/journal.ppat.1000289.

Athman, J. J., Sande, O. J., Groft, S. G., Reba, S. M., Nagy, N., Wearsch, P. A., Richardson, E. T., Rojas, R., Boom, W. H., Shukla, S. and Harding, C. V (2017) 'Mycobacterium tuberculosis Membrane Vesicles Inhibit T Cell Activation.', *Journal of immunology (Baltimore, Md. : 1950)*, 198(5), pp. 2028–2037. doi: 10.4049/jimmunol.1601199.

Athman, J. J., Wang, Y., McDonald, D. J., Boom, W. H., Harding, C. V. and Wearsch, P. A. (2015) 'Bacterial Membrane Vesicles Mediate the Release of Mycobacterium tuberculosis Lipoglycans and Lipoproteins from Infected Macrophages.', *Journal of immunology (Baltimore, Md. : 1950)*, 195(3), pp. 1044–53. doi: 10.4049/jimmunol.1402894.

Avril, T., de Tayrac, M., Leberre, C. and Quillien, V. (2009) 'Not all polyriboinosinic-polyribocytidylic acids (Poly I:C) are equivalent for inducing maturation of dendritic cells: implication for alpha-type-1 polarized DCs.', *Journal of immunotherapy (Hagerstown, Md. : 1997)*, 32(4), pp. 353–62. doi: 10.1097/CJI.0b013e31819d29bf.

Bafica, A., Scanga, C. A., Feng, C. G., Leifer, C., Cheever, A. and Sher, A. (2005) 'TLR9 regulates Th1 responses and cooperates with TLR2 in mediating optimal resistance to *Mycobacterium tuberculosis*', *The Journal of Experimental Medicine*, 202(12), pp. 1715–1724. doi: 10.1084/jem.20051782.

Bafica, A., Scanga, C. a, Schito, M. L., Hieny, S. and Sher, A. (2003) 'Cutting Edge: In Vivo Induction of Integrated HIV-1 Expression by Mycobacteria Is Critically Dependent on Toll-Like Receptor 2', *The Journal of Immunology*, 171(3), pp. 1123–1127. doi:

10.4049/jimmunol.171.3.1123.

Bailer, R. T., Lee, B. and Montaner, L. J. (2000) 'IL-13 and TNF-alpha inhibit dual-tropic HIV-1 in primary macrophages by reduction of surface expression of CD4, chemokine receptors CCR5, CXCR4 and post-entry viral gene expression.', *European journal of immunology*, 30(5), pp. 1340–9. doi: 10.1002/(SICI)1521-4141(200005)30:5<1340::AID-IMMU1340>3.0.CO;2-L.

Balboa, L., Romero, M. M., Yokobori, N., Schierloh, P., Geffner, L., Basile, J. I., Musella, R. M., Abbate, E., De La Barrera, S., Sasiain, M. C. and Alemán, M. (2010) 'Mycobacterium tuberculosis impairs dendritic cell response by altering CD1b, DC-SIGN and MR profile', *Immunology and Cell Biology*, 88(7), pp. 716–726. doi: 10.1038/icb.2010.22.

Banaiee, N., Kincaid, E. Z., Buchwald, U., Jacobs, W. R. and Ernst, J. D. (2006) 'Potent Inhibition of Macrophage Responses to IFN- by Live Virulent Mycobacterium tuberculosis Is Independent of Mature Mycobacterial Lipoproteins but Dependent on TLR2', *The Journal of Immunology*, 176(5), pp. 3019–3027. doi: 10.4049/jimmunol.176.5.3019.

Bansal-Mutalik, R. and Nikaido, H. (2014) 'Mycobacterial outer membrane is a lipid bilayer and the inner membrane is unusually rich in diacyl phosphatidylinositol dimannosides', *Proceedings of the National Academy of Sciences*, 111(13), pp. 4958–4963. doi: 10.1073/pnas.1403078111.

Bañuls, A.-L., Sanou, A., Anh, N. T. Van and Godreuil, S. (2015) 'Mycobacterium tuberculosis: ecology and evolution of a human bacterium.', *Journal of medical microbiology*, 64(11), pp. 1261–9. doi: 10.1099/jmm.0.000171.

Baranyai, T., Herczeg, K., Onódi, Z., Voszka, I., Módos, K., Marton, N., Nagy, G., Mäger, I., Wood, M. J., El Andaloussi, S., Pálinkás, Z., Kumar, V., Nagy, P., Kittel, Á., Buzás, E. I., Ferdinandy, P. and Giricz, Z. (2015) 'Isolation of Exosomes from Blood Plasma: Qualitative and Quantitative Comparison of Ultracentrifugation and Size Exclusion Chromatography Methods.', *PloS one*, 10(12), p. e0145686. doi: 10.1371/journal.pone.0145686.

Barnes, P. F., Chatterjee, D., Abrams, J. S., Lu, S., Wang, E., Yamamura, M., Brennan, P. J. and Modlin, R. L. (1992) 'Cytokine production induced by Mycobacterium tuberculosis lipoarabinomannan. Relationship to chemical structure.', *Journal of immunology (Baltimore, Md. : 1950)*, 149(2), pp. 541–7. Available at: http://www.ncbi.nlm.nih.gov/pubmed/1624801.

Barré-Sinoussi, F. (1996) 'HIV as the cause of AIDS.', *Lancet (London, England)*, 348(9019), pp. 31–5. doi: 10.1016/S0140-6736(96)09058-7.

Barré-Sinoussi, F., Chermann, J. C., Rey, F., Nugeyre, M. T., Chamaret, S., Gruest, J., Dauguet, C., Axler-Blin, C., Vézinet-Brun, F., Rouzioux, C., Rozenbaum, W. and Montagnier, L. (1983) 'Isolation of a T-lymphotropic retrovirus from a patient at risk for acquired immune deficiency syndrome (AIDS).', *Science (New York, N.Y.)*, 220(4599), pp. 868–71. Available at: http://www.ncbi.nlm.nih.gov/pubmed/6189183.

Barry, C. E., Lee, R. E., Mdluli, K., Sampson, A. E., Schroeder, B. G., Slayden, R. A. and Yuan, Y. (1998) 'Mycolic acids: structure, biosynthesis and physiological functions.', *Progress in lipid research*, 37(2–3), pp. 143–79. doi: 10.1016/S0163-7827(98)00008-3.

Bates, J. H. and Stead, W. W. (1993) 'The history of tuberculosis as a global epidemic.', *The Medical clinics of North America*. Elsevier, 77(6), pp. 1205–17. doi: 10.1099/jmm.0.000171.

Beatty, W. L., Rhoades, E. R., Ullrich, H.-J., Chatterjee, D., Heuser, J. E. and Russell, D. G. (2000) 'Trafficking and Release of Mycobacterial Lipids from Infected Macrophages', *Traffic*, 1(3), pp. 235–247. doi: 10.1034/j.1600-0854.2000.010306.x.

Vander Beken, S., Al Dulayymi, J. R., Naessens, T., Koza, G., Maza-Iglesias, M., Rowles, R., Theunissen, C., De Medts, J., Lanckacker, E., Baird, M. S. and Grooten, J. (2011) 'Molecular structure of the Mycobacterium tuberculosis virulence factor, mycolic acid, determines the elicited inflammatory pattern.', *European journal of immunology*, 41(2), pp. 450–60. doi: 10.1002/eji.201040719.

Bell, L. C. K. and Noursadeghi, M. (2018) 'Pathogenesis of HIV-1 and Mycobacterium tuberculosis co-infection', *Nature reviews. Microbiology*. Nature Publishing Group, 16(2), pp. 80–90. doi: 10.1038/nrmicro.2017.128.

Bhat, K. H., Chaitanya, C. K., Parveen, N., Varman, R., Ghosh, S. and Mukhopadhyay, S. (2012) 'Proline-Proline-Glutamic Acid (PPE) Protein Rv1168c of Mycobacterium tuberculosis Augments Transcription from HIV-1 Long Terminal Repeat Promoter', *Journal of Biological Chemistry*, 287(20), pp. 16930–16946. doi: 10.1074/jbc.M111.327825.

Bhatnagar, S., Shinagawa, K., Castellino, F. J. and Schorey, J. S. (2007) 'Exosomes released from macrophages infected with intracellular pathogens stimulate a proinflammatory response in vitro and in vivo.', *Blood*, 110(9), pp. 3234–44. doi: 10.1182/blood-2007-03-079152.

Bleul, C. C., Farzan, M., Choe, H., Parolin, C., Clark-Lewis, I., Sodroski, J. and Springer, T. A. (1996) 'The lymphocyte chemoattractant SDF-1 is a ligand for LESTR/fusin and blocks HIV-1 entry.', *Nature*, 382(6594), pp. 829–33. doi: 10.1038/382829a0.

Bobardt, M. D., Saphire, A. C. S., Hung, H.-C., Yu, X., Van der Schueren, B., Zhang, Z., David, G. and Gallay, P. A. (2003) 'Syndecan captures, protects, and transmits HIV to T lymphocytes.', *Immunity*, 18(1), pp. 27–39. doi: 10.1016/S1074-7613(02)00504-6.

Bobrie, A., Colombo, M., Raposo, G. and Théry, C. (2011) 'Exosome secretion: molecular mechanisms and roles in immune responses.', *Traffic (Copenhagen, Denmark)*, 12(12), pp. 1659–68. doi: 10.1111/j.1600-0854.2011.01225.x.

Böing, A. N., Pol, E. Van Der, Grootemaat, A. E., Coumans, F. a., Sturk, A. and Nieuwland, R. (2014) 'Single-step isolation of extracellular vesicles from plasma by size-exclusion chromatography', *International Meeting of the of ISEV Rotterdam*, 3, p. 118. doi: 10.3402/jev.v3.23430.

Boonyarattanakalin, S., Liu, X., Michieletti, M., Lepenies, B. and Seeberger, P. H. (2008) 'Chemical synthesis of all phosphatidylinositol mannoside (PIM) glycans from Mycobacterium tuberculosis.', *Journal of the American Chemical Society*, 130(49), pp. 16791–9. doi: 10.1021/ja806283e.

Briken, V., Porcelli, S. A., Besra, G. S. and Kremer, L. (2004) 'Mycobacterial lipoarabinomannan and related lipoglycans: From biogenesis to modulation of the immune response', *Molecular Microbiology*, 53(2), pp. 391–403. doi: 10.1111/j.1365-2958.2004.04183.x.

Camacho, L. R., Constant, P., Raynaud, C., Laneelle, M. A., Triccas, J. A., Gicquel, B., Daffe, M. and Guilhot, C. (2001) 'Analysis of the phthiocerol dimycocerosate locus of Mycobacterium

tuberculosis. Evidence that this lipid is involved in the cell wall permeability barrier.', *The Journal of biological chemistry*, 276(23), pp. 19845–54. doi: 10.1074/jbc.M100662200.

Cambier, C. J., Takaki, K. K., Larson, R. P., Hernandez, R. E., Tobin, D. M., Urdahl, K. B., Cosma, C. L. and Ramakrishnan, L. (2014) 'Mycobacteria manipulate macrophage recruitment through coordinated use of membrane lipids.', *Nature*. Nature Publishing Group, 505(7482), pp. 218–22. doi: 10.1038/nature12799.

Cameron, P. U., Forsum, U., Teppler, H., Granelli-Piperno, A. and Steinman, R. M. (1992) 'During HIV-1 infection most blood dendritic cells are not productively infected and can induce allogeneic CD4+ T cells clonal expansion.', *Clinical and experimental immunology*, 88(2), pp. 226–36. doi: 10.1111/j.1365-2249.1992.tb03066.x.

Cameron, P. U., Freudenthal, P. S., Barker, J. M., Gezelter, S., Inaba, K. and Steinman, R. M. (1992) 'Dendritic cells exposed to human immunodeficiency virus type-1 transmit a vigorous cytopathic infection to CD4+ T cells.', *Science (New York, N.Y.)*, 257(5068), pp. 383–7. doi: 10.1126/science.1352913.

Cameron, P. U., Pope, M., Gezelter, S. and Steinman, R. M. (1994) 'Infection and apoptotic cell death of CD4+ T cells during an immune response to HIV-1-pulsed dendritic cells.', *AIDS research and human retroviruses*, 10(1), pp. 61–71. doi: 10.1089/aid.1994.10.61.

Campbell, E. M. and Hope, T. J. (2015) 'HIV-1 capsid: the multifaceted key player in HIV-1 infection.', *Nature reviews. Microbiology*, 13(8), pp. 471–83. doi: 10.1038/nrmicro3503.

Canaday, D. H., Wu, M., Lu, S., Aung, H., Peters, P., Baseke, J., Mackay, W., Mayanja-Kizza, H. and Toossi, Z. (2009) 'Induction of HIV Type 1 Expression Correlates with T Cell Responsiveness to Mycobacteria in Patients Coinfected with HIV Type 1 and Mycobacterium tuberculosis', *AIDS Research and Human Retroviruses*, 25(2), pp. 213–216. doi: 10.1089/aid.2008.0182.

Cantin, R., Diou, J., Bélanger, D., Tremblay, A. M. and Gilbert, C. (2008) 'Discrimination between exosomes and HIV-1: purification of both vesicles from cell-free supernatants.', *Journal of immunological methods*, 338(1–2), pp. 21–30. doi: 10.1016/j.jim.2008.07.007.

Cardona, P.-J. (2006) 'RUTI: A new chance to shorten the treatment of latent tuberculosis infection', *Tuberculosis*, 86(3–4), pp. 273–289. doi: 10.1016/j.tube.2006.01.024.

Carmona, J., Cruz, A., Moreira-Teixeira, L., Sousa, C., Sousa, J., Osorio, N. S., Saraiva, A. L., Svenson, S., Kallenius, G., Pedrosa, J., Rodrigues, F., Castro, A. G. and Saraiva, M. (2013) 'Mycobacterium tuberculosis Strains Are Differentially Recognized by TLRs with an Impact on the Immune Response', *PLoS ONE*, 8(6), pp. 1–10. doi: 10.1371/journal.pone.0067277.

Carmona, R., Pérez-Alvarez, L., Muñoz, M., Casado, G., Delgado, E., Sierra, M., Thomson, M., Vega, Y., Vázquez de Parga, E., Contreras, G., Medrano, L. and Nájera, R. (2005) 'Natural resistance-associated mutations to Enfuvirtide (T20) and polymorphisms in the gp41 region of different HIV-1 genetic forms from T20 naive patients.', *Journal of clinical virology : the official publication of the Pan American Society for Clinical Virology*, 32(3), pp. 248–53. doi: 10.1016/j.jcv.2004.11.009.

de Carvalho, J. V, de Castro, R. O., da Silva, E. Z. M., Silveira, P. P., da Silva-Januário, M. E., Arruda, E., Jamur, M. C., Oliver, C., Aguiar, R. S. and DaSilva, L. L. P. (2014) 'Nef neutralizes the ability of exosomes from CD4+ T cells to act as decoys during HIV-1 infection.', *PloS one*,

9(11), p. e113691. doi: 10.1371/journal.pone.0113691.

Chahar, H. S., Bao, X. and Casola, A. (2015) 'Exosomes and Their Role in the Life Cycle and Pathogenesis of RNA Viruses.', *Viruses*, 7(6), pp. 3204–25. doi: 10.3390/v7062770.

Chang, C. C., Crane, M., Zhou, J., Mina, M., Post, J. J., Cameron, B. a., Lloyd, A. R., Jaworowski, A., French, M. a. and Lewin, S. R. (2013) 'HIV and co-infections', *Immunological Reviews*, 254(1), pp. 114–142. doi: 10.1111/imr.12063.

Cheruiyot, C., Pataki, Z., Ramratnam, B. and Li, M. (2018) 'Proteomic Analysis of Exosomes and Its Application in HIV-1 Infection', *Proteomics. Clinical applications*, 1700142, p. 1700142. doi: 10.1002/prca.201700142.

Chetty, S., Porichis, F., Govender, P., Zupkosky, J., Ghebremichael, M., Pillay, M., Walker, B. D., Ndung'u, T., Kaufmann, D. E. and Kasprowicz, V. O. (2014) 'Tuberculosis distorts the inhibitory impact of interleukin-10 in HIV infection.', *AIDS (London, England)*, 28(18), pp. 2671–6. doi: 10.1097/QAD.0000000000000437.

Clavel, F., Guétard, D., Brun-Vézinet, F., Chamaret, S., Rey, M. A., Santos-Ferreira, M. O., Laurent, A. G., Dauguet, C., Katlama, C. and Rouzioux, C. (1986) 'Isolation of a new human retrovirus from West African patients with AIDS.', *Science (New York, N.Y.)*, 233(4761), pp. 343–6. Available at: http://www.ncbi.nlm.nih.gov/pubmed/2425430.

Clay, H., Volkman, H. E. and Ramakrishnan, L. (2008) 'Tumor Necrosis Factor Signaling Mediates Resistance to Mycobacteria by Inhibiting Bacterial Growth and Macrophage Death', *Immunity*, 29(2), pp. 283–294. doi: 10.1016/j.immuni.2008.06.011.

De Clercq, E. (2013) 'The nucleoside reverse transcriptase inhibitors, nonnucleoside reverse transcriptase inhibitors, and protease inhibitors in the treatment of HIV infections (AIDS).', *Advances in pharmacology (San Diego, Calif.)*. 1st edn. Copyright © 2013 Elsevier Inc. All rights reserved., 67, pp. 317–58. doi: 10.1016/B978-0-12-405880-4.00009-3.

Cocchi, F., DeVico, A. L., Garzino-Demo, A., Arya, S. K., Gallo, R. C. and Lusso, P. (1995) 'Identification of RANTES, MIP-1 alpha, and MIP-1 beta as the major HIV-suppressive factors produced by CD8+ T cells.', *Science (New York, N.Y.)*, 270(5243), pp. 1811–5. Available at: http://www.ncbi.nlm.nih.gov/pubmed/8525373.

Colombo, M., Raposo, G. and Théry, C. (2014) 'Biogenesis, Secretion, and Intercellular Interactions of Exosomes and Other Extracellular Vesicles', *Annual Review of Cell and Developmental Biology*, 30(1), pp. 255–289. doi: 10.1146/annurev-cellbio-101512-122326.

Columba Cabezas, S. and Federico, M. (2013) 'Sequences within RNA coding for HIV-1 Gag p17 are efficiently targeted to exosomes.', *Cellular microbiology*, 15(3), pp. 412–29. doi: 10.1111/cmi.12046.

Converse, S. E., Mougous, J. D., Leavell, M. D., Leary, J. A., Bertozzi, C. R. and Cox, J. S. (2003) 'MmpL8 is required for sulfolipid-1 biosynthesis and Mycobacterium tuberculosis virulence.', *Proceedings of the National Academy of Sciences of the United States of America*, 100(10), pp. 6121–6. doi: 10.1073/pnas.1030024100.

Cox, J. S., Chen, B., McNeil, M. and Jacobs, W. R. (1999) 'Complex lipid determines tissue-specific replication of Mycobacterium tuberculosis in mice.', *Nature*, 402(6757), pp. 79–83. doi: 10.1038/47042.

Craigie, R. and Bushman, F. D. (2012) 'HIV DNA integration.', *Cold Spring Harbor perspectives in medicine*, 2(7), p. a006890. doi: 10.1101/cshperspect.a006890.

Creery, D., Weiss, W., Graziani-Bowering, G., Kumar, R., Aziz, Z., Angel, J. B. and Kumar, A. (2006) 'Differential regulation of CXCR4 and CCR5 expression by interleukin (IL)-4 and IL-13 is associated with inhibition of chemotaxis and human immunodeficiency Virus (HIV) type 1 replication but not HIV entry into human monocytes.', *Viral immunology*, 19(3), pp. 409–23. doi: 10.1089/vim.2006.19.409.

Cywes, C., Hoppe, H. C., Daffé, M. and Ehlers, M. R. (1997) 'Nonopsonic binding of Mycobacterium tuberculosis to complement receptor type 3 is mediated by capsular polysaccharides and is strain dependent.', *Infection and immunity*, 65(10), pp. 4258–66. Available at: http://www.ncbi.nlm.nih.gov/pubmed/9317035.

Daffé, M., Crick, D. C. and Jackson, M. (2014) 'Genetics of Capsular Polysaccharides and Cell Envelope (Glyco)lipids.', *Microbiology spectrum*, 2(4), pp. MGM2-0021-2013. doi: 10.1128/microbiolspec.MGM2-0021-2013.

Daffé, M., Lacave, C., Lanéelle, M. A., Gillois, M. and Lanéelle, G. (1988) 'Polyphthienoyl trehalose, glycolipids specific for virulent strains of the tubercle bacillus.', *European journal of biochemistry*, 172(3), pp. 579–84. doi: 10.1111/j.1432-1033.1988.tb13928.x.

Daffé, M. and Laneelle, M. a (1988) 'Distribution of phthiocerol diester, phenolic mycosides and related compounds in mycobacteria.', *Journal of general microbiology*, 134(7), pp. 2049–55. doi: 10.1099/00221287-134-7-2049.

Daniel, T. M. (2006) 'The history of tuberculosis.', *Respiratory medicine*, 100(11), pp. 1862–70. doi: 10.1016/j.rmed.2006.08.006.

Davis, J. M. and Ramakrishnan, L. (2009) 'The Role of the Granuloma in Expansion and Dissemination of Early Tuberculous Infection', *Cell*. Elsevier Inc., 136(1), pp. 37–49. doi: 10.1016/j.cell.2008.11.014.

Delabranche, X., Berger, A., Boisramé-Helms, J. and Meziani, F. (2012) 'Microparticles and infectious diseases', *Médecine et Maladies Infectieuses*. Elsevier Masson SAS, 42(8), pp. 335–343. doi: 10.1016/j.medmal.2012.05.011.

Delogu, G., Sali, M. and Fadda, G. (2013) 'The biology of mycobacterium tuberculosis infection.', *Mediterranean journal of hematology and infectious diseases*, 5(1), p. e2013070. doi: 10.4084/MJHID.2013.070.

Diedrich, C. R. and Flynn, J. L. (2011) 'HIV-1/mycobacterium tuberculosis coinfection immunology: how does HIV-1 exacerbate tuberculosis?', *Infection and immunity*, 79(4), pp. 1407–17. doi: 10.1128/IAI.01126-10.

Dinadayala, P., Lemassu, A., Granovski, P., Cérantola, S., Winter, N. and Daffé, M. (2004) 'Revisiting the structure of the anti-neoplastic glucans of Mycobacterium bovis Bacille Calmette-Guerin. Structural analysis of the extracellular and boiling water extract-derived glucans of the vaccine substrains.', *The Journal of biological chemistry*, 279(13), pp. 12369–78. doi: 10.1074/jbc.M308908200.

Divangahi, M., Mostowy, S., Coulombe, F., Kozak, R., Guillot, L., Veyrier, F., Kobayashi, K. S., Flavell, R. A., Gros, P. and Behr, M. A. (2008) 'NOD2-Deficient Mice Have Impaired Resistance

to Mycobacterium tuberculosis Infection through Defective Innate and Adaptive Immunity', *The Journal of Immunology*, 181(10), pp. 7157–7165. doi: 10.4049/jimmunol.181.10.7157.

Dkhar, H. K., Nanduri, R., Mahajan, S., Dave, S., Saini, A., Somavarapu, A. K., Arora, A., Parkesh, R., Thakur, K. G., Mayilraj, S. and Gupta, P. (2014) 'Mycobacterium tuberculosis Keto-Mycolic Acid and Macrophage Nuclear Receptor TR4 Modulate Foamy Biogenesis in Granulomas: A Case of a Heterologous and Noncanonical Ligand-Receptor Pair', *The Journal of Immunology*, 193(1), pp. 295–305. doi: 10.4049/jimmunol.1400092.

Dobson G, Minnikin D.E., Minnikin S.M., Parlett M., Goodfellow M., Ridell M. et al. (1985) Systematic analysis of complex mycobacterial lipids. Chemical Methods in Bacterial Systematics. London: Academic Press. pp. 237–265

Domenech, P., Reed, M. B., Dowd, C. S., Manca, C., Kaplan, G. and Barry, C. E. (2004) 'The role of MmpL8 in sulfatide biogenesis and virulence of Mycobacterium tuberculosis.', *The Journal of biological chemistry*, 279(20), pp. 21257–65. doi: 10.1074/jbc.M400324200.

Dong, C., Janas, A. M., Wang, J.-H., Olson, W. J. and Wu, L. (2007) 'Characterization of human immunodeficiency virus type 1 replication in immature and mature dendritic cells reveals dissociable cis- and trans-infection.', *Journal of virology*, 81(20), pp. 11352–62. doi: 10.1128/JVI.01081-07.

van Dongen, H. M., Masoumi, N., Witwer, K. W. and Pegtel, D. M. (2016) 'Extracellular Vesicles Exploit Viral Entry Routes for Cargo Delivery.', *Microbiology and molecular biology reviews : MMBR*, 80(2), pp. 369–86. doi: 10.1128/MMBR.00063-15.

Dorosko, S. M. and Connor, R. I. (2010) 'Primary human mammary epithelial cells endocytose HIV-1 and facilitate viral infection of CD4+ T lymphocytes', *J Virol*, 84(20), pp. 10533–10542. doi: 10.1128/JVI.01263-10.

Dorr, P., Westby, M., Dobbs, S., Griffin, P., Irvine, B., Macartney, M., Mori, J., Rickett, G., Smith-Burchnell, C., Napier, C., Webster, R., Armour, D., Price, D., Stammen, B., Wood, A. and Perros, M. (2005) 'Maraviroc (UK-427,857), a potent, orally bioavailable, and selective small-molecule inhibitor of chemokine receptor CCR5 with broad-spectrum anti-human immunodeficiency virus type 1 activity.', *Antimicrobial agents and chemotherapy*, 49(11), pp. 4721–32. doi: 10.1128/AAC.49.11.4721-4732.2005.

Le Douce, V., Janossy, A., Hallay, H., Ali, S., Riclet, R., Rohr, O. and Schwartz, C. (2012) 'Achieving a cure for HIV infection: do we have reasons to be optimistic?', *The Journal of antimicrobial chemotherapy*, 67(5), pp. 1063–74. doi: 10.1093/jac/dkr599.

Doz, E., Rose, S., Court, N., Front, S., Vasseur, V., Charron, S., Gilleron, M., Puzo, G., Fremaux, I., Delneste, Y., Erard, F., Ryffel, B., Martin, O. R. and Quesniaux, V. F. J. (2009) 'Mycobacterial phosphatidylinositol mannosides negatively regulate host toll-like receptor 4, MyD88-dependent proinflammatory cytokines, and TRIF-dependent co-stimulatory molecule expression', *Journal of Biological Chemistry*, 284(35), pp. 23187–23196. doi: 10.1074/jbc.M109.037846.

Doz, E., Rose, S., Nigou, J., Gilleron, M., Puzo, G., Erard, F., Ryffel, B. and Quesniaux, V. F. J. (2007) 'Acylation determines the toll-like receptor (TLR)-dependent positive versus TLR2-, mannose receptor-, and SIGNR1-independent negative regulation of pro-inflammatory cytokines by mycobacterial lipomannan.', *The Journal of biological chemistry*, 282(36), pp. 26014–25. doi: 10.1074/jbc.M702690200.

Driessen, N. N., Ummels, R., Maaskant, J. J., Gurcha, S. S., Besra, G. S., Ainge, G. D., Larsen, D. S., Painter, G. F., Vandenbroucke-Grauls, C. M. J. E., Geurtsen, J. and Appelmelk, B. J. (2009) 'Role of Phosphatidylinositol Mannosides in the Interaction between Mycobacteria and DC-SIGN', *Infection and Immunity*, 77(10), pp. 4538–4547. doi: 10.1128/IAI.01256-08.

Dubnau, E., Chan, J., Raynaud, C., Mohan, V. P., Lanéelle, M. A., Yu, K., Quémard, A., Smith, I. and Daffé, M. (2000) 'Oxygenated mycolic acids are necessary for virulence of Mycobacterium tuberculosis in mice.', *Molecular microbiology*, 36(3), pp. 630–7. doi: 10.1046/j.1365-2958.2000.01882.x.

Ehlers, M. R. W. and Daffé, M. (1998) 'Interactions between Mycobacterium tuberculosis and host cells: Are mycobacterial sugars the key?', *Trends in Microbiology*, 6(8), pp. 328–335. doi: 10.1016/S0966-842X(98)01301-8.

Ehlers, S. (2010) 'DC-SIGN and mannosylated surface structures of Mycobacterium tuberculosis: a deceptive liaison', *European Journal of Cell Biology*. Elsevier, 89(1), pp. 95–101. doi: 10.1016/j.ejcb.2009.10.004.

Equils, O., Schito, M. L., Karahashi, H., Madak, Z., Yarali, A., Michelsen, K. S., Sher, A. and Arditi, M. (2003) 'Toll-Like Receptor 2 (TLR2) and TLR9 Signaling Results in HIV-Long Terminal Repeat Trans-Activation and HIV Replication in HIV-1 Transgenic Mouse Spleen Cells: Implications of Simultaneous Activation of TLRs on HIV Replication', *The Journal of Immunology*, 170(10), pp. 5159–5164. doi: 10.4049/jimmunol.170.10.5159.

Esser, M. T., Graham, D. R., Coren, L. V, Trubey, C. M., Bess, J. W., Arthur, L. O., Ott, D. E. and Lifson, J. D. (2001) 'Differential incorporation of CD45, CD80 (B7-1), CD86 (B7-2), and major histocompatibility complex class I and II molecules into human immunodeficiency virus type 1 virions and microvesicles: implications for viral pathogenesis and immune regulation.', *Journal of virology*, 75(13), pp. 6173–82. doi: 10.1128/JVI.75.13.6173-6182.2001.

Falvo, J. V., Ranjbar, S., Jasenosky, L. D. and Goldfeld, A. E. (2011) 'Arc of a vicious circle: pathways activated by Mycobacterium tuberculosis that target the HIV-1 long terminal repeat.', *American journal of respiratory cell and molecular biology*, 45(6), pp. 1116–24. doi: 10.1165/rcmb.2011-0186TR.

Fang, Y., Wu, N., Gan, X., Yan, W., Morrell, J. C. and Gould, S. J. (2007) 'Higher-order oligomerization targets plasma membrane proteins and HIV Gag to exosomes', *PLoS Biology*, 5(6), pp. 1267–1283. doi: 10.1371/journal.pbio.0050158.

Ferwerda, G., Girardin, S. E., Kullberg, B. J., Le Bourhis, L., De Jong, D. J., Langenberg, D. M. L., Van Crevel, R., Adema, G. J., Ottenhoff, T. H. M., Van Der Meer, J. W. M. and Netea, M. G. (2005) 'NOD2 and toll-like receptors are nonredundant recognition systems of Mycobacterium tuberculosis', *PLoS Pathogens*, 1(3), pp. 0279–0285. doi: 10.1371/journal.ppat.0010034.

Fischer, K., Chatterjee, D., Torrelles, J., Brennan, P. J., Kaufmann, S. H. and Schaible, U. E. (2001) 'Mycobacterial lysocardiolipin is exported from phagosomes upon cleavage of cardiolipin by a macrophage-derived lysosomal phospholipase A2.', *Journal of immunology (Baltimore, Md. : 1950)*, 167(4), pp. 2187–92. doi: 10.4049/jimmunol.167.4.2187.

Flynn, J. L., Goldstein, M. M., Chan, J., Triebold, K. J., Pfeffer, K., Lowenstein, C. J., Schrelber, R., Mak, T. W. and Bloom, B. R. (1995) 'Tumor necrosis factor-α is required in the protective immune response against mycobacterium tuberculosis in mice', *Immunity*, 2(6), pp. 561–572.

doi: 10.1016/1074-7613(95)90001-2.

Foli, A., Saville, M. W., May, L. T., Webb, D. S. and Yarchoan, R. (1997) 'Effects of human immunodeficiency virus and colony-stimulating factors on the production of interleukin 6 and tumor necrosis factor alpha by monocyte/macrophages.', *AIDS research and human retroviruses*, 13(10), pp. 829–39. doi: 10.1089/aid.1997.13.829.

Folks, T. M., Clouse, K. A., Justement, J., Rabson, A., Duh, E., Kehrl, J. H. and Fauci, A. S. (1989) 'Tumor necrosis factor alpha induces expression of human immunodeficiency virus in a chronically infected T-cell clone.', *Proceedings of the National Academy of Sciences of the United States of America*, 86(7), pp. 2365–8. doi: 10.1073/pnas.86.7.2365.

Frank, I., Santos, J. J., Mehlhop, E., Villamide-Herrera, L., Santisteban, C., Gettie, A., Ignatius, R., Lifson, J. D. and Pope, M. (2003) 'Presentation of exogenous whole inactivated simian immunodeficiency virus by mature dendritic cells induces CD4+ and CD8+ T-cell responses.', *Journal of acquired immune deficiency syndromes (1999)*, 34(1), pp. 7–19. Available at: http://www.ncbi.nlm.nih.gov/pubmed/14501788.

Frankel, A. D. and Young, J. A. (1998) 'HIV-1: fifteen proteins and an RNA.', *Annual review of biochemistry*, 67(1), pp. 1–25. doi: 10.1146/annurev.biochem.67.1.1.

Fratti, R. A., Backer, J. M., Gruenberg, J., Corvera, S. and Deretic, V. (2001) 'Role of phosphatidylinositol 3-kinase and Rab5 effectors in phagosomal biogenesis and mycobacterial phagosome maturation arrest.', *The Journal of cell biology*, 154(3), pp. 631–44. doi: 10.1083/jcb.200106049.

Fratti, R. A., Chua, J., Vergne, I. and Deretic, V. (2003) 'Mycobacterium tuberculosis glycosylated phosphatidylinositol causes phagosome maturation arrest.', *Proceedings of the National Academy of Sciences of the United States of America*, 100(9), pp. 5437–42. doi: 10.1073/pnas.0737613100.

Freed, E. O. (2015) 'HIV-1 assembly, release and maturation.', *Nature reviews. Microbiology*. Nature Publishing Group, 13(8), pp. 484–96. doi: 10.1038/nrmicro3490.

Fukuda, T., Matsumura, T., Ato, M., Hamasaki, M., Nishiuchi, Y., Murakami, Y., Maeda, Y., Yoshimori, T., Matsumoto, S., Kobayashi, K., Kinoshita, T. and Morita, Y. S. (2013) 'Critical roles for lipomannan and lipoarabinomannan in cell wall integrity of mycobacteria and pathogenesis of tuberculosis.', *mBio*, 4(1), pp. e00472-12. doi: 10.1128/mBio.00472-12.

Ganser-Pornillos, B. K., Yeager, M. and Pornillos, O. (2012) 'Assembly and architecture of HIV.', *Advances in experimental medicine and biology*, 726, pp. 441–65. doi: 10.1007/978-1-4614-0980-9_20.

Ganser-Pornillos, B. K., Yeager, M. and Sundquist, W. I. (2008) 'The structural biology of HIV assembly.', *Current opinion in structural biology*, 18(2), pp. 203–17. doi: 10.1016/j.sbi.2008.02.001.

Gao, F., Bailes, E., Robertson, D. L., Chen, Y., Rodenburg, C. M., Michael, S. F., Cummins, L. B., Arthur, L. O., Peeters, M., Shaw, G. M., Sharp, P. M. and Hahn, B. H. (1999) 'Origin of HIV-1 in the chimpanzee Pan troglodytes troglodytes.', *Nature*, 397(6718), pp. 436–41. doi: 10.1038/17130.

Garcia, E., Pion, M., Pelchen-Matthews, A., Collinson, L., Arrighi, J. F., Blot, G., Leuba, F.,

Escola, J. M., Demaurex, N., Marsh, M. and Piguet, V. (2005) 'HIV-1 trafficking to the dendritic cell-T-cell infectious synapse uses a pathway of tetraspanin sorting to the immunological synapse', *Traffic*, 6(6), pp. 488–501. doi: 10.1111/j.1600-0854.2005.00293.x.

Garrait, V., Cadranel, J., Esvant, H., Herry, I., Morinet, P., Mayaud, C. and Israël-Biet, D. (1997) 'Tuberculosis generates a microenvironment enhancing the productive infection of local lymphocytes by HIV.', *Journal of immunology (Baltimore, Md. : 1950)*, 159(6), pp. 2824–2830.

Geijtenbeek, T. B. ., Kwon, D. S., Torensma, R., van Vliet, S. J., van Duijnhoven, G. C. ., Middel, J., Cornelissen, I. L. M. H. ., Nottet, H. S. L. ., KewalRamani, V. N., Littman, D. R., Figdor, C. G. and van Kooyk, Y. (2000) 'DC-SIGN, a dendritic cell-specific HIV-1-binding protein that enhances trans-infection of T cells.', *Cell*, 100(5), pp. 587–597. doi: 10.1016/S0092-8674(00)80694-7.

Geijtenbeek, T. B. H., Van Vliet, S. J., Koppel, E. A., Sanchez-Hernandez, M., Vandenbroucke-Grauls, C. M. J. E., Appelmelk, B. and Van Kooyk, Y. (2003) 'Mycobacteria target DC-SIGN to suppress dendritic cell function.', *The Journal of experimental medicine*, 197(1), pp. 7–17. doi: 10.1084/jem.20021229.

Geisel, R. E., Sakamoto, K., Russell, D. G. and Rhoades, E. R. (2005) 'In vivo activity of released cell wall lipids of Mycobacterium bovis bacillus Calmette-Guérin is due principally to trehalose mycolates.', *Journal of immunology (Baltimore, Md. : 1950)*, 174(8), pp. 5007–15. doi: 10.4049/jimmunol.174.8.5007.

Geldmacher, C., Ngwenyama, N., Schuetz, A., Petrovas, C., Reither, K., Heeregrave, E. J., Casazza, J. P., Ambrozak, D. R., Louder, M., Ampofo, W., Pollakis, G., Hill, B., Sanga, E., Saathoff, E., Maboko, L., Roederer, M., Paxton, W. a, Hoelscher, M. and Koup, R. a (2010) 'Preferential infection and depletion of Mycobacterium tuberculosis-specific CD4 T cells after HIV-1 infection', *Journal of Experimental Medicine*, 207(13), pp. 2869–2881. doi: 10.1084/jem.20100090.

Geurtsen, J., Chedammi, S., Mesters, J., Cot, M., Driessen, N. N., Sambou, T., Kakutani, R., Ummels, R., Maaskant, J., Takata, H., Baba, O., Terashima, T., Bovin, N., Vandenbroucke-Grauls, C. M. J. E., Nigou, J., Puzo, G., Lemassu, A., Daffe, M. and Appelmelk, B. J. (2009) 'Identification of Mycobacterial -Glucan As a Novel Ligand for DC-SIGN: Involvement of Mycobacterial Capsular Polysaccharides in Host Immune Modulation', *The Journal of Immunology*, 183(8), pp. 5221–5231. doi: 10.4049/jimmunol.0900768.

Gilleron, M., Nigou, J., Nicolle, D., Quesniaux, V. and Puzo, G. (2006) 'The acylation state of mycobacterial lipomannans modulates innate immunity response through toll-like receptor 2', *Chemistry and Biology*, 13(1), pp. 39–47. doi: 10.1016/j.chembiol.2005.10.013.

Gilmore, S. A., Schelle, M. W., Holsclaw, C. M., Leigh, C. D., Jain, M., Cox, J. S., Leary, J. A. and Bertozzi, C. R. (2012) 'Sulfolipid-1 biosynthesis restricts Mycobacterium tuberculosis growth in human macrophages.', *ACS chemical biology*, 7(5), pp. 863–70. doi: 10.1021/cb200311s.

Giri, P. K. and Schorey, J. S. (2008) 'Exosomes derived from M. Bovis BCG infected macrophages activate antigen-specific CD4+ and CD8+ T cells in vitro and in vivo.', *PloS one*. Edited by W. Bishai, 3(6), p. e2461. doi: 10.1371/journal.pone.0002461.

Goila-Gaur, R. and Strebel, K. (2008) 'HIV-1 Vif, APOBEC, and intrinsic immunity.', *Retrovirology*, 5, p. 51. doi: 10.1186/1742-4690-5-51.

Goldstone, D. C., Ennis-Adeniran, V., Hedden, J. J., Groom, H. C. T., Rice, G. I., Christodoulou, E., Walker, P. A., Kelly, G., Haire, L. F., Yap, M. W., De Carvalho, L. P. S., Stoye, J. P., Crow, Y. J., Taylor, I. A. and Webb, M. (2011) 'HIV-1 restriction factor SAMHD1 is a deoxynucleoside triphosphate triphosphohydrolase', *Nature*. Nature Publishing Group, 480(7377), pp. 379–382. doi: 10.1038/nature10623.

Goletti, D., Carrara, S., Vincenti, D., Giacomini, E., Fattorini, L., Garbuglia, A. R., Capobianchi, M. R., Alonzi, T., Fimia, G. M., Federico, M., Poli, G. and Coccia, E. (2004) 'Inhibition of HIV-1 replication in monocyte-derived macrophages by Mycobacterium tuberculosis.', *The Journal of infectious diseases*, 189(4), pp. 624–633. doi: 10.1086/381554.

Goletti, D., Weissman, D., Jackson, R. W., Collins, F., Kinter, A. and Fauci, a S. (1998) 'The in vitro induction of human immunodeficiency virus (HIV) replication in purified protein derivative-positive HIV-infected persons by recall antigen response to Mycobacterium tuberculosis is the result of a balance of the effects of endogenous interleu', *The Journal of infectious diseases*, 177(5), pp. 1332–1338.

Goletti, D., Weissman, D., Jackson, R. W., Graham, N. M., Vlahov, D., Klein, R. S., Munsiff, S. S., Ortona, L., Cauda, R. and Fauci, A. S. (1996) 'Effect of Mycobacterium tuberculosis on HIV replication. Role of immune activation.', *Journal of immunology (Baltimore, Md. : 1950)*, 157(3), pp. 1271–1278. doi: 10.5402/2011/810565.

González, M. E. (2015) 'Vpu Protein: The Viroporin Encoded by HIV-1.', *Viruses*, 7(8), pp. 4352–68. doi: 10.3390/v7082824.

González, M. E. (2017) 'The HIV-1 Vpr Protein: A Multifaceted Target for Therapeutic Intervention.', *International journal of molecular sciences*, 18(1), pp. 1–21. doi: 10.3390/ijms18010126.

Goren, M. B., Brokl, O. and Schaefer, W. B. (1974) 'Lipids of putative relevance to virulence in Mycobacterium tuberculosis: phthiocerol dimycocerosate and the attenuation indicator lipid.', *Infection and immunity*, 9(1), pp. 150–8. Available at: http://www.ncbi.nlm.nih.gov/pubmed/4271720.

Gottlieb, M. S., Schroff, R., Schanker, H. M., Weisman, J. D., Fan, P. T., Wolf, R. A. and Saxon, A. (1981) 'Pneumocystis carinii pneumonia and mucosal candidiasis in previously healthy homosexual men: evidence of a new acquired cellular immunodeficiency.', *The New England journal of medicine*, 305(24), pp. 1425–31. doi: 10.1056/NEJM198112103052401.

Gould, S. J., Booth, A. M. and Hildreth, J. E. K. (2003) 'The Trojan exosome hypothesis.', *Proceedings of the National Academy of Sciences of the United States of America*, 100(19), pp. 10592–7. doi: 10.1073/pnas.1831413100.

Gould, S. J. and Raposo, G. (2013) 'As we wait: coping with an imperfect nomenclature for extracellular vesicles.', *Journal of extracellular vesicles*, 2(1), pp. 236–43. doi: 10.3402/jev.v2i0.20389.

Granelli-Piperno, A., Delgado, E., Finkel, V., Paxton, W. and Steinman, R. M. (1998) 'Immature dendritic cells selectively replicate macrophagetropic (M-tropic) human immunodeficiency virus type 1, while mature cells efficiently transmit both M- and T-tropic virus to T cells.', *Journal of virology*, 72(4), pp. 2733–7. Available at: http://www.pubmedcentral.nih.gov/articlerender.fcgi?artid=109716&tool=pmcentrez&rendertype=abstract.

Granowitz, E. V, Saget, B. M., Wang, M. Z., Dinarello, C. A. and Skolnik, P. R. (1995) 'Interleukin 1 induces HIV-1 expression in chronically infected U1 cells: blockade by interleukin 1 receptor antagonist and tumor necrosis factor binding protein type 1.', *Molecular medicine (Cambridge, Mass.)*, 1(6), pp. 667–77. Available at: http://www.pubmedcentral.nih.gov/articlerender.fcgi?artid=2229977&tool=pmcentrez&rendertype=abstract.

Grawenhoff, J. and Engelman, A. N. (2017) 'Retroviral integrase protein and intasome nucleoprotein complex structures.', *World journal of biological chemistry*, 8(1), pp. 32–44. doi: 10.4331/wjbc.v8.i1.32.

Gringhuis, S. I., den Dunnen, J., Litjens, M., van het Hof, B., van Kooyk, Y. and Geijtenbeek, T. B. H. (2007) 'C-Type Lectin DC-SIGN Modulates Toll-like Receptor Signaling via Raf-1 Kinase-Dependent Acetylation of Transcription Factor NF-κB', *Immunity*, 26(5), pp. 605–616. doi: 10.1016/j.immuni.2007.03.012.

Gringhuis, S. I., den Dunnen, J., Litjens, M., van der Vlist, M. and Geijtenbeek, T. B. H. (2009) 'Carbohydrate-specific signaling through the DC-SIGN signalosome tailors immunity to Mycobacterium tuberculosis, HIV-1 and Helicobacter pylori', *Nature Immunology*. Nature Publishing Group, 10(10), pp. 1081–1088. doi: 10.1038/ni.1778.

Grzegorzewicz, A. E., de Sousa-d'Auria, C., McNeil, M. R., Huc-Claustre, E., Jones, V., Petit, C., Angala, S. K., Zemanová, J., Wang, Q., Belardinelli, J. M., Gao, Q., Ishizaki, Y., Mikušová, K., Brennan, P. J., Ronning, D. R., Chami, M., Houssin, C. and Jackson, M. (2016) 'Assembling of the Mycobacterium tuberculosis Cell Wall Core.', *The Journal of biological chemistry*, 291(36), pp. 18867–79. doi: 10.1074/jbc.M116.739227.

Guenin-Macé, L., Siméone, R. and Demangel, C. (2009) 'Lipids of Pathogenic Mycobacteria: Contributions to Virulence and Host Immune Suppression', *Transboundary and Emerging Diseases*, 56(6–7), pp. 255–268. doi: 10.1111/j.1865-1682.2009.01072.x.

Gummuluru, S., KewalRamani, V. N. and Emerman, M. (2002) 'Dendritic cell-mediated viral transfer to T cells is required for human immunodeficiency virus type 1 persistence in the face of rapid cell turnover.', *Journal of virology*, 76(21), pp. 10692–701. doi: 10.1128/JVI.76.21.10692-10701.2002.

Gupta, S. and Rodriguez, G. M. (2018) 'Mycobacterial extracellular vesicles and host pathogen interactions.', *Pathogens and disease*, 76(4), pp. 1–6. doi: 10.1093/femspd/fty031.

Haites, R. E., Morita, Y. S., McConville, M. J. and Billman-Jacobe, H. (2005) 'Function of phosphatidylinositol in mycobacteria.', *The Journal of biological chemistry*, 280(12), pp. 10981–7. doi: 10.1074/jbc.M413443200.

Hamasaki, N., Isowa, K., Kamada, K., Terano, Y., Matsumoto, T., Arakawa, T., Kobayashi, K. and Yano, I. (2000) 'In vivo administration of mycobacterial cord factor (Trehalose 6, 6'-dimycolate) can induce lung and liver granulomas and thymic atrophy in rabbits.', *Infection and immunity*, 68(6), pp. 3704–9. doi: 10.1128/IAI.68.6.3704-3709.2000.

Harris, R. S. and Dudley, J. P. (2015) 'APOBECs and virus restriction.', *Virology*, 479–480, pp. 131–45. doi: 10.1016/j.virol.2015.03.012.

Hernández, J. C., Stevenson, M., Latz, E. and Urcuqui-Inchima, S. (2012) 'HIV Type 1 Infection Up-Regulates TLR2 and TLR4 Expression and Function in Vivo and in Vitro', *AIDS Research and*

Human Retroviruses, 28(10), pp. 1313–1328. doi: 10.1089/aid.2011.0297.

Hickman, S. P., Chan, J. and Salgame, P. (2002) 'Mycobacterium tuberculosis Induces Differential Cytokine Production from Dendritic Cells and Macrophages with Divergent Effects on Naive T Cell Polarization', *The Journal of Immunology*, 168(9), pp. 4636–4642. doi: 10.4049/jimmunol.168.9.4636.

Hildreth, J. E. K. (2017) 'HIV As Trojan Exosome: Immunological Paradox Explained?', *Frontiers in immunology*, 8(DEC), p. 1715. doi: 10.3389/fimmu.2017.01715.

Hoagland, D. T., Liu, J., Lee, R. B. and Lee, R. E. (2016) 'New agents for the treatment of drug-resistant Mycobacterium tuberculosis', *Advanced Drug Delivery Reviews*. The Authors, 102, pp. 55–72. doi: 10.1016/j.addr.2016.04.026.

Hoffmann, C., Leis, A., Niederweis, M., Plitzko, J. M. and Engelhardt, H. (2008) 'Disclosure of the mycobacterial outer membrane: cryo-electron tomography and vitreous sections reveal the lipid bilayer structure.', *Proceedings of the National Academy of Sciences of the United States of America*, 105(10), pp. 3963–7. doi: 10.1073/pnas.0709530105.

Homhuan, A., Kogure, K., Akaza, H., Futaki, S., Naka, T., Fujita, Y., Yano, I. and Harashima, H. (2007) 'New packaging method of mycobacterial cell wall using octaarginine-modified liposomes: Enhanced uptake by and immunostimulatory activity of dendritic cells', *Journal of Controlled Release*, 120(1–2), pp. 60–69. doi: 10.1016/j.jconrel.2007.03.017.

Hong, C.-S., Funk, S., Muller, L., Boyiadzis, M. and Whiteside, T. L. (2016) 'Isolation of biologically active and morphologically intact exosomes from plasma of patients with cancer.', *Journal of extracellular vesicles*, 5(7), p. 29289. doi: 10.3402/jev.v5.29289.

Hoshino, Y., Hoshino, S., Gold, J. A., Raju, B., Prabhakar, S., Pine, R., Rom, W. N., Nakata, K. and Weiden, M. (2007) 'Mechanisms of Polymorphonuclear Neutrophil–Mediated Induction of HIV-1 Replication in Macrophages during Pulmonary Tuberculosis', *The Journal of Infectious Diseases*, 195(9), pp. 1303–1310. doi: 10.1086/513438.

Hoshino, Y., Nakata, K., Hoshino, S., Honda, Y., Tse, D. B., Shioda, T., Rom, W. N. and Weiden, M. (2002) 'Maximal HIV-1 replication in alveolar macrophages during tuberculosis requires both lymphocyte contact and cytokines.', *The Journal of experimental medicine*, 195(4), pp. 495–505. doi: 10.1084/jem.20011614.

Hoshino, Y., Tse, D. B., Rochford, G., Prabhakar, S., Hoshino, S., Chitkara, N., Kuwabara, K., Ching, E., Raju, B., Gold, J. a, Borkowsky, W., Rom, W. N., Pine, R. and Weiden, M. (2004) 'Mycobacterium tuberculosis-induced CXCR4 and chemokine expression leads to preferential X4 HIV-1 replication in human macrophages.', *Journal of immunology (Baltimore, Md. : 1950)*, 172(10), pp. 6251–6258. doi: 15128813.

Hossain, M. M. and Norazmi, M.-N. (2013) 'Pattern Recognition Receptors and Cytokines in Mycobacterium tuberculosis Infection—The Double-Edged Sword?', *BioMed Research International*, 2013, pp. 1–18. doi: 10.1155/2013/179174.

Houben, D., Demangel, C., van Ingen, J., Perez, J., Baldeón, L., Abdallah, A. M., Caleechurn, L., Bottai, D., van Zon, M., de Punder, K., van der Laan, T., Kant, A., Bossers-de Vries, R., Willemsen, P., Bitter, W., van Soolingen, D., Brosch, R., van der Wel, N. and Peters, P. J. (2012) 'ESX-1-mediated translocation to the cytosol controls virulence of mycobacteria.', *Cellular microbiology*, 14(8), pp. 1287–98. doi: 10.1111/j.1462-5822.2012.01799.x.

Hu, W.-S. and Hughes, S. H. (2012) 'HIV-1 reverse transcription.', *Cold Spring Harbor perspectives in medicine*, 2(10), p. a006882-. doi: 10.1101/cshperspect.a006882.

Huang, Y., Paxton, W. A., Wolinsky, S. M., Neumann, A. U., Zhang, L., He, T., Kang, S., Ceradini, D., Jin, Z., Yazdanbakhsh, K., Kunstman, K., Erickson, D., Dragon, E., Landau, N. R., Phair, J., Ho, D. D. and Koup, R. A. (1996) 'The role of a mutant CCR5 allele in HIV-1 transmission and disease progression', *Nature Medicine*, 2(11), pp. 1240–1243. doi: 10.1038/nm1196-1240.

Hussein, W. M., Liu, T., Skwarczynski, M. and Toth, I. (2014) 'Toll-like receptor agonists: a patent review (2011 – 2013)', *Expert Opinion on Therapeutic Patents*, 24(4), pp. 453–470. doi: 10.1517/13543776.2014.880691.

Hütter, G., Nowak, D., Mossner, M., Ganepola, S., Müssig, A., Allers, K., Schneider, T., Hofmann, J., Kücherer, C., Blau, O., Blau, I. W., Hofmann, W. K. and Thiel, E. (2009) 'Long-term control of HIV by CCR5 Delta32/Delta32 stem-cell transplantation.', *The New England journal of medicine*, 360(7), pp. 692–8. doi: 10.1056/NEJMoa0802905.

Indrigo, J., Hunter, R. L. and Actor, J. K. (2002) 'Influence of trehalose 6,6'-dimycolate (TDM) during mycobacterial infection of bone marrow macrophages.', *Microbiology (Reading, England)*, 148(Pt 7), pp. 1991–8. doi: 10.1099/00221287-148-7-1991.

Indrigo, J., Hunter, R. L. and Actor, J. K. (2003) 'Cord factor trehalose 6,6'-dimycolate (TDM) mediates trafficking events during mycobacterial infection of murine macrophages', *Microbiology*, 149(8), pp. 2049–2059. doi: 10.1099/mic.0.26226-0.

Ioerger, T. R., Feng, Y., Ganesula, K., Chen, X., Dobos, K. M., Fortune, S., Jacobs, W. R., Mizrahi, V., Parish, T., Rubin, E., Sassetti, C. and Sacchettini, J. C. (2010) 'Variation among genome sequences of H37Rv strains of Mycobacterium tuberculosis from multiple laboratories.', *Journal of bacteriology*, 192(14), pp. 3645–53. doi: 10.1128/JB.00166-10.

Iraci, N., Leonardi, T., Gessler, F., Vega, B. and Pluchino, S. (2016) 'Focus on extracellular vesicles: Physiological role and signalling properties of extracellular membrane vesicles', *International Journal of Molecular Sciences*, 17(2). doi: 10.3390/ijms17020171.

Ishikawa, E., Ishikawa, T., Morita, Y. S., Toyonaga, K., Yamada, H., Takeuchi, O., Kinoshita, T., Akira, S., Yoshikai, Y. and Yamasaki, S. (2009) 'Direct recognition of the mycobacterial glycolipid, trehalose dimycolate, by C-type lectin Mincle.', *The Journal of experimental medicine*, 206(13), pp. 2879–88. doi: 10.1084/jem.20091750.

Izquierdo-Useros, N., Lorizate, M., McLaren, P. J., Telenti, A., Kräusslich, H.-G. and Martinez-Picado, J. (2014) 'HIV-1 capture and transmission by dendritic cells: the role of viral glycolipids and the cellular receptor Siglec-1.', *PLoS pathogens*, 10(7), p. e1004146. doi: 10.1371/journal.ppat.1004146.

Izquierdo-Useros, N., Naranjo-Gómez, M., Erkizia, I., Puertas, M. C., Borràs, F. E., Blanco, J. and Martinez-Picado, J. (2010) 'HIV and mature dendritic cells: Trojan exosomes riding the Trojan horse?', *PLoS pathogens*, 6(3), p. e1000740. doi: 10.1371/journal.ppat.1000740.

Jang, S., Uematsu, S., Akira, S. and Salgame, P. (2004) 'IL-6 and IL-10 induction from dendritic cells in response to Mycobacterium tuberculosis is predominantly dependent on TLR2-mediated recognition.', *Journal of immunology (Baltimore, Md. : 1950)*, 173(5), pp. 3392–7. doi: 10.4049/jimmunol.173.5.3392.

Jayappa, K. D., Ao, Z. and Yao, X. (2012) 'The HIV-1 passage from cytoplasm to nucleus: the process involving a complex exchange between the components of HIV-1 and cellular machinery to access nucleus and successful integration.', *International journal of biochemistry and molecular biology*, 3(1), pp. 70–85. Available at: http://www.ncbi.nlm.nih.gov/pubmed/22509482.

Jones, L., McDonald, D. and Canaday, D. H. (2007) 'Rapid MHC-II antigen presentation of HIV type 1 by human dendritic cells.', *AIDS research and human retroviruses*, 23(6), pp. 812–6. doi: 10.1089/aid.2006.0280.

Jurkoshek, K. S., Wang, Y., Athman, J. J., Barton, M. R. and Wearsch, P. A. (2016) 'Interspecies Communication between Pathogens and Immune Cells via Bacterial Membrane Vesicles', *Frontiers in Cell and Developmental Biology*, 4(November), pp. 1–8. doi: 10.3389/fcell.2016.00125.

Kadiu, I., Narayanasamy, P., Dash, P. K., Zhang, W. and Gendelman, H. E. (2012) 'Biochemical and biologic characterization of exosomes and microvesicles as facilitators of HIV-1 infection in macrophages.', *Journal of immunology (Baltimore, Md. : 1950)*, 189(2), pp. 744–54. doi: 10.4049/jimmunol.1102244.

Kalsdorf, B., Scriba, T. J., Wood, K., Day, C. L., Dheda, K., Dawson, R., Hanekom, W. A., Lange, C. and Wilkinson, R. J. (2009) 'HIV-1 infection impairs the bronchoalveolar T-cell response to mycobacteria.', *American journal of respiratory and critical care medicine*, 180(12), pp. 1262–70. doi: 10.1164/rccm.200907-1011OC.

Kalsdorf, B., Skolimowska, K. H., Scriba, T. J., Dawson, R., Dheda, K., Wood, K., Hofmeister, J., Hanekom, W. a., Lange, C. and Wilkinson, R. J. (2013) 'Relationship between chemokine receptor expression, chemokine levels and HIV-1 replication in the lungs of persons exposed to Mycobacterium tuberculosis', *European Journal of Immunology*, 43(2), pp. 540–549. doi: 10.1002/eji.201242804.

Kan-Sutton, C., Jagannath, C. and Hunter, R. L. (2009) 'Trehalose 6,6'-dimycolate on the surface of Mycobacterium tuberculosis modulates surface marker expression for antigen presentation and costimulation in murine macrophages.', *Microbes and infection*, 11(1), pp. 40–8. doi: 10.1016/j.micinf.2008.10.006.

Kang, P. B., Azad, A. K., Torrelles, J. B., Kaufman, T. M., Beharka, A., Tibesar, E., DesJardin, L. E. and Schlesinger, L. S. (2005) 'The human macrophage mannose receptor directs Mycobacterium tuberculosis lipoarabinomannan-mediated phagosome biogenesis.', *The Journal of experimental medicine*, 202(7), pp. 987–99. doi: 10.1084/jem.20051239.

Karn, J. and Stoltzfus, C. M. (2012) 'Transcriptional and posttranscriptional regulation of HIV-1 gene expression.', *Cold Spring Harbor perspectives in medicine*, 2(2), p. a006916. doi: 10.1101/cshperspect.a006916.

Kawasaki, N., Rillahan, C. D., Cheng, T.-Y., Van Rhijn, I., Macauley, M. S., Moody, D. B. and Paulson, J. C. (2014) 'Targeted Delivery of Mycobacterial Antigens to Human Dendritic Cells via Siglec-7 Induces Robust T Cell Activation', *The Journal of Immunology*, 193(4), pp. 1560–1566. doi: 10.4049/jimmunol.1303278.

Kawasaki, T. and Kawai, T. (2014) 'Toll-Like Receptor Signaling Pathways', *Frontiers in Immunology*, 5(September), pp. 1–8. doi: 10.3389/fimmu.2014.00461.

Kedzierska, K. and Crowe, S. M. (2001) 'Cytokines and HIV-1: Interactions and clinical implications', *Antiviral Chemistry and Chemotherapy*, pp. 133–150.

Kelly, B. and O'Neill, L. A. J. (2015) 'Metabolic reprogramming in macrophages and dendritic cells in innate immunity.', *Cell research*. Nature Publishing Group, 25(7), pp. 771–84. doi: 10.1038/cr.2015.68.

Khademi, F., Taheri, R. A., Momtazi-Borojeni, A. A., Farnoosh, G., Johnston, T. P. and Sahebkar, A. (2018) 'Potential of Cationic Liposomes as Adjuvants/Delivery Systems for Tuberculosis Subunit Vaccines.', *Reviews of physiology, biochemistry and pharmacology*, 175(July), pp. 47–69. doi: 10.1007/112_2018_9.

Khader, S. A., Pearl, J. E., Sakamoto, K., Gilmartin, L., Bell, G. K., Jelley-Gibbs, D. M., Ghilardi, N., DeSauvage, F. and Cooper, A. M. (2005) 'IL-23 compensates for the absence of IL-12p70 and is essential for the IL-17 response during tuberculosis but is dispensable for protection and antigen-specific IFN-gamma responses if IL-12p70 is available.', *Journal of immunology (Baltimore, Md. : 1950)*, 175(2), pp. 788–95. doi: 10.4049/jimmunol.175.2.788.

Khatua, A. K., Taylor, H. E., Hildreth, J. E. K. and Popik, W. (2009) 'Exosomes packaging APOBEC3G confer human immunodeficiency virus resistance to recipient cells.', *Journal of virology*, 83(2), pp. 512–21. doi: 10.1128/JVI.01658-08.

Kim, J., De La Cruz, J., Lam, K., Ng, H., Daar, E. S., Balamurugan, A. and Yang, O. O. (2018) 'CD8+ Cytotoxic T Lymphocyte Responses and Viral Epitope Escape in Acute HIV-1 Infection.', *Viral immunology*, 31(7), pp. 525–536. doi: 10.1089/vim.2018.0040.

Kim, J. T., Chang, E., Sigal, A. and Baltimore, D. (2018) 'Dendritic cells efficiently transmit HIV to T Cells in a tenofovir and raltegravir insensitive manner.', *PloS one*, 13(1), p. e0189945. doi: 10.1371/journal.pone.0189945.

Konoshenko, M. Y., Lekchnov, E. A., Vlassov, A. V. and Laktionov, P. P. (2018) 'Isolation of Extracellular Vesicles: General Methodologies and Latest Trends.', *BioMed research international*, 2018, p. 8545347. doi: 10.1155/2018/8545347.

Van Kooyk, Y., Appelmelk, B. and Geijtenbeek, T. B. H. (2003) 'A fatal attraction: Mycobacterium tuberculosis and HIV-1 target DC-SIGN to escape immune surveillance', *Trends in Molecular Medicine*, 9(4), pp. 153–159. doi: 10.1016/S1471-4914(03)00027-3.

Koppel, E. a., Ludwig, I. S., Sanchez Hernandez, M., Lowary, T. L., Gadikota, R. R., Tuzikov, A. B., Vandenbroucke-Grauls, C. M. J. E., van Kooyk, Y., Appelmelk, B. J. and Geijtenbeek, T. B. H. (2004) 'Identification of the mycobacterial carbohydrate structure that binds the C-type lectins DC-SIGN, L-SIGN and SIGNR1', *Immunobiology*, 209(1–2), pp. 117–127. doi: 10.1016/j.imbio.2004.03.003.

Kruh-Garcia, N. A., Wolfe, L. M. and Dobos, K. M. (2015) 'Deciphering the role of exosomes in tuberculosis.', *Tuberculosis (Edinburgh, Scotland)*. Elsevier Ltd, 95(1), pp. 26–30. doi: 10.1016/j.tube.2014.10.010.

Krupa, A., Fol, M., Dziadek, B. R., Kepka, E., Wojciechowska, D., Brzostek, A., Torzewska, A., Dziadek, J., Baughman, R. P., Griffith, D. and Kurdowska, A. K. (2015) 'Binding of CXCL8/IL-8 to Mycobacterium tuberculosis Modulates the Innate Immune Response.', *Mediators of inflammation*. Hindawi Publishing Corporation, 2015, p. 124762. doi: 10.1155/2015/124762.

Kulkarni, R. and Prasad, A. (2017) 'Exosomes Derived from HIV-1 Infected DCs Mediate Viral trans-Infection via Fibronectin and Galectin-3.', *Scientific reports*. Springer US, 7(1), p. 14787. doi: 10.1038/s41598-017-14817-8.

Kumar, P., Schelle, M. W., Jain, M., Lin, F. L., Petzold, C. J., Leavell, M. D., Leary, J. a, Cox, J. S. and Bertozzi, C. R. (2007) 'PapA1 and PapA2 are acyltransferases essential for the biosynthesis of the Mycobacterium tuberculosis virulence factor sulfolipid-1.', *Proceedings of the National Academy of Sciences of the United States of America*, 104(27), pp. 11221–6. doi: 10.1073/pnas.0611649104.

Kvaratskhelia, M., Sharma, A., Larue, R. C., Serrao, E. and Engelman, A. (2014) 'Molecular mechanisms of retroviral integration site selection', *Nucleic Acids Research*, 42(16), pp. 10209–10225. doi: 10.1093/nar/gku769.

Kwan, C. K. and Ernst, J. D. (2011) 'HIV and Tuberculosis: a Deadly Human Syndemic', *Clinical Microbiology Reviews*, 24(2), pp. 351–376. doi: 10.1128/CMR.00042-10.

Kyei, G. B., Dinkins, C., Davis, A. S., Roberts, E., Singh, S. B., Dong, C., Wu, L., Kominami, E., Ueno, T., Yamamoto, A., Federico, M., Panganiban, A., Vergne, I. and Deretic, V. (2009) 'Autophagy pathway intersects with HIV-1 biosynthesis and regulates viral yields in macrophages.', *The Journal of cell biology*, 186(2), pp. 255–68. doi: 10.1083/jcb.200903070.

Laguette, N., Sobhian, B., Casartelli, N., Ringeard, M., Chable-Bessia, C., Ségéral, E., Yatim, A., Emiliani, S., Schwartz, O. and Benkirane, M. (2011) 'SAMHD1 is the dendritic- and myeloid-cell-specific HIV-1 restriction factor counteracted by Vpx.', *Nature*, 474(7353), pp. 654–7. doi: 10.1038/nature10117.

Lahaye, X. and Manel, N. (2015) 'Viral and cellular mechanisms of the innate immune sensing of HIV', *Current Opinion in Virology*. Elsevier B.V., 11, pp. 55–62. doi: 10.1016/j.coviro.2015.01.013.

Lane, B. R., King, S. R., Bock, P. J., Strieter, R. M., Coffey, M. J. and Markovitz, D. M. (2003) 'The C-X-C chemokine IP-10 stimulates HIV-1 replication.', *Virology*, 307(1), pp. 122–34. doi: 10.1016/S0042-6822(02)00045-4.

Lane, B. R., Markovitz, D. M., Woodford, N. L., Rochford, R., Strieter, R. M. and Coffey, M. J. (1999) 'TNF-alpha inhibits HIV-1 replication in peripheral blood monocytes and alveolar macrophages by inducing the production of RANTES and decreasing C-C chemokine receptor 5 (CCR5) expression.', *Journal of immunology (Baltimore, Md. : 1950)*, 163(7), pp. 3653–61. doi: 10.1111/jgh.12727.5.

Larson, E. C., Novis, C. L., Martins, L. J., Macedo, A. B., Kimball, K. E., Bosque, A., Planelles, V. and Barrows, L. R. (2017) 'Mycobacterium tuberculosis reactivates latent HIV-1 in T cells in vitro.', *PloS one*. Edited by P.-J. Cardona, 12(9), p. e0185162. doi: 10.1371/journal.pone.0185162.

Larsson, M., Fonteneau, J.-F., Lirvall, M., Haslett, P., Lifson, J. D. and Bhardwaj, N. (2002) 'Activation of HIV-1 specific CD4 and CD8 T cells by human dendritic cells: roles for cross-presentation and non-infectious HIV-1 virus.', *AIDS (London, England)*, 16(10), pp. 1319–29. Available at: http://www.ncbi.nlm.nih.gov/pubmed/12131208.

Law, K. F., Jagirdar, J., Weiden, M. D., Bodkin, M. and Rom, W. N. (1996) 'Tuberculosis in HIV-positive patients: cellular response and immune activation in the lung.', *American journal of*

respiratory and critical care medicine, 153(4 Pt 1), pp. 1377–84. doi: 10.1164/ajrccm.153.4.8616569.

Lawn, S. D., Bekker, L. G. and Miller, R. F. (2005) 'Immune reconstitution disease associated with mycobacterial infections in HIV-infected individuals receiving antiretrovirals', *Lancet Infectious Diseases*, 5, pp. 361–373. doi: http://dx.doi.org/10.1016/S1473-3099%2805%2970140-7.

Lawn, S. D., Butera, S. T. and Folks, T. M. (2001) 'Contribution of Immune Activation to the Pathogenesis and Transmission of Human Immunodeficiency Virus Type 1 Infection', *Clinical Microbiology Reviews*, 14(4), pp. 753–777. doi: 10.1128/CMR.14.4.753-777.2001.

Lawn, S. D., Pisell, T. L., Hirsch, C. S., Wu, M., Butera, S. T. and Toossi, Z. (2001) 'Anatomically compartmentalized human immunodeficiency virus replication in HLA-DR+ cells and CD14+ macrophages at the site of pleural tuberculosis coinfection.', *The Journal of infectious diseases*, 184(9), pp. 1127–33. doi: 10.1086/323649.

Leake, E. S., Myrvik, Q. N. and Wright, M. J. (1984) 'Phagosomal membranes of Mycobacterium bovis BCG-immune alveolar macrophages are resistant to disruption by Mycobacterium tuberculosis H37Rv.', *Infection and immunity*, 45(2), pp. 443–6. Available at: http://www.ncbi.nlm.nih.gov/pubmed/6430807.

Lee, J.-H., Schierer, S., Blume, K., Dindorf, J., Wittki, S., Xiang, W., Ostalecki, C., Koliha, N., Wild, S., Schuler, G., Fackler, O. T., Saksela, K., Harrer, T. and Baur, A. S. (2016) 'HIV-Nef and ADAM17-Containing Plasma Extracellular Vesicles Induce and Correlate with Immune Pathogenesis in Chronic HIV Infection.', *EBioMedicine*. The Authors, 6, pp. 103–113. doi: 10.1016/j.ebiom.2016.03.004.

Lee, J., Kim, S.-H., Choi, D.-S., Lee, J. S., Kim, D.-K., Go, G., Park, S.-M., Kim, S. H., Shin, J. H., Chang, C. L. and Gho, Y. S. (2015) 'Proteomic analysis of extracellular vesicles derived from Mycobacterium tuberculosis.', *Proteomics*, 15(19), pp. 3331–7. doi: 10.1002/pmic.201500037.

Lenassi, M., Cagney, G., Liao, M., Vaupotic, T., Bartholomeeusen, K., Cheng, Y., Krogan, N. J., Plemenitas, A. and Peterlin, B. M. (2010) 'HIV Nef is secreted in exosomes and triggers apoptosis in bystander CD4+ T cells.', *Traffic (Copenhagen, Denmark)*, 11(1), pp. 110–22. doi: 10.1111/j.1600-0854.2009.01006.x.

Levy, J. A., Hoffman, A. D., Kramer, S. M., Landis, J. A., Shimabukuro, J. M. and Oshiro, L. S. (1984) 'Isolation of lymphocytopathic retroviruses from San Francisco patients with AIDS.', *Science (New York, N.Y.)*, 225(4664), pp. 840–2. Available at: http://www.ncbi.nlm.nih.gov/pubmed/6206563.

Li, J., Liu, K., Liu, Y., Xu, Y., Zhang, F., Yang, H., Liu, J., Pan, T., Chen, J., Wu, M., Zhou, X. and Yuan, Z. (2013) 'Exosomes mediate the cell-to-cell transmission of IFN-α-induced antiviral activity.', *Nature immunology*, 14(8), pp. 793–803. doi: 10.1038/ni.2647.

Li, L., Cheng, Y., Emrich, S. and Schorey, J. (2018) 'Activation of endothelial cells by extracellular vesicles derived from Mycobacterium tuberculosis infected macrophages or mice.', *PloS one*, 13(5), p. e0198337. doi: 10.1371/journal.pone.0198337.

Lin, Y., Zhang, M. and Barnes, P. F. (1998) 'Chemokine production by a human alveolar epithelial cell line in response to Mycobacterium tuberculosis.', *Infection and immunity*,

66(3), pp. 1121–6. Available at: http://www.ncbi.nlm.nih.gov/pubmed/9488404%5Cnhttp://www.pubmedcentral.nih.gov/articlerender.fcgi?artid=PMC108024.

Linares, C., Bernabéu, A., Luquin, M. and Valero-Guillén, P. L. (2012) 'Cord factors from atypical mycobacteria (Mycobacterium alvei, Mycobacterium brumae) stimulate the secretion of some pro-inflammatory cytokines of relevance in tuberculosis.', *Microbiology (Reading, England)*, 158(Pt 11), pp. 2878–85. doi: 10.1099/mic.0.060681-0.

Liu, P. T., Stenger, S., Li, H., Wenzel, L., Tan, B. H., Krutzik, S. R., Ochoa, M. T., Schauber, J., Wu, K., Meinken, C., Kamen, D. L., Wagner, M., Bals, R., Steinmeyer, A., Zügel, U., Gallo, R. L., Eisenberg, D., Hewison, M., Hollis, B. W., Adams, J. S., Bloom, B. R. and Modlin, R. L. (2006) 'Toll-like receptor triggering of a vitamin D-mediated human antimicrobial response.', *Science (New York, N.Y.)*, 311(5768), pp. 1770–3. doi: 10.1126/science.1123933.

Lobb, R. J., Becker, M., Wen, S. W., Wong, C. S. F., Wiegmans, A. P., Leimgruber, A. and Möller, A. (2015) 'Optimized exosome isolation protocol for cell culture supernatant and human plasma.', *Journal of extracellular vesicles*, 4(27031), p. 27031. doi: 10.3402/jev.v4.27031.

de los Angeles García, M., Borrero, R., Marrón, R., Lanio, M. E., Canet, L., Otero, O., Kadir, R., Suraiya, S., Zayas, C., López, Y., Nor Norazmi, M., Sarmiento, M. E. and Acosta, A. (2013) 'Evaluation of specific humoral immune response and cross reactivity against Mycobacterium tuberculosis antigens induced in mice immunized with liposomes composed of total lipids extracted from Mycobacterium smegmatis.', *BMC immunology*. BioMed Central Ltd, 14 Suppl 1(Suppl 1), p. S11. doi: 10.1186/1471-2172-14-S1-S11.

Lugo-Villarino, G., Hudrisier, D., Tanne, A. and Neyrolles, O. (2011) 'C-type lectins with a sweet spot for Mycobacterium tuberculosis', *European Journal of Microbiology and Immunology*, 1(1), pp. 25–40. doi: 10.1556/EuJMI.1.2011.1.6.

Maartens, G., Celum, C. and Lewin, S. R. (2014) 'HIV infection: epidemiology, pathogenesis, treatment, and prevention', *The Lancet*. Elsevier Ltd, 384(9939), pp. 258–271. doi: 10.1016/S0140-6736(14)60164-1.

Mack, M., Kleinschmidt, A., Bruhl, H., Klier, C., Nelson, P. J., Cihak, J., Plachy, J., Stangassinger, M., Erfle, V. and Schlondorff, D. (2000) 'Transfer of the chemokine receptor CCR5 between cells by membrane-derived microparticles: a mechanism for cellular human immunodeficiency virus 1 infection', *Nat Med*, 6(7), pp. 769–775. doi: 10.1038/77498.

Madison, M. N. and Okeoma, C. M. (2015) 'Exosomes: Implications in HIV-1 Pathogenesis.', *Viruses*, 7(7), pp. 4093–118. doi: 10.3390/v7072810.

Manca, C., Tsenova, L., Barry, C. E., Bergtold, A., Freeman, S., Haslett, P. A., Musser, J. M., Freedman, V. H. and Kaplan, G. (1999) 'Mycobacterium tuberculosis CDC1551 induces a more vigorous host response in vivo and in vitro, but is not more virulent than other clinical isolates.', *Journal of immunology (Baltimore, Md. : 1950)*, 162(11), pp. 6740–6. Available at: http://www.jimmunol.org/cgi/content/abstract/162/11/6740%5Cnhttp://www.jimmunol.org/content/162/11/6740.full.

Manca, C., Tsenova, L., Bergtold, A., Freeman, S., Tovey, M., Musser, J. M., Barry, C. E., Freedman, V. H. and Kaplan, G. (2001) 'Virulence of a Mycobacterium tuberculosis clinical isolate in mice is determined by failure to induce Th1 type immunity and is associated with induction of IFN-alpha /beta.', *Proceedings of the National Academy of Sciences of the United*

States of America, 98(10), pp. 5752–7. doi: 10.1073/pnas.091096998.

Mancino, G., Placido, R., Bach, S., Mariani, F., Montesano, C., Ercoli, L., Zembala, M. and Colizzi, V. (1997) 'Infection of human monocytes with Mycobacterium tuberculosis enhances human immunodeficiency virus type 1 replication and transmission to T cells.', *The Journal of infectious diseases*, 175(6), pp. 1531–1535.

Margolis, L. and Shattock, R. (2006) 'Selective transmission of CCR5-utilizing HIV-1: The "gatekeeper" problem resolved?', *Nature Reviews Microbiology*, 4(4), pp. 312–317. doi: 10.1038/nrmicro1387.

Marlink, R., Kanki, P., Thior, I., Travers, K., Eisen, G., Siby, T., Traore, I., Hsieh, C. C., Dia, M. C. and Gueye, E. H. (1994) 'Reduced rate of disease development after HIV-2 infection as compared to HIV-1.', *Science (New York, N.Y.)*, 265(5178), pp. 1587–90. doi: 10.1126/science.7915856.

Masur, H., Michelis, M. A., Greene, J. B., Onorato, I., Stouwe, R. A., Holzman, R. S., Wormser, G., Brettman, L., Lange, M., Murray, H. W. and Cunningham-Rundles, S. (1981) 'An outbreak of community-acquired Pneumocystis carinii pneumonia: initial manifestation of cellular immune dysfunction.', *The New England journal of medicine*, 305(24), pp. 1431–8. doi: 10.1056/NEJM198112103052402.

Mathivanan, S., Ji, H. and Simpson, R. J. (2010) 'Exosomes: extracellular organelles important in intercellular communication.', *Journal of proteomics*. Elsevier B.V., 73(10), pp. 1907–20. doi: 10.1016/j.jprot.2010.06.006.

Mayanja-Kizza, H., Wu, M., Aung, H., Liu, S., Luzze, H., Hirsch, C. and Toossi, Z. (2009) 'The Interaction of Monocyte Chemoattractant Protein-1 and Tumour Necrosis Factor-α in Mycobacterium tuberculosis -induced HIV-1 Replication at Sites of Active Tuberculosis', *Scandinavian Journal of Immunology*, 69(6), pp. 516–520. doi: 10.1111/j.1365-3083.2009.02246.x.

Mayer, L. D., Hope, M. J. and Cullis, P. R. (1986) 'Vesicles of variable sizes produced by a rapid extrusion procedure', *Biochimica et Biophysica Acta (BBA) - Biomembranes*, 858(1), pp. 161–168. doi: 10.1016/0005-2736(86)90302-0.

Mazurek, J., Ignatowicz, L., Kallenius, G., Svenson, S. B., Pawlowski, A. and Hamasur, B. (2012) 'Divergent effects of mycobacterial cell wall glycolipids on maturation and function of human monocyte-derived dendritic cells.', *PloS one*. Edited by S. Kovats, 7(8), p. e42515. doi: 10.1371/journal.pone.0042515.

Mazzolini, J., Herit, F., Bouchet, J., Benmerah, A., Benichou, S. and Niedergang, F. (2010) 'Inhibition of phagocytosis in HIV-1-infected macrophages relies on Nef-dependent alteration of focal delivery of recycling compartments.', *Blood*, 115(21), pp. 4226–36. doi: 10.1182/blood-2009-12-259473.

McDonald, D., Wu, L., Bohks, S. M., KewalRamani, V. N., Unutmaz, D. and Hope, T. J. (2003) 'Recruitment of HIV and its receptors to dendritic cell-T cell junctions.', *Science (New York, N.Y.)*, 300(5623), pp. 1295–7. doi: 10.1126/science.1084238.

McDonough, K. A., Kress, Y. and Bloom, B. R. (1993) 'The interaction of Mycobacterium tuberculosis with macrophages: a study of phagolysosome fusion.', *Infectious agents and disease*, 2(4), pp. 232–5. doi: .

McNamara, R. P., Costantini, L. M., Myers, T. A., Schouest, B., Maness, N. J., Griffith, J. D., Damania, B. A., MacLean, A. G. and Dittmer, D. P. (2018) 'Nef Secretion into Extracellular Vesicles or Exosomes Is Conserved across Human and Simian Immunodeficiency Viruses.', *mBio*, 9(1), pp. 1–20. doi: 10.1128/mBio.02344-17.

Means, T. K., Wang, S., Lien, E., Yoshimura, A., Golenbock, D. T. and Fenton, M. J. (1999) 'Human toll-like receptors mediate cellular activation by Mycobacterium tuberculosis', *Journal of Immunology*, 163(7), pp. 3920–3927. Available at: papers3://publication/uuid/789CF37E-F503-4F6B-8BF2-7C57378FD21E.

Meckes, D. G. (2015) 'Exosomal communication goes viral.', *Journal of virology*, 89(10), pp. 5200–3. doi: 10.1128/JVI.02470-14.

Meintjes, G., Lawn, S. D., Scano, F., Maartens, G., French, M. A., Worodria, W., Elliott, J. H., Murdoch, D., Wilkinson, R. J., Seyler, C., John, L., van der Loeff, M. S., Reiss, P., Lynen, L., Janoff, E. N., Gilks, C. and Colebunders, R. (2008) 'Tuberculosis-associated immune reconstitution inflammatory syndrome: case definitions for use in resource-limited settings', *The Lancet Infectious Diseases*, 8(8), pp. 516–523. doi: 10.1016/S1473-3099(08)70184-1.

Métifiot, M., Marchand, C. and Pommier, Y. (2013) 'HIV integrase inhibitors: 20-year landmark and challenges.', *Advances in pharmacology (San Diego, Calif.)*, 67, pp. 75–105. doi: 10.1016/B978-0-12-405880-4.00003-2.

Modrow, S., Falke, D., Truyen, U. and Schätzl, H. (2013) *Molecular Virology*. Berlin, Heidelberg: Springer Berlin Heidelberg. doi: 10.1007/978-3-642-20718-1.

Mogensen, T. H., Melchjorsen, J., Larsen, C. S. and Paludan, S. R. (2010) 'Innate immune recognition and activation during HIV infection', *Retrovirology*, 7, pp. 1–19. doi: 10.1186/1742-4690-7-54.

Mohan, V. P., Scanga, C. A., Yu, K., Holly, M., Tanaka, K. E., Tsang, E., Tsai, M. C., Flynn, J. L., Chan, J., Mohan, V. P., Scanga, C. A., Yu, K. and Scott, H. M. (2001) 'Effects of Tumor Necrosis Factor Alpha on Host Immune Response in Chronic Persistent Tuberculosis : Possible Role for Limiting Pathology', *Infection and immunity*, 69(3), pp. 1847–1855. doi: 10.1128/IAI.69.3.1847.

van Montfort, T., Nabatov, A. a, Geijtenbeek, T. B. H., Pollakis, G. and Paxton, W. a (2007) 'Efficient capture of antibody neutralized HIV-1 by cells expressing DC-SIGN and transfer to CD4+ T lymphocytes.', *Journal of immunology (Baltimore, Md. : 1950)*, 178(5), pp. 3177–3185. doi: 10.4049/jimmunol.178.5.3177.

Moris, A., Pajot, A., Blanchet, F., Guivel-Benhassine, F., Salcedo, M. and Schwartz, O. (2006) 'Dendritic cells and HIV-specific CD4+ T cells: HIV antigen presentation, T-cell activation, and viral transfer.', *Blood*, 108(5), pp. 1643–51. doi: 10.1182/blood-2006-02-006361.

Muller, L., Hong, C.-S., Stolz, D. B., Watkins, S. C. and Whiteside, T. L. (2014) 'Isolation of biologically-active exosomes from human plasma.', *Journal of immunological methods*, 411(Lm), pp. 55–65. doi: 10.1016/j.jim.2014.06.007.

Müller, M., Wandel, S., Colebunders, R., Attia, S., Furrer, H., Egger, M. and IeDEA Southern and Central Africa (2010) 'Immune reconstitution inflammatory syndrome in patients starting antiretroviral therapy for HIV infection: a systematic review and meta-analysis.', *The Lancet. Infectious diseases*, 10(4), pp. 251–61. doi: 10.1016/S1473-3099(10)70026-8.

Muñoz-Fernández, M. A., Navarro, J., Garcia, A., Punzón, C., Fernández-Cruz, E. and Fresno, M. (1997) 'Replication of human immunodeficiency virus-1 in primary human T cells is dependent on the autocrine secretion of tumor necrosis factor through the control of nuclear factor-kappa B activation.', *The Journal of allergy and clinical immunology*, 100(6 Pt 1), pp. 838–45. Available at: http://www.ncbi.nlm.nih.gov/pubmed/9438495.

Muratori, C., Cavallin, L. E., Krätzel, K., Tinari, A., De Milito, A., Fais, S., D'Aloja, P., Federico, M., Vullo, V., Fomina, A., Mesri, E. A., Superti, F. and Baur, A. S. (2009) 'Massive secretion by T cells is caused by HIV Nef in infected cells and by Nef transfer to bystander cells.', *Cell host & microbe*, 6(3), pp. 218–30. doi: 10.1016/j.chom.2009.06.009.

Mvubu, N. E., Pillay, B., McKinnon, L. R. and Pillay, M. (2018) 'Mycobacterium tuberculosis strains induce strain-specific cytokine and chemokine response in pulmonary epithelial cells.', *Cytokine*. Elsevier, 104(3), pp. 53–64. doi: 10.1016/j.cyto.2017.09.027.

Naarding, M. a., Dirac, A. M., Ludwig, I. S., Speijer, D., Lindquist, S., Vestman, E. L., Stax, M. J., Geijtenbeek, T. B. H., Pollakis, G., Hernell, O. and Paxton, W. a. (2006) 'Bile salt-stimulated lipase from human milk binds DC-SIGN and inhibits human immunodeficiency virus type 1 transfer to CD4+ T cells', *Antimicrobial Agents and Chemotherapy*, 50(10), pp. 3367–3374. doi: 10.1128/AAC.00593-06.

Naarding, M. a., Ludwig, I. S., Groot, F., Berkhout, B., Geijtenbeek, T. B. H., Pollakis, G. and Paxton, W. a. (2005) 'Lewis X component in human milk binds DC-SIGN and inhibits HIV-1 transfer to CD4+ T lymphocytes', *Journal of Clinical Investigation*, 115(11), pp. 3256–3264. doi: 10.1172/JCI25105.

Naing, C., Mak, J. W., Maung, M., Wong, S. F. and Kassim, A. I. B. M. (2013) 'Meta-analysis: the association between HIV infection and extrapulmonary tuberculosis.', *Lung*, 191(1), pp. 27–34. doi: 10.1007/s00408-012-9440-6.

Nakata, K., Rom, W. N., Honda, Y., Condos, R., Kanegasaki, S., Cao, Y. and Weiden, M. (1997) 'Mycobacterium tuberculosis enhances human immunodeficiency virus-1 replication in the lung.', *American journal of respiratory and critical care medicine*, 155(3), pp. 996–1003. doi: 10.1164/ajrccm.155.3.9117038.

Narayanan, A., Iordanskiy, S., Das, R., Van Duyne, R., Santos, S., Jaworski, E., Guendel, I., Sampey, G., Dalby, E., Iglesias-Ussel, M., Popratiloff, A., Hakami, R., Kehn-Hall, K., Young, M., Subra, C., Gilbert, C., Bailey, C., Romerio, F. and Kashanchi, F. (2013) 'Exosomes derived from HIV-1-infected cells contain trans-activation response element RNA', *Journal of Biological Chemistry*, 288(27), pp. 20014–20033. doi: 10.1074/jbc.M112.438895.

Näslund, T. I., Paquin-Proulx, D., Paredes, P. T., Vallhov, H., Sandberg, J. K. and Gabrielsson, S. (2014) 'Exosomes from breast milk inhibit HIV-1 infection of dendritic cells and subsequent viral transfer to CD4+ T cells', *Aids*, 28(2), pp. 171–180. doi: 10.1097/QAD.0000000000000159.

Neil, S. J. D., Zang, T. and Bieniasz, P. D. (2008) 'Tetherin inhibits retrovirus release and is antagonized by HIV-1 Vpu', *Nature*, 451(7177), pp. 425–430. doi: 10.1038/nature06553.

Neyrolles, O., Gicquel, B. and Quintana-Murci, L. (2006) 'Towards a crucial role for DC-SIGN in tuberculosis and beyond', *Trends in Microbiology*, 14(9), pp. 383–387. doi: 10.1016/j.tim.2006.07.007.

Nieto-Garai, J. A., Glass, B., Bunn, C., Giese, M., Jennings, G., Brankatschk, B., Agarwal, S., Börner, K., Contreras, F. X., Knölker, H.-J., Zankl, C., Simons, K., Schroeder, C., Lorizate, M. and Kräusslich, H.-G. (2018) 'Lipidomimetic Compounds Act as HIV-1 Entry Inhibitors by Altering Viral Membrane Structure.', *Frontiers in immunology*, 9(September), p. 1983. doi: 10.3389/fimmu.2018.01983.

Nigou, J., Gilleron, M., Cahuzac, B., Bounéry, J. D., Herold, M., Thurnher, M. and Puzo, G. (1997) 'The phosphatidyl-myo-inositol anchor of the lipoarabinomannans from Mycobacterium bovis bacillus Calmette Guérin. Heterogeneity, structure, and role in the regulation of cytokine secretion.', *The Journal of biological chemistry*, 272(37), pp. 23094–103. doi: 10.1074/jbc.272.37.23094.

Nordin, J. Z., Lee, Y., Vader, P., Mäger, I., Johansson, H. J., Heusermann, W., Wiklander, O. P. B., Hällbrink, M., Seow, Y., Bultema, J. J., Gilthorpe, J., Davies, T., Fairchild, P. J., Gabrielsson, S., Meisner-Kober, N. C., Lehtiö, J., Smith, C. I. E., Wood, M. J. A. and El Andaloussi, S. (2015) 'Ultrafiltration with size-exclusion liquid chromatography for high yield isolation of extracellular vesicles preserving intact biophysical and functional properties.', *Nanomedicine : nanotechnology, biology, and medicine*. The Authors, 11(4), pp. 879–83. doi: 10.1016/j.nano.2015.01.003.

Okamoto, T., Matsuyama, T., Mori, S., Hamamoto, Y., Kobayashi, N., Yamamoto, N., Josephs, S. F., Wong-Staal, F. and Shimotohno, K. (1989) 'Augmentation of human immunodeficiency virus type 1 gene expression by tumor necrosis factor alpha.', *AIDS research and human retroviruses*, 5(2), pp. 131–8. doi: 10.1089/aid.1989.5.131.

Okeoma, C. M., Huegel, A. L., Lingappa, J., Feldman, M. D. and Ross, S. R. (2010) 'APOBEC3 proteins expressed in mammary epithelial cells are packaged into retroviruses and can restrict transmission of milk-borne virions.', *Cell host & microbe*, 8(6), pp. 534–43. doi: 10.1016/j.chom.2010.11.003.

Ordway, D., Henao-Tamayo, M., Harton, M., Palanisamy, G., Troudt, J., Shanley, C., Basaraba, R. J. and Orme, I. M. (2007) 'The hypervirulent Mycobacterium tuberculosis strain HN878 induces a potent TH1 response followed by rapid down-regulation.', *Journal of immunology (Baltimore, Md. : 1950)*, 179(1), pp. 522–31. doi: 10.4049/jimmunol.179.1.522.

Ozaki, D. A., Gao, H., Todd, C. A., Greene, K. M., Montefiori, D. C. and Sarzotti-Kelsoe, M. (2012) 'International technology transfer of a GCLP-compliant HIV-1 neutralizing antibody assay for human clinical trials.', *PloS one*, 7(1), p. e30963. doi: 10.1371/journal.pone.0030963.

Pai, R. K., Pennini, M. E., Tobian, A. A. R., Canaday, D. H., Boom, W. H. and Harding, C. V. (2004) 'Prolonged toll-like receptor signaling by Mycobacterium tuberculosis and its 19-kilodalton lipoprotein inhibits gamma interferon-induced regulation of selected genes in macrophages', *Infection and Immunity*, 72(11), pp. 6603–6614. doi: 10.1128/IAI.72.11.6603-6614.2004.

Patel, N. R., Swan, K., Li, X., Tachado, S. D. and Koziel, H. (2009) 'Impaired M. tuberculosis-mediated apoptosis in alveolar macrophages from HIV+ persons: potential role of IL-10 and BCL-3.', *Journal of leukocyte biology*, 86(1), pp. 53–60. doi: 10.1189/jlb.0908574.

Patel, N. R., Zhu, J., Tachado, S. D., Zhang, J., Wan, Z., Saukkonen, J. and Koziel, H. (2007) 'HIV impairs TNF-alpha mediated macrophage apoptotic response to Mycobacterium tuberculosis.', *Journal of immunology (Baltimore, Md. : 1950)*, 179(10), pp. 6973–80. doi:

10.4049/jimmunol.179.10.6973.

Pathak, S., Wentzel-Larsen, T. and Åsjö, B. (2010) 'Effects of in vitro HIV-1 infection on mycobacterial growth in peripheral blood monocyte-derived macrophages', *Infection and Immunity*, 78(9), pp. 4022–4032. doi: 10.1128/IAI.00106-10.

Paxton, W. A., Martin, S. R., Tse, D., O'Brien, T. R., Skurnick, J., VanDevanter, N. L., Padian, N., Braun, J. F., Kotler, D. P., Wolinsky, S. M. and Koup, R. A. (1996) 'Relative resistance to HIV-1 infection of CD4 lymphocytes from persons who remain uninfected despite multiple high-risk sexual exposure.', *Nature medicine*, 2(4), pp. 412–7. doi: 10.1038/nm0496-412.

Pereira, E. A. and DaSilva, L. L. P. (2016) 'HIV-1 Nef: Taking Control of Protein Trafficking.', *Traffic (Copenhagen, Denmark)*, 17(9), pp. 976–96. doi: 10.1111/tra.12412.

Perez-Caballero, D., Zang, T., Ebrahimi, A., McNatt, M. W., Gregory, D. A., Johnson, M. C. and Bieniasz, P. D. (2009) 'Tetherin Inhibits HIV-1 Release by Directly Tethering Virions to Cells', *Cell*. Elsevier Ltd, 139(3), pp. 499–511. doi: 10.1016/j.cell.2009.08.039.

Petrik, J. (2016) 'Immunomodulatory effects of exosomes produced by virus-infected cells.', *Transfusion and apheresis science : official journal of the World Apheresis Association : official journal of the European Society for Haemapheresis*. Elsevier Ltd. doi: 10.1016/j.transci.2016.07.014.

Philips, J. A. (2008) 'Mycobacterial manipulation of vacuolar sorting', *Cellular Microbiology*, 10(12), pp. 2408–2415. doi: 10.1111/j.1462-5822.2008.01239.x.

Philips, J. a. and Ernst, J. D. (2012) 'Tuberculosis Pathogenesis and Immunity', *Annual Review of Pathology: Mechanisms of Disease*, 7(1), pp. 353–384. doi: 10.1146/annurev-pathol-011811-132458.

Pino, M., Erkizia, I., Benet, S., Erikson, E., Fernández-Figueras, M. T., Guerrero, D., Dalmau, J., Ouchi, D., Rausell, A., Ciuffi, A., Keppler, O. T., Telenti, A., Kräusslich, H.-G., Martinez-Picado, J. and Izquierdo-Useros, N. (2015) 'HIV-1 immune activation induces Siglec-1 expression and enhances viral trans-infection in blood and tissue myeloid cells.', *Retrovirology*, 12(1), p. 37. doi: 10.1186/s12977-015-0160-x.

Pitarque, S., Herrmann, J.-L., Duteyrat, J.-L., Jackson, M., Stewart, G. R., Lecointe, F., Payre, B., Schwartz, O., Young, D. B., Marchal, G., Lagrange, P. H., Puzo, G., Gicquel, B., Nigou, J. and Neyrolles, O. (2005) 'Deciphering the molecular bases of Mycobacterium tuberculosis binding to the lectin DC-SIGN reveals an underestimated complexity.', *The Biochemical journal*, 392(Pt 3), pp. 615–624. doi: 10.1042/BJ20050709.

Plantier, J.-C., Leoz, M., Dickerson, J. E., De Oliveira, F., Cordonnier, F., Lemée, V., Damond, F., Robertson, D. L. and Simon, F. (2009) 'A new human immunodeficiency virus derived from gorillas.', *Nature medicine*, 15(8), pp. 871–2. doi: 10.1038/nm.2016.

Popovic, M., Sarngadharan, M. G., Read, E. and Gallo, R. C. (1984) 'Detection, isolation, and continuous production of cytopathic retroviruses (HTLV-III) from patients with AIDS and pre-AIDS.', *Science (New York, N.Y.)*, 224(4648), pp. 497–500. doi: 10.1126/science.6200936.

Puissegur, M.-P., Lay, G., Gilleron, M., Botella, L., Nigou, J., Marrakchi, H., Mari, B., Duteyrat, J.-L., Guerardel, Y., Kremer, L., Barbry, P., Puzo, G. and Altare, F. (2007) 'Mycobacterial lipomannan induces granuloma macrophage fusion via a TLR2-dependent, ADAM9- and

beta1 integrin-mediated pathway.', *Journal of immunology (Baltimore, Md. : 1950)*, 178(5), pp. 3161–9. doi: 10.4049/jimmunol.178.5.3161.

Puryear, W. B., Yu, X., Ramirez, N. P., Reinhard, B. M. and Gummuluru, S. (2012) 'HIV-1 incorporation of host-cell-derived glycosphingolipid GM3 allows for capture by mature dendritic cells.', *Proceedings of the National Academy of Sciences of the United States of America*, 109(19), pp. 7475–80. doi: 10.1073/pnas.1201104109.

Quesniaux, V. J., Nicolle, D. M., Torres, D., Kremer, L., Guerardel, Y., Nigou, J., Puzo, G., Erard, F. and Ryffel, B. (2004) 'Toll-Like Receptor 2 (TLR2)-Dependent-Positive and TLR2-Independent-Negative Regulation of Proinflammatory Cytokines by Mycobacterial Lipomannans', *The Journal of Immunology*, 172(7), pp. 4425–4434. doi: 10.4049/jimmunol.172.7.4425.

Quesniaux, V. J., Nicolle, D. M., Torres, D., Kremer, L., Guérardel, Y., Nigou, J., Puzo, G., Erard, F. and Ryffel, B. (2004) 'Toll-like receptor 2 (TLR2)-dependent-positive and TLR2-independent-negative regulation of proinflammatory cytokines by mycobacterial lipomannans.', *Journal of immunology (Baltimore, Md. : 1950)*, 172(7), pp. 4425–34. doi: 10.4049/jimmunol.172.7.4425.

Quigley, J., Hughitt, V. K., Velikovsky, C. A., Mariuzza, R. A., El-Sayed, N. M. and Briken, V. (2017) 'The Cell Wall Lipid PDIM Contributes to Phagosomal Escape and Host Cell Exit of Mycobacterium tuberculosis.', *mBio*, 8(2), pp. 1–12. doi: 10.1128/mBio.00148-17.

Ramachandra, L., Qu, Y., Wang, Y., Lewis, C. J., Cobb, B. A., Takatsu, K., Boom, W. H., Dubyak, G. R. and Harding, C. V. (2010) 'Mycobacterium tuberculosis synergizes with ATP to induce release of microvesicles and exosomes containing major histocompatibility complex class II molecules capable of antigen presentation', *Infection and Immunity*, 78(12), pp. 5116–5125. doi: 10.1128/IAI.01089-09.

Ranjbar, S., Boshoff, H. I., Mulder, A., Siddiqi, N., Rubin, E. J. and Goldfeld, A. E. (2009) 'HIV-1 replication is differentially regulated by distinct clinical strains of Mycobacterium tuberculosis', *PLoS ONE*, 4(7), pp. 1–8. doi: 10.1371/journal.pone.0006116.

Rao, V., Fujiwara, N., Porcelli, S. A. and Glickman, M. S. (2005) 'Mycobacterium tuberculosis controls host innate immune activation through cyclopropane modification of a glycolipid effector molecule.', *The Journal of experimental medicine*, 201(4), pp. 535–43. doi: 10.1084/jem.20041668.

Rao, V., Gao, F., Chen, B., Jacobs, W. R. and Glickman, M. S. (2006) 'Trans-cyclopropanation of mycolic acids on trehalose dimycolate suppresses Mycobacterium tuberculosis -induced inflammation and virulence.', *The Journal of clinical investigation*, 116(6), pp. 1660–7. doi: 10.1172/JCI27335.

Raposo, G. and Stoorvogel, W. (2013) 'Extracellular vesicles: exosomes, microvesicles, and friends.', *The Journal of cell biology*, 200(4), pp. 373–83. doi: 10.1083/jcb.201211138.

Ratner, L., Gallo, R. C. and Wong-Staal, F. (1985) 'HTLV-III, LAV, ARV are variants of same AIDS virus.', *Nature*, 313(6004), pp. 636–7. doi: 10.1038/313636c0.

Reed, M. B., Domenech, P., Manca, C., Su, H., Barczak, A. K., Kreiswirth, B. N. and Kaplan, G. (2004) 'A glycolipid of hypervirulent tuberculosis strains that inhibits the innate immune response', *Nature*, 431(7004), pp. 84–87. doi: 10.1038/nature02837.

Reuter, M. A., Pecora, N. D., Harding, C. V, Canaday, D. H. and McDonald, D. (2010) 'Mycobacterium tuberculosis promotes HIV trans-infection and suppresses major histocompatibility complex class II antigen processing by dendritic cells.', *Journal of virology*, 84(17), pp. 8549–60. doi: 10.1128/JVI.02303-09.

Riedel, D. D. and Kaufmann, S. H. (1997) 'Chemokine secretion by human polymorphonuclear granulocytes after stimulation with Mycobacterium tuberculosis and lipoarabinomannan.', *Infection and immunity*, 65(11), pp. 4620–3. Available at: http://www.ncbi.nlm.nih.gov/pubmed/9353042.

Rodriguez, M. E., Loyd, C. M., Ding, X., Karim, A. F., McDonald, D. J., Canaday, D. H. and Rojas, R. E. (2013) 'Mycobacterial phosphatidylinositol mannoside 6 (PIM6) up-regulates TCR-triggered HIV-1 replication in CD4+ T cells', *PLoS ONE*, 8(11). doi: 10.1371/journal.pone.0080938.

Rosas-Taraco, A. G., Arce-Mendoza, A. Y., Caballero-Olín, G. and Salinas-Carmona, M. C. (2006) 'Mycobacterium tuberculosis upregulates coreceptors CCR5 and CXCR4 while HIV modulates CD14 favoring concurrent infection.', *AIDS research and human retroviruses*, 22(1), pp. 45–51. doi: 10.1089/aid.2006.22.45.

Rosenkrands, I., Agger, E. M., Olsen, A. W., Korsholm, K. S., Andersen, C. S., Jensen, K. T. and Andersen, P. (2005) 'Cationic liposomes containing mycobacterial lipids: A new powerful Th1 adjuvant system', *Infection and Immunity*, 73(9), pp. 5817–5826. doi: 10.1128/IAI.73.9.5817-5826.2005.

Rothfuchs, A. G., Bafica, A., Feng, C. G., Egen, J. G., Williams, D. L., Brown, G. D. and Sher, A. (2007) 'Dectin-1 Interaction with Mycobacterium tuberculosis Leads to Enhanced IL-12p40 Production by Splenic Dendritic Cells', *The Journal of Immunology*, 179(6), pp. 3463–3471. doi: 10.4049/jimmunol.179.6.3463.

Rousseau, C., Turner, O. C., Rush, E., Bordat, Y., Sirakova, T. D., Kolattukudy, P. E., Ritter, S., Orme, I. M., Gicquel, B. and Jackson, M. (2003) 'Sulfolipid deficiency does not affect the virulence of Mycobacterium tuberculosis H37Rv in mice and guinea pigs.', *Infection and immunity*, 71(8), pp. 4684–90. doi: 10.1128/IAI.71.8.4684.

Rousseau, C., Winter, N., Pivert, E., Bordat, Y., Neyrolles, O., Avé, P., Huerre, M., Gicquel, B. and Jackson, M. (2004) 'Production of phthiocerol dimycocerosates protects Mycobacterium tuberculosis from the cidal activity of reactive nitrogen intermediates produced by macrophages and modulates the early immune response to infection.', *Cellular microbiology*, 6(3), pp. 277–87. doi: 10.1046/j.1462-5822.2004.00368.x.

Rozmyslowicz, T., Majka, M., Kijowski, J., Murphy, S. L., Conover, D. O., Poncz, M., Ratajczak, J., Gaulton, G. N. and Ratajczak, M. Z. (2003) 'Platelet- and megakaryocyte-derived microparticles transfer CXCR4 receptor to CXCR4-null cells and make them susceptible to infection by X4-HIV', *Aids*, 17(1), pp. 33–42. doi: 10.1097/00002030-200301030-00006.

Ruggiero, A., Malatinkova, E., Rutsaert, S., Paxton, W. A., Vandekerckhove, L. and De Spiegelaere, W. (2017) 'Utility of integrated HIV-1 DNA quantification in cure studies', *Future Virology*, 12(4), pp. 215–225. doi: 10.2217/fvl-2016-0130.

Ryll, R., Watanabe, K., Fujiwara, N., Takimoto, H., Hasunuma, R., Kumazawa, Y., Okada, M. and Yano, I. (2001) 'Mycobacterial cord factor, but not sulfolipid, causes depletion of NKT cells and upregulation of CD1d1 on murine macrophages.', *Microbes and infection*, 3(8), pp.

611–9. doi: 10.1016/S1286-4579(01)01416-2.

Sakamoto, K., Kim, M. J., Rhoades, E. R., Allavena, R. E., Ehrt, S., Wainwright, H. C., Russell, D. G. and Rohde, K. H. (2013) 'Mycobacterial trehalose dimycolate reprograms macrophage global gene expression and activates matrix metalloproteinases.', *Infection and immunity*, 81(3), pp. 764–76. doi: 10.1128/IAI.00906-12.

Sallusto, F., Cella, M., Danieli, C. and Lanzavecchia, A. (1995) 'Dendritic cells use macropinocytosis and the mannose receptor to concentrate macromolecules in the major histocompatibility complex class II compartment: downregulation by cytokines and bacterial products.', *The Journal of experimental medicine*, 182(2), pp. 389–400. doi: 10.1084/jem.182.2.389.

Sampey, G. C., Saifuddin, M., Schwab, A., Barclay, R., Punya, S., Chung, M.-C., Hakami, R. M., Asad Zadeh, M., Lepene, B., Klase, Z. A., El-Hage, N., Young, M., Iordanskiy, S. and Kashanchi, F. (2015) 'Exosomes from HIV-1 infected cells stimulate production of pro-inflammatory cytokines through TAR RNA.', *The Journal of biological chemistry*. doi: 10.1074/jbc.M115.662171.

Sanders, R. W., de Jong, E. C., Baldwin, C. E., Schuitemaker, J. H. N., Kapsenberg, M. L. and Berkhout, B. (2002) 'Differential transmission of human immunodeficiency virus type 1 by distinct subsets of effector dendritic cells.', *Journal of virology*, 76(15), pp. 7812–21. doi: 10.1128/JVI.76.15.7812.

Schlesinger, L. S., Hull, S. R. and Kaufman, T. M. (1994) 'Binding of the terminal mannosyl units of lipoarabinomannan from a virulent strain of Mycobacterium tuberculosis to human macrophages.', *Journal of immunology (Baltimore, Md. : 1950)*, 152(8), pp. 4070–9. Available at: http://www.ncbi.nlm.nih.gov/pubmed/8144972.

Schuitemaker, H., Koot, M., Kootstra, N. A., Dercksen, M. W., de Goede, R. E., van Steenwijk, R. P., Lange, J. M., Schattenkerk, J. K., Miedema, F. and Tersmette, M. (1992) 'Biological phenotype of human immunodeficiency virus type 1 clones at different stages of infection: progression of disease is associated with a shift from monocytotropic to T-cell-tropic virus population.', *Journal of virology*, 66(3), pp. 1354–60. Available at: http://www.ncbi.nlm.nih.gov/pubmed/1738194%5Cnhttp://www.pubmedcentral.nih.gov/articlerender.fcgi?artid=PMC240857.

Schwab, A., Meyering, S. S., Lepene, B., Iordanskiy, S., van Hoek, M. L., Hakami, R. M. and Kashanchi, F. (2015) 'Extracellular vesicles from infected cells: potential for direct pathogenesis.', *Frontiers in microbiology*, 6(OCT), p. 1132. doi: 10.3389/fmicb.2015.01132.

Shattock, R. J., Friedland, J. S. and Griffin, G. E. (1993) 'Modulation of HIV transcription in and release from human monocytic cells following phagocytosis of Mycobacterium tuberculosis.', *Research in virology*, 144(1), pp. 7–12. Available at: http://www.ncbi.nlm.nih.gov/pubmed/8446781.

Singh, P. P., LeMaire, C., Tan, J. C., Zeng, E. and Schorey, J. S. (2011) 'Exosomes released from M. tuberculosis infected cells can suppress IFN-γ mediated activation of naïve macrophages.', *PloS one*, 6(4), p. e18564. doi: 10.1371/journal.pone.0018564.

Singh, P. P., Smith, V. L., Karakousis, P. C. and Schorey, J. S. (2012) 'Exosomes isolated from mycobacteria-infected mice or cultured macrophages can recruit and activate immune cells in vitro and in vivo.', *Journal of immunology (Baltimore, Md. : 1950)*, 189(2), pp. 777–85. doi:

10.4049/jimmunol.1103638.

Singh, P., Rameshwaram, N. R., Ghosh, S. and Mukhopadhyay, S. (2018) 'Cell envelope lipids in the pathophysiology of Mycobacterium tuberculosis.', *Future microbiology*, 13(7), pp. 689–710. doi: 10.2217/fmb-2017-0135.

Singh, S. K., Andersson, A.-M., Ellegård, R., Lindestam Arlehamn, C. S., Sette, A., Larsson, M., Stendahl, O. and Blomgran, R. (2016) 'HIV Interferes with Mycobacterium tuberculosis Antigen Presentation in Human Dendritic Cells.', *The American journal of pathology*. American Society for Investigative Pathology, 186(12), pp. 3083–3093. doi: 10.1016/j.ajpath.2016.08.003.

van der Sluis, R. M., van Montfort, T., Centlivre, M., Schopman, N. C. T., Cornelissen, M., Sanders, R. W., Berkhout, B., Jeeninga, R. E., Paxton, W. A. and Pollakis, G. (2013) 'Quantitation of HIV-1 DNA with a sensitive TaqMan assay that has broad subtype specificity', *Journal of Virological Methods*. Elsevier B.V., 187(1), pp. 94–102. doi: 10.1016/j.jviromet.2012.09.019.

Smith, I. (2003) '*Mycobacterium tuberculosis* pathogenesis and molecular determinants of virulence', *Clinical microbiology reviews*, 16(3), pp. 463–496. doi: 10.1128/CMR.16.3.463.

Sprott, G. D., Dicaire, C. J., Gurnani, K., Sad, S. and Krishnan, L. (2004) 'Activation of Dendritic Cells by Liposomes Prepared from Phosphatidylinositol Mannosides from Mycobacterium bovis Bacillus Calmette-Guerin and Adjuvant Activity In Vivo', *Infection and Immunity*, 72(9), pp. 5235–5246. doi: 10.1128/IAI.72.9.5235-5246.2004.

Stanley, S. A. and Cox, J. S. (2013) 'Host-pathogen interactions during Mycobacterium tuberculosis infections.', *Current topics in microbiology and immunology*, 374(July), pp. 211–41. doi: 10.1007/82_2013_332.

Stax, M. J., van Montfort, T., Sprenger, R. R., Melchers, M., Sanders, R. W., van Leeuwen, E., Repping, S., Pollakis, G., Speijer, D. and Paxton, W. a. (2009) 'Mucin 6 in seminal plasma binds DC-SIGN and potently blocks dendritic cell mediated transfer of HIV-1 to CD4+ T-lymphocytes', *Virology*, 391(2), pp. 203–211. doi: 10.1016/j.virol.2009.06.011.

Stax, M. J., Naarding, M. a., Tanck, M. W. T., Lindquist, S., Hernell, O., Lyle, R., Brandtzaeg, P., Eggesbø, M., Pollakis, G. and Paxton, W. a. (2011) 'Binding of human milk to pathogen receptor DC-SIGN varies with bile salt-stimulated lipase (BSSL) gene polymorphism.', *PloS one*, 6(2), p. e17316. doi: 10.1371/journal.pone.0017316.

Suthar, A. B., Lawn, S. D., del Amo, J., Getahun, H., Dye, C., Sculier, D., Sterling, T. R., Chaisson, R. E., Williams, B. G., Harries, A. D. and Granich, R. M. (2012) 'Antiretroviral therapy for prevention of tuberculosis in adults with hiv: A systematic review and meta-analysis', *PLoS Medicine*, 9(7). doi: 10.1371/journal.pmed.1001270.

Tailleux, L., Schwartz, O., Herrmann, J.-L., Pivert, E., Jackson, M., Amara, A., Legres, L., Dreher, D., Nicod, L. P., Gluckman, J. C., Lagrange, P. H., Gicquel, B. and Neyrolles, O. (2003) 'DC-SIGN is the major Mycobacterium tuberculosis receptor on human dendritic cells.', *The Journal of experimental medicine*, 197(1), pp. 121–127. doi: 10.1084/jem.20021468.

Takehisa, J., Kraus, M. H., Ayouba, A., Bailes, E., Van Heuverswyn, F., Decker, J. M., Li, Y., Rudicell, R. S., Learn, G. H., Neel, C., Ngole, E. M., Shaw, G. M., Peeters, M., Sharp, P. M. and Hahn, B. H. (2009) 'Origin and biology of simian immunodeficiency virus in wild-living western

gorillas.', *Journal of virology*, 83(4), pp. 1635–48. doi: 10.1128/JVI.02311-08.

Tang, H., Kuhen, K. L. and Wong-Staal, F. (1999) 'Lentivirus replication and regulation.', *Annual review of genetics*, 33, pp. 133–70. doi: 10.1146/annurev.genet.33.1.133.

Tang, X., Lu, H., Dooner, M., Chapman, S., Quesenberry, P. J. and Ramratnam, B. (2018) 'Exosomal Tat protein activates latent HIV-1 in primary, resting CD4+ T lymphocytes.', *JCI insight*, 3(7), p. e95676. doi: 10.1172/jci.insight.95676.

Tanne, A., Ma, B., Boudou, F., Tailleux, L., Botella, H., Badell, E., Levillain, F., Taylor, M. E., Drickamer, K., Nigou, J., Dobos, K. M., Puzo, G., Vestweber, D., Wild, M. K., Marcinko, M., Sobieszczuk, P., Stewart, L., Lebus, D., Gicquel, B. and Neyrolles, O. (2009) 'A murine DC-SIGN homologue contributes to early host defense against *Mycobacterium tuberculosis*', *The Journal of Experimental Medicine*, 206(10), pp. 2205–2220. doi: 10.1084/jem.20090188.

Taylor, D. D. and Shah, S. (2015) 'Methods of isolating extracellular vesicles impact down-stream analyses of their cargoes.', *Methods (San Diego, Calif.)*. Elsevier Inc., 87, pp. 3–10. doi: 10.1016/j.ymeth.2015.02.019.

Théry, C., Amigorena, S., Raposo, G. and Clayton, A. (2006) 'Isolation and characterization of exosomes from cell culture supernatants and biological fluids.', *Current protocols in cell biology*, Chapter 3, p. Unit 3.22. doi: 10.1002/0471143030.cb0322s30.

Théry, C., Ostrowski, M. and Segura, E. (2009) 'Membrane vesicles as conveyors of immune responses.', *Nature reviews. Immunology*, 9(8), pp. 581–93. doi: 10.1038/nri2567.

Theus, S. A., Cave, M. D. and Eisenach, K. D. (2005) 'Intracellular Macrophage Growth Rates and Cytokine Profiles of *Mycobacterium tuberculosis* Strains with Different Transmission Dynamics', *The Journal of Infectious Diseases*, 191(3), pp. 453–460. doi: 10.1086/425936.

Theus, S., Eisenach, K., Fomukong, N., Silver, R. F. and Cave, M. D. (2007) 'Beijing family Mycobacterium tuberculosis strains differ in their intracellular growth in THP-1 macrophages.', *The international journal of tuberculosis and lung disease : the official journal of the International Union against Tuberculosis and Lung Disease*, 11(10), pp. 1087–93. Available at: http://www.ncbi.nlm.nih.gov/pubmed/17945065.

Tomlinson, G. S., Bell, L. C. K., Walker, N. F., Tsang, J., Brown, J. S., Breen, R., Lipman, M., Katz, D. R., Miller, R. F., Chain, B. M., Elkington, P. T. G. and Noursadeghi, M. (2014) 'HIV-1 infection of macrophages dysregulates innate immune responses to Mycobacterium tuberculosis by inhibition of interleukin-10.', *The Journal of infectious diseases*, 209(7), pp. 1055–65. doi: 10.1093/infdis/jit621.

Toossi, Z., Mayanja-Kizza, H., Hirsch, C. S., Edmonds, K. L., Spahlinger, T., Hom, D. L., Aung, H., Mugyenyi, P., Ellner, J. J. and Whalen, C. W. (2001) 'Impact of tuberculosis (TB) on HIV-1 activity in dually infected patients.', *Clinical and experimental immunology*, 123(2), pp. 233–8. Available at: http://onlinelibrary.wiley.com/doi/10.1046/j.1365-2249.2001.01401.x/full.

Torrelles, J. B., Knaup, R., Kolareth, A., Slepushkina, T., Kaufman, T. M., Kang, P., Hill, P. J., Brennan, P. J., Chatterjee, D., Belisle, J. T., Musser, J. M. and Schlesinger, L. S. (2008) 'Identification of Mycobacterium tuberculosis clinical isolates with altered phagocytosis by human macrophages due to a truncated lipoarabinomannan', *Journal of Biological Chemistry*, 283(46), pp. 31417–31428. doi: 10.1074/jbc.M806350200.

Torrelles, J. B. and Schlesinger, L. S. (2010) 'Diversity in Mycobacterium tuberculosis mannosylated cell wall determinants impacts adaptation to the host.', *Tuberculosis (Edinburgh, Scotland)*. Elsevier Ltd, 90(2), pp. 84–93. doi: 10.1016/j.tube.2010.02.003.

Trkola, A., Paxton, W. A., Monard, S. P., Hoxie, J. A., Siani, M. A., Thompson, D. A., Wu, L., Mackay, C. R., Horuk, R. and Moore, J. P. (1998) 'Genetic subtype-independent inhibition of human immunodeficiency virus type 1 replication by CC and CXC chemokines.', *Journal of virology*, 72(1), pp. 396–404. Available at: http://www.pubmedcentral.nih.gov/articlerender.fcgi?artid=109387&tool=pmcentrez&rendertype=abstract.

Tumne, A., Prasad, V. S., Chen, Y., Stolz, D. B., Saha, K., Ratner, D. M., Ding, M., Watkins, S. C. and Gupta, P. (2009) 'Noncytotoxic suppression of human immunodeficiency virus type 1 transcription by exosomes secreted from CD8+ T cells.', *Journal of virology*, 83(9), pp. 4354–64. doi: 10.1128/JVI.02629-08.

Turville, S. G., Cameron, P. U., Handley, A., Lin, G., Pöhlmann, S., Doms, R. W. and Cunningham, A. L. (2002) 'Diversity of receptors binding HIV on dendritic cell subsets.', *Nature immunology*, 3(10), pp. 975–83. doi: 10.1038/ni841.

Turville, S. G., Santos, J. J., Frank, I., Cameron, P. U., Wilkinson, J., Miranda-Saksena, M., Dable, J., Stössel, H., Romani, N., Piatak, M., Lifson, J. D., Pope, M. and Cunningham, A. L. (2004) 'Immunodeficiency virus uptake, turnover, and 2-phase transfer in human dendritic cells.', *Blood*, 103(6), pp. 2170–9. doi: 10.1182/blood-2003-09-3129.

Turville, S., Wilkinson, J., Cameron, P., Dable, J. and Cunningham, A. L. (2003) 'The role of dendritic cell C-type lectin receptors in HIV pathogenesis.', *Journal of leukocyte biology*, 74(5), pp. 710–718. doi: 10.1189/jlb.0503208.

Underhill, D. M., Ozinsky, A., Smith, K. D. and Aderem, A. (1999) 'Toll-like receptor-2 mediates mycobacteria-induced proinflammatory signaling in macrophages.', *Proceedings of the National Academy of Sciences of the United States of America*, 96(25), pp. 14459–63. Available at: http://www.ncbi.nlm.nih.gov/pubmed/10588727.

Usami, Y., Popov, S., Popova, E., Inoue, M., Weissenhorn, W. and G. Göttlinger, H. (2009) 'The ESCRT pathway and HIV-1 budding: Figure 1', *Biochemical Society Transactions*, 37(1), pp. 181–184. doi: 10.1042/BST0370181.

Vandergeeten, C., Fromentin, R., Merlini, E., Lawani, M. B., DaFonseca, S., Bakeman, W., McNulty, A., Ramgopal, M., Michael, N., Kim, J. H., Ananworanich, J. and Chomont, N. (2014) 'Cross-clade ultrasensitive PCR-based assays to measure HIV persistence in large-cohort studies.', *Journal of virology*, 88(21), pp. 12385–96. doi: 10.1128/JVI.00609-14.

van de Veerdonk, F. L., Teirlinck, A. C., Kleinnijenhuis, J., Kullberg, B. J., van Crevel, R., van der Meer, J. W. M., Joosten, L. A. B. and Netea, M. G. (2010) 'Mycobacterium tuberculosis induces IL-17A responses through TLR4 and dectin-1 and is critically dependent on endogenous IL-1', *Journal of Leukocyte Biology*, 88(2), pp. 227–232. doi: 10.1189/jlb.0809550.

Vergne, I., Chua, J. and Deretic, V. (2003) 'Tuberculosis toxin blocking phagosome maturation inhibits a novel Ca2+/calmodulin-PI3K hVPS34 cascade.', *The Journal of experimental medicine*, 198(4), pp. 653–659. doi: 10.1084/jem.20030527.

Vidya Vijayan, K. K., Karthigeyan, K. P., Tripathi, S. P. and Hanna, L. E. (2017) 'Pathophysiology

of CD4+ T-Cell Depletion in HIV-1 and HIV-2 Infections.', *Frontiers in immunology*, 8(MAY), p. 580. doi: 10.3389/fimmu.2017.00580.

Vignal, C., Guérardel, Y., Kremer, L., Masson, M., Legrand, D., Mazurier, J. and Elass, E. (2003) 'Lipomannans, but not lipoarabinomannans, purified from Mycobacterium chelonae and Mycobacterium kansasii induce TNF-alpha and IL-8 secretion by a CD14-toll-like receptor 2-dependent mechanism.', *Journal of immunology (Baltimore, Md. : 1950)*, 171(4), pp. 2014–23. doi: 10.4049/jimmunol.171.4.2014.

Wahid Ansari, a., Kamarulzaman, A. and Schmidt, R. E. (2013) 'Multifaceted impact of host C-C chemokine CCL2 in the immuno-pathogenesis of HIV-1/M. tuberculosis co-infection', *Frontiers in Immunology*, 4(OCT), pp. 1–7. doi: 10.3389/fimmu.2013.00312.

Wang, X., Chao, W., Saini, M. and Potash, M. J. (2011) 'A common path to innate immunity to HIV-1 induced by toll-like receptor ligands in primary human macrophages', *PLoS ONE*, 6(8). doi: 10.1371/journal.pone.0024193.

van der Wel, N., Hava, D., Houben, D., Fluitsma, D., van Zon, M., Pierson, J., Brenner, M. and Peters, P. J. (2007) 'M. tuberculosis and M. leprae translocate from the phagolysosome to the cytosol in myeloid cells.', *Cell*, 129(7), pp. 1287–98. doi: 10.1016/j.cell.2007.05.059.

Welin, A., Winberg, M. E., Abdalla, H., Särndahl, E., Rasmusson, B., Stendahl, O. and Lerm, M. (2008) 'Incorporation of Mycobacterium tuberculosis lipoarabinomannan into macrophage membrane rafts is a prerequisite for the phagosomal maturation block.', *Infection and immunity*, 76(7), pp. 2882–7. doi: 10.1128/IAI.01549-07.

Welsh, K. J., Hunter, R. L. and Actor, J. K. (2013) 'Trehalose 6,6'-dimycolate--a coat to regulate tuberculosis immunopathogenesis.', *Tuberculosis (Edinburgh, Scotland)*. Elsevier Ltd, 93 Suppl(SUPPL.), pp. S3-9. doi: 10.1016/S1472-9792(13)70003-9.

Wilen, C. B., Tilton, J. C. and Doms, R. W. (2012) 'HIV: cell binding and entry.', *Cold Spring Harbor perspectives in medicine*, 2(8), pp. 1–14. doi: 10.1101/cshperspect.a006866.

Wiley, R. D. and Gummuluru, S. (2006) 'Immature dendritic cell-derived exosomes can mediate HIV-1 trans infection.', *Proceedings of the National Academy of Sciences of the United States of America*, 103(3), pp. 738–43. doi: 10.1073/pnas.0507995103.

de Witte, L., Bobardt, M., Chatterji, U., Degeest, G., David, G., Geijtenbeek, T. B. H. and Gallay, P. (2007) 'Syndecan-3 is a dendritic cell-specific attachment receptor for HIV-1.', *Proceedings of the National Academy of Sciences of the United States of America*, 104(49), pp. 19464–9. doi: 10.1073/pnas.0703747104.

Wu, L. (2008) 'Biology of HIV mucosal transmission.', *Current opinion in HIV and AIDS*, 3(5), pp. 534–40. doi: 10.1097/COH.0b013e32830634c6.

Wu, L., Paxton, W. A., Kassam, N., Ruffing, N., Rottman, J. B., Sullivan, N., Choe, H., Sodroski, J., Newman, W., Koup, R. A. and Mackay, C. R. (1997) 'CCR5 levels and expression pattern correlate with infectability by macrophage-tropic HIV-1, in vitro.', *The Journal of experimental medicine*, 185(9), pp. 1681–91. doi: 10.1084/jem.185.9.1681.

Wurdinger, T., Gatson, N. N., Balaj, L., Kaur, B., Breakefield, X. O. and Pegtel, D. M. (2012) 'Extracellular vesicles and their convergence with viral pathways.', *Advances in virology*, 2012(1), p. 767694. doi: 10.1155/2012/767694.

Yadav, M. and Schorey, J. S. (2006) 'The beta-glucan receptor dectin-1 functions together with TLR2 to mediate macrophage activation by mycobacteria.', *Blood*, 108(9), pp. 3168–75. doi: 10.1182/blood-2006-05-024406.

Yang, L., Sinha, T., Carlson, T. K., Keiser, T. L., Torrelles, J. B. and Schlesinger, L. S. (2013) 'Changes in the major cell envelope components of Mycobacterium tuberculosis during in vitro growth.', *Glycobiology*, 23(8), pp. 926–34. doi: 10.1093/glycob/cwt029.

Yuan, Y., Maeda, Y., Terasawa, H., Monde, K., Harada, S. and Yusa, K. (2011) 'A combination of polymorphic mutations in V3 loop of HIV-1 gp120 can confer noncompetitive resistance to maraviroc.', *Virology*. Elsevier Inc., 413(2), pp. 293–9. doi: 10.1016/j.virol.2011.02.019.

Zhang, Y., Broser, M., Cohen, H., Bodkin, M., Law, K., Reibman, J. and Rom, W. N. (1995) 'Enhanced interleukin-8 release and gene expression in macrophages after exposure to Mycobacterium tuberculosis and its components.', *The Journal of clinical investigation*, 95(2), pp. 586–92. doi: 10.1172/JCI117702.

Zhang, Y., Nakata, K., Weiden, M. and Rom, W. N. (1995a) 'Mycobacterium tuberculosis enhances human immunodeficiency virus-1 replication by transcriptional activation at the long terminal repeat.', *American journal of respiratory and critical care medicine*, 95(5), pp. 2324–31. doi: 10.1172/JCI117924.

Zhang, Y., Nakata, K., Weiden, M. and Rom, W. N. (1995b) 'Mycobacterium tuberculosis enhances human immunodeficiency virus-1 replication by transcriptional activation at the long terminal repeat.', *The Journal of clinical investigation*, 95(5), pp. 2324–2331.

Zhao, J., Siddiqui, S., Shang, S., Bian, Y., Bagchi, S., He, Y. and Wang, C.-R. (2015) 'Mycolic acid-specific T cells protect against Mycobacterium tuberculosis infection in a humanized transgenic mouse model.', *eLife*, 4(DECEMBER2015), pp. 1–18. doi: 10.7554/eLife.08525.

Zhao, X.-Q., Huang, X., Gupta, P., Borowski, L., Fan, Z., Watkins, S. C., Thomas, E. K. and Rinaldo, C. R. (2002) 'Induction of anti-human immunodeficiency virus type 1 (HIV-1) CD8(+) and CD4(+) T-cell reactivity by dendritic cells loaded with HIV-1 X4-infected apoptotic cells.', *Journal of virology*, 76(6), pp. 3007–14. doi: 10.1128/JVI.76.6.3007.

Zuber, B., Chami, M., Houssin, C., Dubochet, J., Griffiths, G. and Daffé, M. (2008) 'Direct visualization of the outer membrane of mycobacteria and corynebacteria in their native state.', *Journal of bacteriology*, 190(16), pp. 5672–80. doi: 10.1128/JB.01919-07.